An Examination of the inter-relationship between Structure and Kinetics associated with Crystallisation of Single and Mixed Chocolate Confectionery Fats

Alessandra Rossi

Department of Pure and Applied Chemistry
University of Strathclyde

Degree of Doctor of Philosophy
1998

To Mum, Dad, Paola

and

Alberto

Acknowledgements

I am indebted to my supervisor, Professor Kevin J. Roberts for all his assistance and support throughout this project and for giving me the opportunity to come to Scotland. I gratefully acknowledge the help of my industrial sponsors, Mr Martin Wells, Mr Mike Polgreen and Dr Ian Smith, not only for financial support but also for guidance, from carrying out experiments to proof reading this thesis.

For the use of the equipment and facilities, I would like to thank the University of Strathclyde, Department of Pure and Applied Chemistry, where the experiments were carried out for the first eighteen months and Heriot-Watt University, Centre of Molecular and Interface Engineering, where this work was completed. I am very grateful to Mr. Neil Hodgson (Strathclyde University) who build my variable temperature and shear in-situ processing cell and to all technical and academic staff, especially Colin, Alf, Les, Susan and Mary, for all the assistance, help and friendship that I received during my time at Heriot-Watt. I would also like to acknowledge Professor Richard Pethrick for taking over as my supervisor at Strathclyde following the group's move to Heriot-Watt University.

This work, supported through a research studentship by Cadbury Ltd, was part of a wider EPSRC programme funded by this structured materials initiative (GR/K/42820). The experiments at Brookhaven National Laboratory were supported by GR/K/80488. I thank to SRS (Daresbury) and NSLS (Brookhaven) for beamtime. At Daresbury, I would like to thank Dr Liz Town-Andrews for her co-operation on station 16.1, Mrs Sue Slawson for assistance on station 2.1, Dr Chiu Tang and Mr Alfie Neeld for helping and support on station 2.3. At Brookhaven, I would like to thank Dr Malcolm Capel (Brookhaven) for co-operation and assistance on station X12B. I would like to acknowledge Scott Mac Millan (PhD student) for helping me to complete the crashcool experiments discussed in Chapter 7.

I am grateful to Dr Robert Hammond for his essential advice and assistance with the data analysis, Mr Charles Kerr for helping with the software development, Dr Anne Neville for proof reading and Dr Elena Ferrari for her support during the final submission of the thesis. I would like to thank all past and present members of our research group for support throughout the duration of this project, especially Ann, Carol, Lorna, Gillian, Susan and Richard. I would also like to acknowledge Mrs Sheilagh Thompson for her friendship and helping me improve my English, Joyce and Graham for the fun and all the lifts from and to Heriot-Watt.

Finally and especially, I would like to thank Alberto for many reasons: for help using the Autosketch program for drawing figures; support, tolerance and ability to cope throughout the duration of this project.

Abstract

A detailed examination of the crystallisation and subsequent phase transformation of confectionery fats was carried out. The systems studied were: tripalmitin/triacetin; tripalmitin/cocoa butter; tripalmitin/triolein; milk fat/cocoa butter and milk fat/cocoa butter/yn (synthetic lecithin). Three different techniques were used to investigate these systems, i.e. small angle and wide X-ray scattering, nucleation (slowcool and crashcool).

Tripalmitin showed a very low solubility in triacetin and hence it did not follow the behaviour of an ideal solution. Whereas the system tripalmitin/triolein showed an ideal behaviour. In the case of the tripalmitin and cocoa butter mixtures the ideal behaviour was observed only for high concentrations of tripamitin.

It was observed that for the milk fat/cocoa butter mixtures two crystallisation and dissolution processes took place depending on the concentration. This result was confirmed by the SAXS experiments.

During the small angle X-ray scattering studies of tripalmitin and cocoa butter system it was observed that Form I showed a higher stability than that reported in literature.

Measurements of the induction time under well-controlled mixing conditions for the binary mixtures tripalmitin/cocoa butter and milk fat/cocoa butter were carried out using a new crash cool tempering cell. It was found that the induction time decreases as the shear rate increases.

As a part of this work a new variable temperature variable shear processing cell was developed in order to study in-situ the crystallisation process under conditions which are more representative of the industrial process. The effects of shearing, time and temperature on the formation of polymorphic forms of cocoa butter and a mixture of fats were examined. For both systems, the shear and temperature had the effect to vary the induction time of crystallisation of Form V.

Erratum

Due to printing errors the last sentence in the following pages should be amended as:

Pag. 2 earlier by the spanish explorer Don Cortes [Minifie, 1980]. When he conquered

Pag. 108 the results at this heating rate were not considered for the kinetics calculations.

Pag. 140 milk fat in cocoa butter show that a polymorphic transformation has taken place. It was observed that this depends on the cooling/heating rate. The nucleation experiments do not provide information of the type of phases formed during the

Pag. 228 From knowledge of the interfacial energy and supersaturation of a system the

Table of contents

Chapter 1

Introduction

1.1 *Industrial background*

Crystallisation is one of the dominant techniques used by the chemical and food industry for particle separation and purification. There is a limited understanding of the detailed structure-kinetics mechanisms associated with the formation of crystalline particles from the liquid phase. The control of solid-state structure represents a key processing variable for the production of many particulate systems.

In chocolate manufacturing, careful control of the solidification processes is very important. First of all it significantly influences the rheological properties of chocolate, which determines the workability in the production processes [Martin, 1987; Nelson, 1994]. Secondly the physical properties of end products such as gloss, snap, texture, heat resistance and fat bloom stability are also influenced by the solidification process [Kleinert, 1961; Musser, 1973; Murray, 1978; Jewell, 1981]. The physical properties are related to the polymorphism of cocoa butter, which is the major component of solid fat present in chocolate. Thus, control of the molecular structure and polymorphic forms of fats is particularly important in the manufacture of chocolate confectionery products.

Consumers enjoy eating confections because they taste good and produce a feeling of satisfaction and pleasure. The pleasure derived from consuming chocolate may also be due in part to the cocoa butter which is a major component of the product formulation. Due to the high price of cocoa butter, it is important that this vital ingredient be used to its maximum benefit.

1.2 *The story of chocolate*

Chocolate production involves formulating a mixture of cocoa butter, cocoa solids, sugar, vegetable fats, lecithin and, in the case of milk chocolate, milk solids (Figure 1.1).

Cocoa was first introduced into England during the Seventeenth century by Nicholas Sanders [Cook, 1984], although it had been brought to Europe over a century

Mexico in 1519, Don Cortes discovered that the Aztecs in Central America had been drinking chocolate made from cocoa beans for hundreds of years. This thick rich liquid flavoured with spices was called "chocolatl" and was a favourite drink of the Aztec Emperor, Moctezuma [Whymper, 1912]. Cortes brought cocoa beans back to Spain where the flavour of the drink was improved by adding sugar. The way it was prepared was a closely guarded secret for almost a century. The chocolate drink was finally introduced into England in the 1650's as an expensive luxury. When the first chocolate house opened in 1657, chocolate cost 6/8d a pound, and the high price was sustained for many years by heavy import duties. In 1853, import taxes were reduced and the Industrial Revolution made transport easier, so chocolate became available to a larger percentage of the population. Chocolate was exclusively for drinking until the early Victorian times when the technique of making solid "eating" chocolate was perfected.

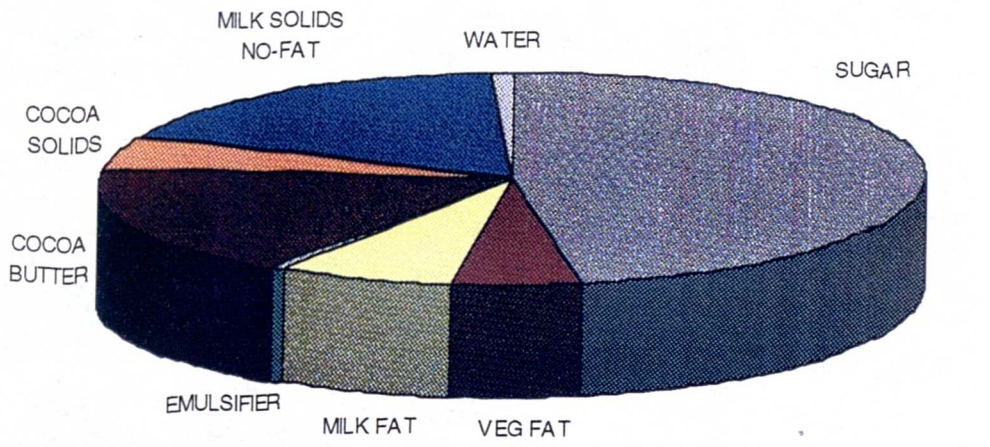

Figure 1.1. Composition of U.K. milk chocolate

1.2.1 *The cultivation of cocoa*

Cocoa and chocolate are derived from the cocoa bean, which grows in pods on the cocoa tree [Dunbar, 1994; Hancock, 1994]. The botanical name of the cocoa tree is *Theobroma cacao*, so called by Linnaeus because of its reputation for providing the "food of the gods" (Greek: theos (god), broma (food)). Originating in the Amazon forests, the cocoa tree thrives in a humid tropical climate, characterised by regular rains and a short dry season. Cocoa is now grown commercially in a number of countries where the climate is similar to the natural habitat: Ghana, Ivory Coast, Nigeria, Cameroon in West Africa; Brazil, Ecuador in South America; Malaysia and Indonesia [Wood, 1986]. But the sources of cocoa and cocoa butter in these countries are different. This is related to the climate in which the cocoa is grown. In a hot climate, there is an increase in the level of saturated fatty acids and a hard fat is produced. Many of the properties of chocolate change if a different source of cocoa butter is used. October to December is the main harvesting period in West Africa when the ripe pods are cut from the trees, split and the pulp and beans removed from the husk.

Fermentation is the next vital stage in the cocoa and chocolate making process, developing chocolate flavour and removing the astringency of the unfermented bean. The cocoa beans are piled up on a layer of large banana leaves, with more leaves covering the beans. The fermentation process takes five or six days and the contents of the heap must be turned from time to time as it proceeds. During fermentation, alcohol and acidic, vinegar-like liquids are produced and drain away. The temperature rises to about 50°C/122°F.

When fermentation is complete, the wet mass of beans is dried, traditionally by being spread in the sun. The farmer then takes his produce to the buying station where the fermented beans are packed into sacks for transportation all over the world. Stringent quality control procedures are carried out as samples are checked to ensure standards are maintained before the cocoa beans are brought from the farmer.

1.2.2 *The manufacture of cocoa and chocolate*

On arrival at the factory the cocoa beans are subjected to the following essential process:

- *Cleaning and Roasting*: The cocoa beans are sorted and cleaned. They are then roasted in revolving drums at a temperature of 135°C. During roasting, the shells become brittle and the cocoa beans acquire their characteristic flavour and aroma. Roasting time is about an hour at the above temperature.

- *Kibbling and Winnowing*: The roasted beans are then broken into small pieces (kibbled) in preparation for winnowing. In the winnower, the fractured shell and bean fragments are separated by sieving and air elutriation. The separation process is dependent on a difference in density between the bean cotyledon fragments and the shell. The broken pieces of cocoa bean, with shells removed, are known as 'nibs'.

- *Grinding*: The nibs are then ground becoming a thick chocolate-coloured liquid with the consistency of thick cream which is known as 'mass' or liquor. The mass, which contains ~ 55% cocoa butter, solidifies on cooling and is the basis for all chocolate and cocoa products. Cocoa is made by compressing the cocoa butter under high pressure, till the solid has around 11-20% remaining fat in total. The solid block of cocoa, which remains, is ground into a fine powder to produce cocoa for beveraging and cooking with a fat content specified by law.

For the production of milk chocolate the cocoa mass is mixed with full cream milk and sugar, which have been condensed into a rich creamy liquid. The product is dried to give milk chocolate "crumb", that is pulverised and ground. Now, additional cocoa butter and special chocolate flavourings are added. Plain chocolate is made by virtually the same process but uses a mixture of cocoa mass, sugar and cocoa butter as its main ingredient (see Figure 1.2).

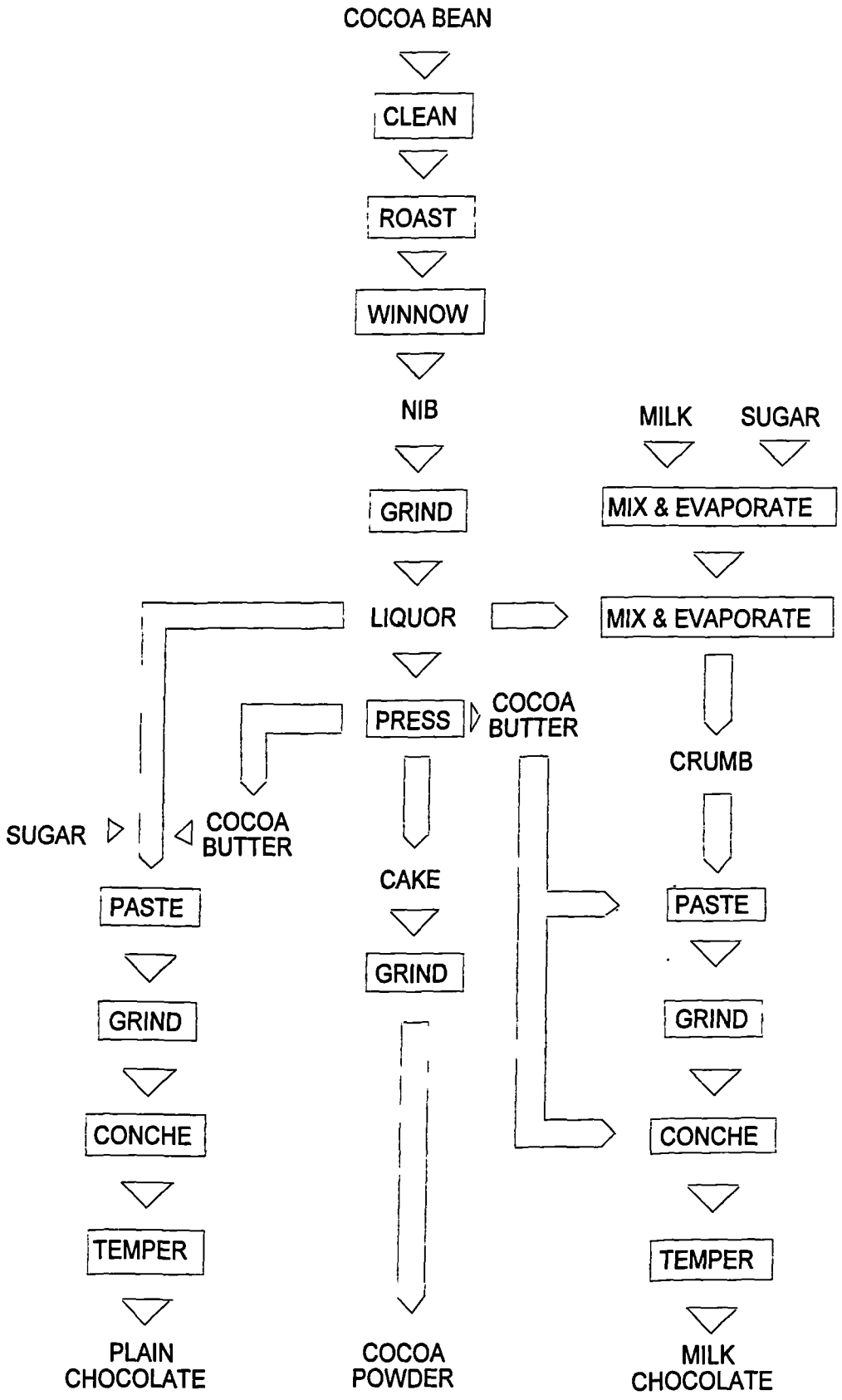

Figure 1.2. Schematic representation of the industrial process involved in the production of chocolate

The chocolate paste has to be refined. This is an important operation to produce the smooth texture [Minifie, 1980]. The roll refiners are made of five horizontal rolls mounted vertically above one another, with the bottom feed roll offset. The speed of rotation of the rolls increases from bottom to top and this allows the chocolate film to be transferred from one roll to the next. The pressure between the rolls is controlled hydraulically and each roll is cooled internally with water jets, with the water to each roll being thermostatically regulated. Correct cooling is essential as the refiners generate a great deal of frictional heat. Another part of the machine is the scraper knife, which removes the film of chocolate from the top roll. This must be set at the correct angle and pressure to ensure that the film is completely removed.

After a small particle size (< 25μm) has been established in the refiners, the chocolate blend is conched. The conching is the last process in the manufacture of bulk chocolate. This is an essential process for the development of the full desirable chocolate flavour and the conversion of the powdery, crumbly refined product into a flowable suspension of sugar, cocoa and milk powder particles in a liquid phase of cocoa butter (and other fats as appropriate). The viscosity is reduced by lowering the moisture content.

Before the liquid chocolate is moulded into bars or used for covering the centres of other confections, it has to be tempered. This process is one of the most important stages in production as it influences the texture, gloss and lasting qualities of the chocolate. This step is essential because it ensures that the confectionery fat constituent is crystallised and that the chocolate will set in a stable condition with a good permanent colour and gloss. Immediately after tempering, the chocolate is moulded and cooled to approximately 16°C for proper setting and contraction. If the chocolate is shock cooled or if the cooling time is too short, the product quality may be affected. The biggest problem associated with poor temper is the formation of fat bloom which visually appears as grey swirl or as large white circular fat crystals on the surface.

The physical properties of chocolate are related to the polymorphism of cocoa butter [Wille and Lutton, 1966]. The properties of cocoa butter, both chemical and physical, have drawn the attention of many investigators, owing to their significance,

they assume, in confectionery production and storage. The unique palatable characteristics of cocoa butter, which are due mainly to the melting of the fat at body temperature, make it the undisguised ingredient of confectionery product formulations.

Cocoa butter is a yellow fat that shows brittleness below 20°C, begins softening at 30° to 32°C, and exhibits a sharp and complete melting below body temperature. The solid/liquid ratio of the fat at different temperatures characterises its fundamental thermal behaviour. This ratio is widely used in the fat industry as a functional estimate of the melting properties of the fat. Cocoa butter is a relatively tasteless fat, the melting behaviour of which is responsible, not only for the mouthfeel, but also for release of the flavour deriving from the cocoa powder dispersed within the fat. Since the fat constitutes a major phase in chocolate and binds together other ingredients, its physical properties have a large influence on the quality and acceptability of the confectionery products. Cocoa butter can occur in numerous polymorphic crystalline forms and the form has a large impact on the final quality of a confectionery product. Snap, gloss, proper melting point, contraction, and other attributes are dictated by the crystalline forms present [Schlichter-Aronhime, 1988]. Taste, smell, mouthfeel, hearing, and especially sight are involved in the total perception of a food product. If the cocoa butter crystals present in a chocolate product are not in the most desirable form, mouthfeel, hearing and sight are affected in a undesirable manner.

Thus, to achieve efficient processing of chocolate and to ensure the quality of the finished product requires an understanding of the physical properties and structure of cocoa butter and how these are modified by other fats that may also be present e.g. milk fat, vegetable fat and emulsifiers.

1.3 *Scope of thesis*

The aim of this project is to study the crystallisation process of single and mixed confectionery fats. This thesis is divided into nine chapters. Following this introduction, chapter 2 describes background process science relating to crystallography, crystallisation, X-ray diffraction and rheology.

Chapter 3 consists of a summary of a literature study concerning the chemical composition of cocoa butter as a function of the different geographic regions. It provides the conceptual background for the phenomenon of polymorphism and phase transformation of fats. In addition, it illustrates the importance of the right polymorph of cocoa butter to chocolate manufacture.

Chapter 4 investigates the nucleation behaviour of single and mixed triglycerides. Firstly, binary mixtures of triglycerides, such as triapalmitin and triacetin, tripalmitin and triolein, were analysed. Secondly, a study of more complex systems was undertaken, involving the presence of cocoa butter, milk fat and synthetic lecithin.

Chapter 5 examines the structural characterisation of single and mixed confectionery fats under static conditions. The studies were carried out using SAXS (small angle X-ray scattering) diffraction at National Synchrotron Light Source, Brookhaven (USA).

Chapter 6 presents an analysis of the crystallisation of cocoa butter using WAXS (wide angle X-ray scattering) diffraction conducted at the synchrotron radiation source at Daresbury Laboratory.

Chapter 7 describes studies in which the effect of mixing on crystallisation of fats is examined. A new crash cool tempering cell was developed in order to measure induction times to a high degree of accuracy in a stirred system using a novel turbidity probe.

Chapter 8 presents an investigation of the effects of shearing, time and temperature on the formation of polymorphic forms of cocoa butter and a mixture of fats. The composition of the mixture is made up of cocoa butter, milk fat, vegetable fat and YN, in proportions similar to those used in real chocolate. A novel variable temperature shear processing cell was developed in order to study the crystallisation and phase transformation in cocoa butter fat, occurring during the tempering process *in-situ*. This cell enables the structural properties of fats to be continuously monitored 'on-line' so that the processing conditions can be optimised.

Finally, chapter 9 summarises the conclusions of all results chapters and also offers proposals for further work in this area.

1.4 *References*

Cook, L R, in *Chocolate Production and Use*, edited by L R Cook, revised by E H Meursing, Harcout Brace Jovanovich Inc. New York, 1984, pp. 401-423.

Dunbar, P in *The complete Cadbury's cook book*, Chancellor Press, 1994.

Hancock, B. L., in *Industrial chocolate manufacture and use*, edited by S. T. Beckett, Blackie A & P, London, 1994, 2nd edn., chap. 2.

Kleinert, I J, *Int. Choco. Rev.*, 1961, 16, 201-219.

Jewell, G G, *35th P. M. C. A. Production Conference*, 1981, 35, 63-66.

Martin, R A, Jr in *Advances in Food Research*, 31, edited by C O Chichester, E M Mark, and B S Schweigert, Academic Press Inc. New York, 1987, pp. 308-313.

Minifie, B W, in *Chocolate Cocoa and Confectionery*, 2nd edn, Avi Publishing Co. Inc., Westport, Connecticut, 1980.

Murray, G, *Manufacturing Confectioner*, 1978, 58, 35-36.

Musser, J C, *27th P. M. C. A. Production Conference*, 1973, 46-50.

Nelson, R B, in *Industrial Chocolate Manufacture and Use*, edited by S T Beckett, Blackie A & P, London, 1994, 2nd edn., pp. 172-202.

Schlichter-Aronhime, J and Garti, N, in *Crystallisation and Polymorphism of Fats and Fatty Acids*, ed by Garti N and Sato K, Marcel Dekker, Inc. New York and Basel, 1988, chap. 9.

Whymper, R, in *Cocoa and chocolate, Their chemistry and Manufacture*, Churchill, London, 1912.

Wille, R L and Lutton, E S, *J. Amer. Oil Chem. Soc.*, 1966, 43, 491-496.

Wood, G A R, *The Biologist*, 1986, 33, 99-104.

Chapter 2

Related processing theory

2.1 *Introduction*

This chapter describes briefly what a crystal is and defines the way in which a crystal nucleates. It continues with a discussion of some basic aspects of X-ray diffraction. Finally, rheology, which is defined as the study of deformation and flow of matter, will be described.

2.2 *Crystals*

A crystal can be defined as a three dimensional repeating pattern of a structural moiety. This pattern is characterised by lattice points, which are points having an identical environment. Each moiety sits at or near the intersections (the lattice points) of an imaginary grid (the lattice) (Figure 2.1). The smallest repeating moiety is called the asymmetric unit. The repeating unit within a crystal lattice is called the unit cell.

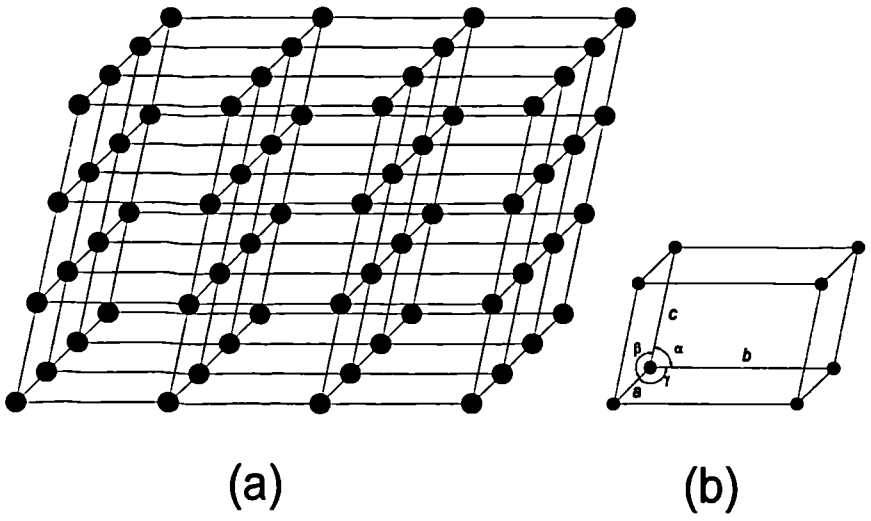

Figure 2.1. (a) Crystal lattice in 3D space; (b) unit cell.

The unit cell contains a number (Z) of asymmetric units and it can be described by the dimensions *a*, *b* and *c* and the angles α, β and γ, with α being the angle between b and c, β between a and c and γ between a and b. These lengths and angles are the *lattice constants* or *lattice parameters* of the unit cell.

Variation in lattice parameters gives rise to seven crystal systems, classified by their fundamental unit cell dimensions and minimal symmetries, and they are listed in table 2.1.

Crystal system	Cell parameters	Minimum symmetry
Cubic	$a = b = c$; $\alpha = \beta = \gamma = 90°$	Four 3-fold rotation axes
Tetragonal	$a = b \neq c$; $\alpha = \beta = \gamma = 90°$	One 4-fold-rotation (or rotation-inversion) axis
Orthorhombic	$a \neq b \neq c$; $\alpha = \beta = \gamma = 90°$	Three perpendicular 2-fold rotation (or rotation-inversion) axes
Trigonal	$a = b = c$; $\alpha = \beta = \gamma \neq 90°$	One 3-fold rotation (or rotation-inversion) axis
Hexagonal	$a = b \neq c$; $\alpha = \beta = 90°$ $\gamma = 120°$	One 6-fold rotation (or rotation-inversion) axis
Monoclinic	$a \neq b \neq c$; $\alpha = \gamma = 90° \neq \beta$	One 2-fold rotation (or rotation-inversion) axis
Triclinic	$a \neq b \neq c$; $\alpha \neq \beta \neq \gamma \neq 90°$	None

Table 2.1. The seven crystal systems and associated symmetry [Myerson and Ginde, 1993].

Bravais (1866) postulated fourteen different ways of arranging the lattice points in three dimensional space (Figure 2.2). These are consistent with the seven crystal systems. Additional lattices are obtained by adding face, base and body centring to certain lattices. The primitive lattice cell (P) has a lattice point only at the corner of the cell. Face centred (F) involves a lattice point at the centre of opposite pairs of faces, while base centred (C) has a lattice point at the centres of the basal planes of the cell. Finally, body centred (I) involves a lattice point at the centre of the cell.

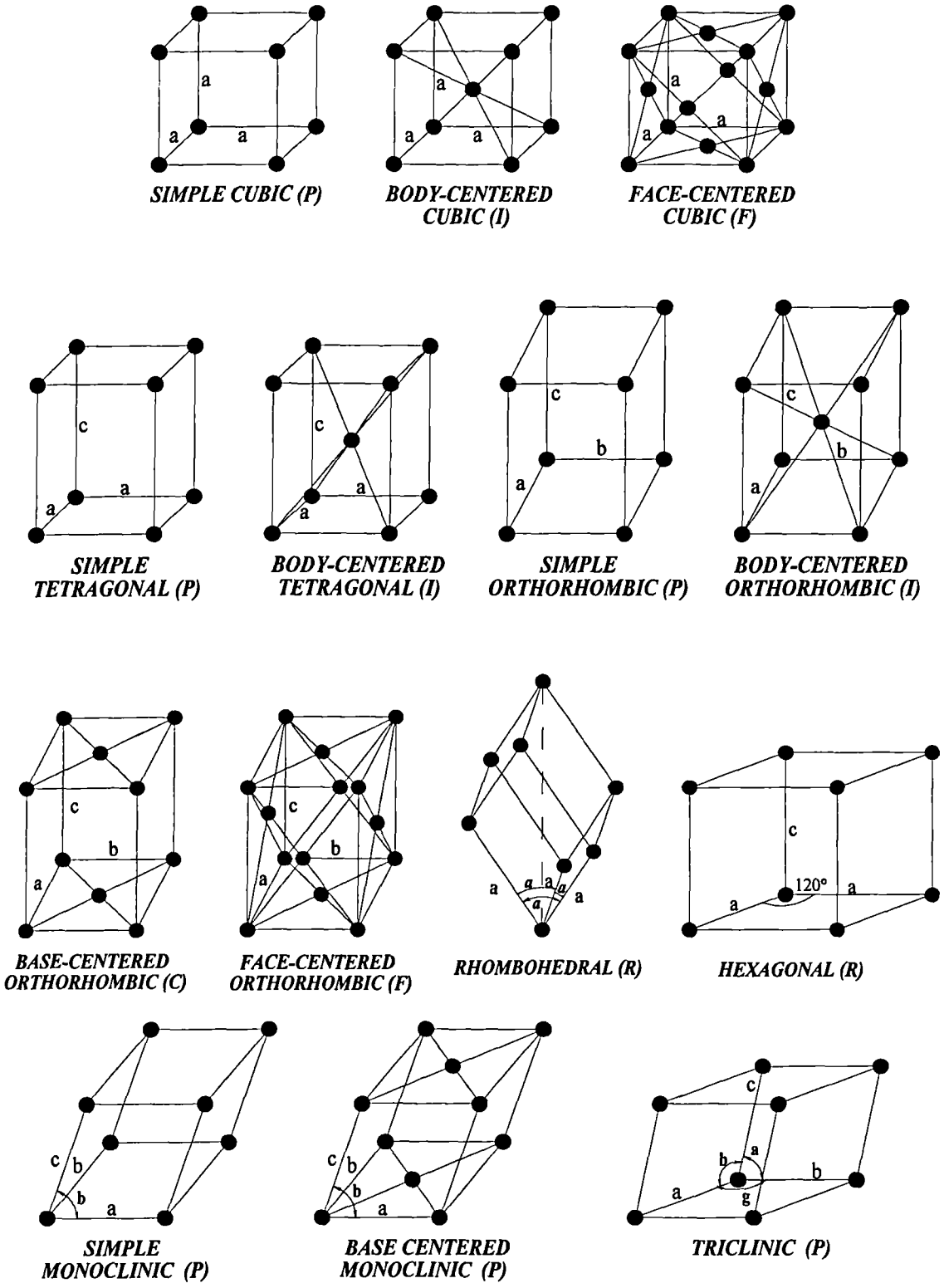

Figure 2.2. The fourteen Bravais lattice.

2.3 *Crystallisation*

Crystallisation is a term used to characterise a number of phenomena: formation of a solid phase from a melt, solution or vapour phases and polymorphic transformation in solid phase. Crystallisation takes place in three stages:

1) achievement of supersaturation;
2) formation of crystal nuclei (nucleation);
3) growth of crystal nuclei (growth).

Analysis of industrial crystallisation processes requires knowledge of both nucleation and crystal growth. A supersaturated solution is required for crystallisation to occur.

2.3.1 *Supersaturation*

Supersaturation is the essential driving force of all crystallisation processes. A solution that contains an excess of concentration over the saturated (equilibrium) value at a given temperature is described as being supersaturated. The supersaturation driving force allows the system to initiate nuclei formation and maintain growth until the degree of supersaturation is relieved.

Ostwald (1897) first classified supersaturation solutions in terms of 'labile' and 'metastable' supersaturated depending on whether spontaneous nucleation did or did not occur, respectively. Miers and Isaac (1906 and 1907), as explained in the text by Mullin (1993), have further advanced the relationship between supersaturation and spontaneous crystallisation, leading to the solubility-supersolubility diagram (Figure 2.3). The metastable zone is the region between equilibrium solubility and the point of bulk nucleation and spontaneous growth. The meta stable zone is important in conventional crystallisation processes, as it gives an insight into the nucleation behaviour of each system.

The lower solubility curve (Figure 2.3) can be located with precision. The upper broken supersolubility curve, which represents temperatures and concentrations at which uncontrolled spontaneous crystallisation occurs, can not be located with the same precision as the solubility curve and its position can be greatly affected by the degree of agitation, the presence of crystals and the presence of trace impurities.

In the case of crystallisation from the liquid phase (liquid/solid phase transition) there are three regions of different behaviour:

1. The stable zone where the solution is unsaturated which respect to the dissolved solid phase and spontaneous crystallisation is impossible.
2. The metastable zone where the solution is supersaturated to a degree and crystallisation takes place only after a certain period of time. The time delay (τ) allows the crystallising molecules to organise themselves into a three dimensional array.
3. The labile zone where the solution is supersaturated and uncontrolled spontaneous crystallisation is likely to occur with no expected time delay.

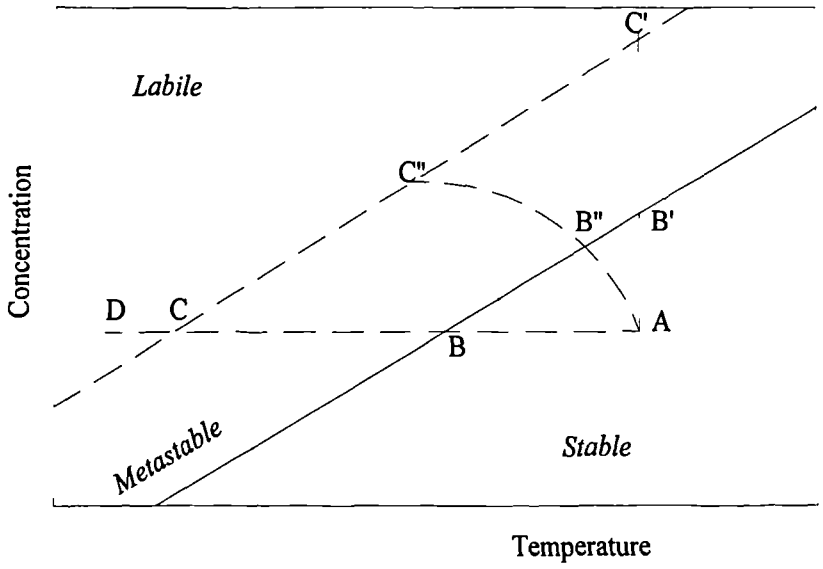

Figure 2.3. Solubility-supersolubility diagram [Mullin, 1993].

Supersaturation can be achieved in a variety of different ways: temperature cooling (ABC), solvent evaporation (AB'C'), a combination of both (AB''C''), the addition of a precipitate or chemical techniques such as the chemical reaction between two homogeneous phases. At the point B, crystallisation is meanly possible or may not

occurred . Crystallisation occurs spontaneously when conditions represented by point C are reached. Within the region BC, the crystallisation may be induced by seeding, agitation or mechanical shock.

Several thermodynamic expressions exist to describe supersaturation [Mullin, 1973]. The concentration driving force, Δc, is defined as:

$$\Delta c = c - c^* \tag{2.1}$$

where c is the solution concentration and c^* is the equilibrium saturation at the given temperature.

The supersaturation ratio, S, is described by:

$$S = \frac{c}{c^*} \tag{2.2}$$

The relative supersaturation, σ is the alternative expression:

$$\sigma = \Delta c / c^* = S^1 \tag{2.3}$$

2.3.2 *Nucleation*

Nucleation can only be achieved once a certain degree of supersaturation exists in the system. Nucleation is a three dimensional process from which two dimensional crystal growth can proceed. In the nucleation stage supersaturation causes the formation and agglomeration of molecular solute clusters. These clusters are maintained in a dynamic equilibrium which is dictated by the balance between the volume and surface contributions to their excess free energy [Walton, 1969; Garside, 1986]. At sufficient cluster size the bulk volume term dominates over the surface term and a viable particle (critical nucleus) is formed. Growth is delayed until the critical nucleus is achieved and continues until the supersaturation is relieved.

Nucleation can be divided into two main processes (Figure 2.4): primary and secondary. The former is defined as a process of formation of nuclei from a pure liquid phase in the absence (homogeneous) and presence (heterogeneous) of foreign particles. Secondary nucleation occurs if attrition particles or seed crystals are present in the mother liquid phase during nucleation.

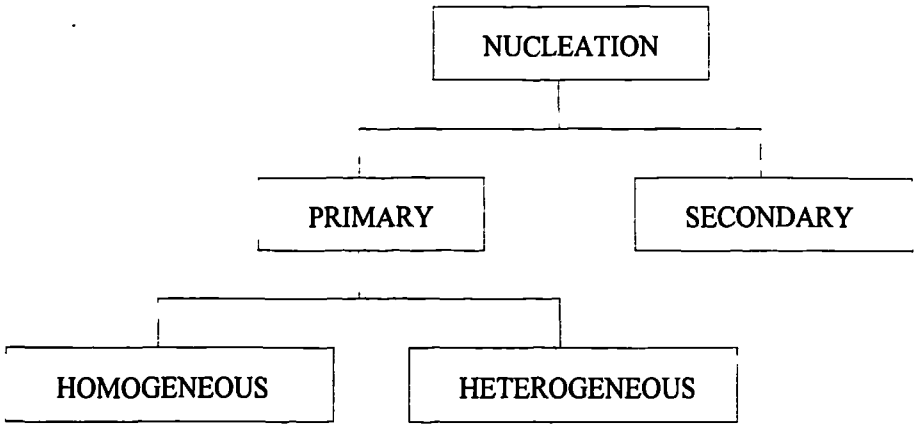

Figure 2.4. Classes of nucleation.

2.3.2.1 *Primary homogeneous nucleation*

Primary homogeneous nucleation is spontaneous nucleation, taking place in systems free from either dissolved or solid impurities. Although it rarely occurs in practice, homogeneous nucleation forms the basis of understanding and explaining the important factors involved in nucleation.

Volmer (1939) assumed that clusters are formed in solution by an addition mechanism:

$$A + A = A_2$$

$$A_2 + A = A_3$$

$$A_{n-1} + A = A_n$$

Further addition of molecules to the critical cluster (A_n) will result in nucleation and subsequent growth of the nucleus. The likelihood of a molecular cluster becoming a stable nucleus is governed by the energy associated with its formation and growth. The construction process can only continue in the very high supersaturation region. The clusters formed will redissolve if they are too small. In the case where the nucleus grows beyond a certain critical size, it becomes stable. However, both processes will result in a decrease in the free energy of the particle. The number of molecules in a stable crystal nucleus can vary from about ten to several thousand.

The classical theory for homogeneous nucleation was developed by Gibbs (1928), Volmer (1939), Becker and Döring (1935) and others. They based their consideration on the condensation of a vapour to a liquid, but this may be extended to crystallisation from melts and solutions. The overall free energy difference, ΔG, between a small solid particle of solute and the solute in solution is the sum of the excess free energy between the surface of the particle and the bulk of the particle, ΔG_S, and the excess free energy between a very large particle ($r = \infty$) and the solute in solution, ΔG_V.

$$\Delta G = \Delta G_S + \Delta G_V \qquad (2.4)$$

Assuming the clusters are spherical, ΔG_S is a positive quantity proportional to r^2, where r is the cluster radius, while ΔG_V is a negative quantity proportional to r^3. Thus:

$$\Delta G = 4\pi r^2\gamma + 4/3\ \pi r^3 \Delta G_v \qquad (2.5)$$

where ΔG_v is the free energy change of the transformation per unit volume and γ is the interfacial tension between the cluster and the surrounding solution. Since ΔG_S and ΔG_V are of opposite sign and depend differently on r, the free energy of formation will pass through a maximum (Figure 2.5).

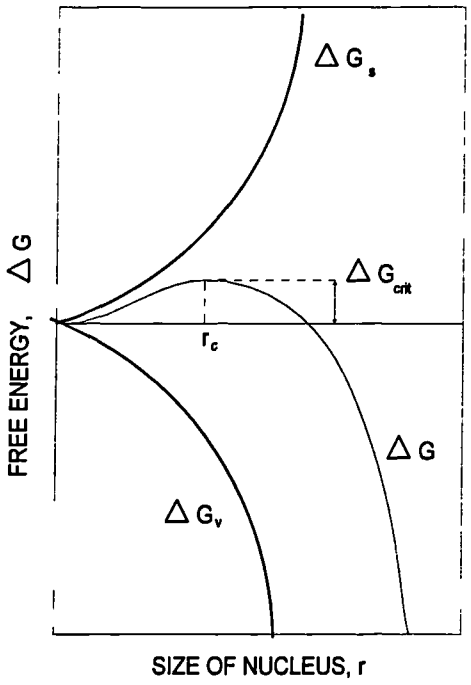

Figure 2.5. Free energy diagram for cluster formation.

The maximum value, ΔG_{crit}, corresponds to the critical nucleus size, r_c. The derivation of the critical nucleus can be found by differentiating ΔG with respect to the nucleus radius in equation (2.5), setting $d\Delta G/dr = 0$:

$$d\Delta G/dr = 8\pi r\gamma + 4\pi r^2 \Delta G_v = 0 \qquad (2.6)$$

thus,

$$r_c = -2\gamma/\Delta G_v \qquad (2.7)$$

Substituting equation (2.7) into equation (2.5) leads to:

$$\Delta G_{crit} = 16\pi\gamma^3/3(\Delta G_v)^2 = 4\pi\gamma r_c^2/3 \qquad (2.8)$$

Using the following thermodynamic definition the critical cluster size can be related to the degree of supersaturation:

$$\Delta G_v = \Delta Hv - T_e \Delta S_v \qquad (2.9)$$

where ΔHv and ΔS_v are the volume enthalpy and entropy of crystallisation, respectively. At equilibrium conditions, where T_e is equivalent to the equilibrium saturation temperature and $\Delta G_v = 0$, equation (2.9) becomes:

$$\Delta S_v = \Delta Hv/T_e = \Delta H_c/ V_m T_e \qquad (2.10)$$

where V_m is the molar volume. Given $\Delta T = (T_e - T)$ and using equations (2.09) and (2.10), the following equation is obtained:

$$\Delta G_v = \Delta H_c/ V_m - T\Delta H_c/ V_m T_e = (\Delta H_c/ V_m)(\Delta T/T_e) \qquad (2.11)$$

For small supersaturations within the metastable zone, supersaturation can be related to the solution's undercooling (ΔT) through the Gibbs-Thomson relationship:

$$\ln (S) = \Delta H_c \Delta T/kT_e^2 \qquad (2.12)$$

where k is the Boltzmann constant.

By eliminating ΔG_v and ΔH_c from equations (2.7), (2.11) and (2.12) then:

$$r^* = 2\gamma V_m/kT_e \ln(S) \qquad (2.13)$$

This equation shows that critical cluster size is inversely proportional to the degree of supersaturation. As the supersaturation increases the critical size decreases. This is the reason why solutions become less and less stable as the degree of supersaturation increases.

Substituting equation (2.13) into equation (2.8) gives:

$$\Delta G_v = 16\pi\gamma^3 V_m^2/3k^2T_e^2(\ln S)^2 \qquad (2.14)$$

The rate of nucleation (J) is the number of nuclei formed per unit time per unit volume. According to Becker and Döring (1935), J can be expressed by an Arrhenius type relationship:

$$J = A \exp(-\Delta G^*/kT) \qquad (2.15)$$

where A is the pre-exponential factor. Combining equations (2.14) and (2.15) J can be expressed as:

$$J = A \exp[-16\pi\gamma^3 V_m^2/3k^3T^3(\ln S)^2] \qquad (2.16)$$

This equation indicates that many variables govern the rate of nucleation: temperature (T), degree of supersaturation (S), interfacial tension (γ) and molecular volume (V_m). A plot of equation (2.16) (Figure 2.6) illustrates the extremely rapid increase in rate of nucleation once some critical level of supersaturation is exceeded.

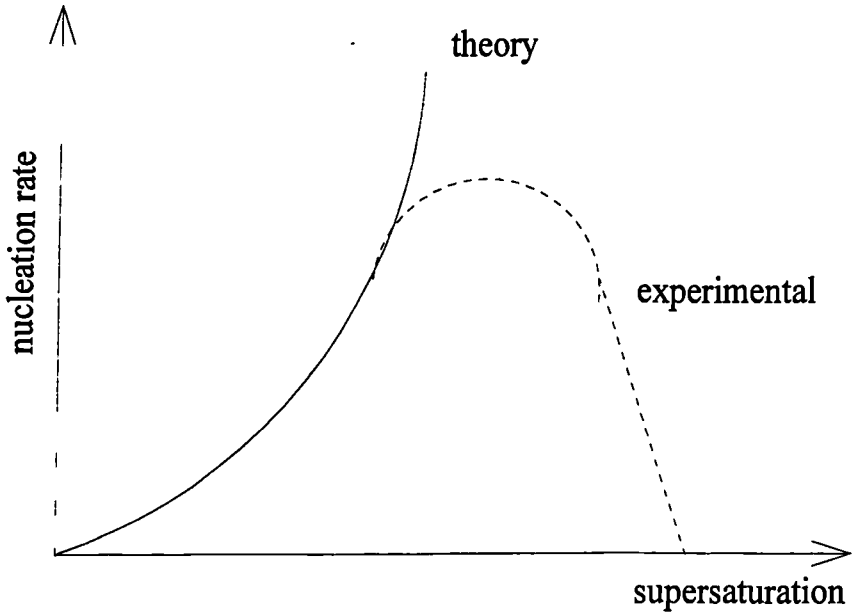

Figure 2.6. Effect of supersaturation on the nucleation rate [Mullin, 1993].

Work on organic melts [Tamman, 1925] demonstrated that the rate of nucleation initially follows an exponential curve as the undercooling is increased but reaches a maximum and subsequently decreases (broken curve). Tamman explained this behaviour by stating that the liquid became too viscous to nucleate, the molecular movement was restricted and therefore the formation of ordered crystal structures inhibited. A similar phenomenon was observed by Mullin and Leci (1969b) for the spontaneous nucleation of citric acid solutions.

The nucleation rate, J, is difficult to measure as the critical cluster may only have a few monomers in it. In practise, the induction time (τ), i.e. the time taken from the achievement of supersaturation to the appearance of the first crystals, is used. Assuming that the nucleation time is primarily due to the formation of the nucleus, then τ is considered inversely proportional to the rate of nucleation, J [Nancollas, 1964; Strickland-Constable, 1968; Saratovkin, 1959; Sohnel and Garside, 1991]:

$$\tau = 1/J \qquad (2.17)$$

Thus from equations (2.16) and (2.17) and taking the natural logarithm, the following equation is obtained:

$$\ln (1/\tau) = \ln (J) = \ln (A) - [-16\pi\gamma^3 V_m^2/3k^3][1/T^3(\ln S)^2] \qquad (2.18)$$

Using equation (2.18) the interfacial energy can be evaluated from measurements of the induction time as a function of supersaturation. The radius of the critical nucleus (the size of nucleus which has a maximum of Gibbs free energy) can be derived from equation (2.13), knowing the interfacial tension and supersaturation. These parameters provide useful base-line information with which to characterise the behaviour of any crystallisation system.

2.3.2.2 *Primary heterogeneous nucleation*

Homogeneous nucleation is difficult to observe in practise due to the presence of trace impurities, which affect the rate of nucleation. It is virtually impossible to achieve a solution completely free of foreign bodies. Generally, solutions may contain 10^6-10^8 solid particles per cm^3 [Mullin, 1993]. The foreign particles act to lower the interfacial energy necessary for cluster formation:

$$\Delta G = 4\pi r^2(\gamma-\gamma_s) + 4/3\pi r^3\Delta G_v \qquad (2.19)$$

where γ_s is the interfacial tension between the hetero-nuclei and any molecular nuclei present within the solution. Heterogeneous nucleation occurs at a lower supersaturation than homogeneous nucleation ($\gamma > \gamma_s$) and hence the induction time and degree of undercooling necessary for bulk crystallisation is lowered. This equation assumes that the hetero-nuclei appear homogeneously throughout the solution. It is difficult to model mathematically heterogeneous nucleation and, in practise, homogeneous nucleation theory is applied to provide a basic understanding of the heterogeneous nucleation process.

2.3.2.3 *Secondary nucleation*

Secondary nucleation differs from primary nucleation in that it is induced by crystals already present in the supersaturated solution. These crystals are able to act by lowering the supersaturation and interfacial tension thus encouraging easier nucleation within the metastable zone. These "parent" crystals have a catalysing effect on the nucleation process. These can form new nuclei by attrition, fracture or by crystalline dust being swept off of them. For these reasons secondary nucleation increases with increased agitation of the solution.

2.3.2.4 *Empirical relationship*

Although many attempts have been made to describe nucleation processes on a theoretical basis, none of these have resulted in a satisfactory quantitative model. One reason for this is the fact that the theory is hard to verify. This is due to the fact that experimental nucleation results are very sensitive to the technique used, the criteria used for judging when nucleation has occurred and the cleanliness of the samples.

An alternative method of modelling nucleation behaviour is the development of a series of empirical relationships. The mass nucleation rate, J_n, may be expressed by the following empirical expression [Mullin, 1993]:

$$J_n = K_n \Delta C_{max}^{\ m} \tag{2.20}$$

where k_n and m are the nucleation rate constant and nucleation reaction order, respectively. ΔC_{max} is the maximum allowable supersaturation.
The nucleation rate can also be expressed as:

$$J_n = (\varepsilon / [1 - c\,(\varepsilon - 1)]\,[(dC^*/dT)\,(dT/dt)] \tag{2.21}$$

Where T is the temperature, t is the time, dC*/dT is the rate of concentration change with temperature and ε is the ratio of molecular weights of hydrated salt to anhydrous salt. When no hydration occurs, the first term in equation (2.21) is equal to one. For a linear range of solubility the metastable limit, ΔC_{max}, may be written as a function of maximum allowable undercooling, ΔT_{max}, before bulk nucleation commences:

$$\Delta C_{max} = (dC^*/dT)\,\Delta T_{max} \tag{2.22}$$

At the metastable limit, a shower of nuclei produce sufficient surface area to prevent a significant further increase in supersaturation with respect to time, due to the cooling then:

$$d\Delta C/dt = 0, \text{ at } \Delta C_{max} \quad (2.23)$$

that is:

$$dC/dt = dC^*/dt \quad (2.24)$$

That is, at the metastable limit, the mass nucleation rate (or rate of change of concentration) is equal to the supersaturation rate due to cooling and hence:

$$J_n = dC/dt = dC^*/dt \quad (2.25)$$

Equation (2.25) can also be expressed in terms of the cooling rate, b (dT/dt):

$$J_n = dC/dt = dC^*/dt = dC^*/dT\ (dT/dt) \quad (2.26)$$

or alternatively:

$$J_n = b\ (dC^*/dT) \quad (2.27)$$

Equating equations (2.20) and (2.27) for J_n gives:

$$K_n \Delta C_{max}^{\ m} = b\ (dC^*/dT) \quad (2.28)$$

and substituting for the supersaturation in terms of equation (2.22) gives:

$$b\ (dC^*/dT) = k_n\ [(dC^*/dT)\ \Delta T_{max}]^m \quad (2.29)$$

Taking the logarithms of equation (2.29) gives:

$$\log b = (m-1) \log (dC^*/dT) + \log k_n + m \log \Delta T_{max} \quad (2.30)$$

Then, the dependence of the logarithm of the maximum undercooling, ΔT_{max}, on the logarithm of the cooling rate, b, should be linear and the slope is equal to the nucleation reaction order, m.

2.3.3 *Crystal growth*

Following nucleation, which involves the formation of stable nuclei via a 3-dimensional process, the next stage is the development of the nuclei in the growth process. The final single crystal is developed by a series of 2-dimensional events taking place on a number of structurally distinct crystal growth interfaces (Figure 2.7). Each of the faces grow in a semi independent manner, with the slowest growing ones dominating the crystal morphology. The fastest growing faces are either very small or grow out of the crystal. It is also possible that each face grows by different mechanisms.

The kinetic stages involved in the growth process are illustrated in Figure 2.8 and summarised below:

- bulk transport (a), which occurs when solvated monomers in the bulk solution are transported towards the growth interface;
- diffusion of the solvated monomers through the boundary layer towards the crystal/solution interface (b);
- surface nucleation/adsorption (c), where the monomers adsorb onto the crystal surface;
- interfacial diffusional processes (d-g). Here the adsorbed monomers find their optimum incorporation sites and undergo varying degrees of desolvation.

Crystal growth rates are affected by the growth conditions. There are three different growth mechanisms, which are dependent on the degree of supersaturation.

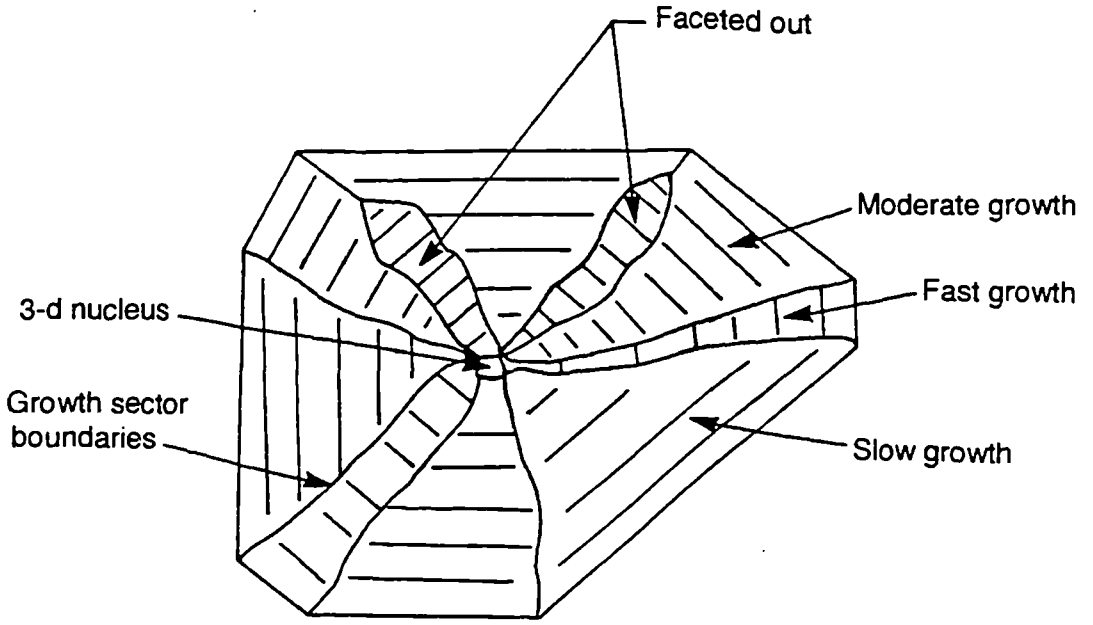

Figure 2.7. Schematic representation of a section cut through a particulate crystal, demonstrating that the 3-dimensional crystal is built from a co-operative series of 2-dimensional growth processes [after Clydesdale, Roberts et al, 1994c].

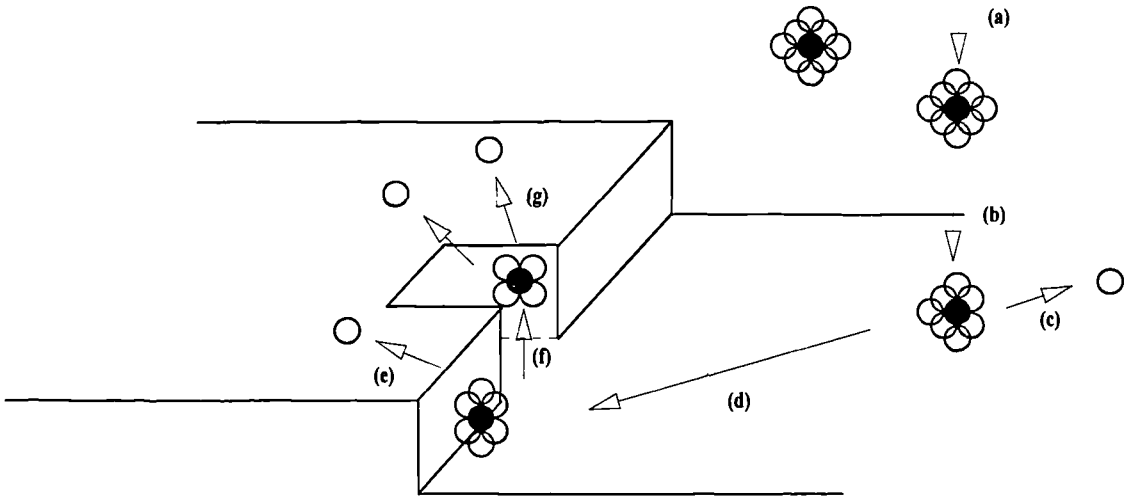

Figure 2.8. Summary of the steps involved at the interface of a growing crystal.

2.3.3.1 *Screw dislocation (BCF) mechanism*

This model, developed by Burton, Cabrera and Frank (1951), occurs at low supersaturation. It requires the presence of screw dislocations for the provision of a permanent source of surface steps and hence binding sites enabling growth to proceed (Figure 2.9(a)).

The 2-dimensional growth continues until the layer is complete. The surface growth rate R is proportional to the supersaturation (σ) squared.

$$R \alpha \sigma^2 \tag{2.31}$$

2.3.3.2 *Birth and spread (B & S) mechanism*

This mechanism occurs at a moderate supersaturation and involves 2-dimensional surface nucleation on a developing crystal [Gilmer and Jackson, 1974]. Then, the nucleus grows across a completed layer and the process repeats (Figure 2.9(b)). The presence of a nucleus is essential for the formation of each new growth layer. The growth rate is roughly proportional to the exponential of the supersaturation.

$$R \alpha \sigma^{5/6} \exp(\sigma) \tag{2.32}$$

2.3.3.3 *Rough interface growth (RIG) mechanism*

At high supersaturation the rough interface growth mechanism occurs and the crystal can grow without the presence of well defined surface layers at the interface [Jackson, 1958]. Due to the rough surface, the oncoming entities are provided with numerous binding positions (Figure 2.9(c)). This method of growth shows a linear dependence with supersaturation.

$$R \alpha \sigma \qquad (2.33)$$

Figure 2.10 shows the growth rate as a function of supersaturation. The unstable and stable regions are indicated. The dominating growth mechanism is also illustrated. The growth rate of the crystals changes from a linear to a parabolic growth law as the supersaturation decreases.

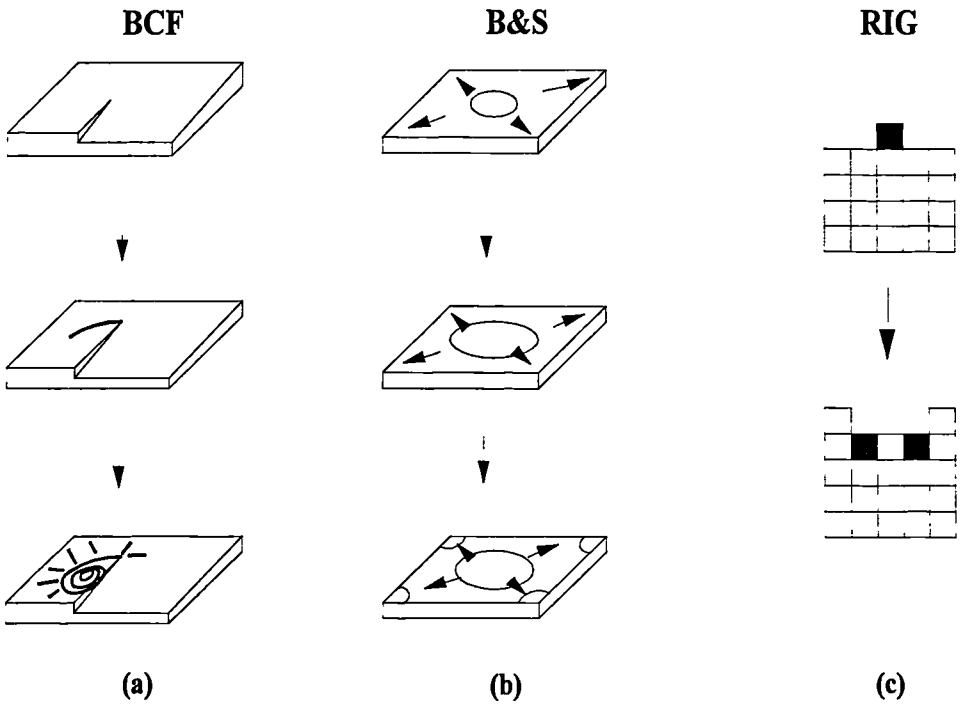

Figure 2.9. Schematic illustration of the three mechanism of crystal growth: (a) the screw dislocation mechanism; (b) the birth and spread mechanism; (c) the rough interface growth mechanism.

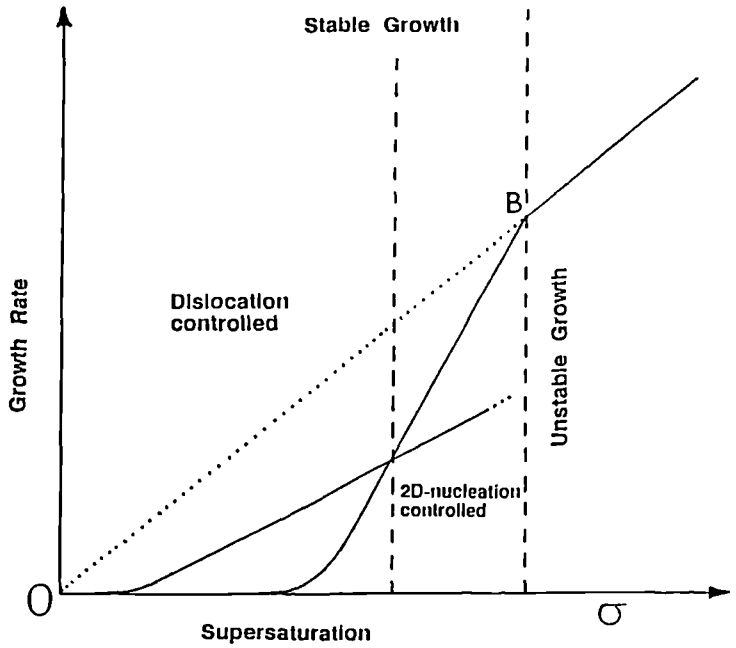

Figure 2.10. The relationship between growth rate and supersaturation, showing the change from BCF to B & S to RIG mechanisms as supersaturation increases [Docherty, 1989].

2.4 *X-ray diffraction*

X-ray diffraction is one of the key techniques used to examine the structural organisation at a molecular level, allowing quantitative molecular orientation parameters to be evaluated in addition to structural parameters such as chain conformation, chain packing, phase transition etc [Klug, 1974].

X-ray diffraction was first discovered by Laue in 1912. He suggested that, if crystals were composed of regularly spaced atoms, and if the wavelength of the X-rays was equal to the interatomic distance in the crystals, a diffraction pattern should result. Experiments were carried on a crystal of copper sulfate. An X-ray was passed through the crystal and a definite diffraction pattern was recorded using a photographic plate.

Bragg successfully analysed the Laue experiment and was able to express the necessary conditions for diffraction in a simple mathematical expression.

$$n\lambda = 2d\sin\theta \qquad (2.34)$$

where n is an integer which is zero for the zeroth order reflection, one for the first order reflection etc, θ is the angle between the atomic planes and the reflected beam and d is the spacing between the planes. The diffracted beams have to be in phase to obey Bragg's law.

The equation (2.34) defines all the values of θ where a reflection can occur for a crystal with spacing d and X-ray wavelength λ. At all other angles no reflected beam will occur because of destructive interference. With this equation, the lattice spacings can be calculated by measuring the angles under which diffraction occurs using a known wavelength of X-rays. From this, the size, shape and orientation of the unit cell can be obtained.

2.4.1 *The production of X-ray*

X-rays are high energy photons, which are produced when fast-moving electrons impinge on matter. The phenomena resulting from the deceleration of such electrons are very complex, and X-rays result from two types of interaction of the electrons with the atoms of the target material. A high-speed electron may strike and displace a tightly bound electron deep in the atom near the nucleus, thereby ionising the atom. When a certain inner shell of an atom has been ionised in this manner, an electron from an outer shell may fall into the vacant place, with the resulting emission of an X-ray characteristic of the atom involved. Such production of X-rays is a quantum process similar to the origin of optical spectra. The foundations of this theory were originally developed by Kossel (1914-1920), on the basis of the Bohr atomic theory [Bohr, 1913] and Moseley's celebrated measurements of X-ray spectra [Moseley, 1913 and 1914].

A high-speed electron may be slowed down by another process. Instead of colliding with an inner electron of an atom of the target material, it may simply be slowed down in passing through the strong electric field near the nucleus of an atom [Klug, 1974]. This is also a quantum process, the decrease in energy ΔE of the electron appearing as an X-ray photon of frequency ν as given by Einstein's equation:

$$h\nu = \Delta E \qquad (2.35)$$

in which h is Planck's constant. X-radiation produced in this manner is independent of the nature of the atoms being bombarded, and appears as a band of continuously varying wavelength whose lower limit is a function of the maximum energy of the bombarding electrons.

X-rays can be produced in three different ways:

- by the use of X-ray tubes;
- from radioactive material which has the disadvantage of producing much lower intensity X-rays;
- from synchrotron radiation sources.

Only the latter will be briefly discussed here as it was the only method used for this work.

2.4.2 *Synchrotron radiation source*

Synchrotron radiation is a powerful X-ray tool for detailed study of fast phase transition processes [Laggner, 1988; Caffrey, 1989]. Synchrotron radiation provides X-rays with a beam divergence which is extremely low, thus enabling high-resolution diffraction data to be collected for use in structure determination. In addition, the intensity of synchrotron radiation is far superior compared with laboratory sources and thus permits data acquisition times of less than 1s compared with many hours in the laboratory. This, together with the high penetrating power of Synchrotron radiation, enables X-ray diffraction measurements to be carried out *in-situ* thus enabling the dynamics of crystallisation processes from the liquid phase to be followed on a structural basis.

The first synchrotron radiation was observed in 1946 from a 70 meV synchrotron at General Electric in Schenactady [Elder et al, 1947]. Synchrotron

radiation is produced when charged particles, and in particular electrons and positrons, are accelerated to relativistic velocity. Magnetic fields of several kilogauss, applied normal to the particle trajectory, produce transverse acceleration which results in large amounts of radiation being emitted. The theory of synchrotron radiation was first developed by Schwinger (1946).

The two synchroton sources to be used for this thesis were the Synchrotron Radiation Source (SRS) at Daresbury Laboratory and the National Synchrotron Light Source (NSLS) at Brookhaven National Laboratory (USA). The former was the world's first ever high energy electron accelerator dedicated to the production and utilisation of synchrotron radiation (Figure 2.11(a)). The X-ray and Vacuum Ultra-Violet (VUV) rings of the NSLS are shown in Figure 2.11(b).

In a typical synchrotron storage ring [Gerson, 1992] electrons or positrons are first accelerated to ~60 MeV in a linear accelerator, then injected into a booster synchrotron in which the energy is increased to 600 MeV by acceleration in the circular orbit. Subsequently, the electrons are injected into the main storage area. The storage ring consists of straight sections linked by curved portions around which the bending magnets are situated. These further increase the speed of the particles to relativistic energies (2-8 GeV). The current decays over a period of several hours due to the collisions of the particles with residual gas molecules and the walls of the ring. Useable radiation is produced as the electrons pass through the bending magnets in the form of a continuum. This radiation has intensity 6-7 orders of magnitude greater than that produced by conventional X-ray sources. It is emitted in the forward direction, tangential to the particle beam and is extracted for use through beam ports into beam lines fully evacuated to the ring vacuum. The synchrotron radiation beam can be maintained for several hours without refill of electrons, even if a progressive fall of intensity with time is noted.

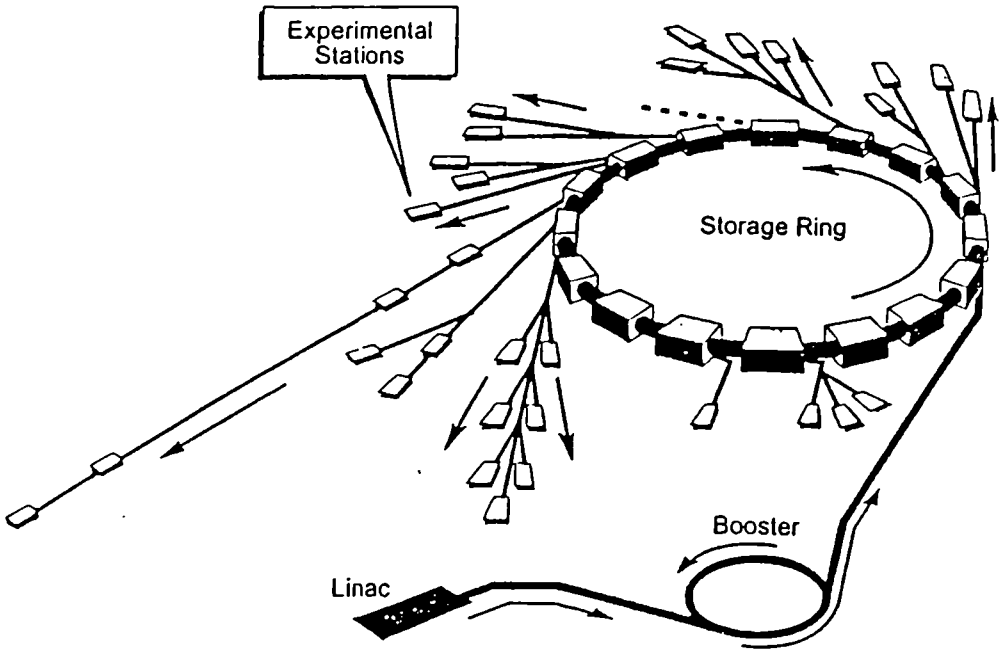

(a)

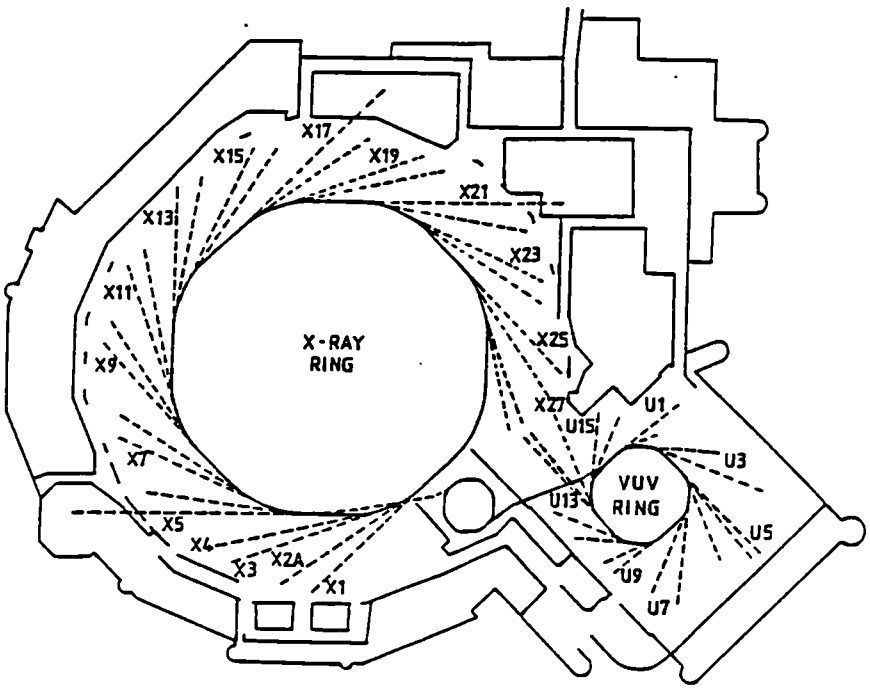

(b)

Figure 2.11 Diagrams of the synchrotron radiation source at Daresbury laboratory, Warrington (a) and at the National Synchrotron Light Source (b).

2.4.2.1 *The advantages of synchrotron radiation*

Synchrotron radiation offers a number of advantages over conventional radiation source and these include:

- a high intensity, which permits data acquisition times of less than 1s compared with many hours in the laboratory. The photon flux is 10^2-10^4 times higher than that from a conventional source;
- low beam divergence (0.1mrad) which provides the high resolution needed for the characterisation of polymorphic systems where the structural changes involved can be subtle;
- a highly polarised beam;
- high photon energy (50-100keV) which allows easy penetration of the growth environment enabling *in-situ* studies to be undertaken;
- a tuneable wavelength.

The beamline stations used at Synchrotron Radiation Source (SRS) at Daresbury Laboratory and at the National Synchrotron Light Source (NSLS) at Brookhaven National Laboratory (USA) will be described in the chapters 5, 6 and 7.

2.5 *Rheology*

Rheology is defined as the science of deformation and flow of matter [British Standard Glossary, 1975]. Deformation pertains to matter which is solid, and flow to matter which is liquid. In the simplest case, the rheological property of interest in solids is elasticity, and in liquids it is viscosity [Barnes, 1989]. Foods, in general, cannot be characterised in so clear cut a manner as solids and liquids. They are neither completely viscous nor completely elastic but are viscoelastic [Borwankar, 1992].

2.5.1 *Historical perspective*

Robert Hooke developed in 1678 his "*True Theory of Elasticity*", regarding the behaviour of an ideal solid and suggested that the power of any spring is in the same proportion with the tension thereof. In 1687, Isaac Newton gave attention to liquids. In "*Principia*" he assumed that the resistance which arises from the lack of slipperiness of the parts of the liquid is proportional to the velocity with which the parts of the liquid are separated from one another. This lack of slipperiness is now called viscosity and is a measure of resistance to flow. In the nineteenth century, Navier and Stokes developed a consistent three-dimensional theory for a Newtonian viscous liquid.

The sample under study is confined between parallel planes of area A (Figure 2.12), separated by a distance d which is small compared to the linear dimensions of the planes [Barnes, 1989].

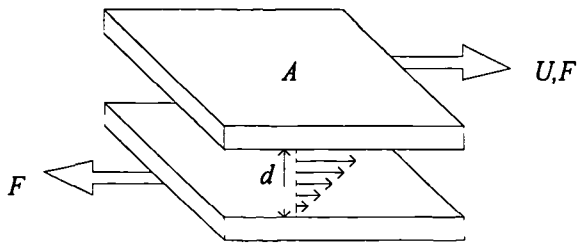

Figure 2.12. Schematic of two parallel planes, each of area A, filled in the space d with shearing liquid.

The upper plane moves with relative velocity U and the length of the arrows between the planes are proportional to the local velocity (v) in the liquid. While the lower plane is held stationary, the test material experiences a "resistance to flow". The force per unit area required to produce the motion is F/A and is denoted by σ (shear stress). σ is related to the "velocity gradient" U/d, otherwise known as the shear rate (γ), through Newton's equation:

$$\sigma = \eta U / d \tag{2.36}$$

$$\sigma = \eta \dot{\gamma} \tag{2.37}$$

where η is the shear viscosity.

For Newtonian liquids, η is called the coefficient of viscosity; for most liquid, η is not a coefficient, but a function of the shear rate γ. The Newton's law is a linear law, which assumes direct proportionality between stress and strain. Newtonian behaviour in experiments conducted at constant temperature and pressure has the following characteristics:

- the only stress generated in simple shear flow is the shear stress σ, the two normal stress differences being zero;
- the shear viscosity does not vary with shear rate;
- the viscosity is constant with respect to the time of shearing and the stress in the liquids falls to zero immediately the shearing is stopped;
- the viscosities measured in different types of deformation are always in simple proportion to one another.

This law is very restrictive. The range of stress over which materials behave linearly is invariably limited, and the limit can be quite low. In other words, material properties such as rigidity modulus and viscosity can change with the applied stress and the stress needs to be low. The change can occur either instantaneously or over a long period of time, and it can appear as either an increase or a decrease of the material parameter. A liquid showing any deviation from the above behaviour is non-Newtonian.

There are two different types of flow behaviour represented by the term non-Newtonian:

- the progressive decrease in the shear viscosity with increase in shear rate is called shear thinning;

- the progressive increase in the shear viscosity with increase in shear rate is known as shear thickening.

Schematic representation of different flow behaviours is shown in Figure 2.13.

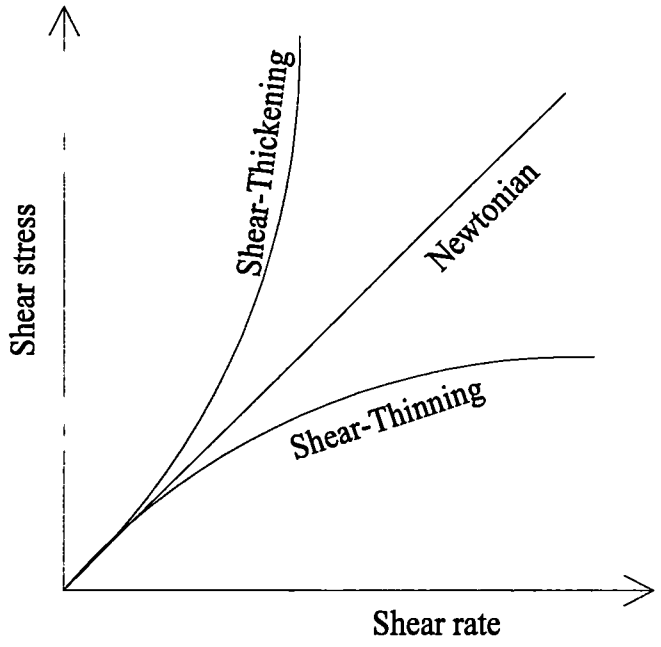

Figure 2.13. Schematic representation of different flow behaviours.

Accuracy of measurement is an importance issue in viscometry. It is possible to calibrate an instrument in terms of speed, geometry and sensitivity, by using standardised Newtonian liquids (usually oils) of known viscosity.

Many types of viscometers rely on rotational motion to achieve a simple shearing flow. For such instruments, the means of inducing the flow are two fold: one can either apply a known shear rate and measure the shear stress or apply a known shear stress and measure the subsequent shear rate.

There are several different rotational viscometers e.g.

- the concentric cylinder viscometer;

- the cone and plate viscometer;
- the parallel plate viscometer;

and a number of other types e.g.

- capillary viscometer;
- slit viscometer.

Concentric cylinder and cone and plate viscometers, used for the study of crystallisation behaviour of fats as a function of different shear rates will be described in chapter 6 and 7, respectively.

2.6 *Conclusion*

This chapter has briefly reviewed the theories which are the basis to an understanding of much of the experimental studies described in the following chapters. The theories reviewed include:

- crystal systems;
- crystallisation;
- X-ray diffraction;
- rheology.

2.7 *References*

Barnes, A H, Hutton, J F and Walters, K., in *An introduction to rheology*, Elsevier, Amsterdam, 1989.

Becker, K and Döring, W, *Annalen der Physik*, 1935, 5, 24, 719-752.

Bohr, N, *Phil. Mag.*, 1913, 26, 6, 1-25.

Borwankar, R P, *J. Food Engineering*, 1992, 16, 1, 55-74.

Bravais, A, *Etudes Crystallographiques*, Gauthie-Villars, Paris, 1866.

British Standard Glossary of Rheological Terms, BS 5168: 1975, British Standard Institution, 1975.

Burton, W K, Cabrera, N and Frank, F C, *Philosophical transactions A243*, 1951, 299-358.

Caffrey, M, *Top. Curr. Chem.*, 1989, 151, 75-109.

Docherty, R, PhD. thesis "*Modelling the Morphology of Molecular Crystals*", University of Strathclyde, 1989.

Clydesdale, G, Roberts, K J and Docherty, R, in Controlled Particle, Droplet and Bubble Formation, ed Wedlock, D J, Butterworth-Heinemann Ltd, 1994c, chapt. 4, p95.

Elder, F R, Grewitsch, A H, Langmuir, R V and Pollock, H C, *Phys. Rev.*, 1947, 71, 829-830.

Garside, J and Larson, M A, *J. Crystal Growth*, 1986, 76, 88-92.

Gerson, A R, Halfpenny, P J, Pizzini, S, Ristic, R, Roberts, K J, Sheen, D B and Sherwood, J N, in *Materials Science and Technology a Comprehensive Treatment*, Vol 2A, Chapter 8, 1992.

Gibbs, J, in *Collected works*, Longmann Green, New York, 1928.

Gilmer, G H and Jackon, K A, in *Crystal Growth and Materials*, ed. by Kaldis, E and Scheel, H. J., North Holland, Amsterdam, 1974, 80-114.

Klug, H P and Alexander, L E, in *X-Ray Diffraction Procedures*, A Wiley-Interscience

Publication, JohnWiley & Sons, New York-London, 1974.

Kossel, W, *Verh. deut. phys. Ges.*, 1914, 14, 953-963.

Kossel, W, *Verh. deut. phys. Ges.*, 1916, 18, 339 and 396.

Kossel, W, *Phys. Z.*, 1917, 18, 240-241.

Kossel, W, *Phys. Z.*, 1920, 1, 119.

Kossel, W, *Phys. Z.*, 1920, 2, 470.

Jackson, K A, in *Liquid Metals and Solidification*, American Society of metals, Cleveland, 1958.

Laggner, P, *Top. Curr. Chem.*, 1988, 145, 173-202.

Miers, H A and Isaac, F, *J. Chem. Soc.*, 1906, 89, 413.

Miers, H A and Isaac, F, *Proceedings of the Royal Society*, 1907, A79, 322-351.

Moseley, H G J, *Phil. Mag.*, 1913, 26, 6, 1024-1034.

Moseley, H G J, *Phil. Mag.*, 1914, 27, 703-713.

Myerson, A S and Ginde, R, in *Handbook on Industrial Crysallisation*, ed. by Myerson, A S, Butterworth-heinemann, 1993.

Mullin, J W and Leci, C L, *J. Cryst. Growth*, 1969b, 5, 75-76.

Mullin, J W, *The Chemical Engineer*, 1973, 274, 316-317.

Mullin, J W, in *Crystallisation*, 3ed Butterworth-Heinemann, London, 1993.

Nancollas, G H and Pudrie, N, *Q. Rev. Chem. Soc.*, 1964, 18, 1-20.

Ostwald, W, *Zietschrift für Physikalische Chemie*, 1897, 22, 289-330.

Saratovkin, D D, *Dentrictic Crystallisation*, Consultants Bureau, New York, 1959.

Schwinger, *Phys. Rev.*, 1946, 70, 798.

Sohnel, O, Garside, J, in *Precipitation: Basic Principles and Industrial Applications*, Butterworth-Heinemann, 1991.

Strickland-Constable, R F, in *Kinetics and Mechanisms of Crystallisation*, Academic Press, London, 1968.

Tamman, G, in *States of Aggregation* (Translated by Mehl, R.F.), Van Nostrand, New York, 1925.

Volmer, M, in *Kinetic der Phasenbildung*, Steinkoff, Dresden, Germany, 1939.

Walton, A G, in *Nucleation*, ed. by Zettlemoyer, A C, Marcel Dekker Inc., New York, 1969, 225-307.

Chapter 3

Processing of cocoa butter fat: a structural perspective

3.1 *Introduction*

Most of the chemical and physical properties of chocolate are related directly to the nature of the cocoa butter. The properties of cocoa butter have drawn the attention of many investigators, owing to the significance they assume in the confectionery production and storage.

Cocoa butter, which amounts to 25-36% in finished dark chocolate, is responsible for the smooth texture, contraction, flavour release, and gloss of the product. Cocoa butter is a yellow fat that shows brittleness below 20°C, begins softening at 30 to 32°C, and exhibits a sharp melting point just below human body temperature. This sharp melting point is responsible for the distinctive cool chocolate texture in the mouth.

3.2 *Cocoa butter*

Cocoa butter is a mixture of triglycerides and trace compounds [Davis, 1989]. It is important to firstly consider the structure of triglycerides before describe the composition of cocoa butter.

3.2.1 *Structure of triglycerides*

The nature of the triglycerides and their thermal history are the key factors controlling the type of crystal formed. Triglycerides are formed when three fatty acids react with glycerol. The fatty acids are long chain compounds with 4 to 20 or more carbons atoms in the chain. The chain may be fully saturated as in palmitic ($C_{16:0}$) and stearic ($C_{18:0}$) acids, or contain one or more double bonds and be called unsaturated as in oleic acid ($C_{18:1}$) or polyunsaturated as in linoleic acid ($C_{18:2}$). When the double bonds are present, the configuration across the double bond gives rise to two possible *isomers*, e.g. both oleic and elaidic acids have the C_{18} chain with one double bond; in

the oleic acid it is in the *cis* form, while elaidic is in the *trans* form. In the *cis* form both ends of the chain are on the same side of the double bond, while in the *trans* form the chains project on opposite sides of the double bond. The *cis* form gives rise to a sharp kink and overall curve in the chain, whereas the *trans* produces a straight chain [Jewell, 1988]. Whether the fatty acids are *cis* or *trans* has a marked influence on the crystallisation of the fats.

3.2 *Cocoa butter composition*

Cocoa butter is principally made up of three major triglycerides of C50-C54 aggregate carbons: POP (~ 20%), POS (~ 40%) and SOS (~ 25%) (O = oleic acid, P = palmitic acid, S = stearic acid) , with minor amounts of triglycerides containing linoleic and arachidonic acid. The unsaturated (O) acid favours the R_2 site (Figure 3.1). The minor components also include [Chaisery, 1987; Davis, 1989]: free fatty acid (~1%), glycolipids (0.89%), phospholipids (0.4%), monoglycerides (0.14%), diglycerides (0.3-0.7%), sterols (0.2%), tocopherols (0.02%), pyrazines, thiazoles, oxazoles, pyradines. In a more recent paper [Savage, 1995] phospholipid concentrations of 0.8-0.9% are reported.

Cocoa butter is a relatively simple fat when compared with other fats of multiple fatty acid composition, where there can be hundreds or more different triglyceride types [Minifie, 1980]. In Figure 3.2 the narrow distribution of cocoa butter is compared with other fats, which show broad distribution. This, in part, explains the solids-state properties of the material which is brittle at room temperature but melts sharply at a temperature just below human body temperature. The cocoa butter is one of the most stable fats known and its natural antioxidant content allows it to be stored for up to five years without noticeable rancidity.

Although cocoa butter is one of the most saturated natural edible fats, its fatty acyl composition can vary significantly. Typical ranges are shown in Table 3.1. The major components, palmitate, stearate and oleate, are each subject to around a 7% variation in their relative amounts.

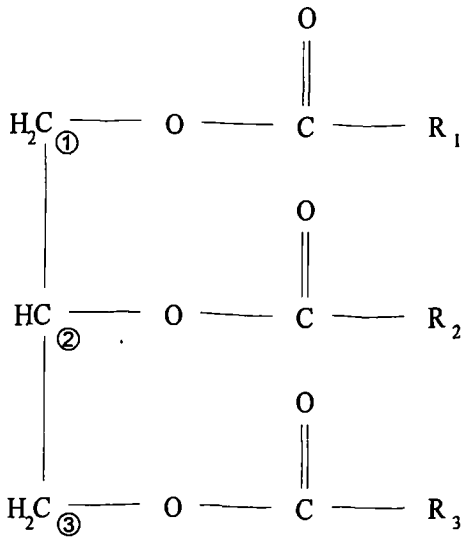

POP	R_1, R_3 = PALMITATE	R_2 = OLEATE	
SOS	R_1, R_3 = STEARATE	R_2 = OLEATE	
POS	R_1 = PALMITATE	R_2 = OLEATE	R_3 = STEARATE

Figure 3.1 Major molecular species of triglycerides in cocoa butter. In order to designate the stereochemistry of asymmetrical triglycerides (i.e. POS), the carbon atoms of glycerol are stereospecifically numbered 1, 2 and 3 from top to bottom. A prefix "sn" (stereospecific numbering) is used to differentiate such numbering from conventional numbering conveying no steric information [Breckenridge, 1978].

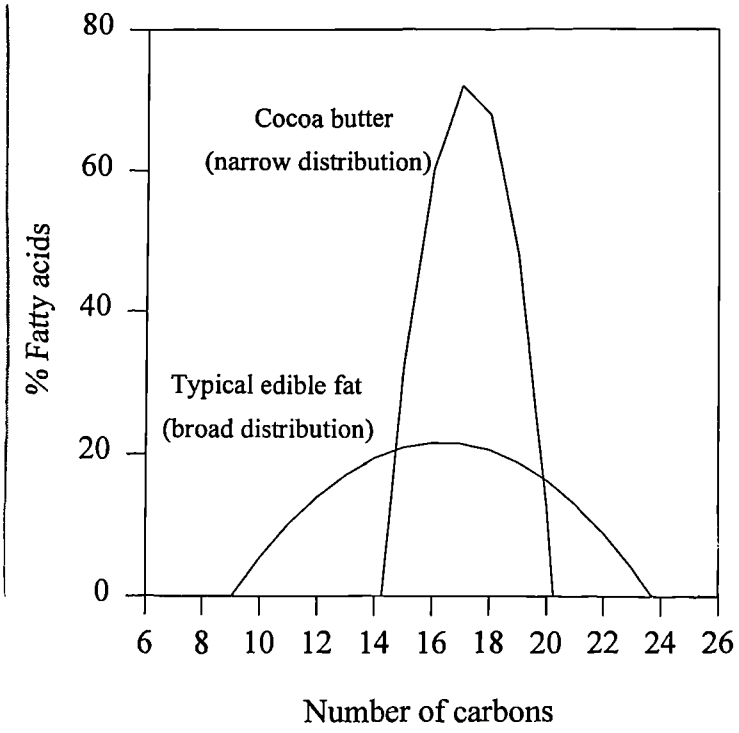

Figure 3.2. Schematic representation of typical fatty acid compositions.

Fatty acid	Range (mol%)
Palmitic	24-31
Stearic	30-37
Oleic	33-39
Linoleic	2-5
Others	2-3

Table 3.1. Variation in the fatty acid composition of different cocoa butters.

In addition, the contribution of linoleate can rise from 2% to about 5%. A major cause of the variability in acyl composition is the environmental temperature during growth of the cocoa tree.

3.2.1 *Characteristics of cocoa butter from different geographic regions*

The climatic variations of cocoa growing areas cause differences in physical and chemical characteristics of cocoa butters. Cocoa butter obtained from fruits grown at low temperature is soft and contains high diunsaturated triacylglycerols [Lehrian, 1980] and high unsaturated fatty acids, i.e. oleic and linoleic acid [Berbert, 1976]. Rainfall causes high concentrations of stearic acid, oleic acid, C56 triacylglycerol and free fatty acid [Chin, 1984]. Sunlight increases the palmitic acid content [Chin, 1984] and the iodine value (= degree of unsaturation) of cocoa butter. Double bonds in the fatty acids in the sn-3 position of diunsaturated triacylglycerols cause extra kinking in the structures that interrupt molecular packing of monounsaturated triacylglycerols, the major components [Jewell, 1981].

Triacylglycerol compositions of cocoa butters from different countries are listed in Table 3.2 [Chaiseri, 1989]. The range for the major triglycerides POP, POS, and SOS, were 17.5 - 22.6%, 35.8 - 41.4%, and 22.8 - 31.3%, respectively. The amounts of POO, SOO, and SLiS vary among the samples from different countries,

whereas PLiP, PLiS, and SOA were constant (Li = linoleic and A = arachidic). The soft cocoa butters which contain high concentrations of POO and SOO (>8%) are from South America; the hardest are from Asia and Oceania. It should be noted that cocoa butters which are low in POO and SOO are concomitantly high in POS and SOS, especially cocoa butters from Malaysia and the Solomon Islands.

The triglycerides, which constitute the cocoa butter, are categorised into high, middle, and low melting point ranges depending upon the degree of fatty acid saturation and unsaturation [Davis, 1989]. The high melting range triglycerides (43°C; 113°F) are saturated with primarily palmitic and stearic acids. The middle melting range group (35.7°C; 96.2°F) is mainly a mixture of POP, POS and SOS. The last group which is the low melting range fraction (0°C; 32°F) contains POO, OOO, SOO. Then, the variation in composition can cause subtle differences in melting properties of cocoa butter, which may be of importance to the end-users.

An understanding of the relationship between the chemical and physical properties of the fats is imperative for the selection of cocoa butter which will successfully temper and solidify upon cooling [Manning, 1984]. There is a limited amount of crystal structure data available. This is due to difficulties in crystallising good quality single crystals of these materials and to the natural polydispersivity and hence the disordered nature of mixed fat systems.

One of the major problems involved in the manufacture of chocolate, is to achieve the required level of snap, gloss, colour and freedom from bloom that the consumer has come to expect in a quality product. It is necessary to pay careful attention to the tempering, cooling and subsequent storage of the product. The reason it is necessary to control carefully all manufacturing process is that the fat components of chocolate exhibits polymorphism, and hence processing must be undertaken in order to ensure the formation of the correct polymorphic form.

Country	PLiP	POO	PLiS	POP	SOO	SliS	POS	SOS	SOA
Bolivia	1.1	3.3	3.5	22.6	4.0	2.1	40.4	22.8	0.5
Brazil	0.9	3.9	3.7	17.9	6.7	3.2	37.1	26.0	0.04
Colombia	1.1	3.3	3.6	20.4	4.4	2.3	39.4	25.0	0.6
Ecuador	1.2	3.0	3.2	19.2	5.4	2.3	38.4	26.9	0.4
Peru	1.5	4.3	3.9	18.3	7.4	3.7	35.8	24.6	0.4
Venezuela	0.9	1.0	3.1	20.4	2.8	1.9	40.4	28.8	0.8
Costa Rica	1.0	2.6	3.5	17.8	5.5	3.0	38.7	27.4	0.4
Guatemala	1.0	2.3	3.4	19.3	4.9	2.2	39.0	27.5	0.4
Mexico	1.1	2.4	3.5	19.1	4.1	3.0	38.8	27.8	0.6
Cameroon	1.0	3.0	3.4	17.9	5.8	2.5	38.3	27.7	0.5
Ghana	1.2	2.2	3.4	17.8	4.9	2.2	39.0	27.5	0.4
Ivory Coast	1.0	1.9	3.0	19.0	3.9	2.5	39.6	28.5	0.6
Indonesia	1.1	1.6	3.0	19.9	3.6	1.7	40.6	28.1	0.5
Malaysia	0.7	1.2	2.8	18.4	2.9	2.2	40.0	31.1	0.8

A = arachidic acid, Li = linoleic acid, O = oleic acid, P = palmitic acid, S = stearic acid

Table 3.2. Triacylglycerol compositions (%)of Cocoa Butter from different origin countries [Chaiseri, 1989]

3.3 *General introduction to polymorphism*

Triglycerides characteristically exist in more than one crystalline form and hence exhibit polymorphism. Timms (1984), Hagemann (1988), Hernqvist (1990) and, more recently, Sato (1996) reviewed studies reported in the last years concerning the polymorphism of triglycerides in pure and mixed systems.

In order to understand the mechanism of fat crystallisation it is first necessary to comprehend how triglycerides crystallise at the molecular level. The phenomenon of triglyceride polymorphism has been known for over 100 years [Duffy, 1852]. Duffy discovered three modifications of tristearin, tripalmitin and other triglycerides, showing different melting points. Throughout recent history numerous scientists have conducted research to demonstrate that the basis for multiple melting points in triglycerides was polymorphism [Clarkson, 1934; Lutton, 1945]. Nearly all fats exhibit polymorphism in a monotropic manner, in that transformations take place from less stable (lower melting forms) to more stable (higher melting forms). Fatty acids and glycerides have been observed in at least two crystalline forms and some may have as many as three or four forms [Bailey, 1950].

When a polymorphic transition occurs, due to a temperature change, the molecular packing of the triglycerides shift to confer greater stability to the crystal. The primary technique employed to determine the molecular packing of triglycerides in a crystalline structure has been X-ray analysis. Clarkson and Malkin (1934) were the first to clearly demonstrate triglyceride polymorphism with X-ray analysis. Much later, Malkin and his associates [Malkin, 1954] also established that, for a given compound, different crystalline forms are distinguishable by their X-ray diffraction pattern. Unfortunately, a great deal of confusion and controversy arose from the early work, since different authors used the same form of nomenclature (α, β' and β), but assigned them to the various crystalline forms on the basis of different criteria. Thus the British school, led primarly by Malkin (1954), assigned them in terms of increasing melting point (the form with the highest melting point was designated β), while the Americans, led primarly by Lutton (1950) used X-ray diffraction data as their basis. The nomenclature developed in two schools was not always strictly

comparable. The confusion continued until Chapman (1962) demonstrated that infrared absorption spectroscopy could be used to study polymorphic forms and use of this technique did allow the controversy to be resolved. Larsson (1966) then suggested a nomenclature based on both X-ray and infrared data, and this is the most accepted terminology to define the different polymorphic forms of triglycerides.

3.3.1 *Crystallisation modes of triglycerides*

The shape of the triglyceride molecule is very important. From X-ray diffraction studies on single crystals it was established that the molecule has a characteristic shape which is usually described as either chair- or tuning fork-shaped and that it is always the 2-position which projects away from the other 2 [Lutton, 1948].

Two associated triglyceride molecules (dimers) form the building blocks in the elementary cells of the crystalline structure of fats. The molecules in the association are antiparallel. For most saturated monoacid triglycerides the structure formed will be the double-chain-length structure (Figure 3.3A) [Lutton, 1948]. Larsson (1964) has altered the conventional tuning fork structure of Figure 3.3A to the modified tuning fork of Figure 3.3B. Data obtained from the β crystal of trilaurin support a modification of the conventional tuning fork structure.

When fats crystallise, the individual triglyceride molecules become associated to form linear arrays of bilayers as depicted in Figure 3.4. The simplest form of packing is that in which the fatty acid chains pack parallel with each other and perpendicular with respect to the plane of the glycerol groups. The chains are thus oriented laterally in a hexagonal array (as a bundle of pipes when viewed end on). Because of the random rotational distribution of the hydrogen atoms, the centres of the chains are separated equidistantly. Using the generally accepted values for interatomic distances and angles, the spacing of this molecular orientation has been calculated to be 4.15Å in all three lateral directions. Structures with this lattice type are designated α and the principal X-ray line is at 4.15Å; this is a so-called *short spacing*.

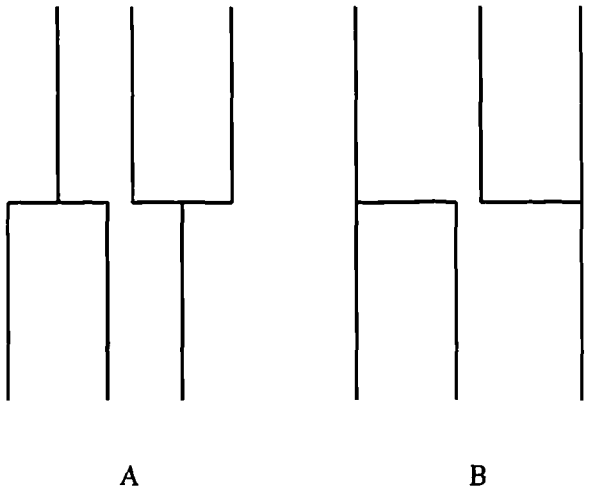

Figure 3.3. Illustration of the arrangement of monoacid saturated triglycerides upon solidification: A) conventional double chain length structure, B) modified double chain length structure.

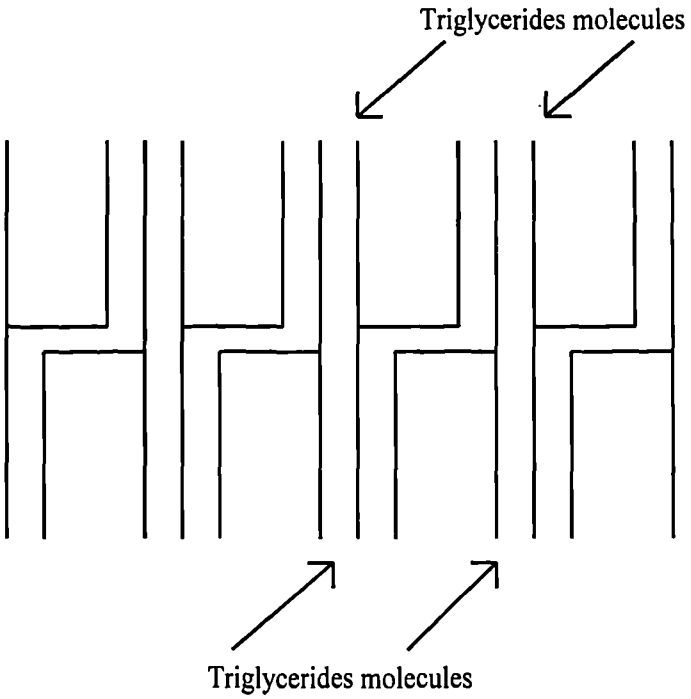

Figure 3.4. Schematic diagram of the bilayer packing in triglycerides.

The *short spacings* describe the cross-sectional arrangement of the fatty acids in the triglycerides [Chapman, 1962]. Additionally, the overall length of the triglyceride will be dependent upon the length of the individual fatty acid chains. This influences the dimension of the bilayer discussed above, and gives rise to a further characteristic dimension which can be deduced from the X-ray data called *long spacing* (Figure 3.5). This represents the distance between the planes formed by the terminal methyl groups of the fatty acids. Typical values are between 30 and 60Å. The α form is the simplest crystal form and has the lowest density. The β' type has a more densely packed crystal structure, and this is achieved by the fatty acid chains being tilted relative to the glycerol chain, at an angle of about 70°. The axes of the molecules are spaced at 3.80Å in two directions and at 4.20Å in the third direction. The long spacings are similar to the α form but slightly shorter due to tilt of the chain axis.
In the third and final crystal type, designated β, the angle of tilt relative to the glycerol chain is even greater, being of the order of 60° [Chaiseri, 1987]. In this polymorph the molecules are spaced at 4.58, 3.85 and 3.65 Å and these are the observed principal short spacings.

The alignment which gives rise to the long spacings can produce two types of structure. Firstly, a form where the long spacings are similar to both the α and β' type, but slightly shorter due to increased angle of tilt. This type of structure can be described as *double packing* as the long spacing is related to the sum of the length of the fatty acids on chains 1 and 2 (Figure 3.5).

In the second type of packing, the length of the bilayer is increased by the fatty acids at the 2-position being aligned preferentially adjacent to each other (Figure 3.6). This packing can be described as a *triple packing*, and results in an increase in the long spacing value of the order of 50% compared with the β' and β double forms (double packing has typical values of about 40 Å while β triple is about 60 Å).

The majority of the natural vegetable fats which contain an unsaturated fatty acid have the cis configuration as in oleic acid ($C_{18:1}$). Also, in nearly all these fats the oleic acid is found in the 2-position. This enables a very precise form of molecular packing which for a 2-oleo triglyceride in the β form is illustrated in Figure 3.7.

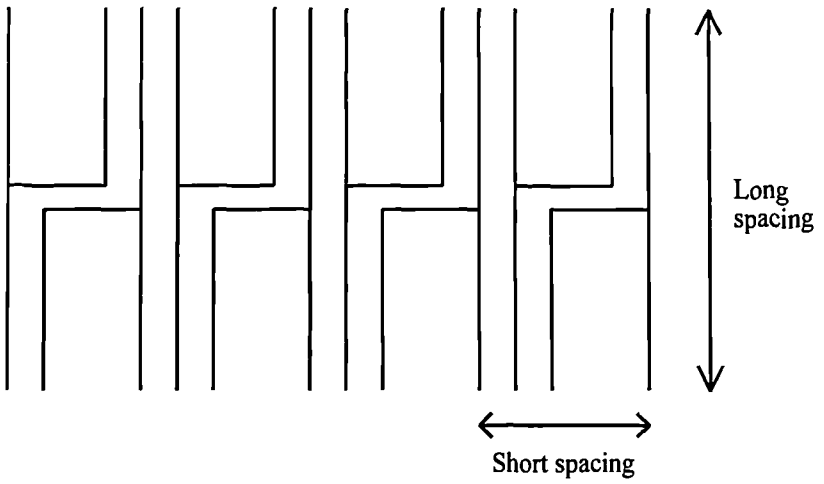

Figure 3.5. Schematic diagram showing the relationship of short and long spacings in α triglycerides.

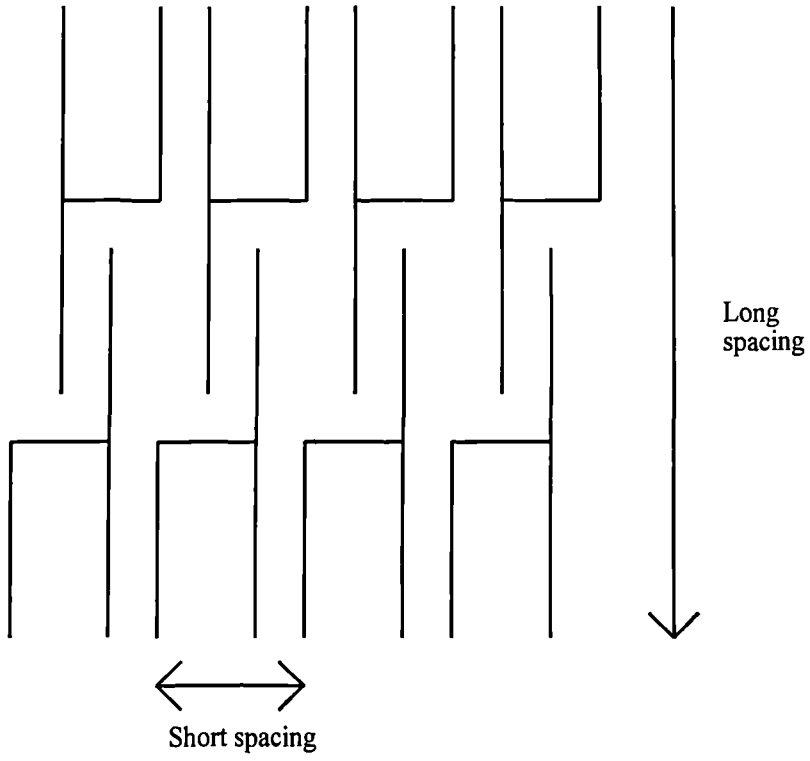

Figure 3.6. Diagrammatic representation of the triple packing in triglycerides.

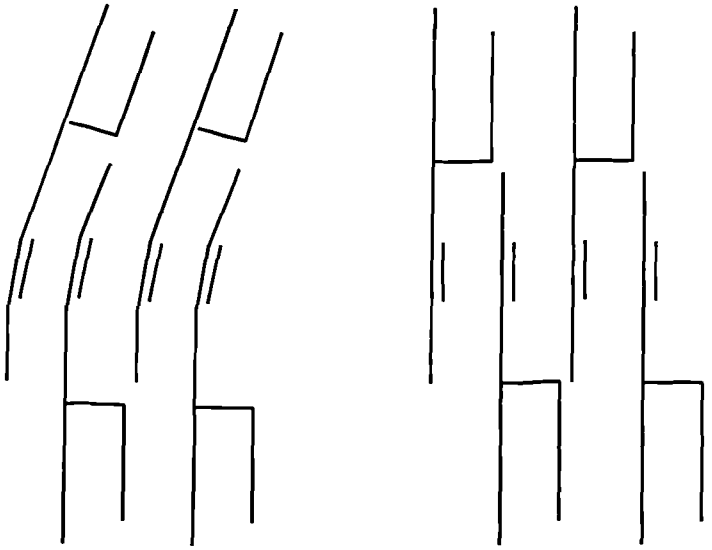

Figure 3.7. Schematic diagram showing the structure of *cis* and *trans* β packing: a) *cis* 2-oleo glyceride; b) *trans* 2-elaido glyceride.

If in some triglycerides the 2-position contains a C_{18} acid of *trans* configuration (e.g. elaidic acid) it is clear that a uniform packing between *cis* and *trans* type is virtually impossible, and extensive crystallisation will be prohibited. This effect is most pronounced with the β crystal and is of less significance with the α type.

In the crystal, the bilayers stack upon themselves and join end-to-end to produce a layered structure. The α crystals, which are the simplest, grow most quickly. The β' type which contains tilted chains needs to grow a little more slowly to achieve the precise packing. However, in the β form, which requires even greater tilt and chain extension, the growth rates will result in differently shaped crystals. This effect has been demonstrated by Hoerr (1960) using polarised light microscopy, and Jewell (1974) using electron microscopy.

The type of fatty acid present in the triglycerides is one of the major factors that controls the ease with which the polymorphic transition can occur. Hernqvist (1988) has studied the mechanism of β'→β transition. He discovered that simple

triglycerides with odd carbon number fatty acids are β' stable, while triglycerides with even carbon number fatty acids are β stable. It is a consequence of the arrangement of the fatty acids around the glyceryl group that the ends of the bilayers are not perfectly planar, but terraced. The height difference between adjacent chains is directly related to the length of the constituent fatty acid (see Figure 3.8).

It has been shown by Larsson (1972) that bilayers with pronounced step heights (more correctly termed methyl terraces) do not build properly to produce crystals. This is not a stable conformation since the contour surface of the terrace allows certain end groups (methyl groups) to become too closely associated.

Thus, it can be seen that the fatty acid composition and configuration are the key factors which control the type of crystal formed. Summarising this, we have:

- The α crystal has the lowest density of molecular packing, has the fastest growth rate, is the least stable and consequently has the lowest melting point.

- The β' type with a more densely packed tilted molecular structure than the α is more stable, and has a higher melting point.

- The β crystal with the highest molecular packing and tilting is the most stable form, and has the highest melting point.

Initial experimentation involved tristearin [Chapman, 1962]. Polymorphic investigations on tristearin were conducted to determine the melting points of the three different forms (α, β' and β) as well as to certain the structural changes occurring in the triglyceride dimers. Tristearin is ideal for studying triglyceride packing due to differences between the width and length of the triglyceride molecules. The data obtained from X-ray analysis can be separated into two groups, long and short spacings. For tristearin, as the melting point increases, the long spacings decrease as shown in Table 3.3. The magnitude of the long spacings recorded for tristearin and other saturated monoacid triglycerides can be related to the length of the fatty acid

hydrocarbon chains present. As the hydrocarbon chains decrease in length from stearic acid to palmitic acid, a decrease in the long spacing is observed. The long spacing recorded for tristearin and most other saturated triglycerides is dictated primarily by the geometry of the triglycerides upon crystallisation.

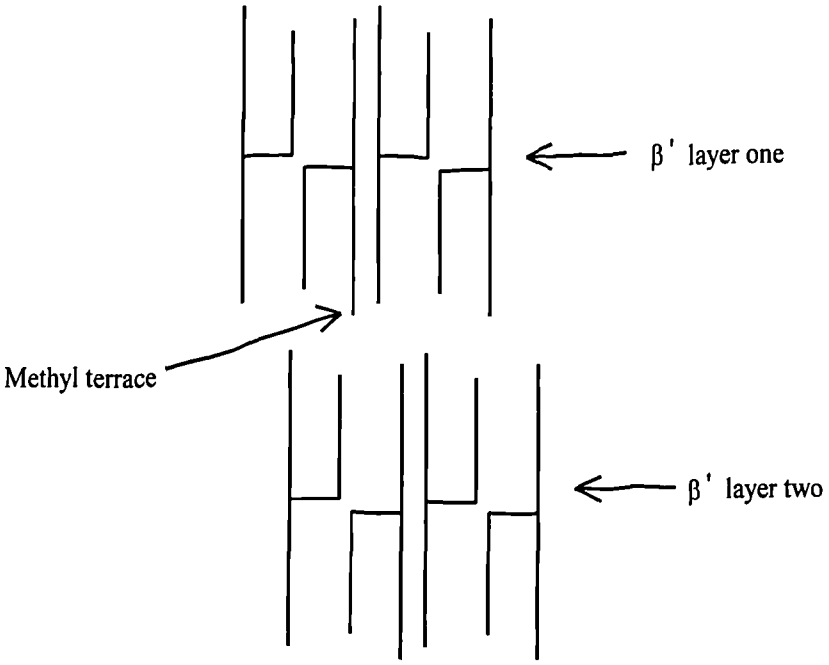

Figure 3.8. Diagrammatic representation of the methyl terraces in adjacent layers in a β' crystal.

Crystalline State	Melting point (°C)	Long spacing (Å)
α	54.0	50.6
β'	64.0	47.2
β	73.1	45.0

Table 3.3. Comparison of the melting points and long spacing for the three crystalline states of tristearin [Chapman, 1962].

When a melt of the triglyceride is quickly cooled, the α form, in which the fatty acid chains segments are aligned parallel to the crystallographic c-axis, is formed (Figure 3.9(a)) [Larsson, 1982]. The triglycerides in the α form are packed in a vertical manner and the molecules are loosely packed in an inefficient manner. The rough appearance of the terminal methyl plane complicates the packing of one bilayer in relation to adjacent layers. During the polymorphic transition, the triglycerides are thought to tilt with respect to the terminal fatty acid methyl plane. For example, if the α crystal of tristearin undergoes a slow transformation into the β' or β form, the long spacing decreases to 47.2 Å and 45.0 Å, respectively (Figure 3.9(b) and (c)). As the angle between the triglyceride and methyl plane decreases, a closer chain packing is adopted and the plane between adjacent bilayers is more even (see Figure 3.3). The closer the chain packing of the triglycerides the more dense will be the structure, resulting in higher melting points of the crystal.

As the triglyceride becomes more complex in its fatty acid composition, a change from the double chain length structure occurs. Variation in the fatty acid composition of the triglycerides has an effect on packing. It may produce differences in the long spacing which would be interpreted as a change in "chain multiplicity". If fatty acid chain lengths on a triglyceride differ by four or more carbons, triple chain length structures may form [Lutton, 1948]. In this case, the alignment of glyceride fatty acids is dictated by sorting of short chain from long chain acids. Depending on the positioning of the fatty acids on the glycerol molecule, a symmetrical tuning fork or chair structure may occur (Figure 3.10(a) and (b)).

In the case of POP, POS and SOS triglycerides, fatty acid alignment involves the separation of saturated from unsaturated acids. Mixed oleic-saturated glycerides tend to form triple chain length structures. X-ray revealed the long spacings for the β form of SOS to be 64Å which corresponds to a triple chain length structure. The 64Å long spacing is characteristic of triple chain length structures while a 45Å long spacing is characteristic of the double chain length structure as in tristearin.

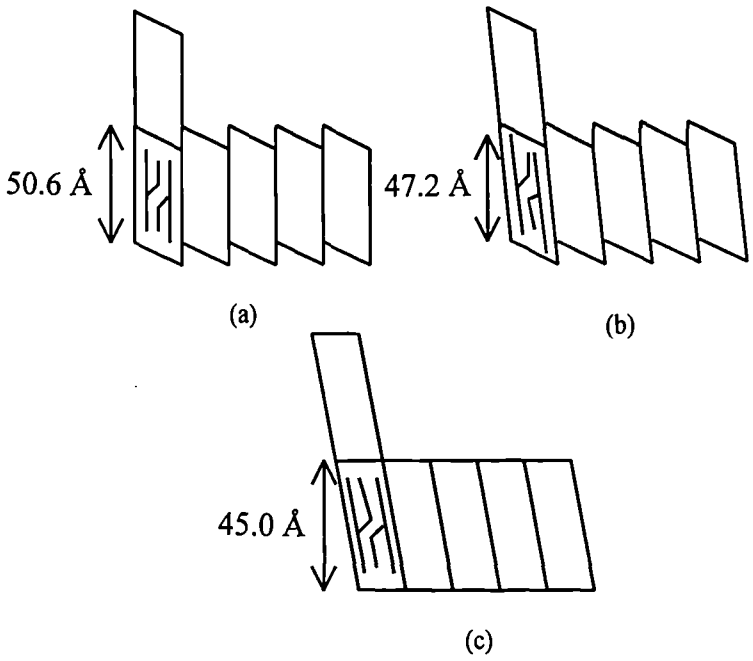

Figure 3.9. Diagrams of saturated triglyceride dimers in a crystalline lattice: Proposed triglyceride structure for the α Form (a), for the β' Form (b), and for the β Form (c) [Larsson, 1982]. Long spacings illustrate the α, β' and β crystals for tristearin [Chapman, 1962].

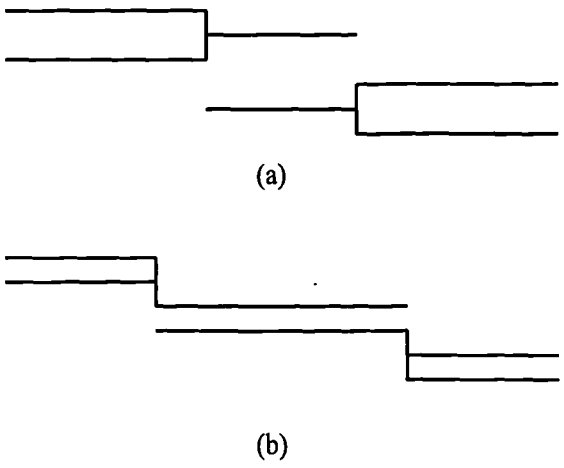

Figure 3.10. Arrangements of saturated mixed triglycerides upon solidification: (a) triple chain length structure; (b) triple chain length chair structure.

Lutton (1972) illustrates the conventional tuning fork packing for a 2-monosaturated triglyceride (Figure 3.11(a)), while Larsson (1972) illustrates the triple chain length structure in the modified tuning fork (Figure 3.11(b)). This happens because the unsaturated O segment in the R_2 position in the triglyceride is likely to lead to deviations from chain linearity in contrast to the straight P and S segments of the saturated acid groups.

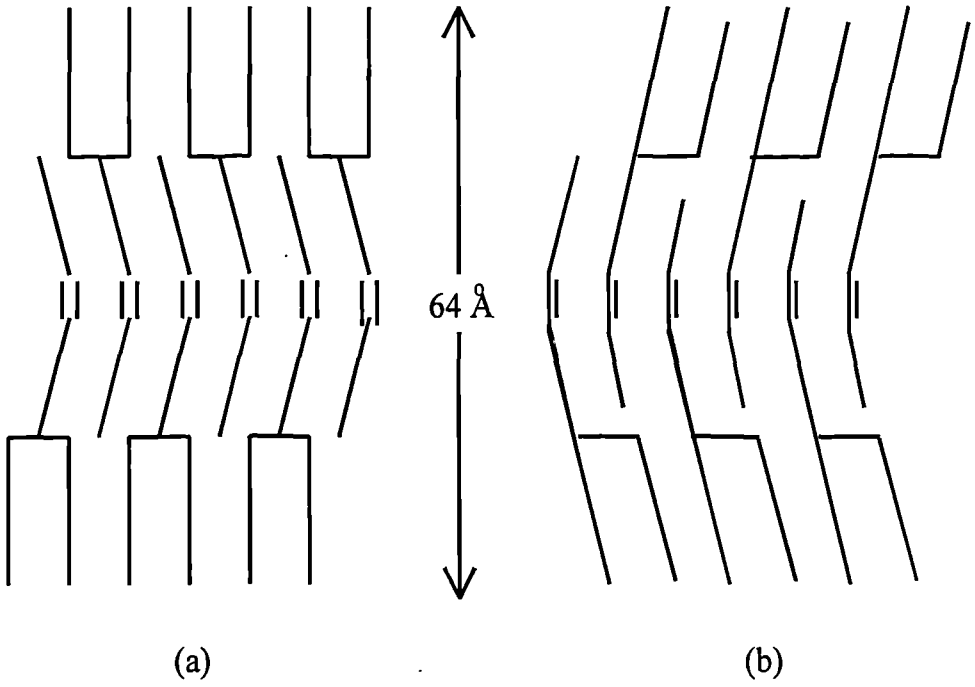

Figure 3.11. Illustration of the arrangements of 2-monounsaturated triglycerides: (a) conventional tuning fork packing; (b) modified tuning fork packing.

The majority of the triglycerides in cocoa butter are of this sn-2-monounsaturated type. The sn-2-monounsaturated arrangement permits close packing of similar triglycerides into a stable structure.

It is important to mention that triglyceride crystallisation in vegetable fats is very complex. Vegetable oils and fats consist of a large number of different triglycerides, but during crystallisation they form a unique crystal lattice. Thus, the triglycerides having different composition and melting point may exist in the same

crystal lattice. Such mixed crystals can be investigated through phase diagrams [Garti, 1988]. In the case of cocoa butter triglycerides, the understanding of the crystallisation mechanism is the key factor in the control of the industrial production of chocolate. Craven (1988) observed that the formation of polymorphic forms of cocoa butter is influenced both by cooling rate and shear forces in the chocolate mass.

3.3.2 *The polymorphic forms in cocoa butter*

Certain fats have been found to have more than three different types of crystal and the most prominent example is cocoa butter, which has been shown to have six crystal types.

One of the most controversial areas in confectionery science is the discrepancy found in the literature used to classify cocoa butter crystal polymorphs. Since the discovery of polymorphism, numerous scientists have reported different numbers of polymorphs and conflicting melting points for the various crystalline forms found in cocoa butter. In general, the various nomenclatures assigned to each classification have compounded the problem due to a lack of consistency (Table 3.4) [Dimick, 1985].

In 1951, four crystalline forms with different melting points were observed and labelled gamma (γ), alpha (α), beta double prime (β''), and beta (β) [Vaeck, 1951]. Nine years later, Vaeck [Vaek, 1960] again examinated cocoa butter and concluded four polymorphic forms, but melting points were slightly different, than previously reported.

In 1964, a fifth polymorphic form was observed and recorded as β' [Duck, 1964]. Two years later, six polymorphic forms were observed. However, the nomenclature denoting the various crystalline forms was changed to Roman numerals [Wille and Lutton, 1966]. The most recent work of Lovegren et al. (1976) revealed six polymorphic forms, but in this case the nomenclature was exactly opposite to that proposed by Wille and Lutton. In addition to these scientists, others have reported classifications dealing with cocoa butter polymorphism [Witzel and Becker, 1969; Huyghebaert and Hendrickx, 1971].

Vaeck (1951)		Vaeck (1960)		Duck (1964)		Wille & Lutton (1966)		Chapman (1971)		Lovergren (1976)	
γ	18.0	γ	17.0	γ	18.0	I	17.3	I		VI	13.0
α	23.5	α	21-24	α	23.5	II	23.3	II		V	20.0
						III	25.5	III		IV	23.0
β"	28.0	β'	28.0	β"	28.0	IV	27.5	IV	25.6	III	25.0
β	34.5	β	34-35	β'	33.0	V	33.8	V	30.8	II	30.0
				β	34.4	VI	36.3	VI	32.2	I	33.5

Table 3.4. Classification and temperature (C°) of cocoa butter crystalline forms

A technique commonly used to analyse the polymorphic crystalline forms of cocoa butter thermally is differential scanning calorimetry (DSC). Huyghebaert and Hendrickx recorded six polymorphic crystalline forms of cocoa butter using DSC. More recent experimentation with the DSC resulted in the reconfirmation of only four polymorphic forms of cocoa butter [Merken and Vaeck, 1980].

As can be seen from the literature data summarised in Table 3.4 there is a wide range of reported structures, the understanding of which is confused due to the different terminology historically adopted. The six polymorphic forms of cocoa butter vary in melting point from 17.3°C (I) to 36.6°C (VI). Form I is the least stable and Form VI the most stable. One aspect of note is the occurrence of two β crystals, i.e. forms V and VI. In this case, a very slight change in the packing at the methyl terrace occurs which results in a marginal shift in the short spacings, but an increase in the melting point of some 3°C. In general terms, this transformation of Form V to VI occurs very slowly taking some 12 weeks at 26°C. In terms of chocolate technology the transition from form V to VI results in bloom formation (see section 3.5). But the Form V is most preferable since it gives rise to better demoulding, desiderable gloss and favorable snap at room temperature. Undesirable demoulding and poor appearance of end products are caused if chocolate is simply solidified with no polymorphic control. This is due to the occurrence and transformation of unstable forms, such as Form III or IV to achieve crystallisation in Form V.

3.4 *Tempering process*

Formulated chocolate is composed of solid matter (sugar, protein, etc.) suspended in a crystalline matrix of cocoa butter, milk fat and vegetable fat. When chocolate solidifies, it is the crystalline fat phase that affects the product's surface finish, colour, and shelf-life stability. As previously stated, cocoa butter and its mixture with vegetable fat and milk fat can crystallise in numerous crystalline forms. Only one of these forms is the most desired form. If chocolate is solidified from the liquid state without any attention to seeding of the cocoa butter constituent or to the

method of cooling, it will be granular in texture and of poor colour or blotchy in appearance.

In order to ensure that the final chocolate product is in the proper crystalline form a process termed "tempering" is undertaken. Melted chocolate must be tempered before moulding. During tempering, therefore, the amount of solid particles is slightly increased and so too its viscosity. Moreover, it is in this state that chocolate is used for moulding, enrobing, shell making, etc.

Temper is the induced partial pre-crystallisation of the chocolate fat phase. The physico-chemical transformations occurring during this process have been reviewed [Jovanovic et al., 1995]. The process of tempering consists of cooling the chocolate down with continous mixing to produce a sufficient number of stable fat seed crystals and distributing these throughout the mass of liquid chocolate [Hachiya, 1990]. It was found that well-tempered chocolate contains approximately 3 to 8 percent cocoa butter seed crystals [Minifie, 1980] and that chocolate tempering quality is related to the quantity of stable crystalline seed present in the fatty phases [Adenier, 1984].

The most commonly used method of tempering involves the following step:

- complete melting;
- cooling to the point of crystallisation;
- crystallisation;
- melting of unstable crystals.

Chocolate has to be heated to at least to 50°C to ensure complete melting of the fat. A scheme of the tempering sequence is shown in Figure 3.12 [Talbot, 1994]. The molten chocolate was rapidly cooled to a minimum temperature that varied between 26 and 29°C, and mixed to induce pre-crystallisation. This is a very important stage because it is necessary to produce a large number of small crystal seeds in the highest possible melting point in the fat phase of the melted mass. Thus, the rapid crystallisation causes the formation of metastable forms (Forms III and IV). This is due to extensive supercooling, which is the driving force for nucleation and crystal growth of the fat. Forms III and IV have lower free energies of crystallisation than the

more stable forms, hence they crystallise more rapidly. However, the unstable forms are not favorable, because they cause poor demoulding and induce fat bloom.

The sample is then heated up to around 30°C for milk chocolate (2°C higher for plain chocolate) to melt the unstable crystals of lower polymorphs and create a uniform-sized crystal population. At the end of a correctly performed tempering process, small stable crystals are uniformly dispersed in the liquid chocolate mass, and they act as seed to promote the crystallisation of stable polymorphic forms in the subsequent cooling step. The chocolate is poured into moulds, and cooled to approximately 16°C. Cooling removes the latent heat of crystallisation to ensure the formation of the largest number of small stable crystals. During cooling, contraction occurs which is an indication of proper temper.

Form V is the preferred polymorph for chocolate since it gives rise to good demoulding, high gloss, favourable snap and rapid meltdown during eating [Hachiya et al., 1990]. Problems of poor texture, lack of contraction and inadequate gloss have been associated with 'lower polymorphs', with no firm data giving the actual polymorph and the amount present. The unsightly 'bloom' formation sometimes seen as a white powdery layer on the surface, particularly of dark chocolate, is usually associated with the formation of Form VI.

Undesirable demoulding and poor appearance of end products are caused if chocolate is simply solidified with no temperature control. This is due to the occurrence and transformation of unstable forms such Forms III and IV. It is also crucial to control very careful the temperature during the moulding and complete crystallisation processes. In the case of "over tempering", which means the crystallisation of too many seed crystals, the stable forms grow quickly, but the viscosity of the chocolate rapidly increases and causes difficulties in moulding. By contrast, the seed crystals at too low a concentration do not solidify in the stable form during the cooling stage.

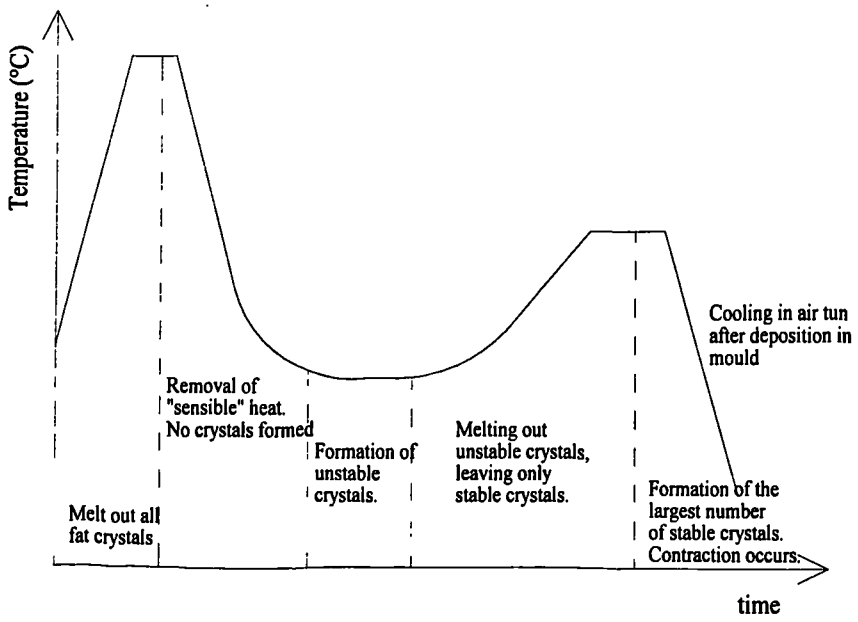

Figure 3.12. A scheme of tempering [Talbot, 1994].

Exactly which crystal form is desired at the completion was speculative. Vaeck (1960) believed that β' or β crystals are present in the final tempered product, while Wille and Lutton [1966] supposed that Form V was the crystal desired in the final product. Problems may occur during tempering for numerous reasons. The presence of unstable crystals after tempering may cause production problems due to the absence of contraction upon cooling. The amount of stable seed formed and the manner in which the product is cooled may lead to large crystal formations and fat bloom. The addition of other fats such as milk fat or vegetable fat affects crystallisation and hence tempering. For example addition of milk fat associated with milk chocolate manufacture requires the reduction of the tempering temperature by approximately 1°C [Koch, 1956].

By using the DSC, HPLC, SEM (Scanning Electron Microscopy), and PLM (Polarized Light Microscopy) to study the properties of cocoa butter crystals, Dimick and Manning (1985) have demonstrated that the initial crystal formed during tempering exhibited the properties of a high-melting-point seed. The stability of the seed increased as the formation temperature in the cycle increased from 26° to 30°C. The composition of the seed is believed to be an SOS-rich fraction. The stable seed

acted as a surface for further crystallisation to continue. After a rapid viscosity increase, the temperature was increased and the viscosity decreased as the crystals partially melt and anneal. Throughout the temperature increase and afterwards, the crystals annealed and exhibited higher melting points. During the tempering cycle, the triglyceride POS is partially excluded from the crystalline structure, whereas POP and other liquid triglycerides are excluded to a greater degree. The resulting crystal formed after the temperature cycle is composed of a high percentage of SOS and lesser amounts of POS.

During tempering there should be adequate agitation to ensure proper heat transfer between the chocolate product and the cooling medium. It is necessary to know quickly whether the chocolate being used is properly tempered. Temperature recording gives some confirmation. One instrument developed to accomplish this is called the Tempermeter. It is based on the principle that under controlled conditions of cooling chocolate there is a relationship between the cooling curve inflection point and the degree of temper [Minifie, 1980].

Figures 3.13 and 3.14 show, respectively, the typical cooling curves and the inclinometer, which greatly facilitates the measurement of the slope of the cooling curve.

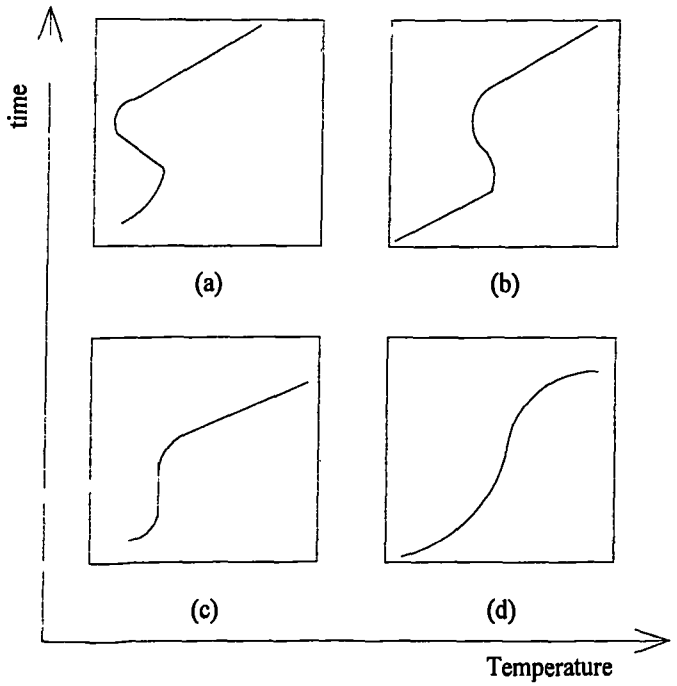

Figure 3.13. Representative curves produced by tempermeter: (a) undertempered; (b) slightly tempered; (c) correctly tempered; (d) overtempered [Minifie, 1980].

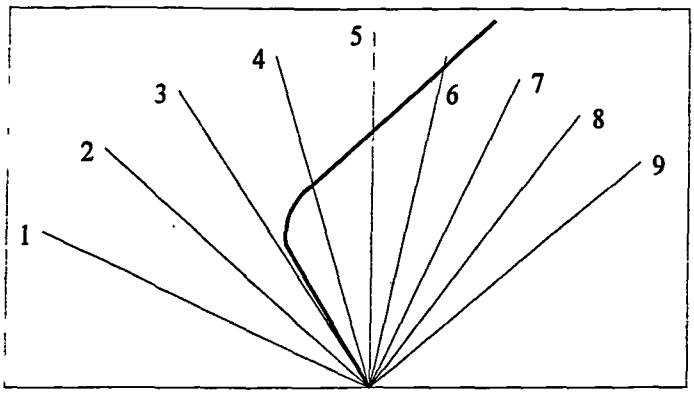

Figure 3.14. Illustration showing the use of inclinometer:
1. very under tempered; 2. Underetempered; 3. sligtly underetempered; 4. very slightly underetempered; 5. correctly tempered; 6. very slightly overtempered; 7. slightly overtempered; 8. Overtempered; 9. much overtempered.

3.5 *Bloom formation*

When chocolate products are stored for a long period above room temperature, the chocolate surface loses its gloss. The phenomenon is called "bloom". Bloom can be of two distinct types, one being "sugar bloom" and the other "fat bloom". Sugar bloom is characterised by a sandy, gritty texture and consists of sugar crystals that have accumulated on the surface of the bar. In most cases sugar bloom forms due to water condensation on the surface of the chocolate. The water solubilizes the surface sugar which eventually crystallises in large white formations that are visible to the naked eye.

The second type of bloom which involves the fat phase is termed fat or chocolate bloom. Fat bloom is a problem that causes the glossy surface of chocolate to became dull and covered with a grey film. This discoloration resembles the bloom on grapes, thus it is termed "bloom" [Cerbulis et al., 1957]. This change is caused by the occurrence of large crystals of cocoa butter.

It is known that bloom on the surface of chocolate is definitely crystalline in structure [Neville et al., 1950]. The mechanism leading to bloom formation is still the subject of controversy today. Numerous theories have been proposed to explain the problem of bloom formation. Whymper (1933) originally proposed that cooling produced an unstable solution in which the individual fat components separated. The higher melting fractions aggregated and separated away from the lower melting fractions thus producing fat bloom.

Becker (1958) proposed a theory involving phase diagrams of various cocoa butter components. His theory stated that the fractionation of triglycerides that ultimately lead to bloom was caused by a transition from an unstable crystal form into the stable form. During this change the crystal volume decreases and air can penetrate into the structure of the chocolate producing a dull reflection. At elevated temperatures the cocoa butter melts and then resolidifies into large crystal formations. These formations may be composed of high melting glycerides.

Kleinert (1961) examined bloom based on practical manufacturing experience. The cooling process after enrobing or moulding should be gentle in order to eliminate

stresses and cracks in the couverture. Bloom may be prevented if tempering and cooling are performed correctly. At high temperatures, fat bloom may form due to unstable crystals melting and the liquid fat migrating to the surface. On the surface, the liquid fat solidifies into stable crystals thus forming bloom [Andersson, 1963]. The crystalline triglycerides present in fat bloom have lower iodine values and higher melting points than those triglycerides dispersed throughout the chocolate mass. The composition of fat bloom was found to be rich in the triglycerides POS and SOS [Steiner and Bonar, 1961].

Fat bloom is most frequently observed on the dark chocolate covering of assortment units particularly those units having centres which contain fats which are incompatible with cocoa butter. Cocoa butter bloom is the most stable, highest melting polymorphic form of cocoa butter (i.e. Form VI). Fat bloom formation is accelerated by a thermal fluctuations, because the transition from Form V to Form VI is caused in the crystalline phase by thermal energy [Hachiya, 1990]. At elevated storage temperatures, 21 to 24°C, cocoa butter polymorphs in the chocolate coating will melt, diffuse to the surface, and recrystallise producing an unappetizing white bloom of Form VI needle-like crystallites on the chocolate surface.

Investigations designed to retard fat bloom formation have been underway for at least 30 years. Most efforts have been aimed at retarding bloom by the addition of different additives to the chocolate or by infrared radiation. Kleinert (1961) retarded bloom formation after enrobing by heating with warm air. After the heat treatment, crystals with melting points above 34.5°C were present. The optimum heat treatment to prevent bloom over a one-year period was 80 min at 32°C.

Most investigations aimed at preventing fat bloom employed chemical food additives. The addition of butterfat or a mixture of sorbitan monostearate 60 and polysorbate 60 has been used extensively in the past to control fat bloom [Musser, 1980]. Milk fat was thought to be a good choice because it is already used in the manufacture of milk chocolate. Milk fat is traditionally thought to work by forming a mixed glyceride crystal with cocoa butter which, when solidified as form V, is stabilised and thereby prevented (possibly by steric hindrance) from transforming to form VI. Campbell et al. (1969) reported bloom inhibition two to four times longer

with the addition of 2.5% hydrogenated milk fat as compared to an equal addition of unhydrogenated milk fat. Hendrickx et al. (1971) observed an inhibition of bloom formation when replacing 10% of the cocoa butter with hydrogenated milk fat. Not so favourable observations were decreased contraction and a less than ideal sharp melting point. Timms and Parekh (1980) reported that the addition of fractionated or hydrogenated milk fat to cocoa butter did not result in an increased amount of solid fat at ambient temperatures.

The addition of a 1% mixture of sorbitan monostearate and polyoxyethylene sorbitan monostearate increased the shelf-life of chocolate over a similar chocolate lacking the modifiers [Easton et al.,1952]. Kleinert (1961), however, disagrees with Easton's results. Its experiments indicated an inability to prevent or delay bloom formation when sorbitan monostearate and polyoxyethylene sorbitan monostearate were added. Of 19 additives tested, only butterfat and hard arachis fat were found to retard bloom formation. It is believed the disagreement between scientists concerning bloom inhibitors may be due to the procedures used to induce bloom after tempering. It appears that many of these inhibitors work only under specific time and temperature parameters.

The bloom problem is very complex and the cause may be a combination of factors instead of one single factor. Above all, the formation of bloom is affected by the way in which the chocolate is handled in the factory and in the marketplace. Correct seeding and moderate cooling go a long way toward the prevention of fat bloom [Schlichter, 1984, Koyano, 1990].

3.6 *Chocolate flow properties*

Molten chocolate is a suspension of particles of sugar, cocoa and/or milk solids in a continuous fat phase of cocoa butter [Chevalley, 1974]. Chocolate processing occurs with the product in the molten state. Liquid chocolate is a non-Newtonian fluid and this means that the rheological properties of this material have to take in consideration when highly automated molding and enrobing machinery are designed

[Minifie, 1980, Nelson, 1994]. Knowledge of rheology provides the industry with measurable properties to assess product quality and processing efficiency [Riedel, 1980].

Plotting shear rate ($\dot{\gamma}$) versus shear stress (σ), three different types of rheogram can be obtained (see Figure 3.15) [Chevalley, 1994]. In the case of Newtonian liquids (line a) it is obtained a straight line, passing through the origin. A flow begins as soon as a force is applied. Viscosity (η) is equal to the reciprocal of the slope of this line as expressed by equation (2.37). Liquid cocoa butter behaves as a Newtonian fluid.

For Bingham fluids (line b), the straight line does not pass through the origin, but intercepts the shear stress axis at the yield value σ_0. In this case, a minimum force (the yield value) must be applied before flow occurs. The reciprocal of the slope of line (b) is called plastic viscosity (η_{pl}) of the fluid and it can be expressed by the equation:

$$\eta_{pl} = (\sigma - \sigma_0) / \dot{\gamma} \qquad (3.1)$$

The equation (3.1) may also be expressed as:

$$\sigma = \sigma_0 + \eta_{pl} \dot{\gamma} \qquad (3.2)$$

An example of Bingham fluid is the toothpaste.

Chocolate flow behaviour is expressed by curve (c), where the rheogram is curved rather than linear. Also in this case a minimum force has to be applied. Many attempts were made to express the curvature of the chocolate rheogram in terms of an equation and the most successful was that of Steiner (1958). He adapted a model proposed by Casson, deriving an equation, which is adopted by the OICC (Office International du Cacao et du Chocolat) (1973):

$$\sigma^{1/2} = (K_0)^{1/2} - (K_1 \dot{\gamma})^{1/2} \qquad (3.3)$$

By taking the square roots of shear stress and shear rate, the rheological behaviour of the chocolate may be expressed by the constants K_0 (yield stress) and K_1 (plastic viscosity) as in the equation (3.2).

Various factors may influence the flow properties of chocolate: fat content, emulsifier content, water content, particle size distribution, temperature, conching time, degree of temper, condition of storage, thixotropy and vibration [Chevalley, 1974 and 1994].

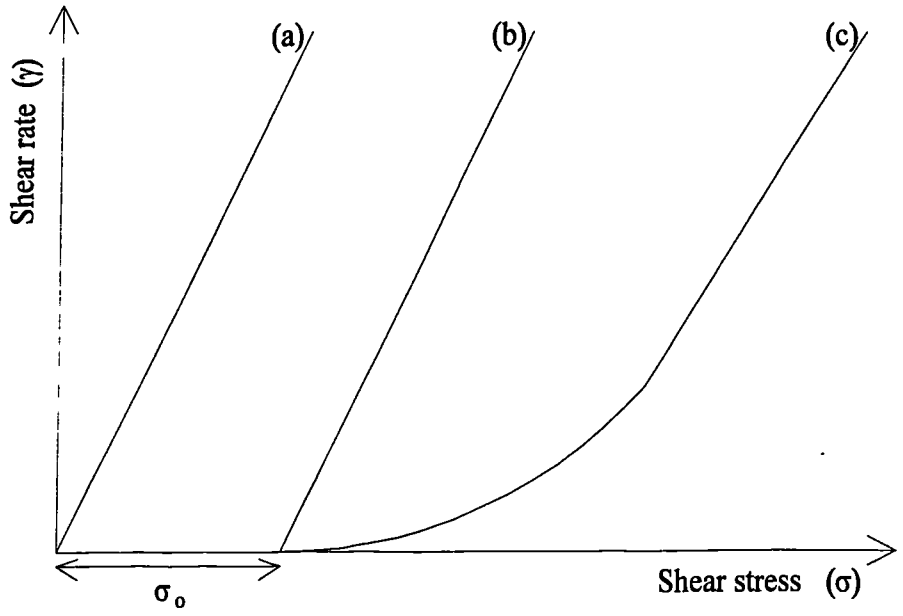

Figure 3.15. Different types of rheogram: (a) Newtonian; (b) Bingham; (c) pseudoplastic [Chevalley, 1994].

3.7 *References*

Adenier, H, Chaveron, H. and Ollivon, M., *Sciences des aliments*, 1984, 4, 213-231.

Andersson, W, *Rev. Int. Choc.*, 1963, 18, 92-98.

Bailey, A E, in *Melting and Solidification of Fats*, Interscience Publishers, Inc., New York, NY, 1950.

Becker, K, *Rev. Int. Choc.*, 1958, 13, 254-256.

Berbert, P R F, *Revista Theobroma*, 1976, 6, 67.

Breckenridge, W C, in *Fatty Acids and Glycerides, Handbook of Lipid Research*, ed by Kuksis, Plenum Press, New York, 1978, chapt. 4.

Campbell, L B, Andersson, D A and Keeney, P G, *J. Dairy Sci.*, 1969, 52, 976-979.

Cerbulis, J, Clay, C and Mack, C, *J. Amer. Oil Chem. Soc.*, 1957, 43,533-537.

Chaiseri, S and Dimick, S P, *Manufacturing confectionery*, 1987, 67, 9, 115-122.

Chaiseri, S and Dimick, S P, *J. Amer. Oil Chem. Soc.*, 1989, 66, 11, 1771-1776.

Chapman, D, *Chem. Rev.*, 1962, 62, 433-456.

Chevalley, J, *Journal Texture Studies*, 1974, 22, 177-196.

Chevalley, J, in *Industrial chocolate manufacture and use*, edited by S T Beckett, Blackie A & P, London, 1994, 2nd edn., pp. 139-155.

Chin, A.H.G. and Zainuddin, N, *Proceedings of the 1984 International Conference in Cocoa and Coconuts*, Malaysia, 1984.

Clarkson, C E and Malkin, T, *J. Chem. Soc.*, 1934, 666-671.

Craven, M B, in *The physical chemistry of lipids, Handbook of lipid research*, ed by Small, Plenum Press, New York, 1988, chapt. 10.

Davis T R and Dimick P S, *J. Amer. Oil Chem. Soc.*, 1989, 66, 10, 1494-1498.

Dimick, P S and Manning, D M, *Food Microstructure*, 1985, 4, 249-265.

Duck, W N, in *Determination of solid fat in melted fat, their role in formation and polymorphic form by viscosimetry*, A master thesis, Lancaster, Pa, 1964, 72.

Duffy, P, *J. Chem. Soc.*, 1852, 5, 197-210.

Easton, N R, Kelly, D J, Bartron, L R, Cross, S t and Griffin, W C, *Food Technology*, 1952, 6, 21-25.

Garti, N and Sato, K, in *Crystallisation and polymorphism of fats and fatty acids*, eds by Garti, N. and Sato, K., Marcel Decker Inc., New York, 1988, 3-7.

Hachiya, I, Koyano, T and Sato K, *Lipid Technology,* 1990, 2, 2, 34-37.

Hagemann, J W, in *Crystallisation and polymorphism of fats and fatty acids*, eds by Garti, N and Sato, K, Marcel Decker Inc., New York, 1988, 9-95.

Hendrickx, H, DeMoor, H, Huybhebaert, A and Jansen, G, *Rev. Int. Choc.*, 1971, 26, 190-193.

Hernqvist, L, *Fat Sci Technol*, 1988, 90, 11, 451-454.

Hernqvist, L, *Food structure*, 1990, 9, 39-44.

Hoerr, C W, *J. Amer. Oil Chem. Soc.*, 1960, 37, 539-546.

Huyghebeart, A and Hendrickx, H, *Lebensm-Wiss u technol.*, 1971, 4, 59.

Kleinert, J, *Rev. Int. Choc.*, 1961, 16, 201-219.

Koch, J, *Rev. Int. Choc.*, 1956, 11, 344-348.

Koyano, T, Hachiya, I and Sato, K, *Food structure*, 1990, 9, 231-240.

Jewell, G G, *Leatherhead Food RA Research Report*, 1974, no. 202.

Jewell, G G, *35th P.M.C.A. Production Conference*, 1981, 35, 63-66.

Jewell, G G and Heathcock, J F, in *Food Structure - its creation and evaluation*, ed by Blanshard, J M V and Mitchell, J R, Butterworths, 1988, chap. 15.

Jovanovic, O, Karlovic, D J and Jakovijevic, J, *Acta alimentaria*, 1995, 24, 3, 225-239.

Larsson, K, *Arkiv for Kemi*, 1964, 23, 5, 35-56.

Larsson, K, *Acta Chemica Scandinavica*, 1966, 20, 2255-2258.

Larsson, K, *Fette Seifen Anstrichmittel*, 1972, 74, 136-142.

Larsson, K, *Food Microstructure*, 1982, 1, 55-62.

Lehrian, D W, Keeney, P G and Butler, D R, *J. Am. Oil Chem. Soc.*, 1980, 57, 66-69.

Lovergren, N V, Gray, M S and Feuge, R O, *J. Amer. Oil Chem. Soc.*, 1976, 53, 108-112.

Lutton, E S, *J. Amer. Oil Chem. Soc.*, 1945, 67, 524-527.

Lutton, E S, *J. Amer. Oil Chem. Soc.*, 1948, 70, 248.

Lutton E S, *J. Amer. Oil Chem. Soc.*, 1950, 27, 276-281.

Lutton, E S, *J. Amer. Chem. Soc.*, 1972, 49, 1-9.

Malkin, T, in *Progress in Chemistry of Fats and Other Lipids*, ed. By Holman, R T et al., Volume 2. London, Pergamon Press, 1954, 1-50.

Manning, D M, Dimick, P S, *38th P.M.C.A. Production Conference*, 1984, 29-33.

Merken, G V and Vaeck, S V, *Lebensm-Wiss u Technol*, 1980, 13, 314-317.

Minifie, B W, in *Chocolate Cocoa and Confectionery*, Science and Technology; 1980.

Musser, J C, *Proceedings of the 34th Annual PMCA Production Conference*, 1980.

Nelson, R B, in *Industrial chocolate manufacture and use*, edited by S T Beckett, Blackie A & P, London, (1994), 2nd edn., pp. 167-210.

Neville, H A, Easton, N R and Bartron, L R, *Food Technology*, 1950, 4, 439.

Office International du Cacao et du Chocolate. Analytical Methods (E/1973) 10, *Rev. Int. Choc*, 1973, 216-218.

Riedel, H R, *Confectionery production*, 1980, 518-519.

Sato, K, *Advances in Applied Lipid Research*, 1996, 2, 213-268.

Savage, C M and Dimick, P S, *49th P.M.C.A. Production conference*, 1995, 54-59.

Schlitchter, J, Garti, N and Sarig, S, *Industrie alimentari*, 1984, 871-877.

Steiner, E H, *Rev. Int. Choc.*, 1958, 13, 290-295.

Steiner, E H and Bonar, A R, *J. Sci. Food Agric.*, 1961, 12, 247-250.

Talbot, G, in *Industrial chocolate manufacture and use*, edited by S T Beckett, Blackie A & P, London, (1994), 2nd edn., chap. 11.

Timms, R E and Parekh, *Lebensm-Wiss u Technol.*, 1980, 13, 177.

Timms, R E, *Prog. Lipid Res.*, 1984, 23, 1-38.

Vaeck, S C, *Rev. Int. Choc.*, 1951, 6, 100-113.

Vaeck, S C, *Manufacturing Confectioners*, 1960, 40, 35-46 and 71-74.

Wille, R L and Lutton, E S, *J. Amer. Oil Chem. Soc.*, 1966, 43, 491-496.

Witzel, H and Becker, K, *Fette Seifen Anstrichmittel*, 1969, 71, 507-516.

Whymper, R, in *The problem of chocolate fat bloom*, The Manufacturing Confectioner Publishing Company, Chicago, IL, 1933.

Chapter 4

An Examination of the Nucleation of Single and Mixed Confectionery Fats

4.1 *Introduction*

The position of identical and/or different fatty acids within the glyceride molecule is responsible for the large differences in melting and polymorphic behaviour of the triglycerides. One way of understanding and interpreting these differences in behaviour is the use of phase diagrams. Kremann and Shoulz (1912) reported the first known study of a triglyceride phase diagram, but they did not understand the difficulties related to polymorphism. Efremov et al. (1927) studied binary mixtures of tristearin (SSS) and tripalmitin (PPP) and took account of the polymorphism. He found eutectic mixtures in each of the three polymorphic modifications possible. Joglekar and Watson (1928 and 1930) also investigated the binary mixtures of SSS and PPP, but they found difficulty mixing SSS and PPP.

Rossell (1967) collected most of the phase diagrams determined up until 1965 and classified them in terms of mixtures of monoacid (simple) triglycerides and mixtures of mixed-acid triglycerides. Afterwards, three further studies of particular interest have been published, concerning all the binary phase diagrams that can be formed from the 6 triglycerides containing only palmitic and / or stearic acids [Perron, 1969 and 1971; Knoester, 1972]. These triglyceride phase diagrams were also reviewed by Small (1986).

In this chapter the nucleation behaviour of single and mixed triglycerides will be examined. Firstly, binary mixtures of triglycerides, such as tripalmitin and triacetin, tripalmitin and triolein, will be investigated. Secondly, studies will proceed to more complex systems, involving the presence of cocoa butter, milk fat and synthetic lecithin (YN).

4.2 *Methodology*

An automated apparatus (Figure 4.1) designed by Gerson (1991) and updated by Taggart et al. (1993) has been used to study the crystallisation kinetics of different fat systems. The system (solute/solvent) is placed in a glass vial (volume ~60 ml) and

is continuously agitated by a teflon magnetic flea. Initially the sample is stirred at a constant speed by the magnetic flea via a turbojet magnetic stirrer, which is powered by the water bath pump. This stirrer, made of plastic material, proved to be impractical because the system required to be heated to a temperature beyond 50°C and the turbojet stirrer warped and required replacing regularly. This proved to be a costly event both in money and time. A substitute metal magnetic stirrer was constructed and this enabled the experiments to operate without further problems. A Sybron Brinkmann stainless steel fibre optic light probe, with associated colorimeter to detect light transmittance through the solution, and a platinum resistance (PT100) thermometer to measure solution temperature are immersed in the solution through a liquid tight lid. The vial is placed into a Haake F3C recirculating bath, filled with water.

The change in resistance in the PT100 due to changes in the solution temperature are interpreted as differences in voltages (Platinum resistance changes by 3.85 ohms/°C). Voltages corresponding to the temperature readings of the solution are converted to digital signals via the OASIS MADA containing an interface analogue to digital converter which are then sent to an Amstrad 1640 computer for subsequent processing in which the digital voltages are converted into solution temperature readings. The sensitivity of the platinum resistance thermometer is approximately 0.01°C.

The turbidity probe is attached to two bundles of fibre optics encased in rubber tubing, connected into a Brinkman PC700 colorimeter. The light is projected from the colorimeter down one of the fibre optic bundles, through 1cm of solution and is reflected back up the other bundle by the external turbidometric probe mirror. In total the light projected from the fibre optic travels a pathlength of 2 cm through the solution. This system was found to be as sensitive to the development of opacity as the human eye, which can detect solid particle sizes of 5-10 μm. The fibre optic turbidity probe detects nucleation by the reduction in light transmittance associated with nuclei formation in the supersaturated solution. This reduction is observed on the colorimeter on a percentage scale from 100 to 0.

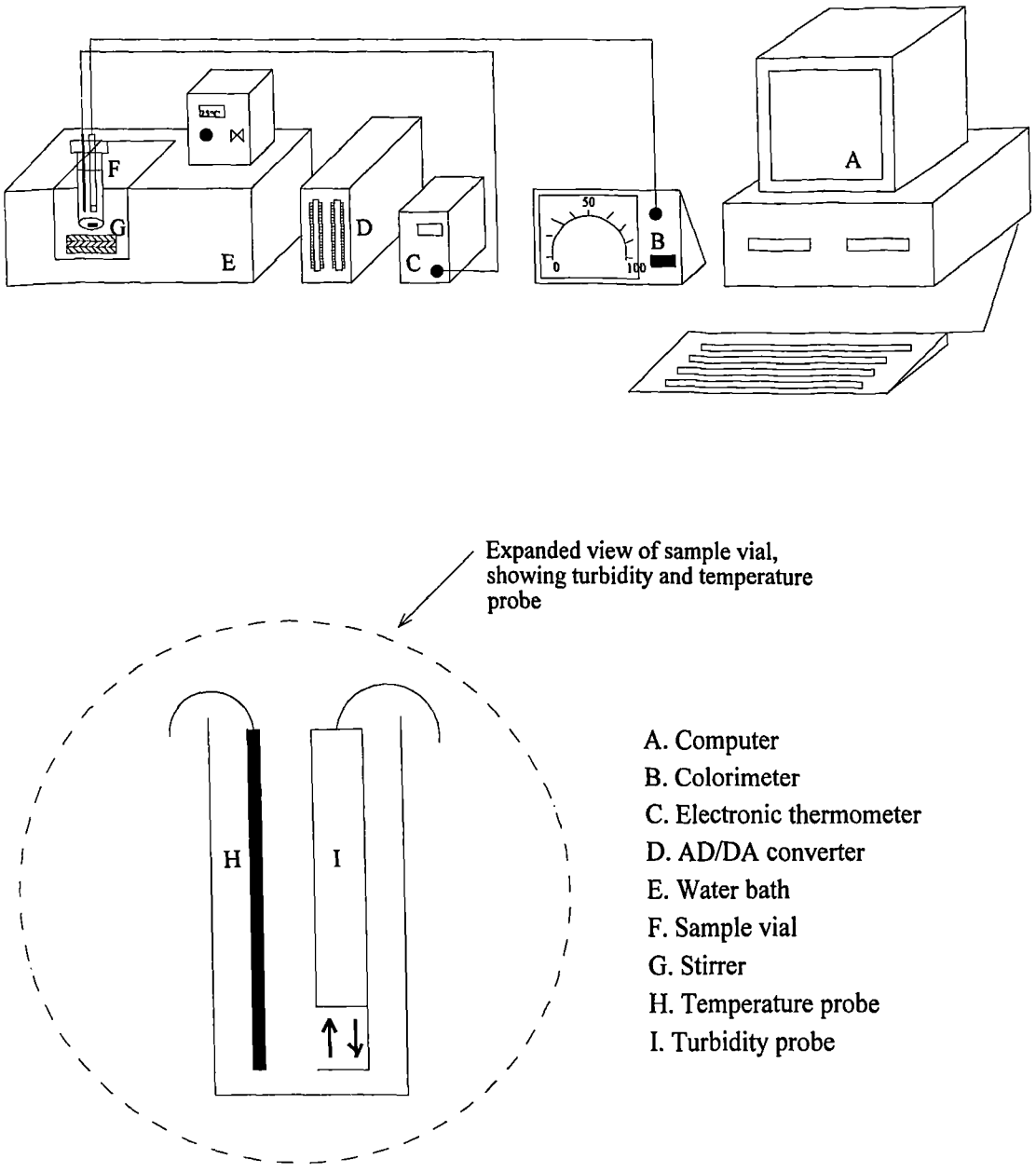

Figure 4.1. Schematic of experimental arrangement and data acquisition used for nucleation measurements. A: Amstrad 1640 computer; B: Brinkmann colorimeter; C: Temperature controller; D: OASIS MADA interface; E: Haake F3C cryostat; F: Glass sample vial containing Pt100 temperature probe and fibre optic light probe in addition to magnetic flea; G: metal magnetic stirrer.

It has to be noted that the measured turbidity is not 'absolute', a reading of 100% transmittance does not represent a totally transparent solution and 0% value does not indicate an opaque solution. The colorimeter produces a voltage output from 1 to 0 volts which is proportional to the light transmittance reading. This voltage is sent to an OASIS MADA containing an interface analogue to digital converter and to an Amstrad 1640 computer where the signal is processed and converted into a percentage transmittance reading.

The computer also controls the temperature of the recirculating bath, transmitting a digital signal to the MADA digital to analogue converter. The signal is converted to an analogue signal between 0 and 1 volts. Then the signal is passed to the F3C digital control head of the recirculating bath where the temperature of approximately 1°C for every 10 mV is signalled. In this way the solution can be subjected to cooling/heating cycles at a desired rate of temperature change.

Prior to the start of the experiments the glass vial, magnetic flea, temperature and turbidity probes must be carefully washed in a solution of water and soap, rinsed in doubly distilled water and dried to try and minimise the possibility of heterogeneous nucleation, although realistically this is rather difficult. At the beginning of the cooling/heating cycle the temperature is raised by at least 10°C above the expected saturation temperature to ensure any nuclei present are totally dissolved.

4.3 *Experimental measurements*

Solutions are subjected to cooling/heating cycles at the following rates: 0.75, 0.50, 0.25 and 0.10°C/min. Each cycle is repeated at least three times to verify the reproducibility of the results. The temperature and light transmittance of the system are recorded as a function of time (every 30 seconds) throughout the controlled temperature program. Between each cycle the sample is held at high pre-determined temperature for approximately 30 minutes to ensure that no crystals are detectable. The light transmittance is recorded at this stage as the average turbidity of the sample over 30 minutes and the value is associated with a clear sample solution. During the cooling

phase of the cycle, the light transmittance remains constant until nucleation starts to occur. This is said to have occurred when the percentage of light transmittance has dropped by 10% or more of the averaged recorded value. The value of 10% was selected so that electronic noise (up to 4%) could not be mistaken for nucleation. Then, the system is held for two minutes at the lowest pre-determined temperature of the cycle (where the crystals start to form) in order to let the solution equilibrate before the heating phase commences. Dissolution was defined as occurring when the percentage of light transmittance came within 10% of the average transmission recorded for the clear solution. A scheme of the change in percentage transmission (Trans (i)) and temperature (T(i)) as a function of time is shown in Figure 4.2.

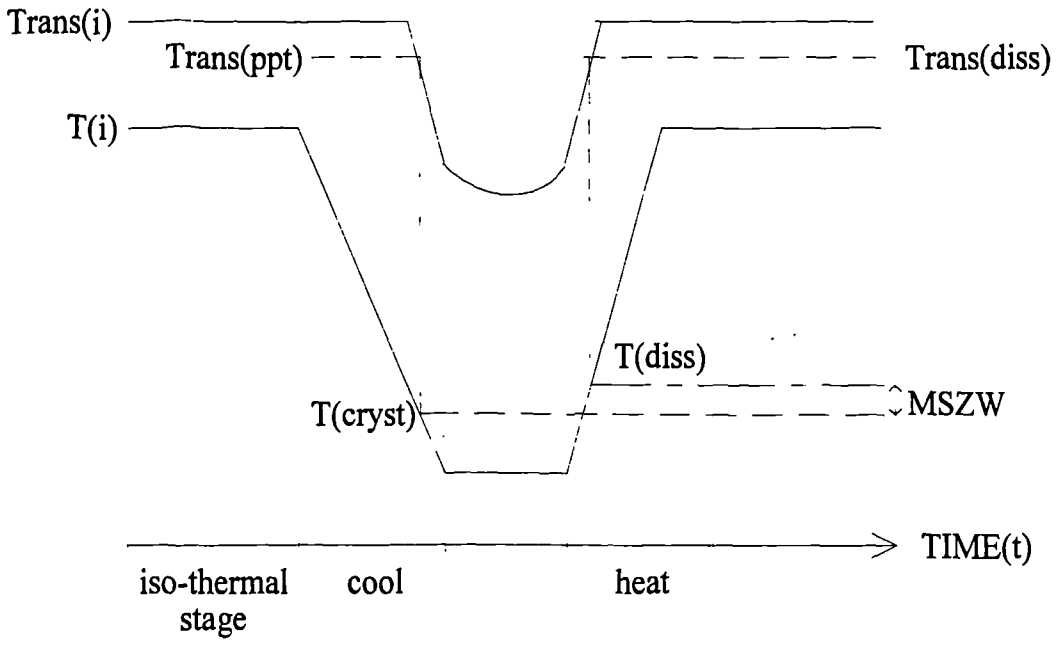

Figure 4.2. Schematic of cooling and heating cycle as a function of time for slow cool cycle measurements. T(i) and Trans(i) are the temperature and light transmittance reading recorded during the high temperature phase of the experimental cycle. Trans(ppt) is approximately 10% lower than the light transmittance recorded during the first iso-thermal stage (Trans(i)) and indicates the onset of crystallisation, T(cryst). T(diss) is the temperature at which the solutions light transmittance comes within 10% of Trans(i) [Trans(diss)] and is associated with the crystals dissolution temperature.

4.3.1 *Slow cooling/heating cycle*

The experimental methodology consists of repeatedly cooling and heating the solution at known and steady rates. During each cycle the temperatures of crystallisation (T_{cryst}) and dissolution (T_{diss}) are recorded as a function of the cooling/heating rate. It is to be expected that the faster the cooling rate the greater the degree of undercooling achieved in the system prior to bulk nucleation. T_{cryst} and T_{diss} are expected to become closer by using slower cooling/heating rate in the measurement technique. But, this does not occur in all experiments, depending on the system studied.

The saturation temperature (T_{sat}) is defined as the temperature where dissolution occurs at an infinitely slow heating rate (i.e. $\rightarrow$ 0°C/min) and it can be determined by plotting temperature of dissolution at different heating rate against the heating rate. The temperature of saturation corresponds to the intercept on the 'y' axis.

The metastable zone width (MSZW) is described by the expression:

$$MSZW = T_{sat} - T_{cryst} \qquad (4.1)$$

The order of reaction can be calculated from the following equation:

$$\log b = (m-1) \log (dc/dt) + \log k_n + m \log \Delta T_{max} \qquad (4.2)$$

where b is the cooling rate, k_n is the rate constant, ΔT_{max} is the maximum undercooling in °K (assumed to be equivalent to MSZW), m is the order of reaction and dc/dt is the rate of equilibrium concentration change with respect to temperature. The order of reaction corresponds to the slope of a plot of the logarithm of the rate of temperature change versus the logarithm of ΔT_{max}.

When the values of saturation temperature for three or more different concentrations of the solution are known, the *van't Hoff* equation can be used to calculate the entropy (ΔS_d) and enthalpy of dissolution (ΔH_d):

$$\ln(\chi) = -\Delta H_d / RT + \Delta S_d / R \qquad (4.3)$$

where χ is the mole fraction of solute in solution, T is the absolute temperature of saturation (°K), and R is the gas constant. This equation assumes ideal solution behaviour in addition to calculating the enthalpies and entropies of the dissolution process.

A linear regression method was used to derive the lines of best fit for the determination of nucleation parameters. The main procedures can be summarised as follows:

- Saturation temperatures were determined from the measured dissolution temperatures as a function of heating rate by extrapolating the dissolution temperature back to equilibrium conditions (b=0°C/min).

- Metastable zone widths (MSZW) at a zero cooling/heating rate were determined by plotting the MSZW values recorded against the cooling rate and extrapolating to zero cooling/heating rate.

- In accordance with equation (4.2) the orders of reaction were found to be the slope of a plot of log (b) versus log (MSZW).

- In accordance with equation (4.3), the enthalpies and entropies of dissolution were calculated from the gradient and intercept, respectively, of a plot of ln (mole fraction of solute) versus 1/saturation temperature (°K).

4.4 *Nucleation kinetic studies of confectionery fats*

4.4.1 *Mixtures of tripalmitin and triacetin*

The concentrations studied were 0.02, 0.05, 0.10 and 0.15 mole percent of tripalmitin (PPP) in triacetin. Also the nucleation behaviour of pure tripalmitin was analysed. No studies on these mixtures have been reported in the literature.

In Figure 4.3 the profile of a typical cooling/heating cycle obtained from the experiments carried out is shown. The nucleation process occurs every district time therefore the turbidity is observed to change over a finite crystallisation time. Hence the trace of transmittance versus time is not perfectly vertical. All the experimental data, collected during the cooling/heating phase at different rates, are summarised in Tables 4.1 and 4.2. Each run has been repeated three times and the value shows good reproducibility. The temperatures of crystallisation and dissolution are shown in Figure 4.4.

Tripalmitin shows a very low solubility in triacetin, and this probably depends on the different length of the fatty acid chain in the two triglycerides (C_{16} in PPP and C_2 in triacetin). For all mixtures studied, the temperature of crystallisation increases from the fastest to the slowest cooling rate. The difference, between the values recorded at 0.75°C/min and those recorded at 0.10°C/min, is about 2-3°C. In the case of the tripalmitin sample alone the difference in the temperature of crystallisation, between these two rates, is approximately 4°C. The temperatures of dissolution show the same trend as that observed for the temperatures of crystallisation, even if the change is much less evident. For the lowest concentration (0.02 mole percent), the change of temperature of dissolution, from the fastest to the slowest heating rate, is about 4°C. For the other concentrations, the temperatures of dissolution are almost constant, with a change of less than 1°C. For the pure tripalmitin sample, the change on temperature of dissolution recorded is more evident (about 3°C).

From the experimental data summarised in Tables 4.1 and 4.2, the temperatures of saturation, the metastable zone width and the order of reaction have been calculated and summarised in Table 4.3.

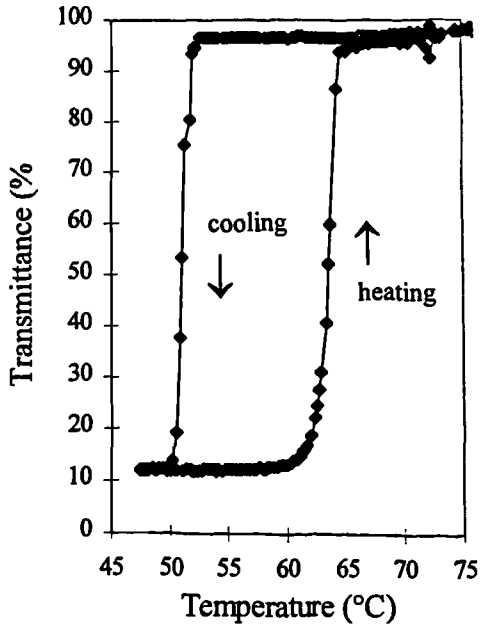

Figure 4.3. Transmittance (%) versus temperature (°C) for the mixture 0.10 mole percent PPP in triacetin, taken at a cooling/heating rate of 0.75°C/min.

	0.02 mole% PPP			0.05 mole% PPP		
Rate (°C/min)	T_{cryst} (°C)	T_{diss} (°C)	MSZW (°C)	T_{cryst} (°C)	T_{diss} (°C)	MSZW (°C)
0.75	47.3	54.4	7.2	48.7	61.4	12.7
	46.7	54.2	7.5	49.6	61.4	11.8
	46.8	54.2	7.4	49.1	61.4	12.3
0.50	47.4	53.1	5.7	50.4	61.3	10.9
	47.3	53.4	6.1	50.0	61.2	11.2
	47.1	53.0	5.9	50.0	61.3	11.3
0.25	48.0	51.4	3.4	51.1	61.2	10.1
	47.0	51.3	4.3	51.0	61.3	10.3
	47.3	51.4	4.1	51.0	61.2	10.2
0.10	48.6	50.2	1.6	52.8	61.1	8.3
	49.2	50.3	1.1	52.6	61.0	8.4
	48.9	50.2	1.3	52.5	61.0	8.5

Table 4.1. The crystallisation and dissolution temperatures and the metastable zone width of the binary system PPP/triacetin at 0.02 and 0.05 mole percent.

Rate (°C/min)	0.10 mole% PPP			0.15 mole% PPP			100% PPP		
	T_{cryst} (°C)	T_{diss} (°C)	MSZW (°C)	T_{cryst} (°C)	T_{diss} (°C)	MSZW (°C)	T_{cryst} (°C)	T_{diss} (°C)	MSZW (°C)
0.75	51.3	64.3	13.0	51.6	64.1	12.5	51.2	71.2	20.0
	51.3	64.3	13.0	51.7	64.1	12.4	51.5	71.7	20.2
	51.2	64.2	13.0	51.4	64.1	12.7	51.8	72.5	20.7
0.50	52.4	64.0	11.6	52.1	64.0	11.9	52.4	70.8	18.4
	52.3	64.0	11.7	52.3	63.9	11.6	52.2	70.0	17.8
	52.2	63.9	11.7	52.3	63.7	11.4	52.0	70.3	18.3
0.25	52.7	63.6	10.9	53.6	63.6	10.0	52.4	69.6	17.2
	52.9	63.7	10.8	53.9	63.7	9.8	52.7	69.7	17.0
	52.8	63.7	10.9	53.8	63.6	9.8	53.1	69.8	16.7
0.10	54.3	63.3	9.0	55.0	63.5	8.5	54.2	68.1	13.9
	54.5	63.3	8.8	54.4	63.4	8.9	54.5	68.0	13.5
	54.0	63.1	9.1	54.5	63.4	8.9	54.4	68.1	13.7

Table 4.2. The crystallisation and dissolution temperatures and the metastable zone width of tripalmitin (100%) and of the binary system PPP/triacetin at 0.10 and 0.15 percent mole.

Concentration (mole percent)	T_{sat} (°C)	MSZW (°C)	m
0.02	49.7 (98%) [1.8]	1.2 (94%) [2.6]	1.1 (94%) [0.7]
0.05	61.0 (80%) [0.1]	8.3 (92%) [1.6]	5.4 (97%) [0.1]
0.10	63.2 (93%) [0.4]	8.9 (93%) [1.5]	5.6 (98%) [0.1]
0.15	63.4 (91%) [0.3]	8.4 (96%) [1.7]	5.4 (97%) [0.2]
100	67.9 (89%) [1.6]	13.6 (91%) [2.7]	5.2 (97%) [0.2]

Table 4.3. The saturation temperatures, metastable zone width (MSZW) and order of reaction (m) calculated for tripalmitin sample and the solutions of tripalmitin in triacetin. Correlation coefficients are given in brackets, with the standard deviations in square brackets.

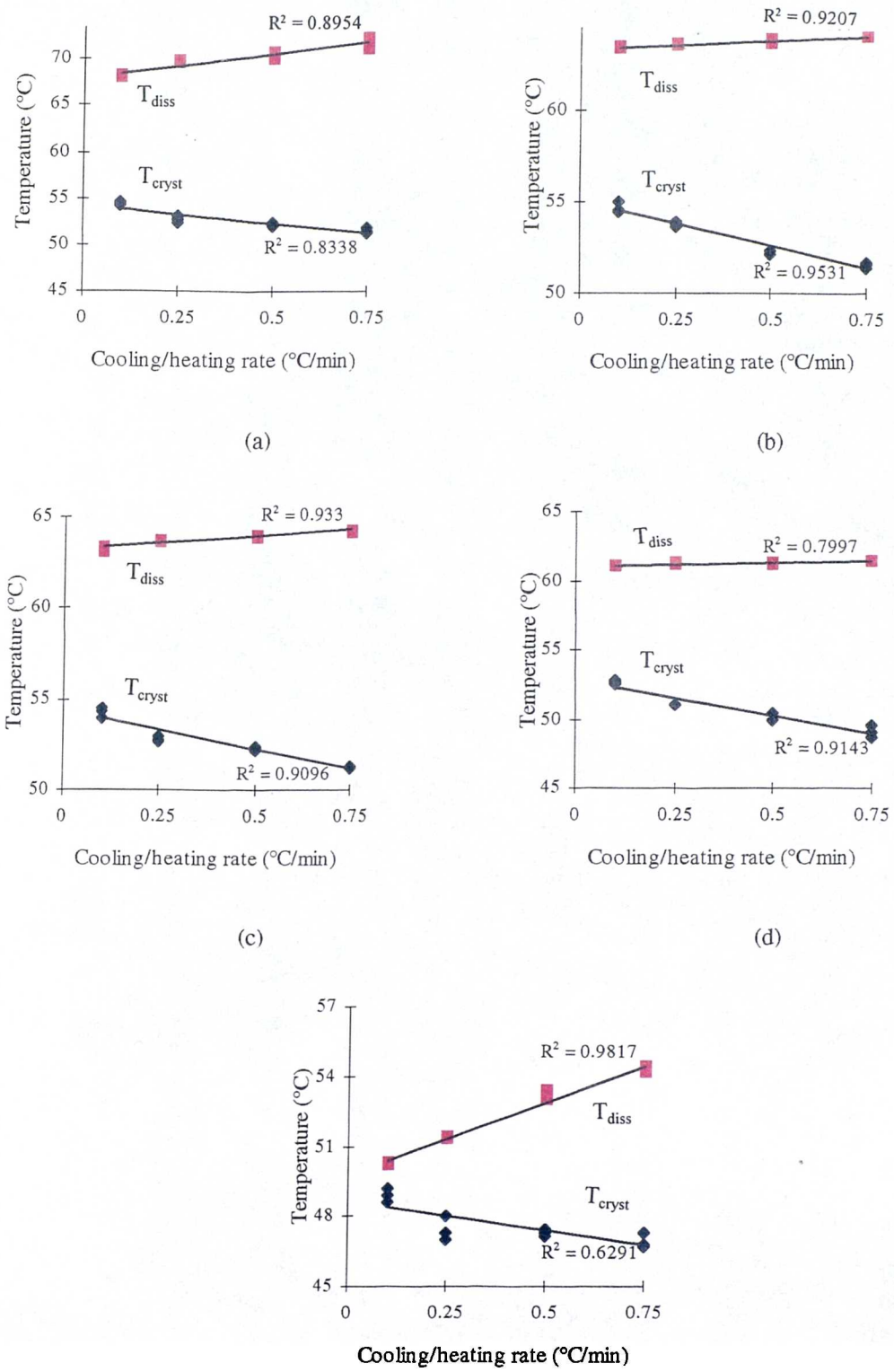

Figure 4.4. The temperature of crystallisation and dissolution of tripalmitin (a) and of 0.15 mole% (b), 0.10 mole% (c), 0.05 mole% (d) and 0.02 mole% (e) solutions of tripalmitin in triacetin.

The temperature of saturation decreases from the smallest to the highest concentration, but the change is not linear. The temperature of saturation calculated for the 0.02 mole percent solution of PPP in triacetin is 49.7°C, while for the solution at 0.05 mole percent the temperature of saturation is 61.0°C. The difference between these two values is 11.3°C. Comparing the value of temperature of saturation observed for 0.05 mole percent solution (61.0°C) with that recorded for 0.10 mole percent solution (63.2°C), it must be noted that the difference is only 2.2°C(see also Figure 4.5).

The values calculated for the metastable zone width show a large difference between 0.02 and 0.05 mole percent solutions, while the metastable zone width is almost constant from 0.05 to 0.15 mole percent solutions. A difference in MSZW value is also noticed between the 0.15 mole percent solution and the pure PPP sample (Figure 4.6).

The large metastable zone width recorded for the PPP sample suggests that it does not easily nucleate, until high supersaturations are reached, therefore it is relatively easy to produce large numbers of small crystals, while the slow growth of few larger crystals will be a more complex process. Adding triacetin, the metastable zone width is reduced considerably with the nucleation and the growth occurring more spontaneously. The low value of metastable zone width observed for 0.02 mole percent solution of PPP in triacetin is only 1.2°C and this could be due to the excessively low quantity of tripalmitin in the system.

The apparent order of nucleation (m) shows the same trend observed for the temperature of saturation. The order of reaction calculated for the 0.02 mole percent solution of PPP in triacetin is 1.1, while for the other concentrations, including the pure PPP sample, the order of reaction varies between 5.2 and 5.6.

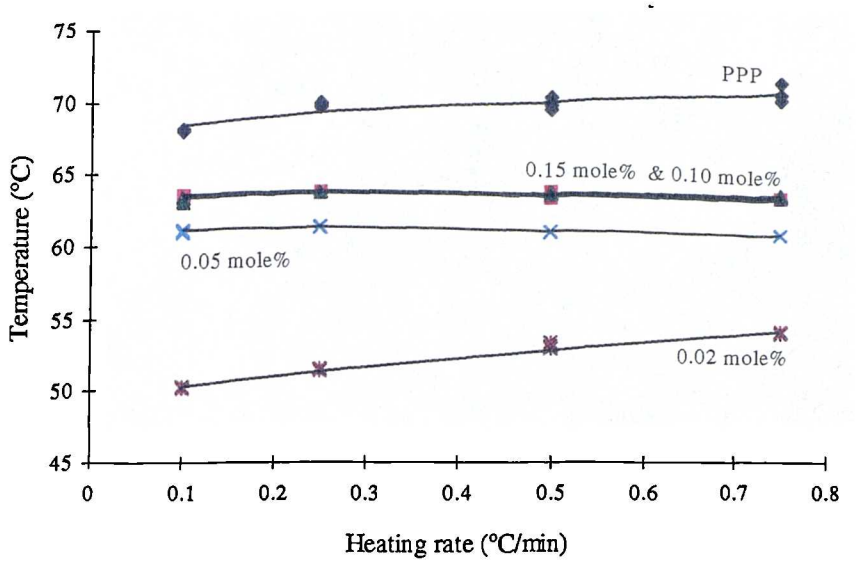

Figure 4.5. Dissolution temperatures as a function of heating rate for the PPP sample, and for the 0.02, 0.05, 0.10 and 0.15 mole% of PPP crystallised from triacetin.

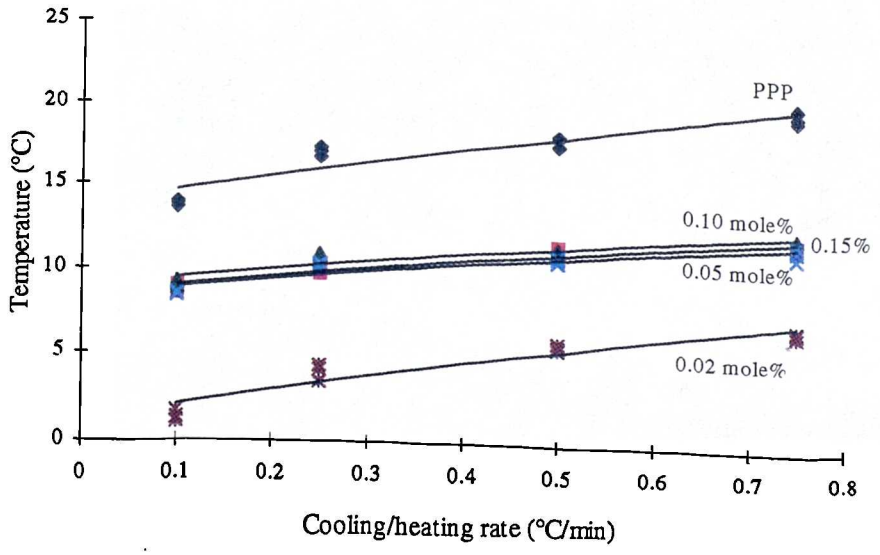

Figure 4.6. Metastable zone width measurements for the tripalmitin sample and for tripalmitin crystallised from triacetin, as a function of cooling rate.

4.4.1.1 *Phase diagram of the binary system tripalmitin and triacetin*

The measured values of temperature of saturation were compared with those predicted using the Hildebrand solubility law [Hildebrand, 1950]. This is essentially an integrated form of the Clausius-Clapeyron equation:

$$1/T = (1/T_m - R\ln\chi/\Delta H_f) \qquad (4.4)$$

where T_m is the absolute melting point of the pure PPP, R is the universal gas constant, χ is the mole fraction of PPP, and ΔH_f is the enthalpy of fusion of the pure PPP. This equation assumes that tripalmitin forms crystals that do not contain solvent. It has been assumed that T_m is 66.4°C and ΔH_f is 165 kJ mol^{-1} [Norton, 1985; Kellens, 1990].

The experimental and ideal behaviours for the tripalmitin and triacetin system are shown in Figure 4.7. The experimental data show a very large positive deviation from ideal behaviour. This could be due to the fact that cohesive forces between like molecules are stronger than those between PPP and triacetin. The molecules seem to prefer to be on their own than together. Then, the difficulty in dissolving PPP in triacetin tends to suggest that the two components are not very compatible and the mixture is almost behaving as a two component mixture with the melting behaviour being close to that of pure PPP. Timms (1984) observed that measurable deviations from ideality occur when the triglycerides differ appreciably in molecular weight (and hence also in molecular volume). This is the case of the binary mixture PPP and triacetin, where the molecular weights are 807.3 and 218 kg/kmol, respectively.

In Figure 4.8 the natural logarithms of the mole fraction are plotted versus the inverse of temperature of saturation ($°K^{-1}$) and the Van't Hoff equation applied to determine the enthalpy and entropy of dissolution from the slope and the intercept, respectively. These parameters give a measure of the energy and disorder within the solute/solvent system.

Two trends can be observed from Figure 4.8. A value of enthalpy and entropy of dissolution can be calculated for each one. The values are summarised on Table 4.4.

Concentrations (mole %)	ΔH_d (kcal mol^{-1})	ΔS_d (cal K^{-1} mol^{-1})	Correlation coefficient
All	27.2	67.2	86
0.05, 0.10 and 0.15	87.0	245.3	91

Table 4.4. The enthalpy and entropy of dissolution of tripalmitin in triacetin.

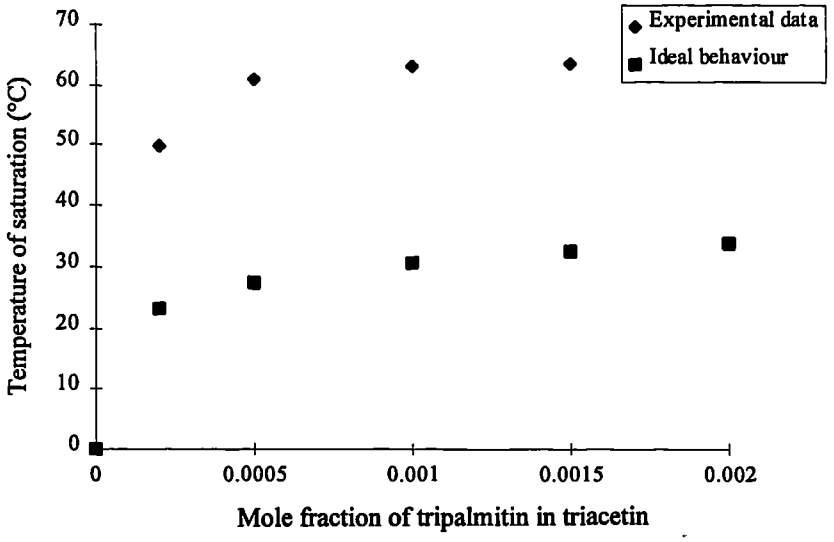

Figure 4.7. Phase diagram of the binary mixture PPP and triacetin.

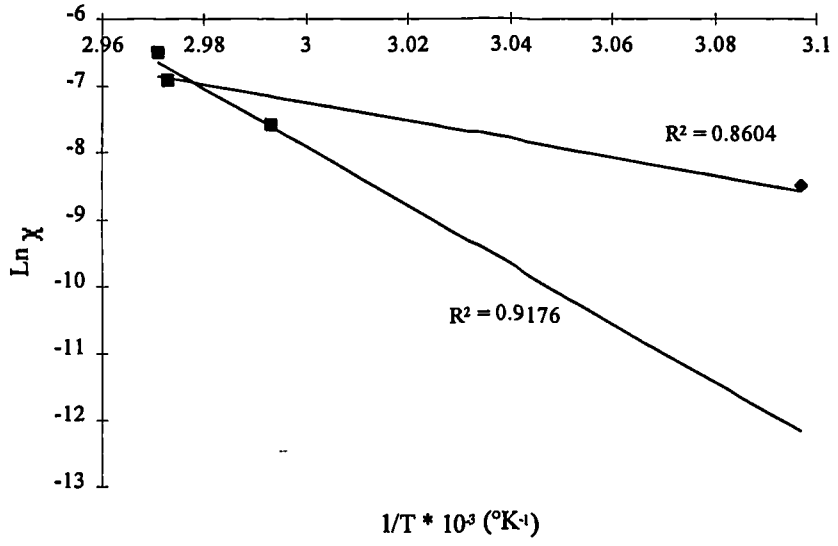

Figure 4.8. Plot of Ln χ versus $1/T_{sat}$ ($°K^{-1}$) for PPP crystallised from triacetin at 0.02, 0.05, 0.10 and 0.15 mole % concentrations.

4.4.2 *Tripalmitin in Triolein*

This binary system is of great interest for many industrial processes of oils and fats because of the large difference in melting point of the two triglycerides [Norton, 1985]. At room temperature, tripalmitin (PPP) is a simple solid saturated triglycerides whereas triolein (OOO) is a simple liquid unsaturated triglyceride. The chain length of the two triglycerides differs by only two carbons (C_{16} for PPP and C_{18} for OOO), but the hydrocarbon chain of OOO is characterised by the presence of a cis double bond in position 9.

Six different tripalmitin concentrations were used to study the crystallisation behaviour of the binary mixture tripalmitin/triolein: 25, 20, 15, 10, 5 and 1 mole percent. Tables 4.5, 4.6 and 4.7 show the summary of all experimental data, including those already discussed for pure PPP. Each run has been repeated three times and very good reproducibility was observed. Figure 4.9 shows the profile of a typical cooling/heating cycle obtained from the experiments. The temperatures of crystallisation and dissolution are shown in Figure 4.10.

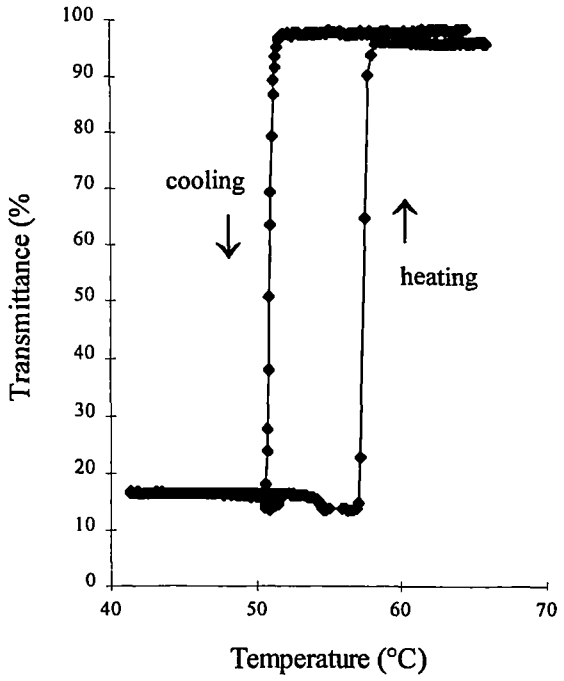

Figure 4.9. Transmittance (%) versus temperature (°C) for 25 mole percent of PPP in OOO. The small reduction in transmittance just prior the dissolution might be to a change in the crystalline phase.

	100% mole PPP			25% mole PPP			20% mole PPP		
Rate (°C/min)	Tcryst (°C)	Tdiss (°C)	MSZW (°C)	Tcryst (°C)	Tdiss (°C)	MSZW (°C)	Tcryst (°C)	Tdiss (°C)	MSZW (°C)
0.75	51.2	71.2	20.0	47.6	60.5	12.9	49.5	57.9	8.4
	51.5	71.7	20.2	48.0	60.6	12.6	49.7	57.5	7.8
	51.8	72.5	20.7	48.1	61.0	12.9	49.2	57.7	8.5
0.50	52.4	70.8	18.4	48.6	59.2	10.6	49.8	57.2	7.4
	52.2	70.0	17.8	48.7	59.3	10.6	49.6	57.2	7.6
	52.0	70.3	18.3	48.7	59.1	10.4	49.4	57.2	7.8
0.25	52.4	69.6	17.2	51.3	58.2	6.9	47.6	56.4	8.8
	52.7	69.7	17.0	51.2	58.2	6.9	47.7	56.9	9.2
	53.1	69.8	16.7	51.2	58.3	7.1	47.5	56.9	9.4
0.10	54.2	68.1	13.9	51.7	57.9	6.2	49.0	56.4	7.4
	54.5	68.0	13.5	51.9	57.8	6.1	49.1	56.1	7.0
	54.4	68.1	13.7	52.5	57.8	5.3	49.0	56.1	7.1

Table 4.5. The crystallisation and dissolution temperatures and the metastable zone width of the PPP sample and 25 and 20 mole percent solutions of PPP in OOO.

	15% mole PPP			10% mole PPP		
Rate (°C/min)	Tcryst (°C)	Tdiss (°C)	MSZW (°C)	Tcryst (°C)	Tdiss (°C)	MSZW (°C)
0.75	43.5	56.1	12.6	41.5	55.4	13.9
	43.9	56.2	12.3	41.3	55.3	14.0
	43.6	56.0	12.4	41.4	55.3	13.9
0.50	44.5	55.9	11.4	41.7	55.1	13.4
	44.4	55.9	11.5	42.0	55.2	13.2
	44.7	55.8	11.1	42.2	55.1	12.9
0.25	45.2	55.7	10.5	42.8	54.4	11.6
	45.8	55.7	9.9	42.6	54.5	11.9
	45.8	55.7	9.9	42.7	54.7	12.0
0.10	46.9	55.4	8.5	45.7	54.3	8.6
	47.3	55.4	8.1	45.1	54.2	9.1
	46.6	55.4	8.8	45.9	54.2	8.3

Table 4.6. The crystallisation and dissolution temperatures and the metastable zone width of 15% and 20% solutions of PPP in OOO.

	5% mole PPP			1% mole PPP		
Rate (°C/min)	Tcryst (°C)	Tdiss (°C)	MSZW (°C)	Tcryst (°C)	Tdiss (°C)	MSZW (°C)
0.75	39.9	50.2	10.3	26.5	41.7	15.2
	40.0	50.2	10.2	26.9	41.6	14.7
	38.6	50.2	11.6	26.9	41.6	14.7
0.50	38.7	49.9	11.2	24.0	41.1	17.0
	38.6	49.9	11.3	24.0	41.0	17.0
	39.0	49.8	10.8	24.3	41.0	16.7
0.25	40.2	49.4	9.2	27.1	41.0	13.9
	40.2	49.5	9.3	28.9	41.0	12.1
	40.2	49.4	9.2	28.4	41.0	12.6
0.10	42.4	49.2	6.8	31.2	40.7	9.5
	42.1	49.2	7.1	31.8	40.8	9.0
	42.2	49.1	6.9	31.2	40.6	9.4

Table 4.7. The crystallisation and dissolution temperatures and the metastable zone width of 5 and 1 mole percent solutions of PPP in OOO.

Concentration (mole percent)	T_{sat} (°C)	MSZW (°C)	m
1*	40.6 (97%) [0.4]	7.7 (97%) [3.2]	3.9 (90%) [0.2]
5*	49.0 (97%) [0.4]	7.1 (78%) [1.9]	3.4 (99%) [0.2]
10	54.1 (93%) [0.5]	8.9 (82%) [2.3]	4.0 (94%) [0.2]
15	55.4 (92%) [0.3]	8.2 (94%) [1.7]	5.2 (97%) [0.2]
20*	56.0 (91%) [0.6]	7.0 (75%) [0.8]	11.4 (66%) [0.1]
25	57.2 (96%) [1.3]	4.6 (98%) [3.2]	2.3 (93%) [0.3]
100	67.9 (89%) [1.5]	13.6 (91%) [2.7]	5.2 (97%) [0.2]

Table 4.8. The saturation temperatures, metastable zone width (MSZW) and order of reaction (m) calculated for tripalmitin sample (100%) and the solutions of tripalmitin in triolein. Correlation coefficients are given in brackets, with the standard deviations in square brackets.

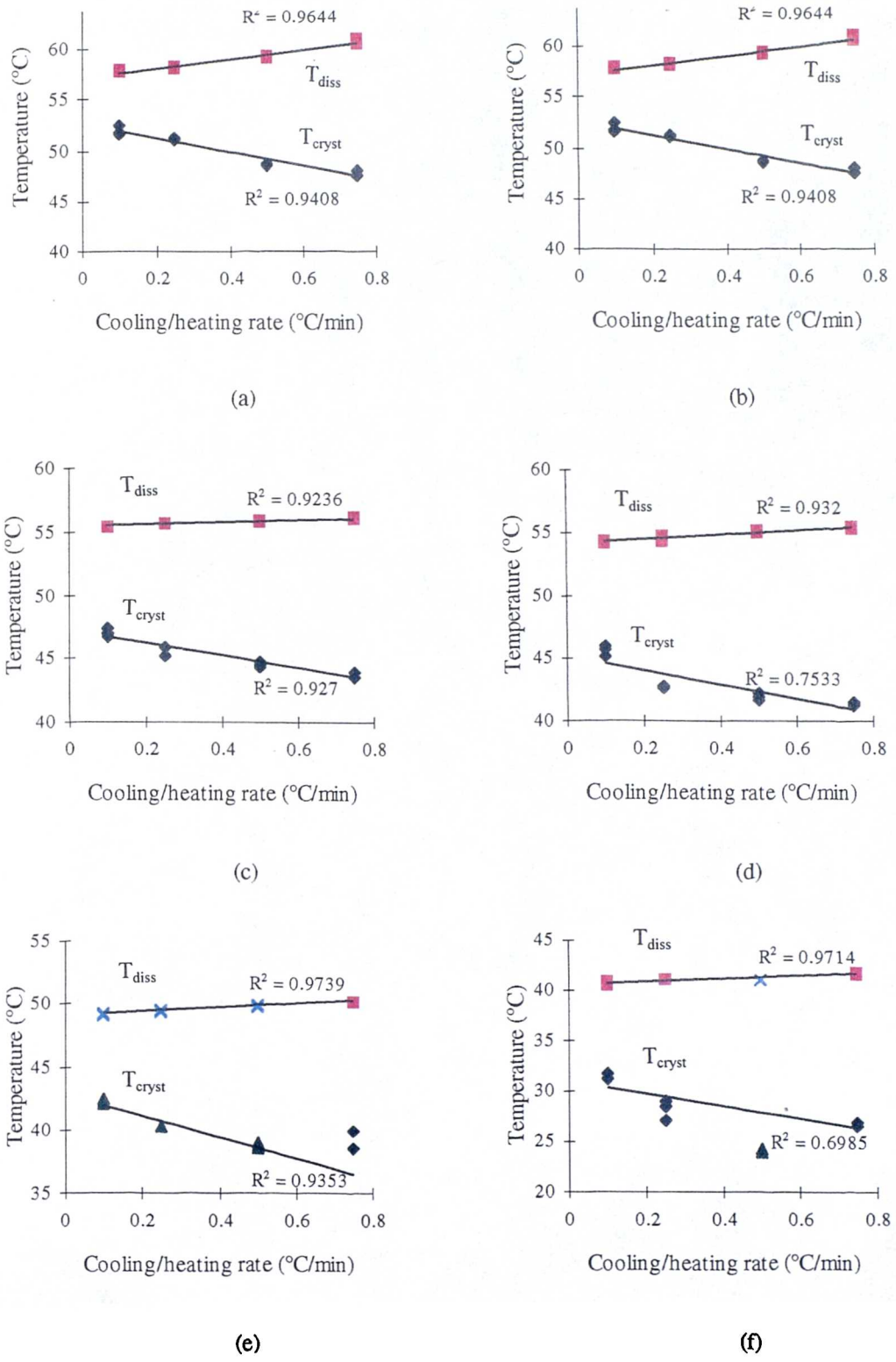

Figure 4.10. The temperature of crystallisation and dissolution of 25 mole% (a), 20 mole% (b), 15 mole% (c), 10 mole% (d), 5 mole% (e) and 1 mole% (f) solutions of tripalmitin in triolein.

4.4.2.1. *Temperatures of crystallisation and dissolution*

The temperature of crystallisation increases from the fastest to the slowest cooling rate for the 25, 20 and 15 mole percent solutions of PPP in OOO (Figure 4.10 (a), (c) and (d), respectively). In the case of the 1 mole percent solution, the values of temperature of crystallisation show a good trend between 0.75, 0.25 and 0.10°C/min, while at a rate of 0.50°C/min the temperatures of crystallisation are smaller than those recorded at 0.75°C/min (Figure 4.10 (f)). A similar situation is observed for 5 mole percent solution, but, in this case, the best trend is detected between the rates 0.50 and 0.10°C/min (Figure 4.10 (e)). At different rates, a change in crystallisation behaviour is noted also for the 20 mole percent solution, but in this case the difference appears at a rate of 0.25°C/min (Figure 4.10 (b) and Table 4.5). This different way of crystallisation as a function of the cooling rate could be indicative of phase separation. In a previous study [Ng, 1989], it has been found that, by increasing the OOO content in the solution, two different polymorphs of PPP can be formed. One of them has been earlier identified to be a β crystal [Norton, 1985], while the other could be either the α- or β'-polymorph of PPP, which melt at 45 and 57°C, respectively.

The temperatures of dissolution decrease from the fastest to the slowest heating rate for all systems studied. The values, recorded at different heating rates, are very close. In the case of the 1 mole percent solution, the values of temperature of dissolution recorded for the rates 0.50 and 0.25°C/min are the same. The greatest change in terms of temperature of dissolution, as a function of heating rate, is observed for the 25 mole percent solution of PPP in OOO and it corresponds to only 2°C. The dissolution phase of the cycle does not seem to be influenced by the heating rate used.

It should be noted that the spread of the values of crystallisation is greater compared with those of dissolution. The scatter of these results is due to the presence of residual nuclei in the solutions, which can be minimised by increasing the preheating time, but cannot be completely removed [Meenan, 1992]

4.4.2.2 *Calculations of kinetic parameters*

Temperatures of saturation, metastable zone width and the orders of reactions were calculated and summarised in Table 4.8. Due to non-linear behaviour occurring when the rates of 0.25, 0.50 and 0.75°C/min are used, respectively, for 20, 5 and 1 mole percent solutions, these results were not employed in the kinetics calculations.

The temperature of saturation increases from the smallest to the highest concentration of tripalmitin in triolein. Between 25 and 10 mole percent solutions, the values of temperature of saturation are very close, they vary in the range from 57.2°C to 54.1°C. It is important to note that between 10 and 1 mole percent solutions, the values of temperature of saturation show the widest degree of variation. In contrast to the binary mixture tripalmitin/triacetin, however it is important to underline that the values of temperature of saturation recorded for the mixture PPP/OOO are very much lower than the value of melting point recorded for pure PPP (Figure 4.11). This might be due or to the fact that PPP and OOO are more compatible than PPP and triacetin (thermodynamic effect) or to a diffusion of the molecules from the surface depending on the different viscosity between triacetin and triolein (kinetic effect).

The metastable zone widths decrease from the smallest to the highest concentration of tripalmitin in triolein (Figure 4.12). This reflects the fact that it becomes easier for the system to nucleate as the solution is more concentrated in tripalmitin.

The apparent order of nucleation (m) increases from 1 to 20 mole percent of tripalmitin in triolein, whereas the value of m calculated for the 25 mole percent solution results to be smallest than the value calculated for 1 mole percent solution.

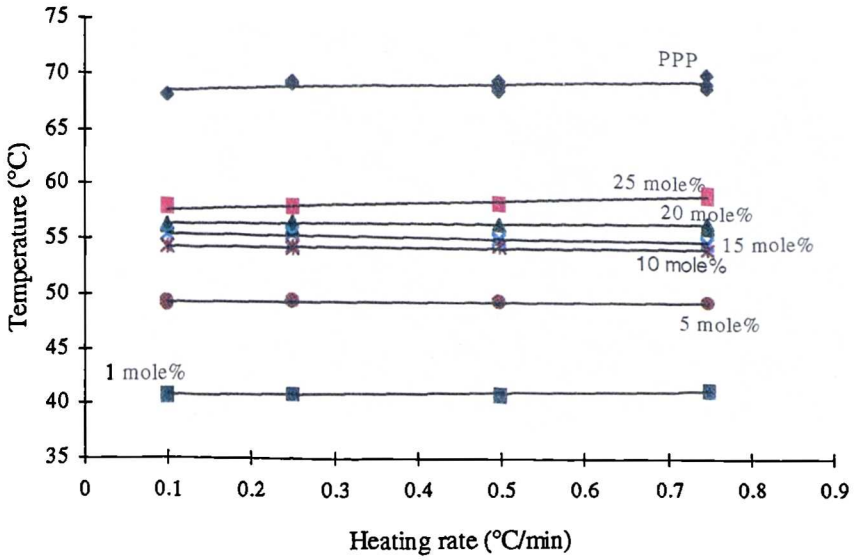

Figure 4.11. Dissolution temperatures as a function of heating rate for the PPP sample, and for the 25, 20, 15, 10, 5 and 1 mol percent of PPP crystallised from triolein.

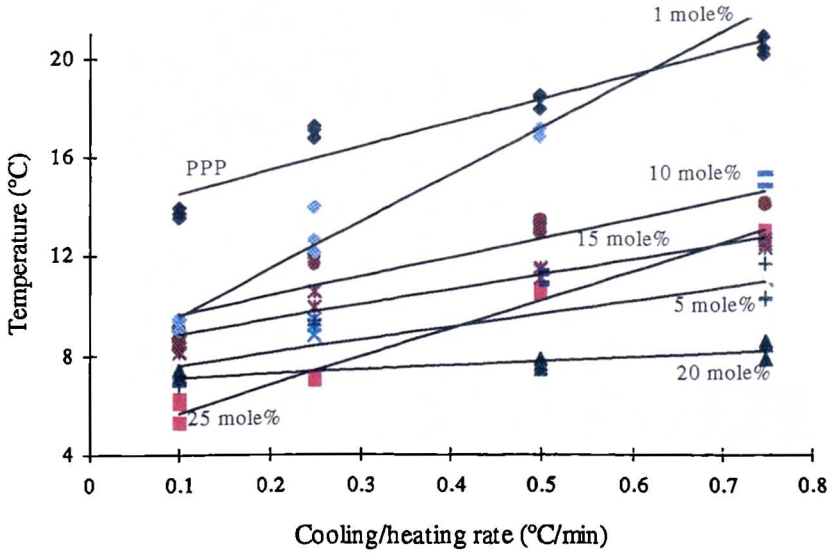

Figure 4.12. Metastable zone width measurements for tripalmitin sample and for tripalmitin crystallised from triolein, as a function of cooling rate.

4.4.2.3 *Phase diagram of the binary system tripalmitin and triolein*

The measured values of temperature of saturation were compared with those predicted using the Hildebrand solubility law [Hildebrand, 1950] (equation (4.4)). The experimental and ideal behaviour for the tripalmitin and triolein system are shown in Figure 4.13. It is clearly evident that the experimental data follow the ideal behaviour. Previously, Kung (1966) studied mixtures corresponding to part of the range of compositions of these two components, and an incomplete diagram similar to that in Figure 4.13 has been constructed from his results. This incomplete solid solutions diagram is associated with a difference in melting points of more than 30°C between the two components. Thus, the phase diagrams exhibit the monotectic nature of the binary mixture [Kerridge, 1952]. Previous work [Rossell, 1967; Hale, 1981] has demonstrated that there is neither a eutectic mixture nor a mixed crystal formation in this binary system. The solidus line has not been clearly worked out and there is some suggestion that there may be a limited region of solid solution of the unsaturated material in a polymorph (probably β) of the saturated material. This could explained the small values of temperature of saturation for the mixture PPP/OOO with respect to pure PPP, due to the presence of OOO in the solid phase.

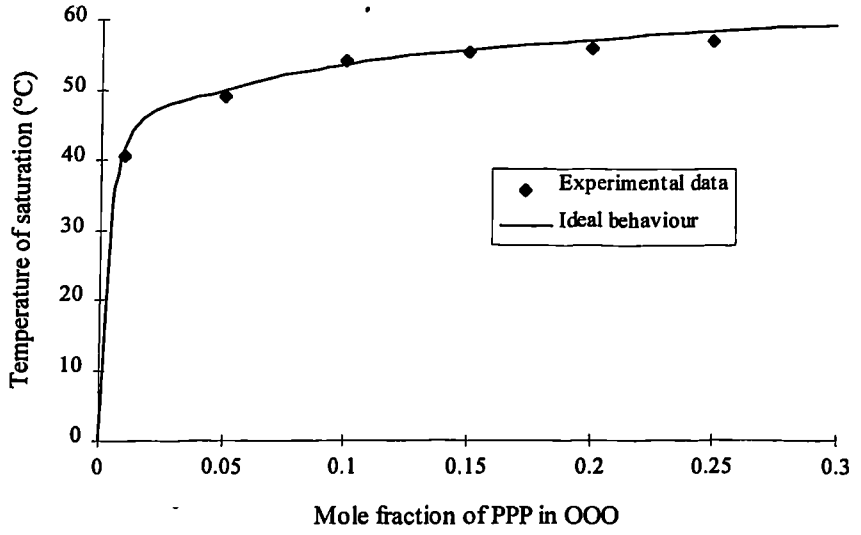

Figure 4.13. Phase diagram of the binary mixtures of tripalmitin and triolein. The system is monotectic

In Figure 4.14 the natural logarithm of the mole fraction is plotted versus the inverse of temperature of saturation ($°K^{-1}$) and the Van't Hoff equation is applied to determine the enthalpy and entropy of dissolution. These parameters give a measure of the energy and disorder within the solute/solvent system. This equation also assesses solution ideality.

For the mixture PPP/OOO the enthalpy and entropy of dissolution were 38.9 kcal mol^{-1} and 114.6 cal$°K^{-1}mol^{-1}$, respectively.

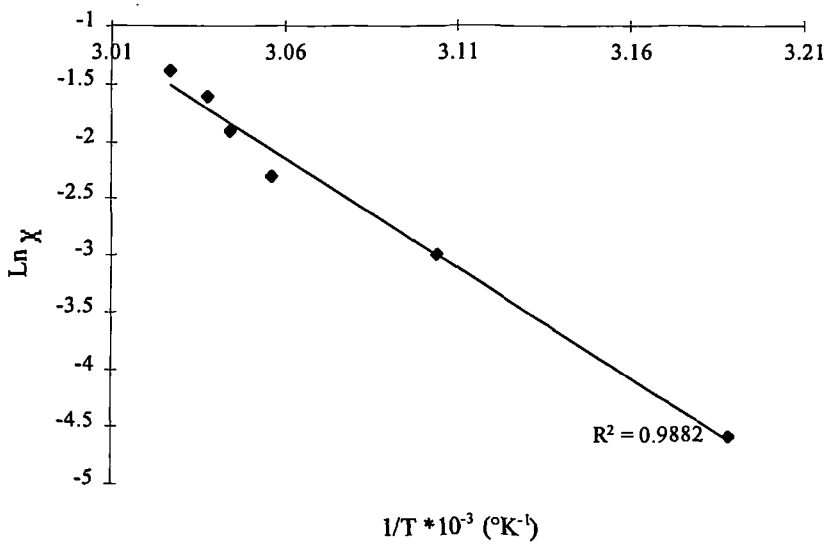

Figure 4.14. Plot of Ln χ versus $1/T_{sat}$ ($°K^{-1}$) for PPP crystallised from OOO at 25, 20, 15, 10, 5 and 1 mole percent concentrations. Correlation coefficient of best fit straight line was 99 %.

4.4.3 *Tripalmitin in Cocoa Butter*

Twelve different concentrations were used to study the crystallisation behaviour of the binary mixture tripalmitin/cocoa butter: 25, 20, 15, 10, 9, 8, 7, 6, 5, 4, 3 and 1 mole percent solutions. Also the nucleation behaviour of pure cocoa butter was analysed. No studies on these mixtures have been reported in literature.

The cocoa butter used for these experiments was analysed by Gas Chromatography (GC) at RSSL (Reading Scientific Service Limited).The GC results are summarised in Table 4.9. The average molecular weight (MW) of cocoa butter was found to be 861.68 g/mol.

The summary of all experimental data, including those obtained for pure tripalmitin and cocoa butter, are given in Tables 4.10, 4.11, 4.12, 4.13 and 4.14. Each run has been repeated three times and, again for this system, good reproducibility was observed. Figure 4.15 shows the profile of typical cooling/heating cycle obtained from the experiments carried out. The temperatures of crystallisation and dissolution are shown in Figures. 4.16, 4.17 and 4.18.

Triglycerides	MW	%
PLiO	856.0	0.4
PLiP	831.4	1.3
POPo	**	0.1
Unknown	**	0.1
OOO	885.4	0.3
POO	859.4	2.2
PLiS	858.0	3.0
POP	833.4	16.1
PPP	807.3	0.3
SOO	887.5	3.1
SLiS	886.0	1.6
POS	861.4	40.0
PPS	834.0	0.6
Unknown	**	0.1
SOS	889.5	29.2
SSP	863.4	0.3
AOS	659.0	1.1
SSS	891.5	0.1

Table 4.9. Gas chromatography analysis of cocoa butter used for these experiments.

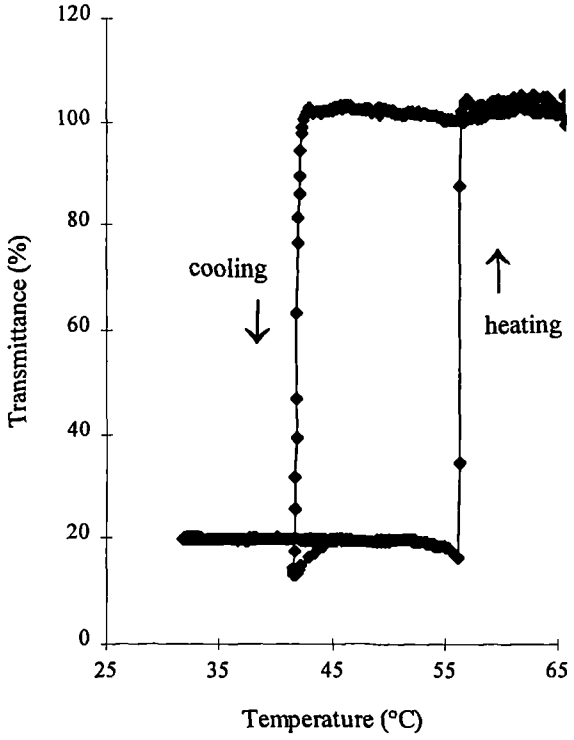

Figure 4.15. Transmittance (%) versus temperature (°C) for the mixture 20 mole percent of PPP in cocoa butter at a rate of 0.25°C/min.

	100% mole PPP			25% mole PPP			20% mole PPP		
Rate (°C/min)	Tcryst (°C)	Tdiss (°C)	MSZW (°C)	Tcryst (°C)	Tdiss (°C)	MSZW (°C)	Tcryst (°C)	Tdiss (°C)	MSZW (°C)
0.75	51.2	71.2	20.0	39.0	60.1	21.1	35.7	57.4	21.7
	51.5	71.7	20.2	39.3	60.0	20.7	35.7	57.3	21.6
	51.8	72.5	20.7	39.6	59.8	20.2	35.7	57.3	21.6
0.50	52.4	70.8	18.4	41.6	59.4	17.8	39.9	56.9	17.0
	52.2	70.0	17.8	42.0	59.5	17.5	40.4	57.1	16.7
	52.0	70.3	18.3	41.7	59.4	17.7	40.0	57.0	17.0
0.25	52.4	69.6	17.2	44.3	58.9	14.6	40.7	56.7	16.0
	52.7	69.7	17.0	44.3	58.9	14.6	41.3	56.7	15.4
	53.1	69.8	16.7	44.9	58.9	14.0	41.0	56.7	15.7
0.10	54.2	68.1	13.9	47.2	58.6	11.4	43.6	56.1	12.5
	54.5	68.0	13.5	47.6	58.4	10.8	43.7	56.0	12.3
	54.4	68.1	13.7	47.4	58.5	11.1	43.3	56.1	12.8

Table 4.10. The crystallisation and dissolution temperatures and the metastable zone width of PPP sample , 25 and 20 mole percent solutions of PPP in cocoa butter.

	15% mole PPP			10% mole PPP			9% mole PPP		
Rate (°C/min)	Tcryst (°C)	Tdiss (°C)	MSZW (°C)	Tcryst (°C)	Tdiss (°C)	MSZW (°C)	Tcryst (°C)	Tdiss (°C)	MSZW (°C)
0.75	32.9	56.2	23.3	28.7	52.6	23.9	27.7	49.7	22.0
	32.7	56.3	23.6	28.8	52.4	23.6	27.8	49.7	21.9
	33.1	56.7	23.6	28.9	52.4	23.5	27.8	49.9	22.1
0.50	33.9	55.4	21.5	29.5	52.1	22.6	28.3	47.7	19.4
	34.1	56.3	22.2	29.2	52.2	23.0	28.1	47.6	19.5
	34.6	56.0	21.4	29.8	52.2	22.4	28.2	47.8	19.6
0.25	38.0	54.9	16.9	31.1	52.3	21.2	30.5	46.9	16.4
	37.6	54.9	17.3	31.5	52.2	20.7	30.2	46.3	16.1
	38.3	55.0	16.7	31.6	52.2	20.6	30.5	46.7	16.2
0.10	41.2	54.7	13.5	36.2	52.4	16.2	34.9	50.8	15.9
	40.7	54.7	14.0	35.5	52.1	16.6	34.7	50.8	16.1
	41.1	54.7	13.6	35.5	52.1	16.6	34.4	50.8	16.4

Table 4.11. The crystallisation and dissolution temperatures and the metastable zone width of 15, 10 and 9 mole percent solutions of PPP in cocoa butter.

	8% mole PPP			7% mole PPP			6% mole PPP		
Rate (°C/min)	Tcryst (°C)	Tdiss (°C)	MSZW (°C)	Tcryst (°C)	Tdiss (°C)	MSZW (°C)	Tcryst (°C)	Tdiss (°C)	MSZW (°C)
0.75	27.2	48.3	21.1	26.2	47.3	21.1	26.0	41.4	15.4
	27.1	48.3	21.2	26.3	47.2	20.9	26.1	41.9	15.8
	27.1	48.2	21.1	26.2	47.1	20.9	26.1	41.5	15.4
0.50	27.3	47.6	20.3	27.2	41.8	14.6	26.2	40.7	14.5
	27.3	47.6	20.3	27.0	42.0	15.0	26.4	40.4	14.0
	27.1	47.4	20.3	27.0	42.0	15.0	26.4	41.1	14.7
0.25	29.2	42.3	13.1	28.0	41.2	13.2	27.5	41.1	13.6
	29.5	42.5	13.0	28.1	41.7	13.6	27.9	40.6	12.7
	29.3	42.3	13.0	28.4	41.8	13.4	27.8	40.3	12.5
0.10	34.4	50.1	15.7	30.8	41.9	11.1	29.9	40.9	11.0
	34.0	50.1	16.1	30.6	41.8	11.2	29.9	41.0	11.1
	34.4	50.1	15.7	30.8	41.9	11.1	29.6	40.8	11.2

Table 4.12. The crystallisation and dissolution temperatures and the metastable zone width of 8, 7 and 6 mole percent solutions of PPP in cocoa butter.

	5% mole PPP			4% mole PPP			3% mole PPP		
Rate (°C/min)	Tcryst (°C)	Tdiss (°C)	MSZW (°C)	Tcryst (°C)	Tdiss (°C)	MSZW (°C)	Tcryst (°C)	Tdiss (°C)	MSZW (°C)
0.75	26.2	40.2	14.0	24.7	37.8	13.1	23.8	36.5	12.7
	26.1	40.4	14.3	24.9	38.0	13.1	23.7	36.5	12.8
	26.1	40.3	14.2	24.8	38.3	13.5	23.8	36.4	12.6
0.50	26.3	39.9	13.6	24.7	37.6	12.9	23.7	36.4	12.7
	26.0	40.1	14.1	24.7	37.5	12.8	23.8	36.4	12.6
	26.0	39.9	13.9	24.7	37.5	12.8	23.7	36.5	12.8
0.25	27.3	40.4	13.1	25.0	38.7	13.7	23.9	38.0	14.1
	27.0	40.2	13.2	24.9	38.8	13.9	23.9	38.5	14.6
	27.2	40.2	13.0	25.0	38.7	13.7	23.9	38.1	14.2
0.10	28.6	40.3	11.7	27.1	39.2	12.1	25.8	39.9	14.1
	28.6	40.2	11.6	27.1	39.3	12.2	25.8	39.8	14.0
	28.7	40.4	11.7	27.2	39.3	12.1	26.0	39.3	13.3

Table 4.13. The crystallisation and dissolution temperatures and the metastable zone width of 5, 4 and 3 mole percent solutions of PPP in cocoa butter.

	1% mole PPP			100% mole Cocoa butter		
Rate (°C/min)	Tcryst (°C)	Tdiss (°C)	MSZW (°C)	Tcryst (°C)	Tdiss (°C)	MSZW (°C)
0.75	22.2	27.6	5.4	20.5	35.6	15.1
	21.8	27.6	5.8	20.9	35.4	14.5
	21.7	27.3	5.6	20.9	35.3	14.4
0.50	21.9	28.2	6.3	21.0	35.3	14.3
	22.0	28.5	6.5	21.0	34.9	13.9
	21.9	28.5	6.6	21.1	35.3	14.2
0.25	21.9	33.4	11.5	23.1	34.3	11.2
	21.9	33.3	11.5	23.3	34.3	11.0
	21.8	33.4	11.6	23.1	34.1	11.0
0.10	22.1	35.2	13.1	25.1	33.4	8.3
	22.1	35.1	13.0	25.6	34.1	8.5
	22.2	35.1	12.9	25.6	33.4	7.8

Table 4.14. The crystallisation and dissolution temperatures and the metastable zone width of 1 mole percent solution of PPP in cocoa butter and of cocoa butter sample.

4.4.3.1 *Temperature of crystallisation*

The temperature of crystallisation increases from the fastest to the slowest cooling rate for all concentrations studied. For 25, 20, 15 and 10 mole percent solutions, the spread of these values is much greater compared with that of the temperatures of dissolution. A difference of approximately 8°C is observed between the temperatures of crystallisation recorded at the rates of 0.75 and 0.10°C/min for the 25 mole percent solution.

With increasing concentration of cocoa butter, this difference decreases. For 1 mole percent solution of PPP in cocoa butter, the temperatures of crystallisation do not seem to be influenced by the cooling rate. Besides, between the concentrations of 5 and 1 mole percent, the values recorded at the rates 0.75 and 0.50°C/min are almost the same.

4.4.3.2 *Temperature of dissolution*

The temperature of dissolution decreases from the fastest to the slowest rate for 25, 20 and 15 mole percent solutions. The values, recorded at different heating rates, differ by less than 1.5°C. In the case of 10 mole percent solution, there is no noticeable change in the temperature of dissolution as measured at different rates. Besides, the values, recorded at the rate of 0.25°C/min, are slightly larger than those observed at a rate of 0.50°C/min. For this reason, the results obtained at a rate of 0.25°C/min were not used in the kinetics experiments of this latter mixture.

Decreasing the concentration of tripalmitin, more complex behaviour is observed. For 9 and 8 mole percent solutions, the temperatures of dissolution decrease from a rate of 0.75 to 0.50°C/min, while the values recorded at a rate of 0.10°C/min are greater than those at a rate of 0.75°C/min. In the case of 7 and 6 mole percent solutions, no reasonable difference in terms of temperatures of dissolution is observed between the two rates 0.25 and 0.10°C/min. For these latter four concentrations, due to the non-linear rate-dependent behaviour occurring when a rate of 0.10°C/min is used,

Different effects are noticed with the 5, 4, 3 and 1 mole percent solutions. For the first three mixtures, the values of temperature of dissolution increase from a rate of 0.50 to 0.10°C/min, while at a rate of 0.75°C/min the values recorded are slightly greater than those at a rate 0.50°C/min (see Table 4.13). In this case, the values recorded at a rate of 0.75°C/min will not be used for calculation of kinetics parameters. In the case of 1 mole percent solution, the temperatures of dissolution increase from the fastest to the slowest rate (Table 4.14). Comparing these results with those obtained for cocoa butter alone, it must be noticed that the temperatures of dissolution, recorded for cocoa butter, decrease from the faster to the slowest rate, as would be expected (Figure 4.16). Therefore, it is possible to deduce that adding 1% of PPP is sufficient to influence the dissolution process of the mixture.

In conclusion, the non-linear rate-dependent behaviour, observed when some rates are used, can be explained as a phase separation has taking place during heating.

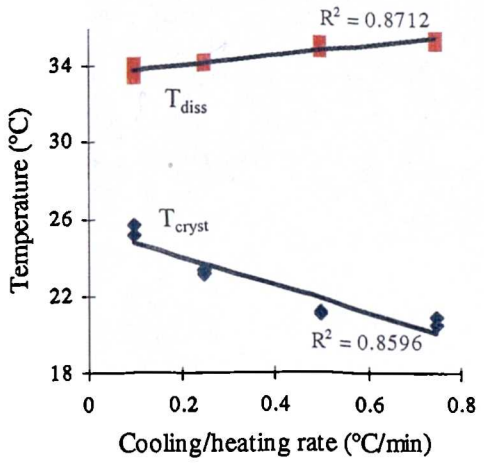

Figure 4.16. The temperature of crystallisation and dissolution of cocoa butter.

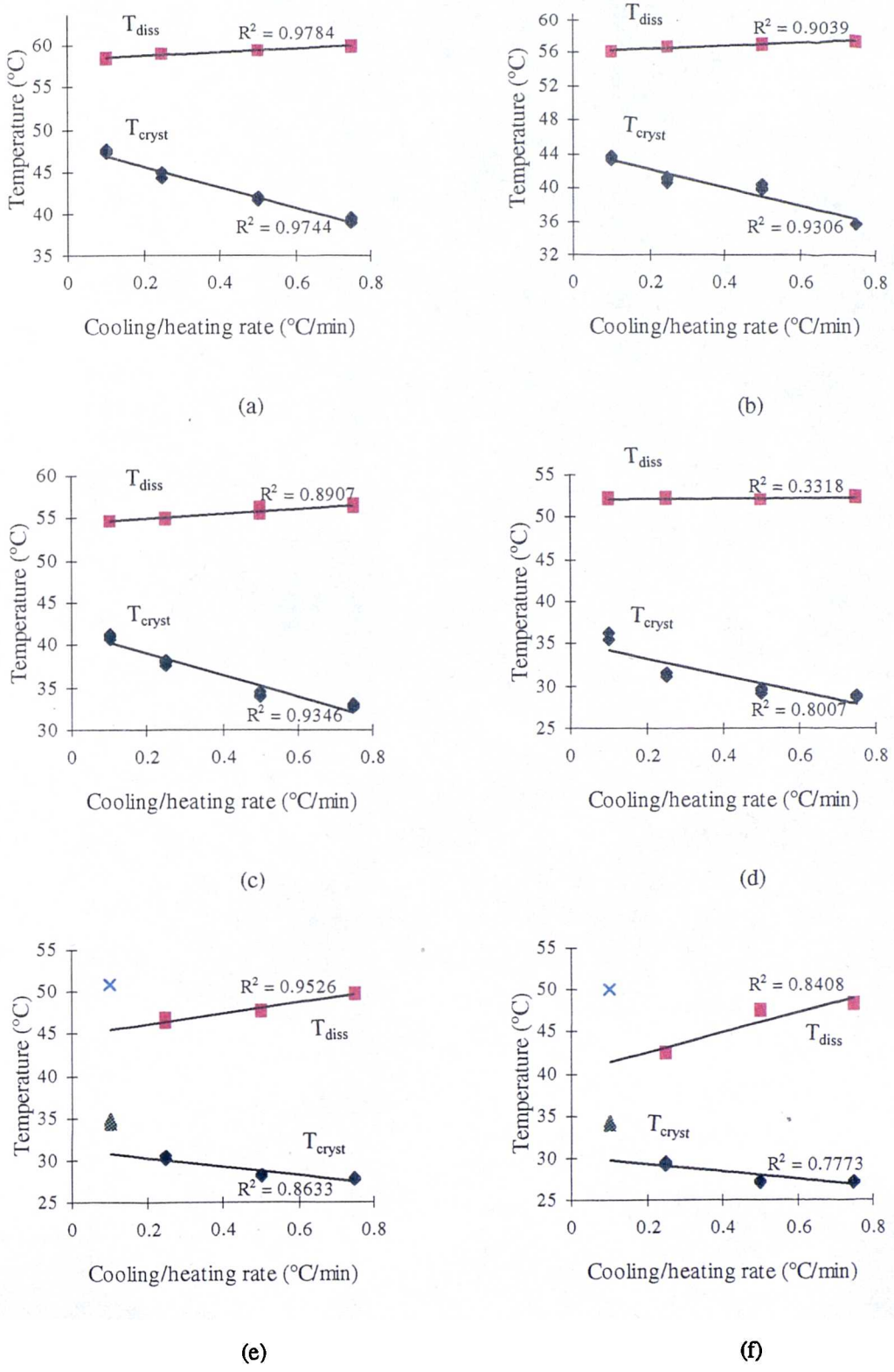

Figure 4.17. The temperature of crystallisation and dissolution of 25 (a), 20 (b), 15 (c), 10 (d), 9 (e), and 8 (f) mole percent solutions of tripalmitin in cocoa butter.

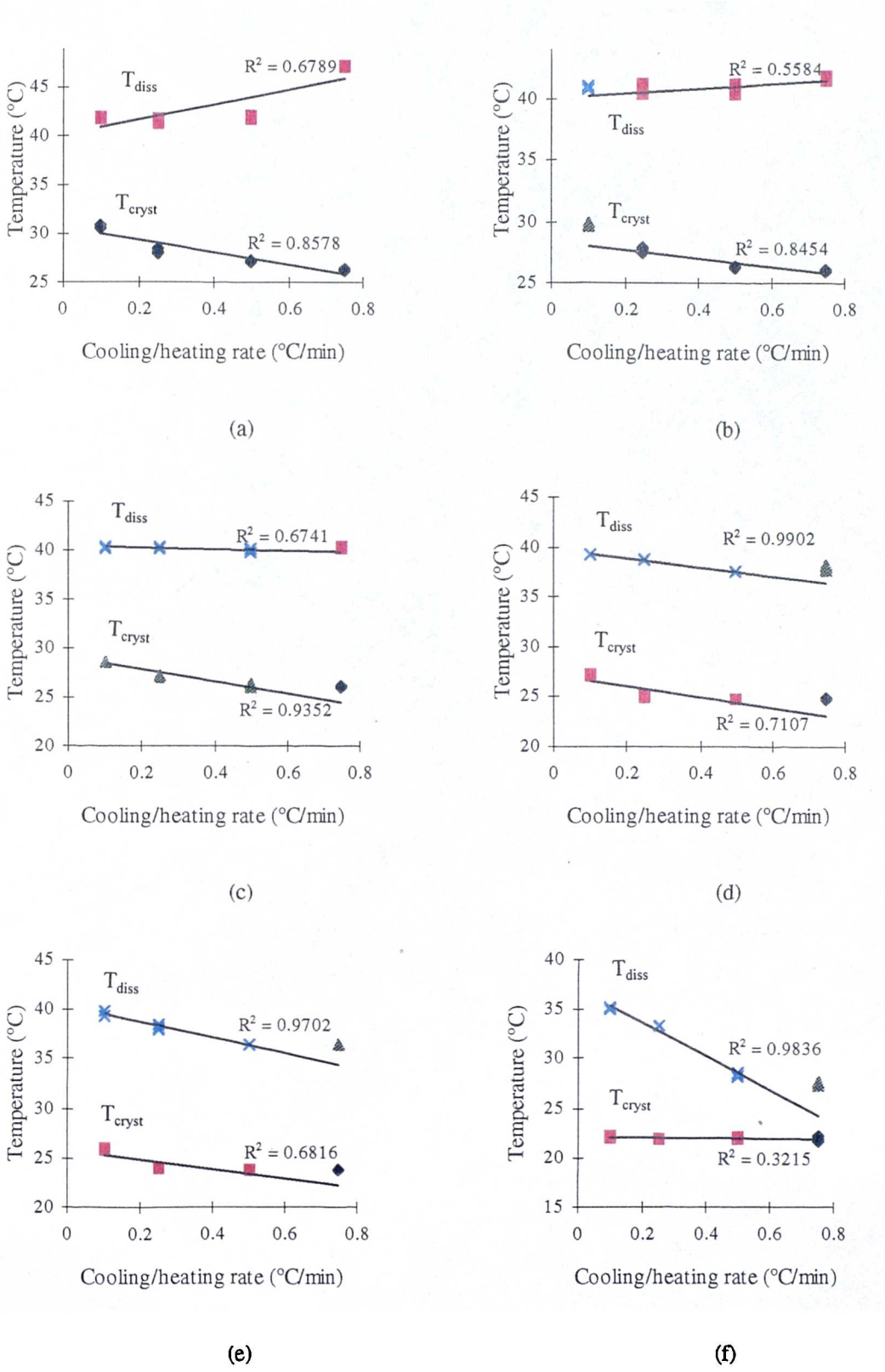

Figure 4.18. The temperature of crystallisation and dissolution of 7 (a), 6 (b), 5 (c), 4 (d), 3 (e) and 1 (f) mole percent solutions of tripalmitin in cocoa butter.

4.4.3.3 *Calculation of nucleation parameters*

Variations in phase composition were observed during the cooling/heating cycle depending on the concentration and the rate used and this phenomenon is more evident during the dissolution process. In this case, some values have not been used for the calculation of nucleation parameters. The details of the data used are given in Table 4.15. Temperatures of saturation and the metastable zone width have been calculated and are summarised in Table 4.16.

Concentration (mole percent)	Rate (°C/min)
25, 20, 15 and 7	All
10	0.75, 0.25 and 0.10
9, 8 and 6	0.75, 0.50 and 0.25
5, 4, 3 and 1	0.50, 0.25 and 0.10
cocoa butter	All

Table 4.15. Detailed of the rates, used for the calculation of nucleation parameters

The temperatures of saturation show a consistent trend between 25 and 8 mole percent solutions of PPP in cocoa butter. As the concentration of tripalmitin is reduced in this range, the temperature of saturation decreases. But between 8 and 3 mole percent solutions of PPP in cocoa butter, it can be noted that the values of temperature of saturation are very close, with a difference of less than 0.5°C (Figure 4.19).

The metastable zone widths and the order of reaction do not show a trend. Moreover, for all systems studied, a high metastable zone is observed and this could be because the system does not easily nucleate. Besides, from Tables 4.13 and 4.14 it can be observed that for the 3 and 1 mole percent concentrations the metastable zone width increases from the fastest to the slowest cooling/heating rate. This could be consistent with the hypothesis that different polymorphic forms could be present at the same time.

The highest values of order of reaction have been observed for 10 and 5 mole percent solutions, while the smallest for 8 and 6 mole percent concentrations. The

order of reaction could not be obtained for 3 and 1 mole percent solutions of PPP in cocoa butter. This is due to the fact that, for both systems, metastable zone width increases as the cooling/heating rate decreases, implying a physically unrealistic negative value for the order of reaction.

Concentration (mole percent)	T_{sat} (°C)	MSZW (°C)	m
Cocoa butter	33.5 (87%) [0.8]	8.1 (88%) [2.9]	3.2 (97%) [0.2]
1% PPP	37.1 (98%) [3.7]	16.7 (97%) [3.7]	**
3% PPP	40.4 (97%) [1.5]	14.5 (52%) [0.8]	**
4% PPP	39.8 (99%) [0.8]	12.6 (12%) [0.7]	6.4 (26%) [0.1]
5% PPP	40.4 (67%) [0.2]	11.4 (88%) [1.1]	8.9 (97%) [0.1]
6% PPP	39.7 (77%) [0.4]	8.8 (89%) [1.9]	2.1 (80%) [0.1]
7% PPP	40.0 (67%) [2.7]	9.4 (93%) [4.2]	3.1 (86%) [0.2]
8% PPP	40.2 (84%) [3.3]	10.1 (83%) [3.8]	2.0 (92%) [0.2]
9% PPP	44.9 (95%) [1.9]	13.5 (99%) [2.8]	3.6 (99%) [0.1]
10% PPP	52.1 (81%) [0.1]	15.8 (93%) [3.2]	5.3 (99%) [0.2]
15% PPP	54.4 (89%) [0.8]	12.7 (95%) [4.5]	3.6 (99%) [0.2]
20% PPP	56.0 (90%) [0.5]	11.5 (94%) [3.8]	3.7 (92%) [0.2]
25% PPP	58.3 (98%) [0.6]	10.2 (98%) [4.1]	3.3 (99%) [0.2]
PPP	67.9 (89%) [1.5]	13.6 (91%) [2.7]	5.2 (97%) [0.2]

Table 4.16. The saturation temperatures, meta stable zone width (MSZW) and order of reaction (m) calculated for tripalmitin sample, for cocoa butter sample and for the solutions of tripalmitin in cocoa butter. Correlation coefficients are given between brackets, with the standard deviations in square brackets. ** - This depicts orders which were undefined and have been omitted from the results table.

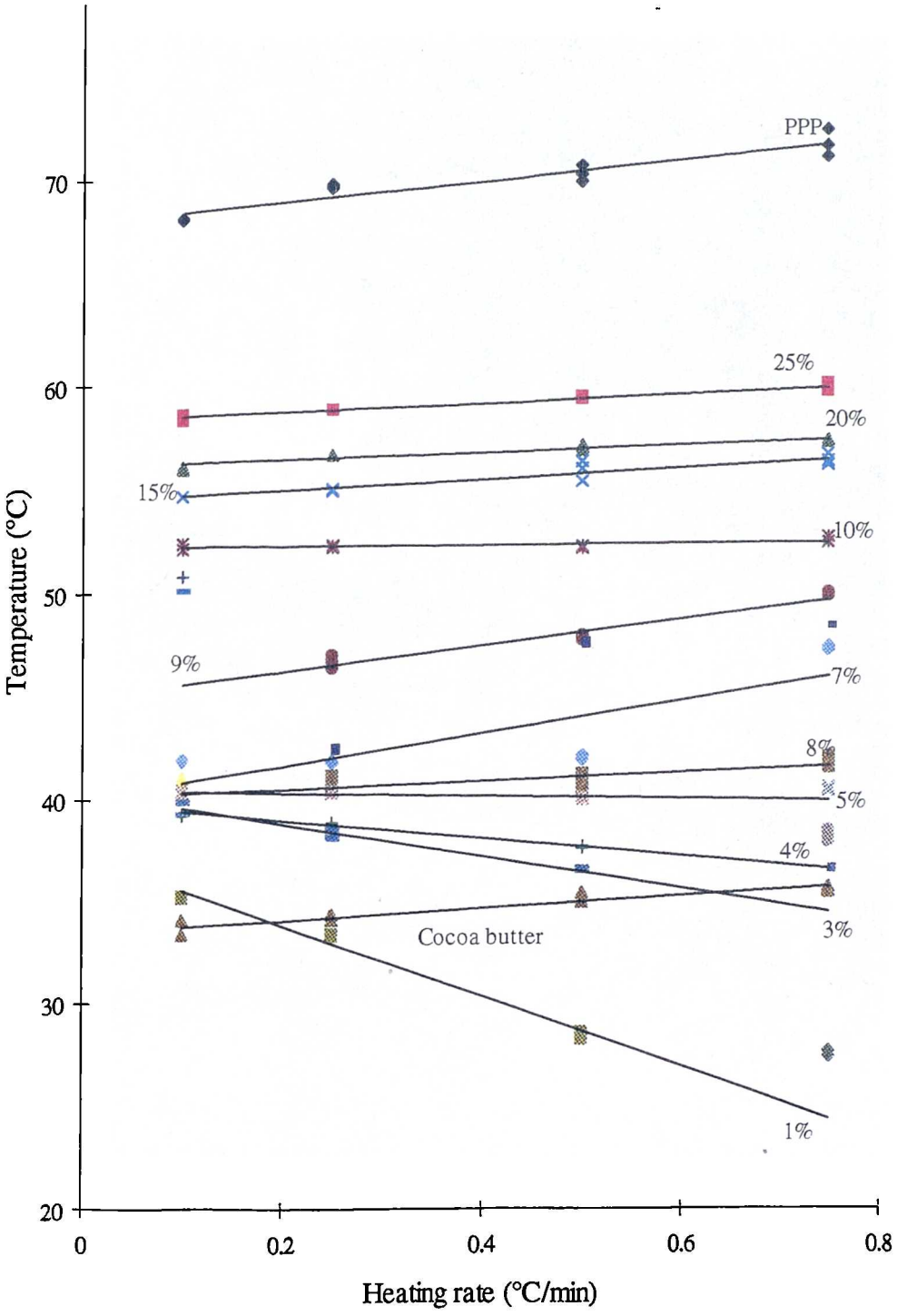

Figure 4.19. Dissolution temperatures as a function of heating rate for pure PPP, cocoa butter, and for the 25, 20, 15, 10, 9, 8, 7, 6, 5, 4, 3 and 1 mole percent solutions of PPP in cocoa butter.

4.4.3.4 *Phase diagram of the binary system tripalmitin and cocoa butter*

This system follows the Hildebrand solubility law [Hildebrand, 1950] (equation (4.4)) only at high concentrations of tripalmitin (Figure 4.20) The experimental and ideal behaviours for the tripalmitin and cocoa butter system are shown in Figure 4.20. It is clear that the experimental data follow the ideal behaviour at 25, 20, 15 and10 mole percent solutions of tripalmitin in cocoa butter. Between 8 and 1 mole percent solutions, remarkable differences are detected in the saturation temperature.

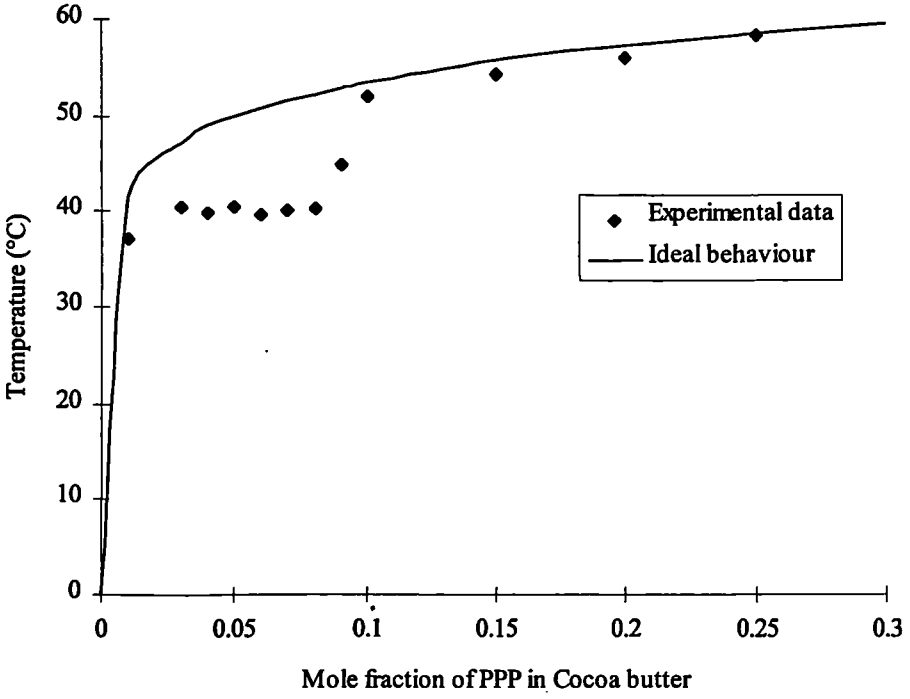

Figure 4.20. Phase diagram of the binary mixtures of tripalmitin and cocoa butter.

In Figure 4.21 the natural logarithms of the mole fraction are plotted versus the inverse of temperature of saturation ($°K^{-1}$). It should be specified that a simplification of a very complex system has been done. PPP and cocoa butter do not behave like two phase components. Assuming that cocoa butter acts like a solvent, the Van't Hoff equation could be used to calculate approximate values of enthalpy and entropy of dissolution for this binary system. This may give an idea of what can be expected.

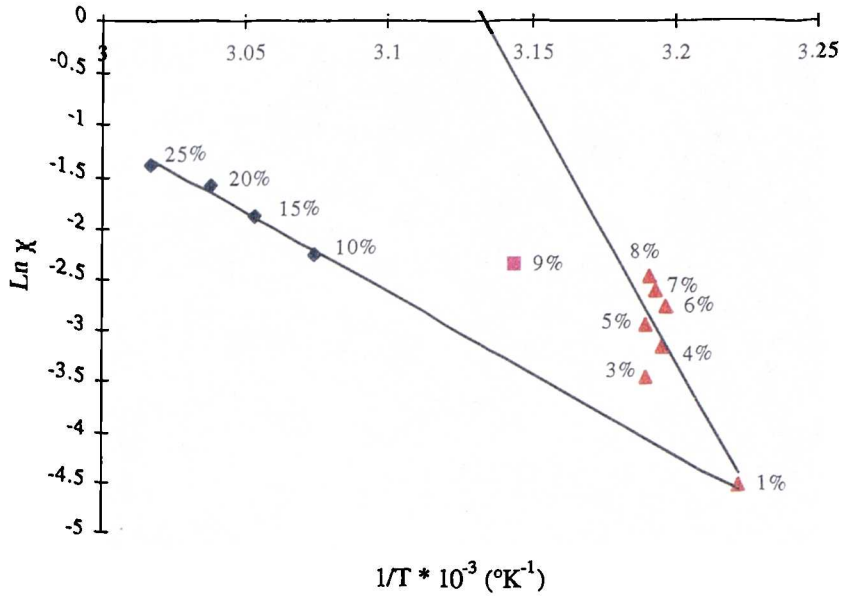

Figure 4.21. Plot of Ln χ versus $1/T_{sat}$ ($^{\circ}K^{-1}$) for PPP crystallised from cocoa butter at different concentrations.

Two phase separations can be observed from Figure 4.21. An approximate value of enthalpy and entropy of dissolution can be calculated for each phase. The values are summarised on Table 4.17.

Concentrations (mol %)	ΔH_d (kcal mol^{-1})	ΔS_d (cal K^{-1} mol^{-1})	Correlation Coefficient
25, 20, 15 and 10	32.0	93.8	98%
8 - 1	100.8	315.8	68%

Table 4.17. The enthalpy and entropy of dissolution of tripalmitin in cocoa butter.

4.4.4 *Milk Fat in Cocoa Butter*

Four different concentrations were used to study the crystallisation behaviour of the binary mixture milk fat/cocoa butter: 75, 50, 25 and 12.5 mole percent of milk fat. Also the nucleation behaviour of milkfat alone was analysed. No studies of these mixtures have been reported in the literature.

The milk fat used for these experiments was analysed by Gas Chromatography (GC) at RSSL (Reading Scientific Service Limited).The GC results are summarised in Table 4.18. The average molecular weight of milk fat was found to be 836.72 g/mol.

A summary of all experimental data are given in the Tables 4.19 and 4.20. Each run has been repeated three times and, again for this system, good reproducibility was observed.

Figures 4.22 and 4.23 show the most significative profiles of crystallisation and dissolution process obtained from the experiments carried out on milk fat and the various mixtures with cocoa butter. Figure 4.22(a) shows the transmittance plotted against the temperature for milk fat at the cooling/heating rate of 0.75°C/min. This is in agreement with a typical curve and shows that precipitation of the solid phase is occurring at approximately at 22.5°C during cooling, and as the temperature is then raised the solid phase is dissolved at around 36°C. The metastable zone width calculated is approximately 13°C when the temperature is reduced at a rate of 0.75°C/min. As the rate decreases, a smaller metastable zone width is observed, but the shape of the cycle is the same. Similar behaviour is observed for the 75 (Figure 4.22 (b)) and 50 mole percent solutions of milk fat in cocoa butter.

In the case of the 25 mole percent solution of milk fat in cocoa butter, different crystallisation/dissolution process were observed between the two rates 0.75 and 0.50°C/min. Figure 4.22 (c) shows a typical curve, taken when the cooling and heating cycle occur at a rate of 0.75°C/min. Precipitation is observed at approximately 21.8°C as the temperature is lowered. As the system is heated up, the solid phase dissolves at around 23.9°C. The metastable zone width calculated is approximately 2°C. In contrast, the curve, for a cooling/heating cycle at a rate of 0.50°C/min (Figure 4.22(d)), is not typical. Precipitation is observed at approximately 21.7°C as the temperature is cooled.

Heating up the system, a transformation process is observed at approximately 23.7°C (the maximum transmittance value is 67%) and this might be due to melting of unstable polymorph followed by re-crystallisation. The transmittance drops to a minimum value of 30% at approximately 28°C. Then, the transmittance immediately increases, due to a gradual dissolution of the stable phase. The system is completely dissolved at around 31.4°C. A similar shape of cooling/heating curve was also observed for the experiments carried out at the slowest rates (0.25 and 0.10°C/min).

Figure 4.23 shows the profile of crystallisation and dissolution processes obtained for 12.5 mole percent solution of milk fat in cocoa butter at different rates. Using a rate of 0.75°C/min (Figure 4.23(a)), precipitation occurs at approximately 21.1°C as the temperature is reduced and dissolution is observed at around 25.6°C as the system is heated up. Using a rate of 0.50°C/min (Figure 4.23(b)), the system starts to crystallise at approximately 20.6°C. Then, upon heating, a transformation process is observed at around 25.7°C (the maximum transmittance value is 87%), but a solid still appears to be present. The transmittance drops to a minimum value of 62%, then it quickly increases to a maximum value of 95% at around 26.9°C. At this stage, the crystals are completely dissolved. In the case of the experiments carried out at a rate of 0.25°C/min (Figure 4.23(c)), it can be observed that, during the heating cycle, the transmittance increases reaching a value of 90% at around 29.2°C. Then, the transmittance is approximately constant until at 32°C, where a further increasing of transmittance is observed. A complete dissolution of the crystals is observed at approximately 33.1°C. In contrast, a different cooling/heating curve is observed at a rate of 0.10°C/min. As the system is cooled, precipitation is observed at 21.7°C. The transmittance decreases rapidly to a minimum value of 10% at 21.5°C. Then, at lower temperatures, the transmittance gradually increases up to a value of 30%. As the system is heated up, the transmittance is kept constant till approximately 25°C. Then, the transmittance decreases again to a minimum value of 10% around 31°C. On further heating, the transmittance quickly increases, reaching its maximum value around 34°C, which indicates the complete dissolution of the crystals.

Peak number	%	Peak number	%	Peak number	%
1	0.1	14	2.3	27	4.7
2	0.3	15	3.3	28 (OOO)	0.8
3	0.4	16	4.1	29 (POO)	3.0
4	0.6	17	3.0	30 (PLiS)	2.0
5	0.3	18	1.4	31 (POP)	5.6
6	1.2	19	2.7	32	0.1
7	2.1	20	1.9	33 (PPP)	2.4
8	1.5	21	3.0	34 (SOO)	0.6
9	4.9	22	3.1	35 (POS)	2.1
10	6.0	23	0.3	36 (PPS)	1.3
11	3.7	24	3.4	37	<0.1
12	11.5	25	3.4	38 (SOS)	0.3
13	11.4	26	0.7	39	0.3

Table 4.18. Gas chromatography analysis of milk fat used for these experiments.

	100 mole% milk fat			75 mole% milk fat			50 mole% milk fat		
Rate (°C/min)	Tcryst (°C)	Tdiss (°C)	MSZW (°C)	Tcryst (°C)	Tdiss (°C)	MSZW (°C)	Tcryst (°C)	Tdiss (°C)	MSZW (°C)
0.75	22.5	36.1	13.6	21.4	35.0	13.6	20.6	32.9	12.3
	22.5	36.0	13.5	20.9	34.7	13.8	20.7	32.9	12.2
	22.6	36.2	13.6	20.9	34.7	13.8	20.7	32.7	12.0
0.50	23.9	35.7	11.8	21.1	34.6	13.5	21.4	33.2	11.8
	23.7	35.8	12.1	21.1	34.6	13.5	21.1	33.0	11.9
	23.9	35.7	11.8	21.1	34.7	13.6	21.1	33.0	11.9
0.25	25.6	35.2	9.6	23.4	34.4	11.0	21.9	33.3	11.5
	25.5	35.3	9.8	23.0	34.4	11.4	21.9	33.3	11.4
	25.6	35.2	9.6	23.0	34.4	11.4	21.8	33.3	11.5
0.10	27.5	36.3	8.8	25.4	34.9	9.5	23.6	34.0	10.4
	27.5	36.1	8.6	25.4	34.9	9.5	23.9	34.2	10.3
	27.7	36.2	8.5	25.9	34.9	9.0	23.7	34.2	10.5

Table 4.19. The crystallisation and dissolution temperatures and the metastable zone width of milk fat and 75 and 50 mole percent solutions of milk fat in cocoa Butter.

	25 mole% milk fat					12.5 mole% milk fat				
Rate (°C/min)	Tcryst (°C)	Tdiss (°C)		MSZW (°C)		Tcryst (°C)	Tdiss (°C)		MSZW (°C)	
		(A)	(B)	(A)	(B)		(A)	(B)	(A)	(B)
0.75	21.8	23.9	--	2.1	--	21.1	25.6	--	4.5	--
	21.7	23.9	--	2.2	--	21.1	25.4	--	4.3	--
	21.7	23.9	--	2.2	--	20.8	25.7	--	4.9	--
0.50	21.7	23.7	31.3	2.0	9.6	20.6	25.7	26.9	5.1	6.3
	21.7	23.8	31.4	2.1	9.7	20.6	25.8	26.9	5.2	6.3
	21.6	23.7	31.2	2.1	9.6	20.8	25.7	27.0	4.9	6.2
0.25	21.6	24.1	32.8	2.5	11.2	21.1	29.2	33.0	8.1	11.9
	21.6	24.3	32.7	2.7	11.1	21.0	29.4	32.9	9.4	11.9
	21.5	24.3	32.8	2.8	11.3	21.0	29.4	33.1	9.4	12.1
0.10	22.6	30.7	34.0	8.1	11.4	21.7	--	34.0	--	12.3
	22.4	31.0	34.0	8.6	11.6	21.7	--	34.0	--	12.3
	22.3	30.9	34.0	8.6	11.7	21.8	--	34.0	--	12.2

Table 4.20. The crystallisation and dissolution temperatures and the metastable zone width of 25 and 12.5 mole percent solutions of milk fat in cocoa butter.

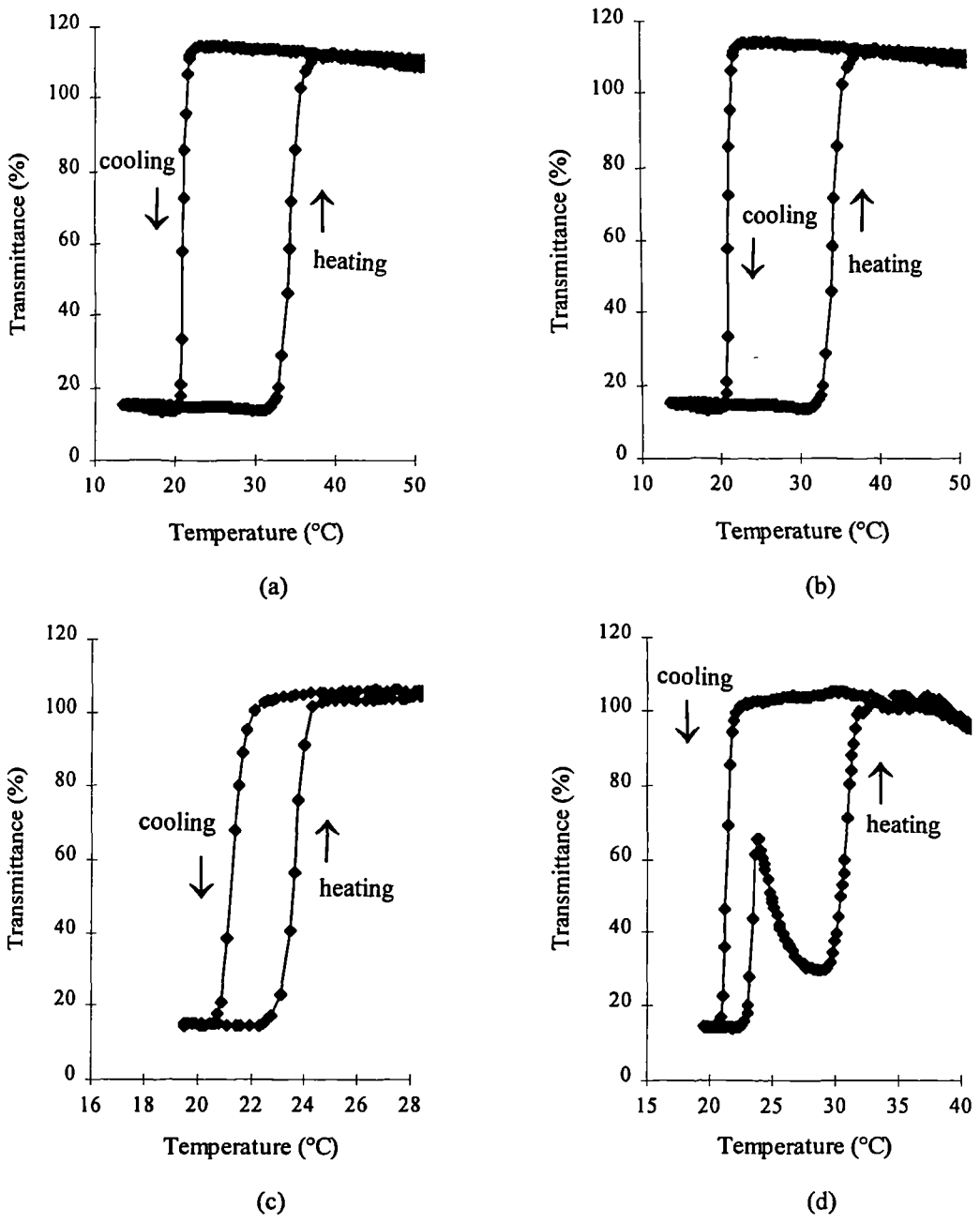

Figure 4.22. Transmittance (%) versus temperature (°C) for: milk fat at 0.75°C/min (a); 75 mole percent solution of milk fat in cocoa butter at 0.75°C/min (b); 25 mole percent solution of milk fat in cocoa butter at the rate 0.75°C/min (c) and 0.50°C/min (d).

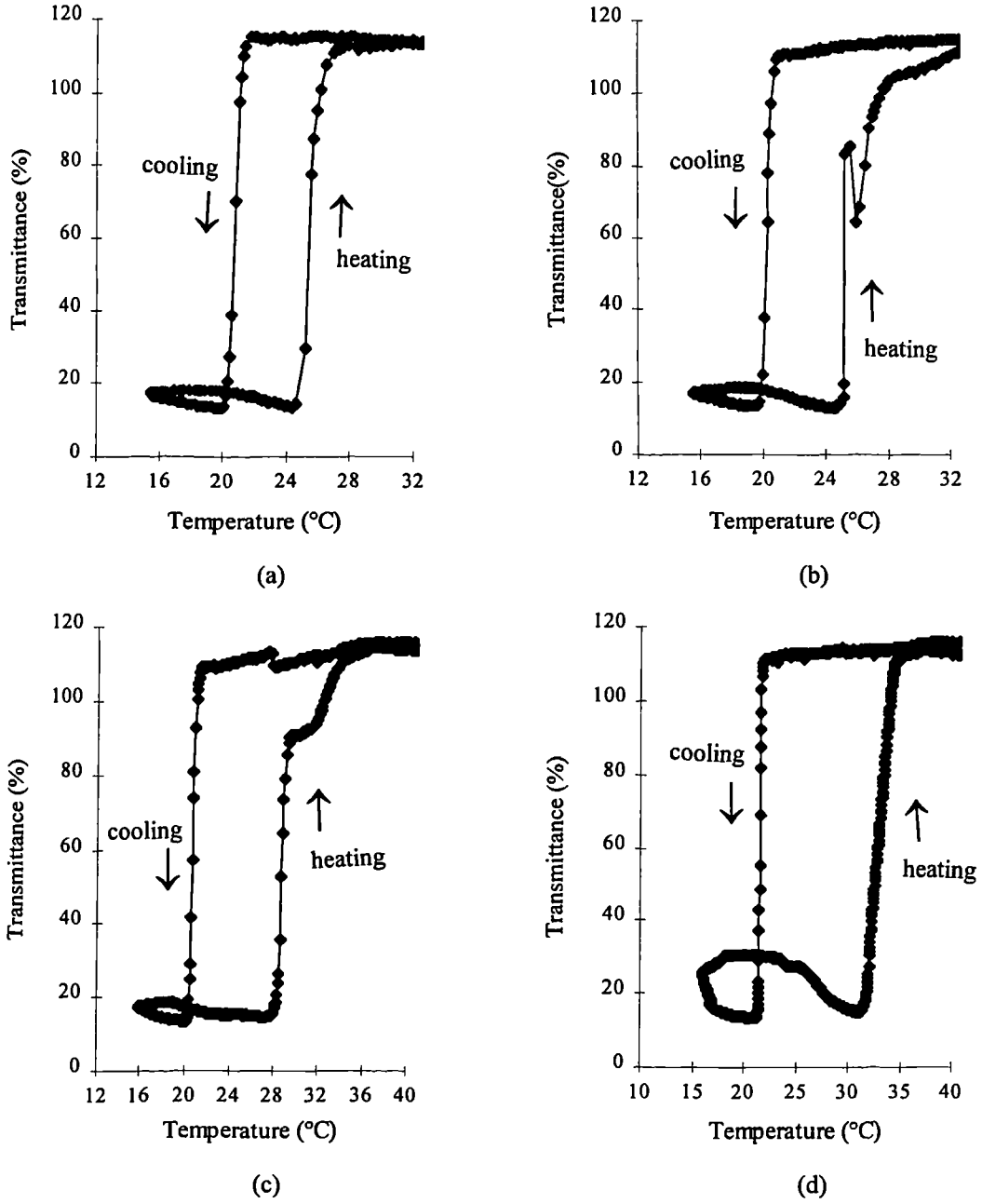

Figure 4.23. Transmittance (%) versus temperature (°C) for 12.5 mole percent solution of milk fat in cocoa butter at different rates: 0.75°C/min (a); 0.50°C/min (b); 0.25°C/min (c) and 0.10°C/min (d).

4.4.4.1 *Temperatures of crystallisation and dissolution*

The temperatures of crystallisation and dissolution are schematically shown in Figure 4.24. The temperatures of crystallisation increase from the fastest to the slowest rate for milk fat and for the 75 and 50 mole percent solutions of milk fat in cocoa butter. In the case of 25 and 12.5 mole percent solutions, the temperatures of crystallisation do not seem to be influenced by the different rates, the values are all very close.

The temperatures of dissolution decrease from the heating rate of 0.75 to 0.25°C/min for milk fat and for the 75 mole percent solution of milk fat in cocoa butter. At a heating rate of 0.10°C/min, both systems show values of dissolution temperatures higher than the values recorded at a rate of 0.75°C/min. Due to these non-linear rate-dependent behaviour occurring when a rate of 0.10°C/min is used, these results were not employed in the kinetics calculations.

In the case of the 50 mole percent solution of milk fat in cocoa butter, the temperatures of dissolution increase from the fastest to the slowest rate. The same behaviour was observed for 25 and 12.5 mole percent solutions. But, as it was already explained in the previous section, between the rates of 0.50 and 0.10°C/min, two values of temperature of dissolution were observed for both mixtures at each rate. Moreover, the values of dissolution temperatures observed at a rate 0.75°C/min are slightly higher than those recorded during the first dissolution occurring at a rate of 0.50°C/min. Due to this non-linear behaviour, the results collected at a rate of 0.75°C/min were not used in the kinetics calculations.

4.4.4.2 *Temperatures of saturation , metastable zone width and order of reaction*

Irregularities were observed during the cooling/heating cycle dependng on the concentration and the rate used. Consequently, some results were not used for the calculation of kinetics parameters. The details of the values used are given in Table 4.21.

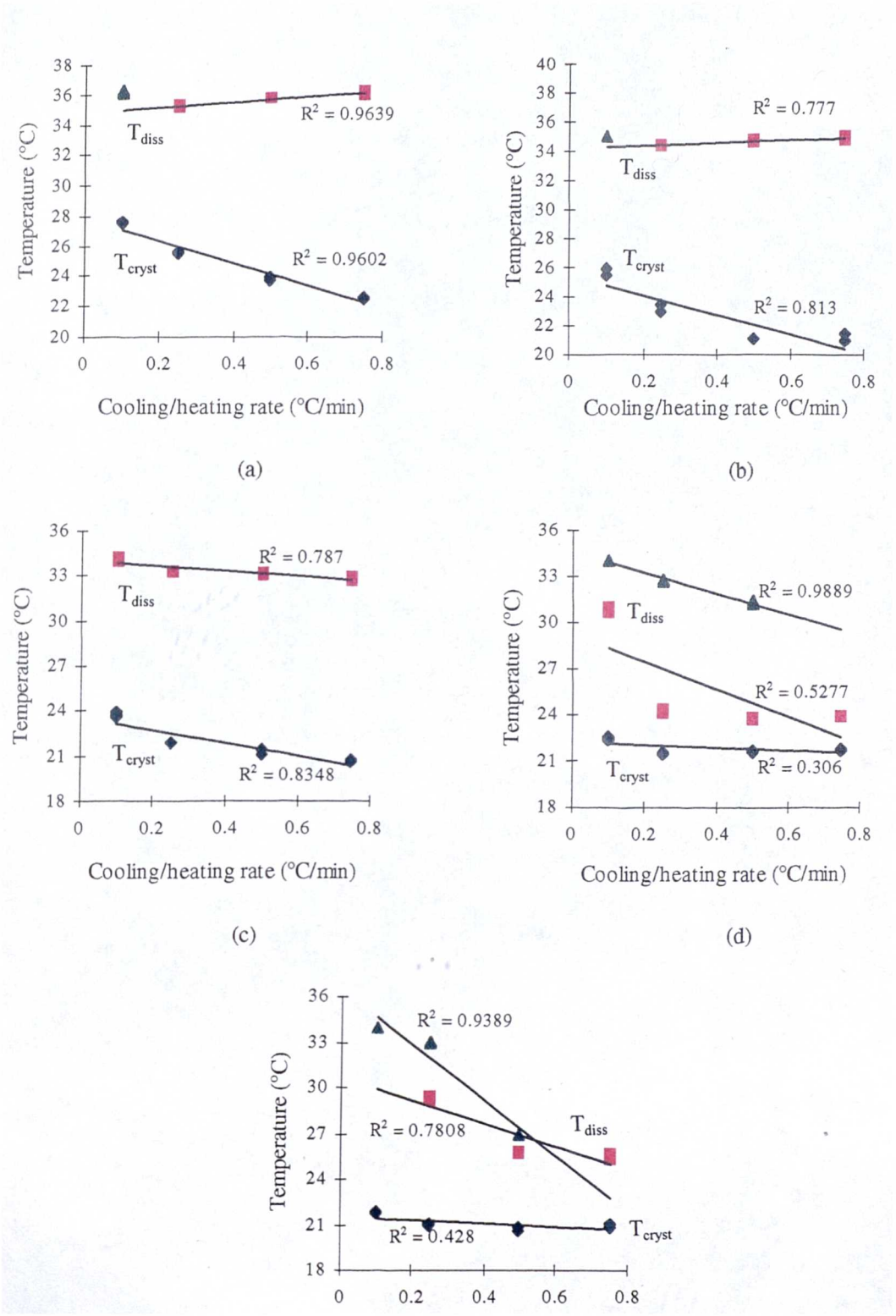

Figure 4.24. The temperature of crystallisation and dissolution of milk fat (a) and 75 (b), 50 (c), 25 (d), 12.5 (e) mole percent solutions of milk fat in cocoa butter.

Temperatures of saturation, the metastable zone width and the order of reaction have been calculated and are summarised in Table 4.22.

Concentration (mole percent)	Rate (°C/min)
100% milk fat	0.75, 0.50 and 0.25
75%	0.75, 0.50 and 0.25
50%	All
25%	0.50, 0.25 and 0.10
12.5 (A) (B)	0.75, 0.50 and 0.25 0.50, 0.25 and 0.10

Table 4.21. Detailed of the rates, used for the calculation of nucleation parameters

Concentration (mole percent)	T_{sat} (°C)	MSZW (°C)	m
100 % Milk fat	34.8 (96%) [0.4]	7.8 (99%) [2.2]	3.21 (99%)
75%	34.2 (78%) [0.2]	10.4 (80%) [2.1]	4.7 (90%)
50%	34.0 (79%) [0.6]	10.5 (84%) [0.8]	12.5 (96%)
25% (A)	29.2 (53%) [3.4]	8.5 (70%) [3.1]	**
25% (B)	34.6 (99%) [1.3]	12.2 (95%) [1.0]	**
12.5% (A)	30.6 (78%) [2.1]	9.7 (84%) [2.4]	**
12.5% (B)	36.5 (94%) [3.8]	14.6 (89%) [3.4]	**
100% Cocoa butter	33.5 (87%) [0.8]	8.1 (88%) [2.9]	3.2 (97%) [0.2]

Table 4.22. The saturation temperatures, metastable zone width (MSZW) and order of reaction (m) calculated for the milk fat sample, for the cocoa butter sample and for the solutions of milk fat in cocoa butter. Correlation coefficients are given in brackets, with the standard deviations in square brackets.
** - This depicts orders which were undefined and have been omitted from the results table.

The temperature of saturation slightly decreases, moving from pure milk fat to a 50 mole percent solution of milk fat in cocoa butter (Figure 4.25). The difference in terms of saturation temperature is less than 1°C. Besides, the temperatures of saturation for 75 and 50 mole percent solutions are approximately equal. Considering the 25 and 12.5 mole percent solutions, two values of saturation temperature can be calculated for each system. This could be related to a polymorphic transformation occurring during the heating process. For both 25 and 12.5 mole percent solutions, the temperature of saturation of the phase "called" B seems to be better correlated with the values obtained for the systems richest in milk fat. However, two different trends should be noted. The temperatures of saturation decrease from milk fat alone to 50 mole percent solution of milk fat in cocoa butter. The value calculated for the latter concentration is slightly higher than that observed for pure cocoa butter solution. Then, the temperature of saturation increases moving from 50 to 12.5 mole percent solutions with respect to the phase "called" (B), while it sensibly decreases, in the same range of concentrations, if the values obtained for the phase "called" (A) are considered.

The metastable zone width increases from the system richest in milk fat to the smallest concentration of milk fat in cocoa butter, if the values obtained for the phase "called" (B) are used. Anyway, for all mixtures studied, a high metastable zone width is observed, and this could be because the system does not easily nucleate.

The order of reaction can be calculated only for milk fat, which appears to have the same value as calculated for cocoa butter, and for the 75 and 50 mole percent solutions of milk fat in cocoa butter. In the case of 25 and 12.5 mole percent solutions, the order of reaction could not be obtained, due to the fact that the metastable zone width increases from the fastest to the slowest rate (Table 4.21). Plotting the metastable zone width recorded against the rate, the slope is negative, implying the existence of a physically unrealistic negative order of reaction.

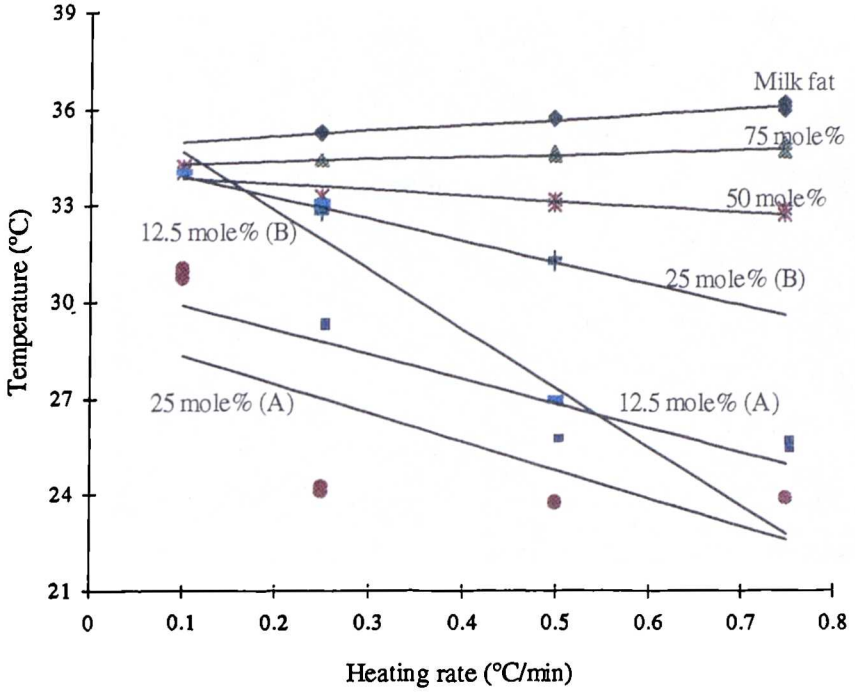

Figure 4.25. Dissolution temperatures as a function of heating rate for pure milk fat and for 75, 50, 25 and 12.5 mole percent solutions of milk fat in cocoa butter.

4.4.4.3 *Enthalphy and entropy of dissolution*

The enthalphy and entropy of dissolution cannot be calculated using the values obtained for the phase "called" (A). As it can be observed in Figure 4.26 (a), the slope is positive. This gives negative values of enthalpy and entropy of dissolution.

Using the values obtained for the phase "called" (B) (Figure 4.26 (b)), the enthalpy and the entropy of dissolution are 61.2 kcal mol^{-1} and 197.6 cal K^{-1} mol^{-1}, respectively. The correlation coefficient is only 46%.

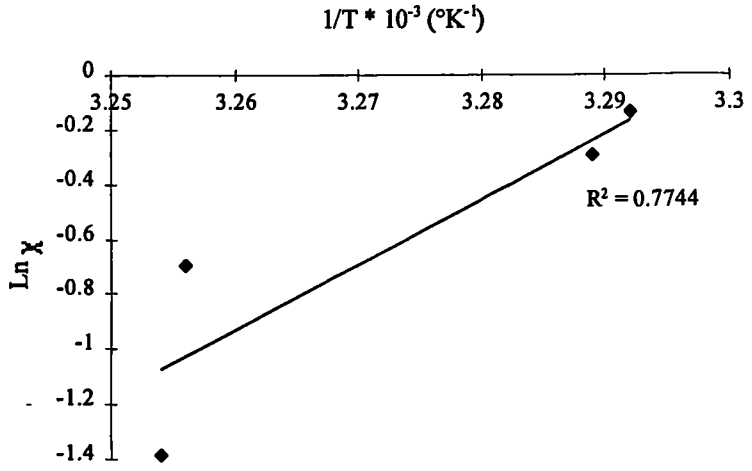

(a)

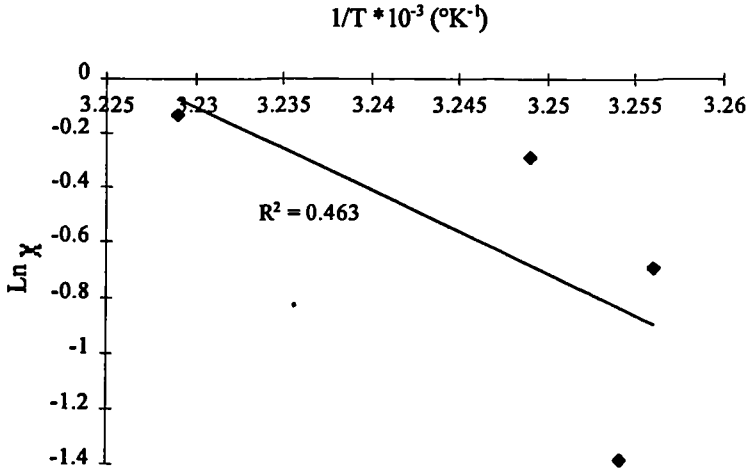

(b)

Figure 4.26. Plot of Ln χ versus 1/Tsat ($°K^{-1}$) for milk fat crystallised from cocoa butter at different concentrations: (a) using the values obtained for phase "A"; (b) using the values obtained for phase "B".

4.4.4.4 *Discussion*

Observing the results obtained for the milk fat and cocoa butter system, two different crystallisation and dissolution process occurring as a function of the concentration can be noted.

The 75 and 50 mole percent solutions of milk fat in cocoa butter show a nucleation behaviour closest to that observed for pure milk fat. For the three systems, only one temperature of dissolution was detected during the cooling/heating cycle at different rates.

In contrast, the 25 and 12.5 mole percent solutions of milk fat in cocoa butter show that a polymorphic transformation has taken place. It was observed that this depends on the cooling/heating rate. In the case of the 25 mole percent solution, a different crystallisation/dissolution process was noted between the rates 0.75 and 0.50°C/min. As the mixture was cooled at a rate of 0.75°C/min, only the crystallisation of the metastable phase was detected (Figure 4.21 (c)). This phase dissolved without giving a chance to the stable form to grow. This could explain the small metastable zone width (approximately 2°C). Using a rate of 0.50°C/min, the metastable form crystallised during the cooling phase of the cycle. As the system is heated up, the meta stable phase dissolves, while a stable phase nucleates and grows for a short period of time before it quickly dissolves (Figure 4.21 (d)). The same behaviour was observed at the two slowest rates.

Four different crystallisation/dissolution processes could be observed for the 12.5 mole percent solution of milk fat in cocoa butter (Figure 4.22). At the rates of 0.75°C/min, only a metastable phase is formed, while a polymorphic trasformation has taken place at a rate of 0.50°C/min. The differences with the 25 mole percent solution are observed at the two slowest rates. As the 12.5 mole percent solution of milk fat in cocoa butter is cooled at a rate of 0.25°C/min, the system initially crystallises into the metastable phase, but also a stable form is formed (Figure 4.22 (c)). The two phases coexist and this could be explained as a highest value of dissolution temperature is observed during the heating phase. The metastable phase dissolves at approximately 29.2°C, while the stable phase is still present. The transmittance values are

approximately constant until about 32°C, where an increase of transmittance is detected and this corresponds to the complete dissolution of the crystals.

As the mixture is cooled at a rate of 0.10°C/min, both metastable and stable phases nucleate at the same time (Figure 4.22(d)). But in this case the complete transformation into the stable form occurs at low temperatures. An increase in transmittance is observed at temperatures below 20°C. This could be due to a dissolution of the metastable phase in the stable form, which is completed at 28°C during the heating cycle. Meanwhile, the stable phase is grown up to reach its maximum around 32°C, where a decrease of transmittance is detected.

The nucleation experiments do not provide specific information of the type of phases formed during the crystallisation process. They do provide supporting evidence for this occurrence.

4.4.5 *Effects of the emulsifier YN on the 25 mole percent solution of Milk Fat in Cocoa Butter*

The synthetic compound lecithin YN (ammonium phosphatides) was added to a solution of milk fat in cocoa butter. The effects of this emulsifier on the crystallisation of confectionery fats will be explained in detail in chapter 5.

The concentration of milk fat was kept constant (25 mole percent) for all experiments. The molecular weight of YN is approximated to ca. 1000 g/mol. Three systems were studied:

- 0.2%YN/25%Milk fat/74.8% Cocoa Butter
- 0.4%YN/25%Milk fat/74.6% Cocoa Butter
- 0.6%YN/25%Milk fat/74.4% Cocoa Butter

The summary of all experimental data is given in Tables 4.23 and 4.24. Each run has been repeated three times and, also for these mixtures, good reproducibility was observed. The most significant profiles of crystallisation and dissolution processes are shown in Figures 4.27 and 4.28.

The mixture with 0.2 mole percent of YN reveals the closest crystallisation/dissolution behaviour to the 25 mole percent solution of milk fat in cocoa butter. The cooling/heating curves shown in Figures 4.27(a) and (b) are similar to that in Figures 4.22(a) and (b). At a rate of 0.50°C/min (Figure 4.27(b)), two values of dissolution temperature are detected, and they are almost certainly related to a phase transformation occurring during the dissolution process. Cooling the 0.2 mole percent solution of YN in milk fat/cocoa butter at a rate of 0.50°C/min, precipitation is observed at approximately 20.8°C. As the system is heated up, a transformation process is observed at around 29.2°C (the maximum transmittance value is 88%). Immediately, the transmittance drops to a minimum value of 26% at approximately 30.1°C. This could be due to a complete transformation into another phase. Then, the transmittance quickly increases due to a rapid dissolution at 33.3°C of the new phase. This behaviour agrees with that observed in the binary mixture (Figure 4.22(a)), even

if the latter system shows the smaller temperatures of dissolution. But, in the case of the ternary mixture, the phase transformation is observed only at a rate of 0.50°C/min, while, in the binary system, it is possible to distinguish two dissolution temperatures also at the slowest rates.

The 0.4 mole percent solution of YN in milk fat/cocoa butter system reveals the presence of phase transformation at the rates of 0.75 and 0.50°C/min (Figure 4.28(a) and (b), respectively), while at the two slowest rates (Figure 4.28(c)), the cooling/heating curves have a typical curve profile. Cooling the ternary mixture at a rate of 0.75°C/min (Figure 4.28(a)), precipitation occurs at around 20.3°C. As the system is heated up, the transmittance increases and reaches the maximum value of 75% at 29.8°C, then it drops down to a minimum value of 30% at around 30.1°C. This is probably due to a phase transformation during re-heating. Heating further, the complete dissolution occurs at approximately 33.6°C. Using a rate of 0.50°C/min, precipitation occurs at the same temperature as that observed at a rate of 0.75°C/min. A difference is noted during the dissolution phase (Figure 4.28(b)). As the system is heated up, the transmittance increases up to a value of 48% around 29.4°C. Then, the transmittance stays constant until 32.3°C, then it increases to reach a value of 90% at 34.2°C, which corresponds to the dissolution temperature of the system at this rate.

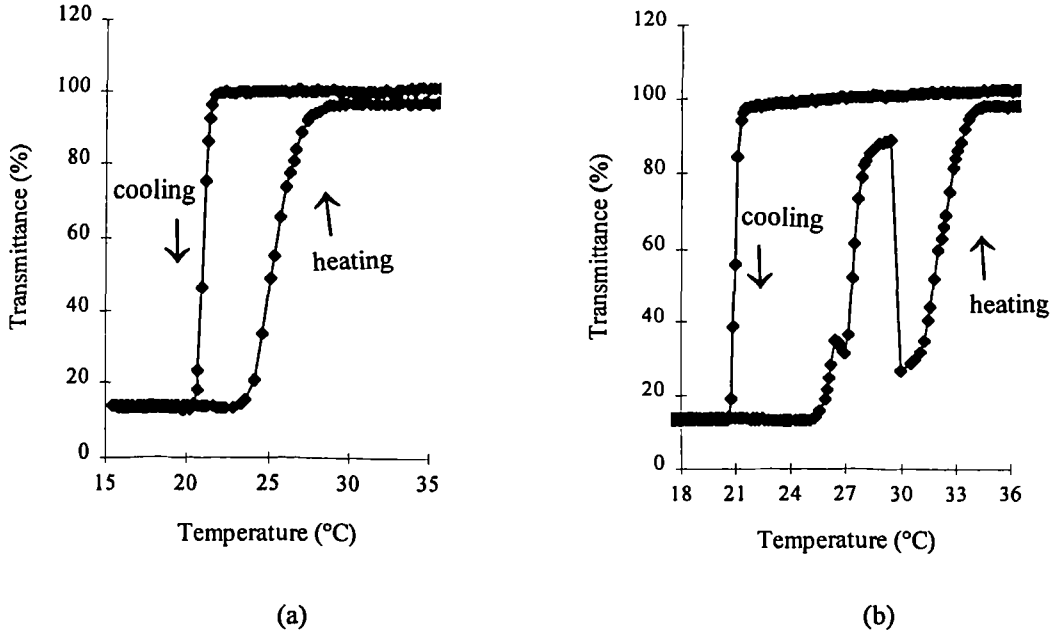

Figure 4.27. Transmittance (%) versus temperature (°C) for 0.2 mole percent solution of YN in milk fat/cocoa butter at two different cooling/heating rates: 0.75°C/min (a) and 0.50°C/min (b).

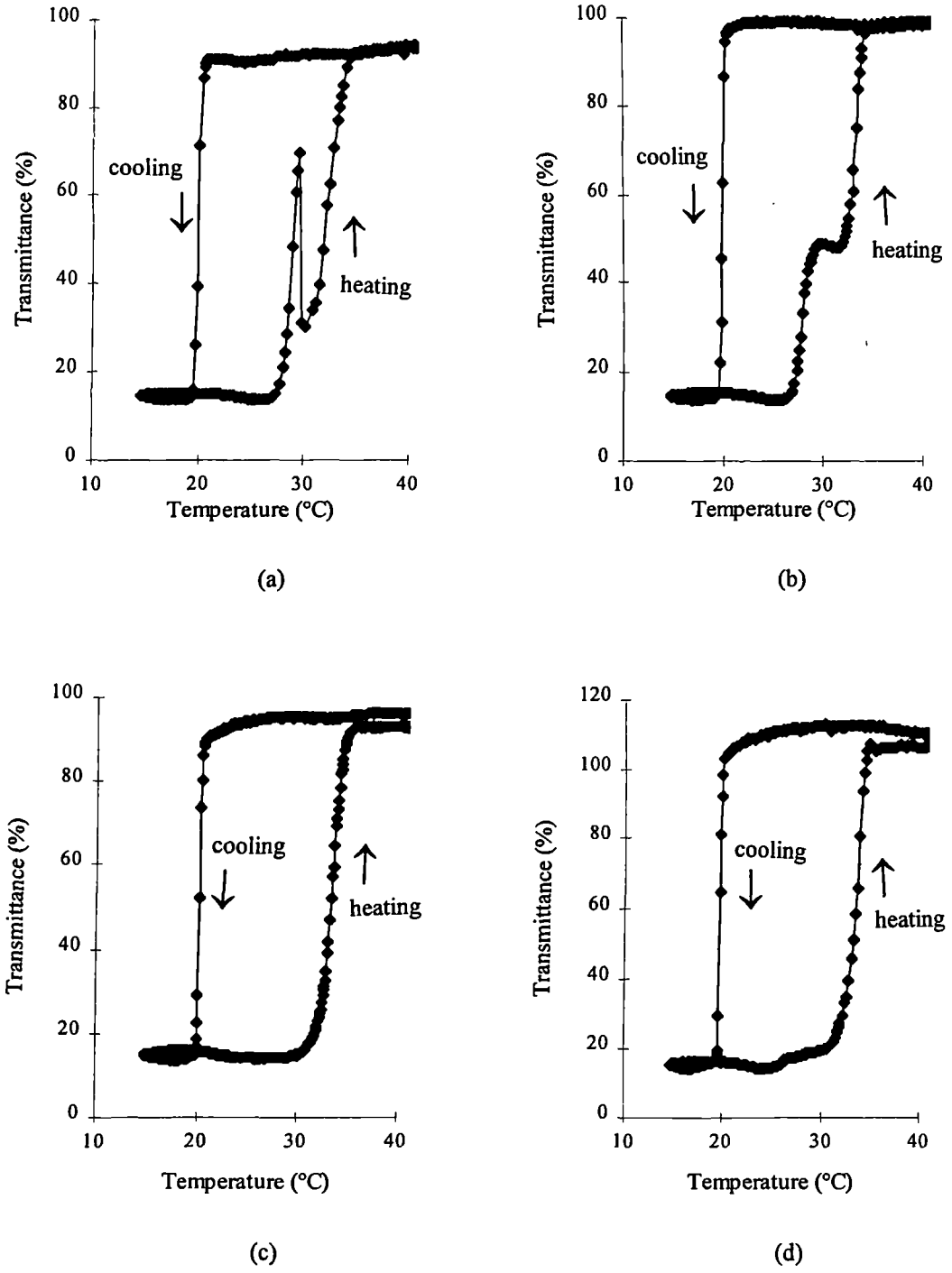

Figure 4.28. Transmittance (%) versus temperature (°C) for 0.4 mole percent solution of YN in milk fat/cocoa butter at three different cooling/heating rates: 0.75°C/min (a), 0.50°C/min (b), 0.10°C/min (c) and for 0.6 mole percent solution at a rate of 0.10°C/min (d).

Rate (°C/min)	25 mole% Milk fat					0.2 mole% YN		
	Tcryst (°C)	Tdiss (°C)		MSZW (°C)		Tcryst (°C)	Tdiss (°C)	MSZW (°C)
0.75	21.8	23.9	--	2.1	--	20.7	27.0	6.3
	21.7	23.9	--	2.2	--	20.8	27.4	6.6
	21.7	23.9	--	2.2	--	20.9	28.0	7.1
0.50	21.7	23.7	31.3	2.0	9.6	20.8	29.2	8.4
	21.7	23.8	31.4	2.1	9.7	21.0	29.2	8.2
	21.6	23.7	31.2	2.1	9.6	20.8	29.2	8.4
0.25	21.6	24.1	32.8	2.5	11.2	21.1	32.4	11.3
	21.6	24.3	32.7	2.7	11.1	21.3	32.0	10.7
	21.5	24.3	32.8	2.8	11.3	21.3	31.9	10.6
0.10	22.6	30.7	34.0	8.1	11.4	23.0	33.8	10.8
	22.4	31.0	34.0	8.6	11.6	22.9	34.1	11.2
	22.3	30.9	34.0	8.6	11.7	22.7	34.0	11.3

Table 4.23. The crystallisation and dissolution temperatures and the metastable zone width of 25 mole percent solution of milk fat in cocoa butter compared with 0.2 mole percent of YN in a solution of milk fat/cocoa butter

Rate (°C/min)	0.4 mole% YN			0.6 mole% YN		
	Tcryst (°C)	Tdiss (°C)	MSZW (°C)	Tcryst (°C)	Tdiss (°C)	MSZW (°C)
0.75	20.3	33.3	13.0	20.3	33.1	12.8
	20.2	33.6	13.4	20.2	33.2	13.0
	20.4	33.7	13.3	20.3	33.5	13.2
0.50	20.3	34.0	13.7	20.3	33.9	13.6
	20.3	34.2	13.9	20.3	33.9	13.6
	20.4	34.2	13.8	20.4	34.0	13.8
0.25	20.5	34.5	14.0	20.5	34.5	14.0
	20.5	34.5	14.0	20.5	34.5	14.0
	20.4	34.5	14.1	20.4	34.5	14.1
0.10	24.2	35.5	11.3	23.3	35.5	12.2
	23.8	35.5	11.7	23.4	35.5	12.1
	24.0	35.2	11.2	23.8	35.5	11.7

Table 4.24. The crystallisation and dissolution temperatures and the metastable zone width of 0.4 and 0.6 mole percent of YN in a solution of milk fat/cocoa butter.

Analysing the crystallisation and dissolution process occurring in the 0.6 mole percent solution of YN (Figure 4.28 (d)), phase separation is not detected for any of the rates used.

4.4.5.1 *Temperatures of crystallisation and dissolution*

The temperatures of crystallisation increase from the fastest to the slowest rate for all the three ternary systems studied (Figure 4.29). Comparing these results with those obtained for the binary mixture (25 mole percent of milk fat in cocoa butter), it can be noted that the crystallisation temperatures are smaller in the range of rates between 0.75 and 0.25°C/min, while, at the slowest rate, they show higher values, especially in the case of 0.4 and 0.6 mole percent solutions of YN. These two latter systems show similar temperatures of crystallisation. Moreover, for both ternary mixtures, no differences in terms of crystallisation temperatures are detected between the rates 0.75 and 0.25°C/min. At a rate of 0.10°C/min, the temperatures of crystallisation are much higher than those observed at the three faster rates.

The temperatures of dissolution increase from the fastest to the slowest rates for the three ternary systems studied. At a rate of 0.50°C/min for 0.2 mole percent solution of YN and at the rates of 0.75 and 0.50°C/min for the 0.4 mole percent solution of YN, two dissolution temperatures were detected. This could be related to polymorphic transformation, but further structural studies would be needed to clarify this.

4.4.5.2 *Temperature of saturation and metastable zone width*

The temperature of saturation and the metastable zone width were calculated and summarised in Table 4.25. Non linear rate-dependent behaviours are observed when the rates of 0.25 and 0.10°C/min are employed for 0.4 and 0.6 mole percent solutions of YN in milk fat/cocoa butter system. Due to these problems, the results

obtained for 0.10°C/min have not been used for the calculation of the kinetics parameters.

The order of reaction resulted in negative values for all ternary mixtures, due to the fact the metastable zone width increases from the fastest to the the slowest rate. This was observed also for the related binary mixture. Then, these latter values were not considered.

The saturation temperatures for the three ternary mixtures are very close (Figure 4.30). No difference is noted between the temperatures of saturation calculated for 0.4 and 0.6 mole percent solutions of YN in milk fat/cocoa butter, while the value observed for the 0.2 mole percent solution of YN is the same as that found for the phase "called" (B) of the correspondent binary mixture (25 mole percent of milk fat in cocoa butter).

The metastable zone width values show the same trend observed for the saturation temperatures.

Concentration (mole percent)	T_{sat} (°C)	MSZW (°C)
25% Milk fat in cocoa butter (A)	29.2 (53%) [3.4]	8.5 (70%) [3.1]
25 Milk fat in cocoa butter (B)	34.6 (99%) [1.3]	12.2 (95%) [1.0]
0.2 YN	34.7 (97%) [2.9]	12.2 (95%) [2.1]
0.4 YN	35.0 (91%) [0.8]	14.5 (85%) [1.2]
0.6 YN	35.1 (96%) [0.9]	14.6 (91%) [0.9]

Table 4.25. The saturation temperatures and metastable zone width (MSZW) calculated for 0.2, 0.4 and 0.6 mole percent solutions of YN in milk fat/cocoa butter and for 25 mole percent solution of milk fat in cocoa butter. Correlation coefficients are given in brackets, with the standard deviations in square brackets.

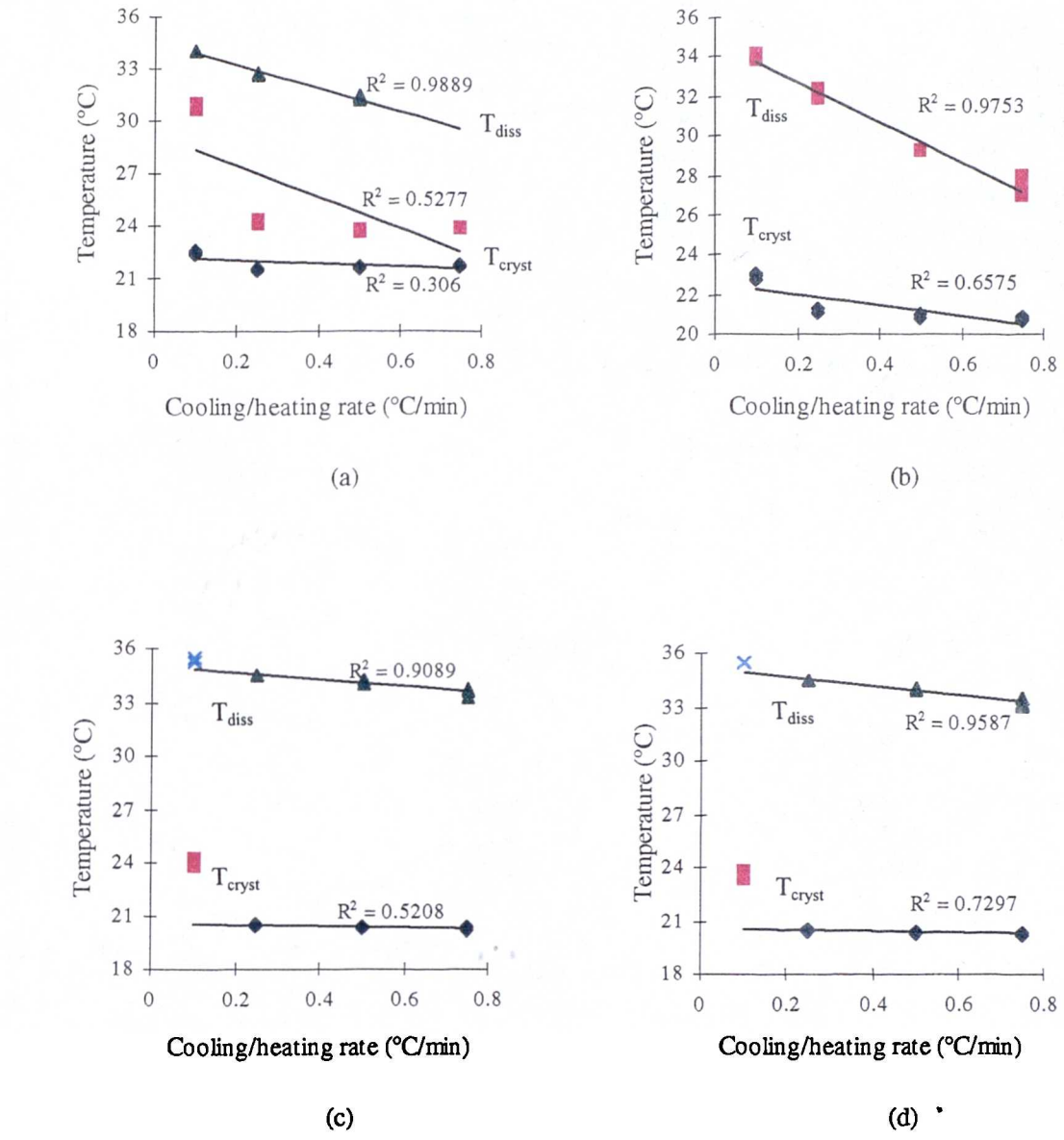

Figure 4.29. The temperature of crystallisation and dissolution of 25 mole percent solution of milk fat in cocoa butter (a) and of three different concentrations of YN in milk fat/cocoa butter system: 0.2 (b), 0.4 (c) and 0.6 (d) mole percent solutions.

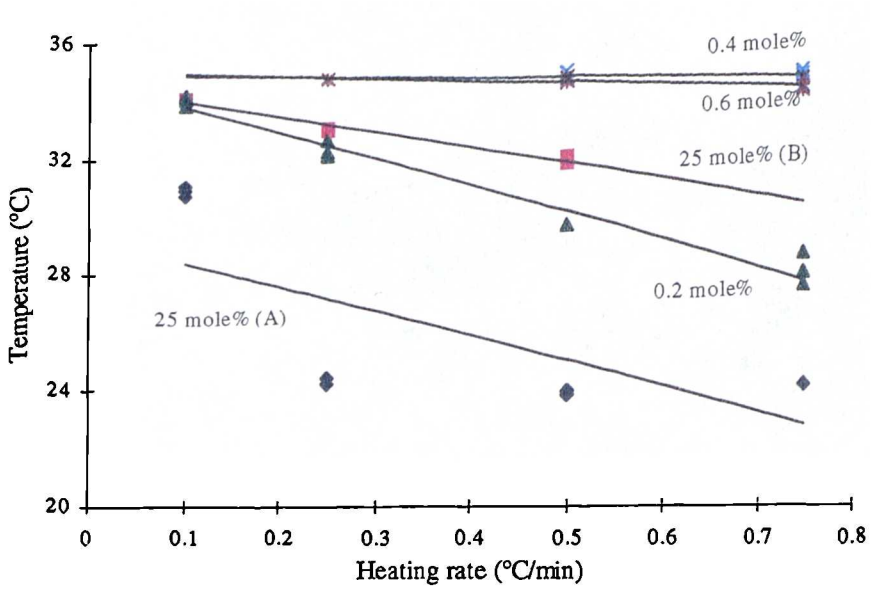

Figure 4.30. Dissolution temperatures as a function of heating rate for 25 mole percent solution of milk fat in cocoa butter and for 0.2, 0.4 and 0.6 mole percent concentrations of YN in milk fat/cocoa butter system.

4.4.5.3 *Discussion*

The effect of addition of the synthetic lecithin YN to a 25 mole percent solution of milk fat in cocoa butter is noted between 0.2 and 0.4 mole percent of YN. In a study of the reduction of viscosity of chocolate by addition of YN [Harris, 1968], the maximum reduction in viscosity was observed at 0.3 mole percent of YN, and at levels above this no thickening occurred.

The 0.2 mole percent concentration of YN shows the closest crystallisation and dissolution processes to that of the binary mixture with no YN. The same values of temperature of saturation and metastable zone width were calculated for both mixtures. But the addition of YN to 25 mole percent of milk fat in cocoa butter affects the presence of the two phases observed for the binary mixture. In the case of the 0.2 mole percent solution of YN, the two phases are only observed at a rate of 0.50°C/min.

But the addition of YN to 25 mole percent of milk fat in cocoa butter affects the presence of the two phases observed for the binary mixture. In the case of the 0.2 mole percent solution of YN, the two phases are only observed at a rate of 0.50°C/min.

The 0.4 and 0.6 mole percent solutions of YN results do not show remarkable differences. In both cases, between the rates of 0.75 and 0.25°C/min, the crystallisation and dissolution temperatures do not undergo variations, while at a rate of 0.10°C/min a difference of more than 3°C is observed for the temperatures of crystallisation. This could be explained by a different phase being present, but this information is too limited to understand which crystallisation process is involved.

4.5 *Discussion summarised*

4.5.1 *Nucleation behaviour of tripalmitin in different solvent*

An examination of the nucleation behaviour of tripalmitin has revealed differences depending on the type of solvent used. Tripalmitin shows a very low solubility in triacetin, and this probably depends on the different length of the fatty acid chain in the two triglycerides. However, a very large positive deviation from the ideal behaviour is observed. This could be due to the fact that cohesive forces between like molecules are stronger than those between PPP and triacetin. Then, the difficulty in dissolving PPP in triacetin tends to suggest that the two components are not very compatible and the mixture is almost behaving as a two component mixture with the melting behaviour being close to that of pure PPP.

In the case of the binary mixture tripalmitin/triolein, the experimental data follow the ideal behaviour. This might be due or to the fact that the two components PPP and OOO are more compatible than PPP and triacetin or to a diffusion of the molecules from the surface depending on the different viscosity triacetin and triolein.

Whereas, the tripalmitin and cocoa butter system follows the Hildebrand solubility law only at high concentrations of tripalmitin. The experimental data follow the ideal behaviour at 25, 20, 15 and 10 mole percent solutions of tripalmitin in cocoa

butter. Between 8 and 1 mole percent solutions, remarkable difference are detected on temperature of saturation. Phase separation was observed.

Both binary systems tripalmitin/triacetin and tripalmitin/cocoa butter they have shown large metastable zone width. In the case of tripalmitin in triolein, the metastable zone widths decrease from the smallest to the highest concentration of tripalmitin in triolein. This reflects the fact that it becomes easier for the system to nucleate as the solution is more concentrated in tripalmitin.

The values of enthalpy and entropy of dissolution relative to the systems mentioned above are summarised in Table 4.26. It is not possible to compare the ΔH_d and ΔS_d relative to PPP/triacetin with those relative to PPP/OOO and PPP/CB because they refer to different systems. However, it must be noted that the values of enthalpy and entropy of dissolution relative to the system PPP/cocoa butter at high concentration of PPP are similar to those observed for PPP/OOO. This behaviour can be explained as cocoa butter behaves as a solvent in a system rich of tripalmitin.

Binary systems	ΔH_d (kcal mol^{-1})	ΔS_d (cal K^{-1} mol^{-1}
PPP/triacetin (all concentrations)	27.2	67.2
PPP/triacetin (between 0.05 - 0.15 mole % of PPP)	87.0	245.3
PPP/OOO	38.9	114.6
PPP (at higher conc.)/CB	32.0	93.8
PPP (at lower conc.)/CB	100.8	315.8

Table 4.26. Summary of the enthalpy and entropy calculated for PPP in different solvent.

4.5.2 *The nucleation behaviour of confectionery fats*

In the case of the milk fat and cocoa butter system, two different crystallisation and dissolution process occur, depending on the concentration. The 75 and 50 mole percent solutions of milk fat in cocoa butter show a nucleation behaviour closest to that observed for pure milk fat. In contrast, the 25 and 12.5 mole percent solutions of

crystallisation process.

The effect of addition of the synthetic lecithin YN to a 25 mole percent solution of milk fat in cocoa butter is observed between 0.2 and 0.4 mole percent of YN. The 0.2 mole percent concentration of YN shows the closest crystallisation and dissolution processes to those of the binary mixture with no YN. But the addition of YN to 25 mole percent of milk fat in cocoa butter affects the presence of the two phases observed in the binary mixture. Phase separation is observed only in the case of the 0.2 mole percent solution of YN, at a rate of 0.50°C/min. The 0.4 and 0.6 mole percent solutions of YN do not show remarkable differences.

4.6 *Conclusions*

- Tripalmitin shows a very low solubility in triacetin. A large positive deviation of the experimental data from ideal behaviour is observed.

- In the case of tripalmitin and triolein the experimental data follow the ideal behaviour.

- The tripalmitin and cocoa butter system follows the Hildebrand solubility law only at high concentrations of tripalmitin. Two phase separation are observed.

- The phase diagrams of the binary mixtures tripalmitin/triacetin, tripalmitin/triolein and tripalmitin/cocoa butter exhibit monotectic behaviour.

- The binary system milk fat/cocoa butter system shows two different crystallisation/dissolution process as a function of the concentration. The 75 and 50 mole percent solutions of milk fat in cocoa butter show a nucleation behaviour closest to that observed for pure milk fat. In contrast, the 25 and 12.5 mole percent solutions of milk fat in cocoa butter show that a polymorphic transformation has taken place.

- The effect of addition of the synthetic lecithin YN to a 25 mole percent solution of milk fat in cocoa butter is observed between 0.2 and 0.4 mole percent of YN. The 0.2 mole percent concentration of YN shows the closest crystallisation and dissolution processes to those of the binary mixture with no YN.

4.7 *References*

Efremov, N N, Ravich, G and Vol'nova, V A, *Izv. Sektora Fiz. Khim. Analizo, Inst. Obshch. Neorgan. Khim. Akad. Nauk SSSR*, 1927, 16, 3, 142-155.

Gerson, A R, Roberts, K J and Sherwood, J N, *Powder Technology*, 1991, 65, 243-249.

Hale, J E and Shroeder, F, *Lipids*, 1981, 16, 11, 805-809.

Harris, T L, *SCI Monograph*, 1968, 32, 108-122.

Hildebrand, J H and Scott, R L, in *Solubility of Nonelectrolytes*, 3rd ed. Reinhold Publishing Corporation, New York, 1950.

Joglekar, R B and Watson, H E, *J. Indian Chem. Soc.*, 1928, 47, 365T.

Joglekar, R B and Watson, H E, *J. Indian Inst. Sci.*, 1930, A13, 119-146.

Kellens, M, Meeussen, W and Reynsers, H, *Chem. Phys. Lipids*, 1990, 55, 163-178.

Kerridge, R, *J. Chem. Soc.*, 1952, 4577-4579.

Knoester, M, De Bruijne, P and Van Den Tempel, M, *Chem. Phys. Lipids*, 1972, 9, 309-319.

Kremann, R and Shoulz, R, *Monotsh. Chem.*, 1912, 33, 1063.

Larson, M A and Garside, J, *Journal of Crystal Growth*, 1986, 76, 88-92.

Meenan, P, in *Experimental and Theoretical Studies On The Nucleation, Growth and Habit Modification of Some Inorganic Carbonates, Phosphates and Sulphates*, Ph.D. Thesis, University of Strathclyde, Glasgow (1992).

Ng, W L, *J. Am. Oil Chem. Soc.*, 1989, 66, 8, 1103-1106.

Norton, I T, Lee-Tuffnell, C D, Ablett, S and Bociek, S M, *J. Am. Oil Chem. Soc.*, 1985, 62, 8, 1237-1244.

Perron, R, Petit, J and Mathieu, A, *Chem. Phys. Lipids*, 1969, 3, 11-28.

Perron, R, Petit, J and Mathieu, A, *Chem. Phys. Lipids*, 1971, 6, 58-94.

Rossell, J B, *Adv. Lipid Res.*, 1967, 5, 353-408.

Small, D M, in *The Physical Chemistry of Lipids, Handbook of Lipid Research 4*, Plenum, New York, 1986, chap 10.

Taggart, A M, Gerson, A R, Jackson, G, Roberts, K J and Sherwood, J N, *J. Cryst. Growth*, 1993, 128, 1176-1181.

Timms, R E, *Prog. Lip. Res.*, 1984, 23, 1-38.

Chapter 5

In-situ Crystallisation studies of Confectionery Fats under static conditions using small angle X-ray scattering (SAXS)

5.1 *Introduction*

The knowledge of the detailed structural aspects associated with the formation of crystalline solids from their mother phases following nucleation remains quite limited. The nucleation results discussed in Chapter 4 did not identify the solid phases formed.

This chapter will investigate the structural characterisation of single and mixed confectionery fats under static conditions. The studies were carried out using SAXS (small angle X-ray scattering) diffraction at NSLS, Brookhaven (USA).

5.2 *Small Angle X-ray Scattering experiments*

The small angle X-ray scattering (SAXS) data provide information on long spacing. The long spacings correspond to the planes formed by the terminating methyl end groups in fats and are dependent on the chain length and angle of tilt of the component fatty acids of the triglyceride molecules. All SAXS experiments were carried out at the NSLS in Brookhaven (New York) on station X12B (Figure 5.1), using a 2D-Multi-wire Proportional Detector [Capel, 1995].

5.2.1 *Description of station X12B*

All beamline operational controls, including optics and spectrometer motions, sample handlers and detector operation are implemented via a PC-compatible 486 class machine (DOS), based on a control system named "CONSOLE" [Capel, 6/8/1997]. The CONSOLE system consists of development and execution environments, accessible via a windowing graphical user interface. The scripting language is called Console Control Language (CCL), and is a procedural language system, using a unique syntax. Data flow and reduction handled by a combination of DEC VAX station 3600 (VMS) and Silicon Graphics Iris-crimson (IRIX).

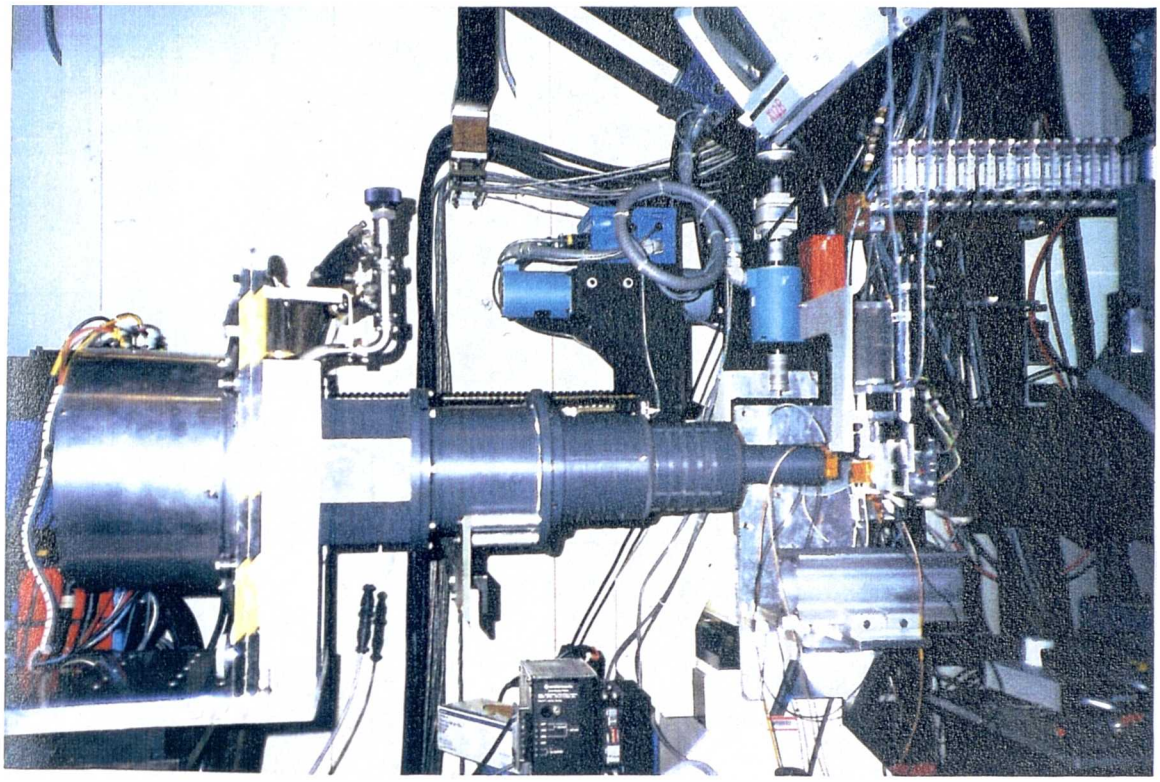

Figure 5.1. Photograph of station X12B.

The diffractometer mechanism controls the orientation and alignment of the sample handling and detector systems in relation to the incident and diffracted X-ray beams [Capel, 2/9/1996]. The diffractometer consists of:

- 6.3 m rail, carrying;
- lift table/carriage, which in turn carries;
- sample stage;
- detector theta arm.

The carriage translates on the rail to permit alignment of the sample and detector in relation to the focal point of the monochromatic beam. The sample stage consists of a Huber 420 goniometer mounted on a compound x-z translation table. The axes of the goniometer and the detector arm are coaxial. The entire carriage assembly is mounted on a vertical translation stage to permit alignment of the sample rotation and detector arm axis in relation to the X-ray beam. The detector arm pivots from -15° to 45°

relative to the incident beam. Detector systems are mounted on an upright that translates along the detector arm. The detector upright incorporates a scanning motion for the detector along the x-axis and a gimbal to allow adjustment of the azimuthal orientation of the detector. The detector upright also carries a mount point for evacuated flight paths or helium snouts to minimise gas scatter and attenuation of the diffracted beam.

Just after entry to the end-station hutch the beam passes through a beryllium window and into the collimator assembly, consisting of lengths of 8" pipe, containing x-y slit arrays, maintained at a low vacuum by a roughing pump. All slit drive screws are connected to stepping motors via vacuum feed-throughs. By varying the lengths of the flight path segments between the slit modules, it is possible to configure a near collimation geometry for any given sample-to-detector distance. Both ends of the flight path are terminated in 0.005 inch Kapton windows. The first section of the flight path telescopes to permit fine-tuning of the path length.

The beam stop is fixed to the downstream kapton window. The beamstop is a lead cup, 3 mm in diameter, glued to a small samarium/cobalt magnetic disk. A second magnetic disc placed on the downstream side of the window holds the beamstop in place by friction generated by the magnetic couple.

The detector is mounted on a gimbal on the downstream side of the upright that carries the flight path. The detector mounting plate is hinged to the upright so that the detector can be swung out to permit beam stop positioning and to protect from window failure during pump-down of the flight path.

The beamline optics provide a very stable monochromatic, doubly focused beam in the wavelength range between 1.61 and 0.92 Å [Capel, 20/2/1997]. The principal components of the optical train are :

- primary mirror of toroidal figure, Rh working surface
- water-cooled aperture array
- water-cooled beryllium window
- double-crystal, fixed-exit Si (111) monochromator
- refocusing (secondary) mirror, Rh working surface
- collimator surface

The primary mirror operates as a condenser-collimator, and serves to transport the effective source towards the experimental end station.

The monochromator is a double flat crystal fixed-exit using two Si (111) flats, with an angular range of 8.4-70° in steps of 3.78×10^{-4}°. The orientation and separation of the two Si flats are controlled by a boomerang cam, driven by a single stepping motor. Second crystal orientation is controlled trough a piezoelectric translator, which operates in two angular ranges -8° to 15° and 13.5° to 70°. A water-cooled beryllium window, just upstream of the monochromator, help limit the head load on the led Si crystal, which is further stabilised by a passive heat transfer line to a water-cooled block.

The monochromatic beam is refocused by a secondary mirror consisting of a bent cylinder (fabricated in Al, coated with Rh). Like the primary, the secondary mirror is mounted on a motorised kinematic support with lateral axes to control yaw. The bending of the secondary mirror is effected by two weighted cantilevers attached to the ends of the mirror. The cantilevers, driven by two motor-driven micrometers, induce deflections of the two ends of the mirror in order to establish the desired focus. The primary and secondary mirrors are inverted with respect to one another. This configuration results in a beam that is nearly parallel to the electron orbit plane (after the secondary mirror). In addition, this geometry results in a beam that is nearly rectangular in form, even at large distances from the monochromatic focal point. The most important result of this is that even with the maximum sample-to-detector distance, the area of sample illuminated by the beam (4×1.5 mm) is minimised when the beam focus is placed at the detector plane.

5.2.2 *Description of the in-situ X-ray cell*

An in-situ cell with a water-jacket was used and the sample was held between two Kapton windows (Figure 5.2). Kapton windows were used instead of mica since the use of mica can result in spurious diffraction spots in the wide angle region. A small aperture (2 mm in diameter) in the brass block allows the X-rays to pass through

the sample. Using a Haake F3C recirculating bath, water of a controlled temperature circulates through the brass block. The temperature of the bath and thus of the cell is remotely controlled using a PG-20 temperature programmer. A Pt100 platinum resistance temperature probe is placed inside the brass block close to the cell to measure the sample temperature during the experiments. By keeping the size of the aperture in the brass block to a minimum, a uniform temperature through the sample is ensured.

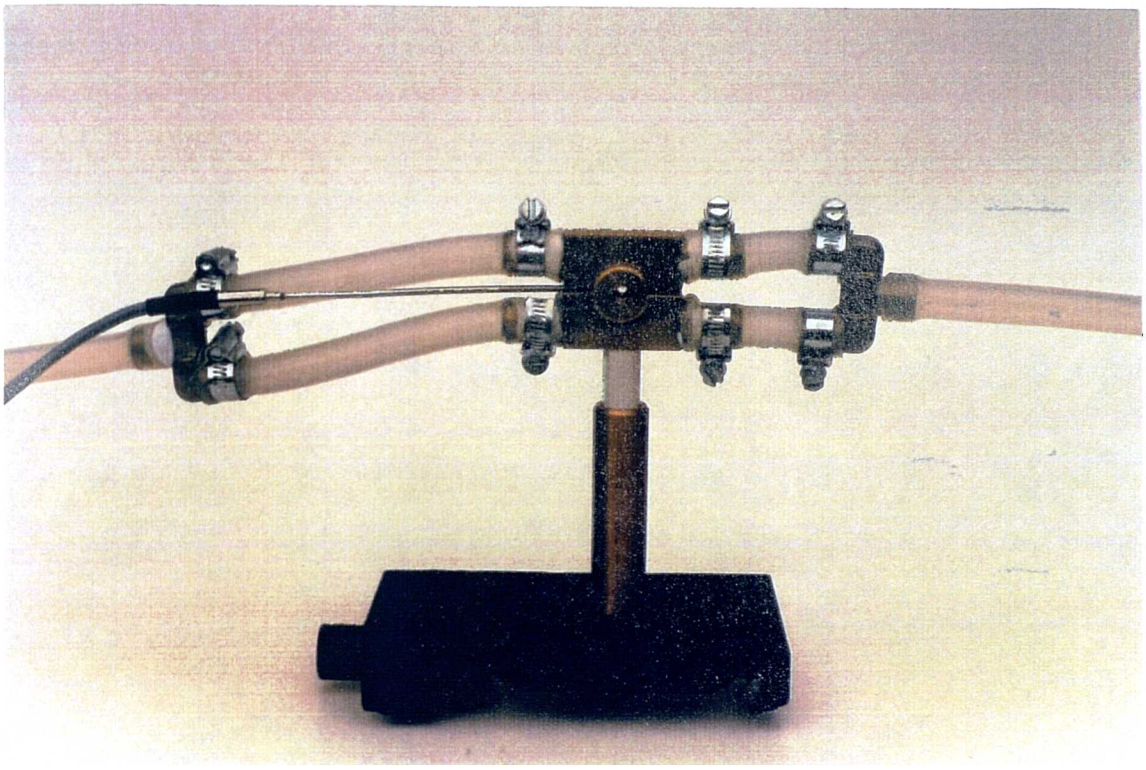

Figure 5.2. Photograph of the in-situ cell used at station X12B at NSLS (Brookhaven).

5.2.3 *Data collection and analysis*

All samples were subjected to a constant heating/cooling rate of 0.75°C/min during which X-ray data were collected with a counting time of 60 seconds per data frame. The raw data were circularly integrated using the program FI_GUI and analysed with the programs FRNEW, INT_VIEW and GEOMVIEW.

5.3 *Effect of presence of tripalmitin on crystallisation of cocoa butter*

Several different concentrations of the binary system tripalmitin/cocoa butter have been analysed in order to study the crystallisation of cocoa butter in the presence of saturated triglycerides such as tripalmitin. First, the single components of the mixture have been investigated, and subsequently, several mixtures have been analysed.

5.3.1 *Cocoa butter*

The sample was cooled from 50°C to 8°C at 0.75°C/min. All data, collected during the cooling stage of the cycle, are summarised in Table 5.1. Crystallisation is first observed at 19.3°C. Cocoa butter starts to crystallise in Form III (Figure 5.3(a)). At 17.2°C, another ring (Figure 5.3(b)) appears and corresponds to the 1st order diffraction pattern of Form I (Table 5.2) [Wille & Lutton, 1966]. The ring, corresponding to the 2nd order of Form I, appears at 16.3°C (Figure 5.3(c)). The d-spacing relative to 2nd order of Form I is half of the d-spacing of 1st order of Form I. During the whole cooling stage, the intensity of Form I is less than the value of intensity recorded for Form III, suggesting that Form III is the dominant form. The sample is kept at a constant temperature (10°C) for approximately 40 minutes. During this period of time, the intensity of Form III increases, while the intensity of Form I decreases, until the latter disappeared completely after 24 minutes at 10°C.

From Figure 5.3(d) it can be observed that a shoulder is formed in the peak corresponding to Form III at 11.9°C. The shoulder became more intense on decreasing the temperature, but not enough to form an independent peak. A 3-D plot of the integrated data is shown in Figure 5.4.

As cocoa butter is heated up to 40°C, the intensity of the shoulder in Form III increases and it shows a proper shape (independent from Form III) at 15.8°C. This latter peak corresponds to Form IV (d = 44.7Å) (Table 5.3). However, Form III is still the predominant form. At 19.9°C, the two peaks show the same intensity, suggesting

that at this temperature cocoa butter crystallised in Forms III and IV in equal quantities. This equilibrium does not last for long; at 20.5°C Form IV became the predominant crystalline form. Form III melts and the peak becomes the shoulder of the peak for Form IV. The recorded melting point of Form III is 22.6°C, this in accordance with literature data [Wille and Lutton, 1966]. Form IV melts at 28.1°C.

Temperature (°C)	d-spacing (Å)	Polymorphic form	Intensity
19.3	49.3	III	60
18.4	49.3	III	225
16.3	54.1 49.0 26.7	I (1^{st} order) III I (2^{nd} order)	629 1893 157
15.0	54.1 49.0 26.7	I (1^{st} order) III I (2^{nd} order)	1928 3420 383
13.6	54.2 48.8 26.7	I (1^{st} order) III I (2^{nd} order)	2705 5994 590
11.4	54.0 48.8 26.6	I (1^{st} order) III I (2^{nd} order)	2314 8959 439
10.7	54.0 48.8 26.6	I (1^{st} order) III I (2^{nd} order)	2105 9342 367
10.0	54.0 48.8 26.6	I (1^{st} order) III I (2^{nd} order)	1096 10131 118
10.0	48.5	III	10049

Table 5.1. Small angle X-ray diffraction data of cocoa butter collected during the cooling stage.

Polymorphs of Cocoa butter	I	II	III	IV	V	VI
long spacing (Å)	55.1 34.0 26.8	49.0	49.0 24.6	45.0 22.6	63.1 32.2	63.1 32.0

Table 5.2. The long spacing of cocoa butter [Wille & Lutton, 1966].

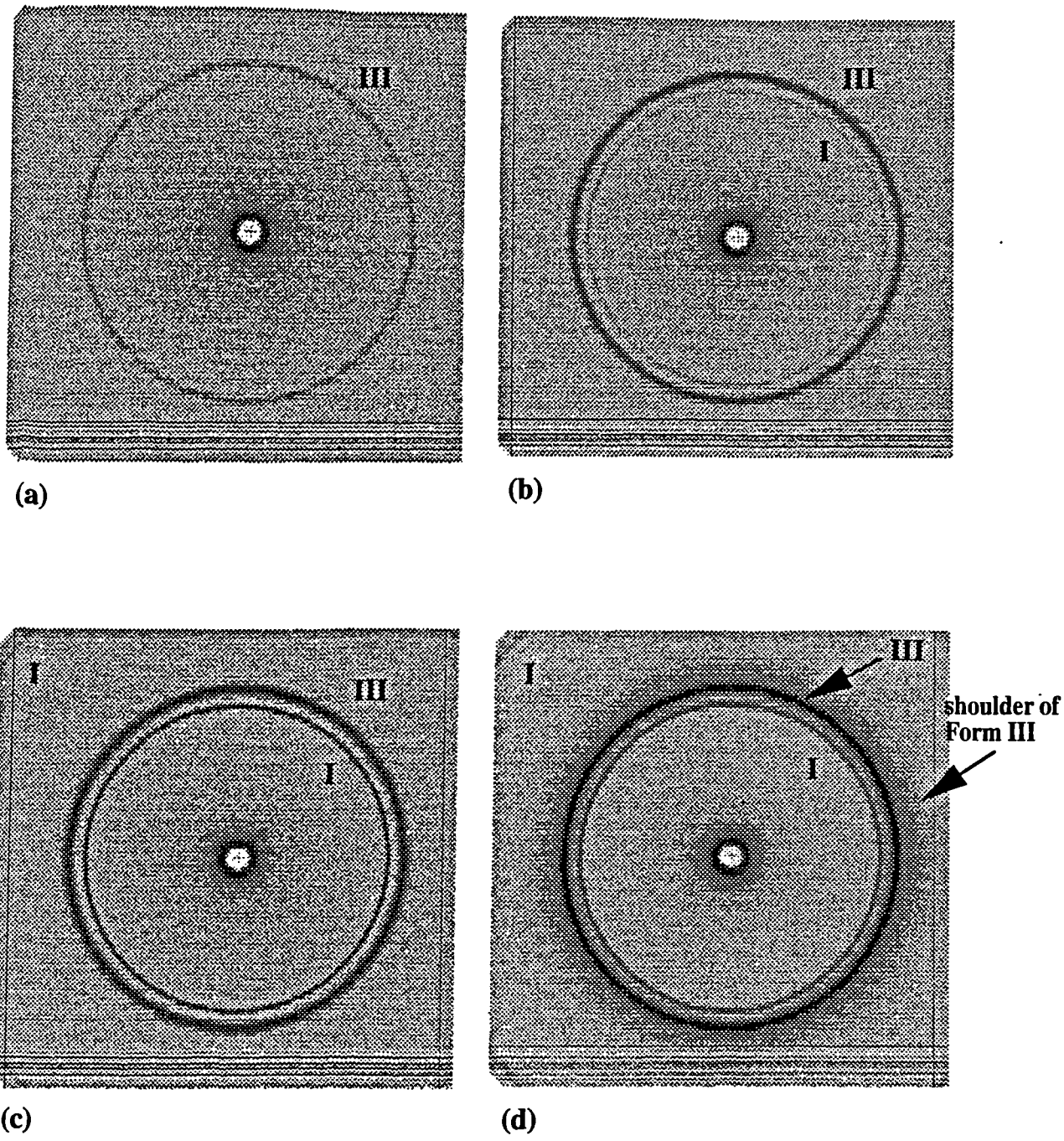

Figure 5.3. Small angle X-ray diffraction data collected during the crystallisation process of cocoa butter: 19.3°C (a); 17.2°C (b); 16.3°C (c) and 11.9°C (d).

Temperature (°C)	d-spacing (Å)	Polymorphic form	Intensity
12.0	48.4 44.7	III IV	7430 2590
15.8	48.4 44.7	III IV	6403 2863
17.3	48.4 44.7	III IV	5317 2896
19.9	48.4 44.7	III IV	3070 2964
20.5	48.2 44.7	III IV	2497 2998
22.6	44.7	IV	2771
28.1	-	-	-

Table 5.3. Small angle X-ray diffraction data of cocoa butter collected during the heating stage.

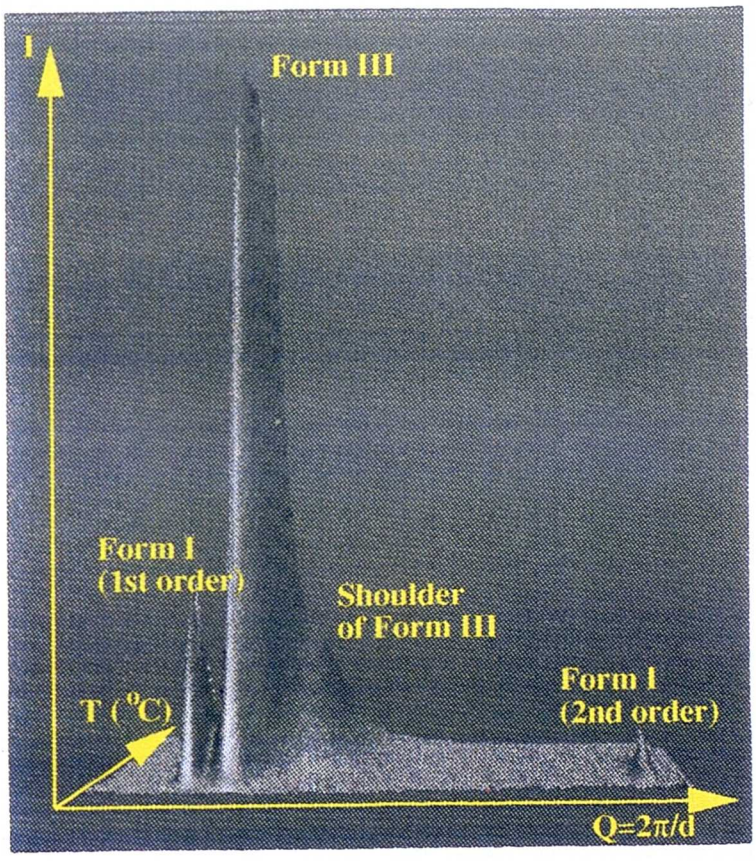

Figure 5.4. A three-dimensional plot of SAXS data collected during the cooling phase of cocoa butter. The sample was cooled from 50 to 8°C. The Q range is from 0.08 to 0.25.

The integration of the raw data shown that a constant intensity is present throughout the 360° thus showing that no preferred orientation is observed (see i.e. Figure 5.5). Similarly effect was observed for any of the systems discussed in this chapter.

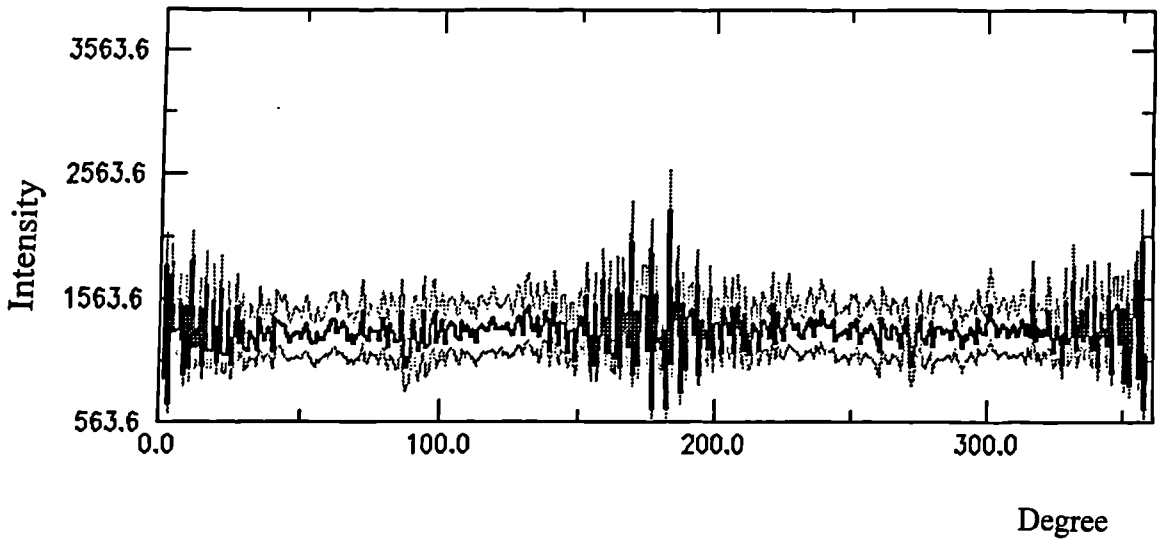

Figure 5.5. Integrated data of cocoa butter sample taken at 18.4°C, during the cooling stage. A constant intensity is present throughout the 360°.

5.3.2 *Tripalmitin*

Melted tripalmitin was cooled from 70°C to 15°C at a rate of 0.75°C/min. The crystallisation starts at 48.2°C. The d-spacing recorded is equal to 41.7Å, which corresponds to the polymorphic form β' (Table 5.4) [Lutton, 1969]. The maximum intensity of the peak corresponding to form β' is reached at 43.7°C and it is constant through the whole cooling stage (Figure 5.6(a) and Table 5.5). During the cooling stage, no polymorphic transitions are observed.

Then, the sample was heated up to 70°C. During heating, the d-spacing is constant up to 51.0°C (see Table 5.6). At this temperature the integrated frame shows a doublet (Figure 5.7), which is due to the coexistence of two phases: β'and β. At 51.7°C only form β is observed. The polymorphic transition is clear immediately, as

shown in the Figure 5.6(b). The transition β' to β takes place rapidly and during the melting of the β'-form. The long-spacing decrease of approximately 1Å is due to the smaller layer thickness of the β-form. This explanation is supported from previous work [Kellens et al., 1991]. At 66.5°C the sample is liquid, since this temperature corresponds to the melting point of form β of tripalmitin.

Polymorphs of PPP	α	β'	β
long spacing (Å)	46.0	42.3	40.9

Table 5.4. The long spacing of tripalmitin [Lutton, 1969].

Temperature (°C)	d-spacing (Å)	Polymorphic Form	Intensity
48.2	41.7	β'	594
44.5	41.7	β'	34418
43.7	41.7	β'	38333
15.0	41.7	β'	39914

Table 5.5. X-ray diffraction data collected during the cooling stage of the cycle for pure tripalmitin

Temperature (°C)	d-spacing (Å)	Polymorphic Form	Intensity
19.0	41.7	β'	39649
42.5	41.6	β'	38947
46.2	41.6	β'	36842
51.0	41.4 40.5	β' β	25131 24868
51.7	40.3	β	34386
59.2	40.3	β	40026
66.5	-	-	-

Table 5.6. X-ray diffraction data collected during the heating stage of the cycle for pure tripalmitin

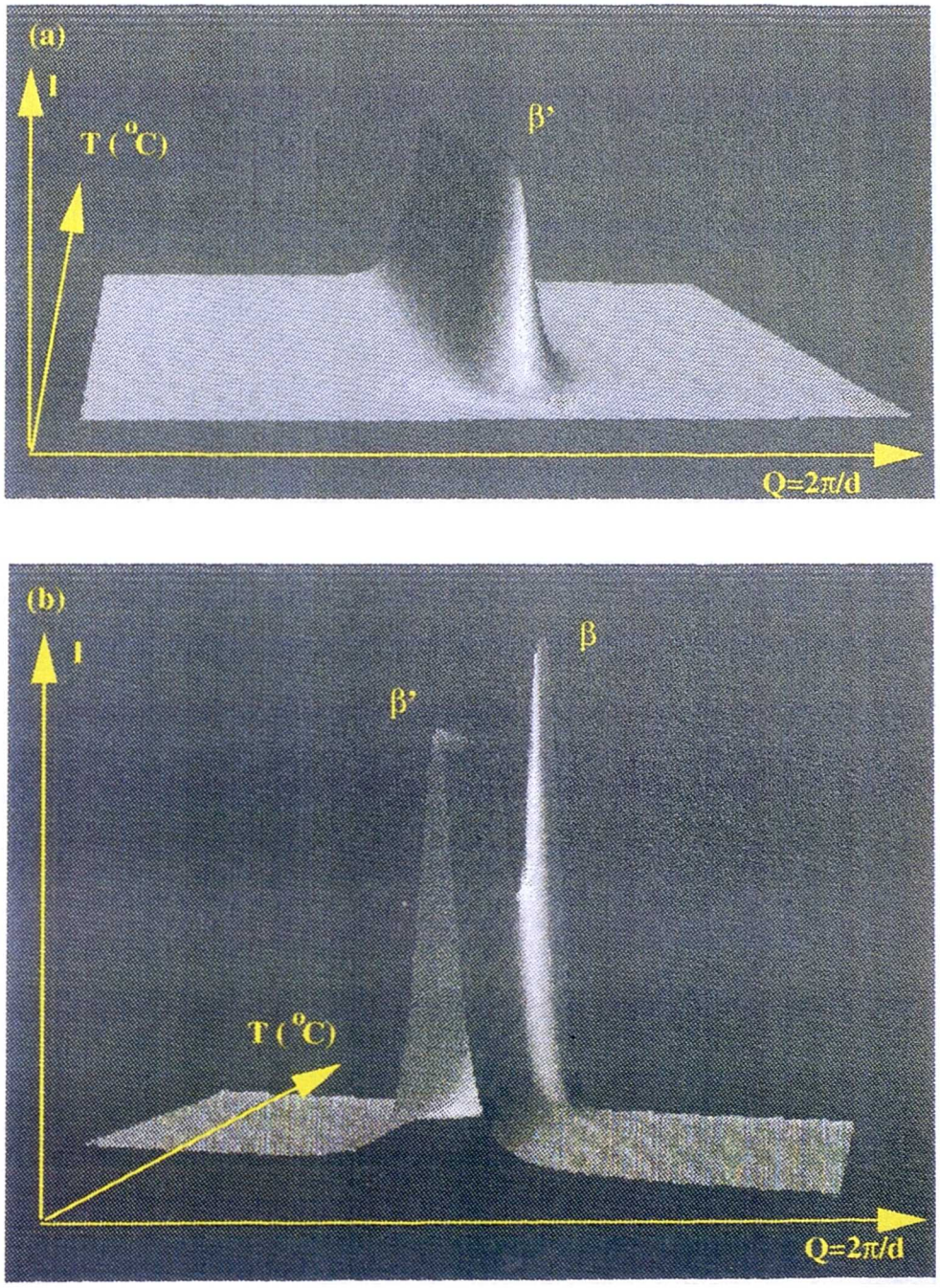

Figure 5.6. A three-dimensional plot of SAXS data of tripalmitin taken as a function of time every 60 seconds during: (a) cooling stage: the sample was cooled from 70 to 15°C; (b) heating stage: the sample was heated back to 70°C. The Q range is from 0.12 to 0.18.

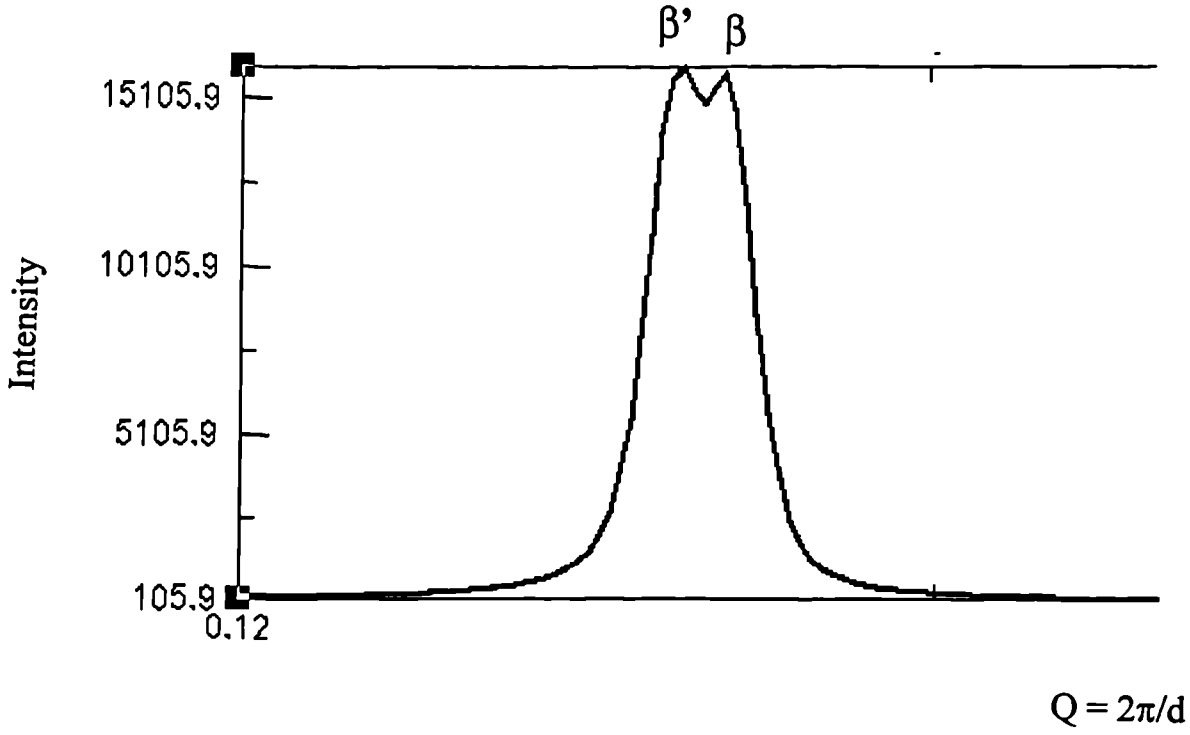

Figure 5.7. Integrate X-ray spectrum taken at 51°C, during the heating stage. The presence of a doublet is due to the coexistence of two phases: β' and β.

After analysing the single components, the crystallisation behaviour of several mixtures of tripalmitin/cocoa butter at different concentrations was investigated.

5.3.3 *25% Tripalmitin in Cocoa Butter*

The mixture was cooled from 70°C to 18°C. It starts to crystallise at 34.2°C. The binary system crystallises first like form α of PPP. The d-spacing found was 45.0Å. The temperature of 34.2°C is too high to suppose that the cocoa butter crystallises and the d-spacing value found (45.0Å) is smaller than the value found in the literature for form α of pure PPP [Lutton, 1969]. The two values can be explained assuming that cocoa butter dissolves in tripalmitin. This influences the crystallisation process of PPP and shifts the d-spacing toward smaller values.

At 32.7°C, a shoulder is formed on the main peak (Figure 5.8). Cooling further, the d-spacing is shifted from 45.0Å to 42.4Å. This is consistent with form α transforming gradually to form β' and the intensity of the peak increases (Table 5.7).

The sample was left at 18.0°C for approximately 15 minutes to allow the data to be transferred from the vax systems to the workstation.

The first frame, collected during the heating phase of the cycle (T=18.9°C), shows that another peak has formed. The relative d-spacing was found to be 34.6Å. This value is too low to correspond to any phases of PPP, but it is consistent with Form I of cocoa butter [Wille and Lutton, 1966]. Form I is also present in the diffraction patterns collected for the cocoa butter sample, but with a different value of d-spacing (54.1Å). The two values correspond to two different crystallisation packing of the same polymorphic phase. The peak at approximately 34.0Å is also be present in the other PPP/CB binary systems described in the following sections.

Form I was found to melt at 26.3°C. After heating further, it was observed that the d-spacing of form β' shifts to 40.2Å and transforms to form β at 48.4°C (Table 5.8). At this temperature, the intensity of the peak corresponding to the form β slightly increases. The mixture melted completely at 59.2°C.

Temperature (°C)	d-spacing (Å)	d-spacing observed for PPP (Å)	Polymorphic form	Intensity
34.2	45.0		α	70
32.7	43.1		α/β'	330
30.0	42.3	41.7	β'	1185
22.5	42.4		β'	1348
18.9	42.4		β'	1425

Table 5.7. Small angle X-ray diffraction data collected during cooling for the 25 mole percent solution of PPP in cocoa butter. The table also includes the d-spacing value observed for PPP alone.

Temperature (°C)	d-spacing (Å)	d-spacing observed for PPP and CB alone	Polymorphic form	Intensity
18.9	42.4 34.6	41.7 (PPP) 54.1 (CB)	β' I	1448 64
20.1	42.4 34.6	41.7 (PPP) 54.1 (CB)	β' I	1435 57
26.3	42.4	41.7 (PPP)	β'	1378
33.5	42.2		β'	1282
39.1	41.9		β'/β	876
42.7	40.8		β'/β	512
48.4	40.2	40.3 (PPP)	β	546
59.2	-		-	-

Table 5.8. Small angle X-ray diffraction data collected during heating for the 25 mole percent solution of PPP in cocoa butter. The table also includes the d-spacing values observed for PPP and cocoa butter (CB) alone.

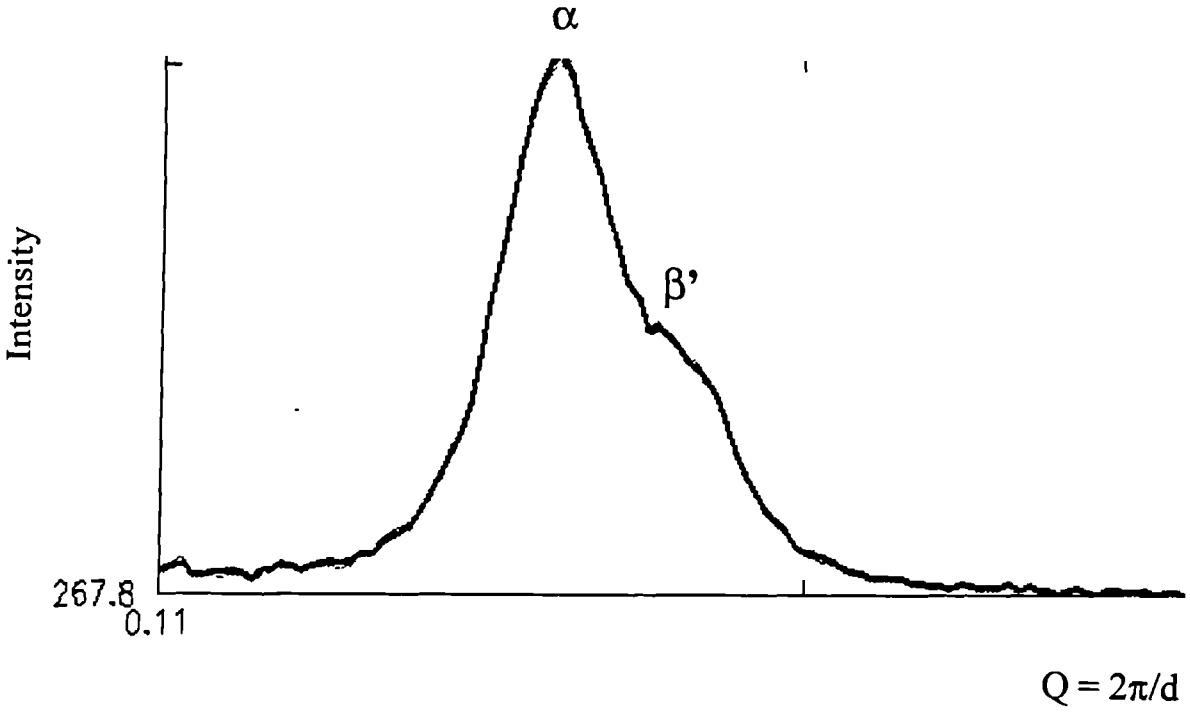

Figure 5.8. Small angle X-ray diffraction data collected during the crystallisation process of 25 mole percent solution of PPP in cocoa butter at 32.7°C: (a) form α and (b) form β'.

5.3.4 *20% Tripalmitin in Cocoa Butter*

The sample was cooled from 70°C to 15°C at 0.75°C/min. Initially this mixture shows the same behaviour observed for the 25 mole percent solution of PPP in cocoa butter. The temperature of crystallisation of form α of the 20 mole percent solution of PPP in cocoa butter was 32.8°C, slightly lower than that recorded for the 25 mole percent solution of PPP in cocoa butter. This is probably due to the lower concentration of PPP. During cooling, the transformation from α to β' was observed. The d-spacing shifts gradually and the intensity increases. The polymorphic transformation occurs at approximately 28.7°C (Table 5.9).

The mixture was cooled further to 15°C, and it was possible to detect two more phases. The first appears at 16.9°C and it has long spacing of 47.3Å. This corresponds to Form III of cocoa butter dissolved in tripalmitin. The second phase crystallises at 16.1°C and it shows a long spacing of 34.9 Å. The latter solid phase was also recorded for the 25 mole percent solution of PPP in cocoa butter. It should be noted that the two phases formed almost at the same time and they could be related. At the lowest temperatures, the concentration of cocoa butter in the solid phase increases, and this leads to the formation of two crystalline forms characteristic of cocoa butter.

Temperature (°C)	d-spacing (Å)	d-spacing observed for PPP and CB alone	Polymorphic form	Intensity
32.8	44.9	--	α	874
31.5	44.2	--	α	1428
30.1	43.2	--	α/β'	2868
28.7	42.6	41.7 (PPP)	β'	4189
19.3	42.6	41.7 (PPP)	β'	6728
16.9	47.3 42.9	49.0 (CB) 41.7 (PPP)	III β'	980 6825
16.1	47.3 42.9 34.9	49.0 (CB) 41.7 (PPP) 54.1 (CB)	III β' I	2272 6651 263

Table 5.9. Small angle X-ray diffraction data collected during cooling of the 20 mole percent solution of PPP in cocoa butter. The table also includes the d-spacing values observed for PPP and cocoa butter (CB) alone.

The system was held at 16°C for approximately 15 minutes. The first frame, collected during heating, did not show the crystalline form at 47.3Å. Form III is melted and the intensities of form β' and Form I are slightly higher, because they are grown up in the constant temperature region. While heating up, the intensities decrease gradually, until at 26.3°C Form I melts on Form β'. The intensity of Form β' increases, because cocoa butter melts and the mixture becomes richer in tripalmitin.

Then, the d-spacing of form β' is gradually shifted to 40.3Å, transforming to form β. The complete polymorphic transformation was recorded at 45.4°C, where the intensity of the peak slightly increases (Table 5.10). The melting point of β was found to be 57.0°C.

Temperature (°C)	d-spacing (Å)	d-spacing observed for PPP and CB alone	Polymorphic form	Intensity
16.2	43.0 34.2	41.7 (PPP) 54.1 (CB)	β' I	7158 908
22.1	43.0 34.1	41.7 (PPP) 54.1 (CB)	β' I	6903 1064
26.3	42.5	41.7 (PPP)	β'	6772
36.2	42.2		β'/β	5331
39.1	42.0		β'/β	4084
43.4	40.6		β'/β	2326
45.4	40.3	49.0 (CB)	β	2561
57.0	-		-	-

Table 5.10. Small angle X-ray diffraction data collected during heating of the 20 mole percent solution of PPP in cocoa butter. The table also includes the d-spacing values observed for PPP and cocoa butter (CB) alone.

5.3.5 *15% and 10% of Tripalmitin in Cocoa Butter*

The 15 mole percent solution of PPP in cocoa butter was cooled from 70°C to 25°C. The system starts to crystallise at 30.8°C like form α (d = 46.4Å). Form I was not observed because the final temperature (25°C) was not low enough to allow the system to crystallise in this crystalline form (Table 5.11). Also the transformation from

Form α to Form β' was missed. The system was not cooled further as the synchrotron beam needed to be refilled.

Temperature (°C)	d-spacing (Å)	d-spacing observed for PPP (Å)	Polymorphic form	Intensity
30.8	46.4	46.0	α	68
28.7	46.2		α	2382
27.3	46.0		α	2668
26.6	46.0		α	2915
25.9	45.7		α	3162

Table 5.11. Small angle X-ray diffraction data collected during cooling for the 15 mole percent solution of PPP in cocoa butter. The table also includes the d-spacing value observed for PPP alone.

Then, the mixture was heated back to 70°C. The first frame shows that the transformation from α to β' has already occurred (Table 5.12). During the heating stage, the d-spacing of form β' shifts gradually to 40.4Å, due to the polymorphic transformation from β' to β. The complete transformation occurs at 47.0°C, where an increasing of the intensity of the peak is observed. Finally, the melting point of the latter phase was recorded at 54.8°C.

Temperature (°C)	d-spacing (Å)	d-spacing observed for PPP (Å)	Polymorphic form	Intensity
25.3	43.1	41.7	β'	5367
30.1	43.1		β'	4849
36.2	42.4		β'/β	2620
38.4	42.1		β'/β	2339
40.3	41.8		β'/β	1789
44.2	41.0		β'/β	632
47.0	40.4	40.3	β	1111
54.8	-		-	-

Table 5.12. Small angle X-ray diffraction data collected during heating of the 15 mole percent solution of PPP in cocoa butter. The table also includes the d-spacing value observed for PPP alone.

Also the 10 mole percent solution of tripalmitin in cocoa butter was cooled to 25°C. This system shown the same behaviour of the previous mixture (Table 5.13). The temperature of 25°C was not low enough to allow the system to crystallise into the low melting fraction. During heating, form β' transformed gradually to form β, but an increasing of the intensity was not noticed (Table 5.14). The melting point of this mixture was observed at 52.8°C.

Temperature (°C)	d-spacing (Å)	d-spacing observed for PPP (Å)	Polymorphic form	Intensity
28.8	46.8	46.0	α	522
28.1	46.6		α	1375
26.7	46.5		α	2403
25.9	46.5		α	2618
25.4	46.5		α	2770

Table 5.13. Small angle X-ray diffraction data collected during cooling for the 10 mole percent solution of PPP in cocoa butter. The table also includes the d-spacing value observed for PPP alone.

Temperature (°C)	d-spacing (Å)	d-spacing observed for PPP (Å)	Polymorphic form	Intensity
25.4	43.5	41.7	β'	5977
27.3	43.4		β'	5834
30.1	43.1		β'	4824
33.0	42.8		β'	4516
35.8	42.5		β'/β	3224
38.7	42.2		β'/β	2401
41.5	41.9		β'/β	1428
43.6	41.8		β'/β	595
46.0	40.2	40.3	β	60
49.8	40.2		β	94
52.8	-		-	-

Table 5.14. Small angle X-ray diffraction data collected during heating of the 10 mole percent solution of PPP in cocoa butter. The table also includes the d-spacing value observed for PPP alone.

5.3.6 *9% of Tripalmitin in Cocoa Butter*

The sample was cooled from 60°C to 15°C. The system crystallises at 25.2°C. The value of long spacing recorded (47.5Å) is consistent with Form III of the mixture rich in cocoa butter. A higher temperature of crystallisation and a smaller value of d-spacing depends on the presence of tripalmitin which crystallises and influences the crystallisation packing of cocoa butter (Table 5.15).

The system was held at 15°C for approximately 20 minutes. Two more forms were observed in the first frame collected during heating (Table 5.16). The peak at 44.8Å could correspond to Form IV of the mixture rich in cocoa butter. This peak does not have a proper shape (Figure 5.9), but it is the shoulder of the peak at 48.3Å (Form III). The peak at 34.2Å is consistent with Form I of cocoa butter. From Figure 5.9 it is evident that the form at 48.3Å dominates the other two.

During heating, Form III is still the most intense, but its intensity decreases step by step, while the intensity of Form IV increases. When the temperature reaches the value of 25.3°C, the intensity of the Form IV peak is greater than that of Form III, and this suggests that Form III melts into Form IV. Form I and Form III melted completely at 26.1°C and 26.8°C, respectively. The two melting points are very close, and this could be due to the fact that two crystalline forms are related.

After the melting of the Forms I and III, the solid phase is richer in tripalmitin. The long spacing shifts gradually to the right. At 37.3°C, the d-spacing is 42.59Å, similar to Form β' of tripalmitin. While the temperature increases, this latter crystalline phase transforms in Form β and the complete transformation is observed at 45.9°C, where the intensity of the latter form increases. Finally, its melting point is recorded at 50.4°C.

Temperature (°C)	d-spacing (Å)	d-spacing observed for CB (Å)	Polymorphic form	Intensity
25.2	47.5	49.0-48.5	III	878
23.8	47.5		III	6400
21.6	47.5		III	10272
19.4	47.6		III	15672
16.3	47.6		III	23295
14.7	47.9		III	33625

Table 5.15. Small angle X-ray diffraction data collected during heating of the 10 mole percent solution of PPP in cocoa butter. The table also includes the d-spacing value observed for cocoa butter alone.

Temperature (°C)	d-spacing (Å)	d-spacing observed for PPP and CB alone (Å)	Polymorphic form	Intensity
14.9	48.3 44.8 34.2	49.0 (CB) 44.7 (CB) 54.1 (CB)	III IV I	30294 7290 1870
18.7	48.1 44.6 34.2		III IV I	26843 8645 1595
23.1	47.5 44.7 34.2		III IV I	16653 10232 1260
25.3	47.5 44.6 34.4		III IV I	8619 9408 650
26.1	47.5 44.4		III IV	6580 8346
26.8	44.3		IV	7640
34.3	43.0		IV→β'	5930
37.3	42.6	41.7 (PPP)	β'	3561
40.3	41.8		β'	1283
43.6	41.1		β'→β	1236
45.9	40.8	40.3 (PPP)	β	6913
50.4	-		-	-

Table 5.16. Small angle X-ray diffraction data collected during heating of the 9 mole percent solution of PPP in cocoa butter. The table also includes the d-spacing value observed for cocoa butter alone.

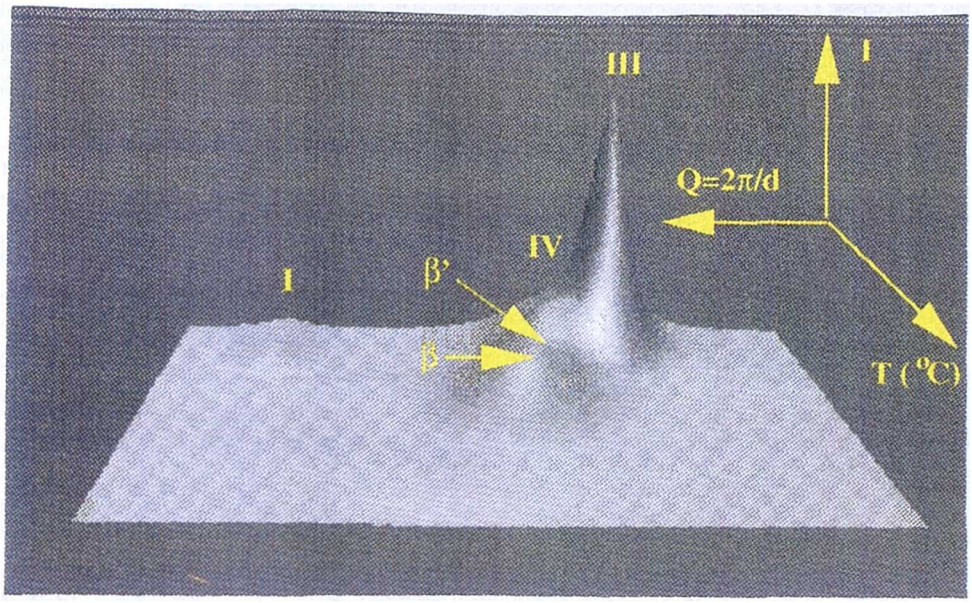

Figure 5.9. A three-dimensional plot of SAXS data collected during the heating stage of 9 mole percent solution of PPP in cocoa butter. The mixture was heated from 15°C to 50°C. The Q range is from 0.08 to 0.21.

5.3.7 *9%, 8% and 7% of Tripalmitin in Cocoa Butter*

The similarities and differences, observed in the behaviour of these three mixtures, have been summarised in Table 5.17. During cooling, all systems show the same crystallisation behaviour. The temperature of first crystallisation is slightly different, this perfectly agrees with the difference in concentration of tripalmitin in cocoa butter (Tables 5.18 and 5.20).

During heating, Forms I and III melt together for all concentrations and this supports the hypothesis that the forms could be related (Tables 5.19 and 5.21). Heating further, a shift in the d-spacing is observed for the three systems. The polymorphic transformation from β' to β was clearly observed for the 9 and 8 mole percent solutions. In the case of the 7 mole percent solution of PPP in cocoa butter, the long spacing shifts gradually to 41.7Å, assuming a value very close to that corresponding to form β' of tripalmitin. Because the temperature at which the frame was taken is close to the melting point of the solid phase and the intensity of the corresponding peak is

very low, it is not possible to know for certain if the polymorphic transformation had really taken place.

Concentration	9%	8%	7%
Crystallisation temperature of Form III	25.5°C	25.2°C	24.6°C
Melting point of Forms I and III	26.1°C	25.4°C	25.3°C
Temperature of transformation from β' to β	45.9°C	44.6°C	41.8°C
Melting point of β	50.4°C	48.4°C	45.7°C

Table 5.17. Comparison of the small angle X-ray data obtained for 9, 8 and 7 mole percent solutions of PPP in cocoa butter.

Temperature (°C)	d-spacing (Å)	d-spacing observed for CB (Å)	Polymorphic form	Intensity
25.5	47.8	49.0-48.5	III	553
24.1	47.7		III	5059
22.7	47.7		III	9670
20.7	47.7		III	14780
18.8	47.8		III	20475
16.9	48.0		III	28158

Table 5.18. Small angle X-ray diffraction data collected during cooling of the 8 mole percent solution of PPP in cocoa butter. The table also includes the d-spacing value observed for cocoa butter alone.

Temperature (°C)	d-spacing (Å)	d-spacing observed for PPP and CB alone	Polymorphic form	Intensity
14.9	48.1 44.5 34.3	49.0 (CB) 44.7 (CB) 54.1 (CB)	III IV I	28226 15280 994
18.2	48.0 44.5 34.3		III IV I	25325 15845 1116
23.2	47.6 44.4 34.3		III IV I	15281 18291 643
24.6	47.5 44.4		III IV	9416 17230
26.1	44.2		IV	10201
27.6	43.8		IV→β'	6216
29.1	43.5		IV→β'	6823
30.6	43.4		IV→β'	6802
33.7	43.1	41.7 (PPP)	β'	4939
35.1	42.9		β' →β	3833
37.4	42.5		β' →β	1940
40.4	41.4		β' →β	1104
44.6	40.9	40.3 (PPP)	β	920
48.4	-		-	-

Table 5.19. Small angle X-ray diffraction data collected during heating of the 8 mole percent solution of PPP in cocoa butter. The table also includes the d-spacing values observed for PPP and cocoa butter alone.

Temperature (°C)	d-spacing (Å)	d-spacing observed for CB (Å)	Polymorphic form	Intensity
24.6	48.1	49.0-48.5	III	1303
23.2	48.0		III	7471
21.7	48.0		III	12073
19.6	47.9		III	18650
16.7	47.9		III	32250
15.1	48.0		III	41976
14.9	48.0		III	51347

Table 5.20. Small angle X-ray diffraction data collected during cooling of the 7 mole percent solution of PPP in cocoa butter. The table also includes the d-spacing value observed for cocoa butter alone.

Temperature (°C)	d-spacing (Å)	d-spacing observed for PPP and CB alone	Polymorphic form	Intensity
14.9	48.5	49.0 (CB)	III	59223
	44.6	44.7 (CB)	IV	8281
	34.3	54.1 (CB)	I	902
17.3	48.3		III	45928
	44.6		IV	10687
	34.3		I	1033
21.6	48.0		III	22309
	44.6		IV	14350
	34.3		I	1244
24.5	47.6		III	7707
	44.4		IV	10498
	34.3		I	373
26.0	44.3		IV	6263
27.4	43.9		IV→β'	5347
29.7	43.6		IV→β'	5916
34.2	43.1		IV→β'	3788
37.2	42.9	41.7 (PPP)	β'	2843
40.2	41.7		β'	457
41.8	40.5	40.3 (PPP)	β	433
45.7	-		-	-

Table 5.21. Small angle X-ray diffraction data collected during heating of the 7 mole percent solution of PPP in cocoa butter. The table also includes the d-spacing values observed for PPP and cocoa butter alone.

5.3.8 *6% Tripalmitin in Cocoa Butter*

This mixture was cooled from 54°C to 15°C and it was found to crystallise at 24.9°C. The long spacing recorded was 48.0Å, similar to that of Form III of the cocoa butter sample, but slightly smaller (Table 5.22). The crystalline phase is very rich in cocoa butter, but the presence of tripalmitin still influences the crystallisation process.

Then, the system was held at 15°C for approximately 30 minutes. During this period of time, Forms IV and I were formed. The Form IV peak is a shoulder of the peak for Form III. The heating stage of the cycle shows the same behaviour as that observed for all the other systems (Table 5.23). Form III is the predominant crystalline form, until the system reaches the temperature of 24.2°C where the intensity of the

Form IV peak is greater than that of Form III. Slowly, Forms I and III melt leaving Form IV. Form I disappears at 26.6°C, while Form III melts completely leaving Form IV at 27.4°C (Figure 5.10). Further heating causes the d-spacing of Form IV to be slightly shifted to the right and this suggests the presence of a morphological form similar to Form β' of tripalmitin, although the percentage of tripalmitin is low (only 6%). However, the polymorphic transition from β' to β is not observed. Finally, the melting point is observed at 46.1°C.

Temperature (°C)	d-spacing (Å)	d-spacing observed for CB (Å)	Polymorphic form	Intensity
24.6	48.9	49.0-48.5	III	301
24.3	48.2		III	2279
23.6	48.1		III	5891
22.2	48.0		III	12830
20.9	48.0		III	18308
19.7	48.0		III	23537
18.4	48.0		III	30323
17.3	48.0		III	39269

Table 5.22. Small angle X-ray diffraction data collected during cooling of the 6 mole percent solution of PPP in cocoa butter. The table also includes the d-spacing value observed for cocoa butter alone.

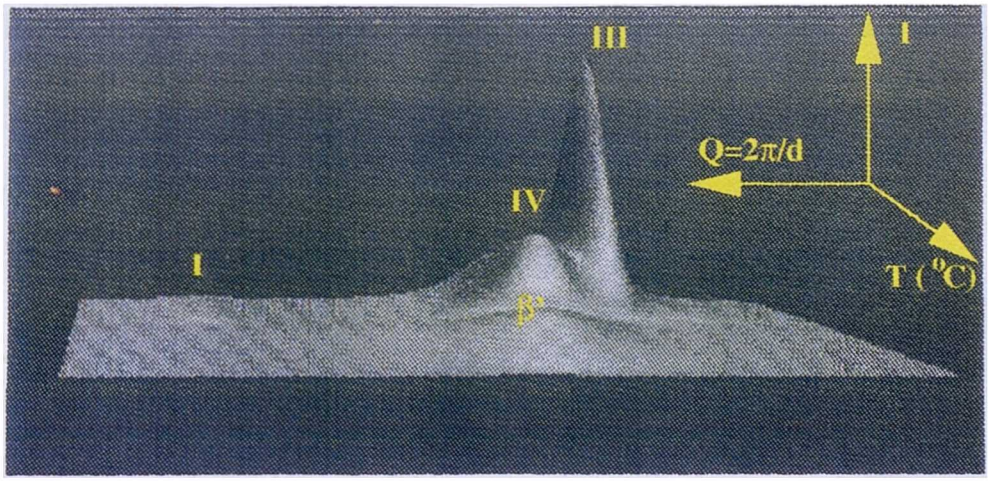

Figure 5.10. A three-dimensional plot of SAXS data collected during the heating stage of 6 mole percent solution of PPP in cocoa butter. The mixture was heated from 15 to 60°C. The Q range is from 0.08 to 0.21.

Temperature (°C)	d-spacing (Å)	d-spacing observed for PPP and CB alone	Polymorphic form	Intensity
15.0	48.5 44.8 34.3	49.0 (CB) 44.7 (CB) 54.1 (CB)	III IV I	71468 15100 1194
20.4	48.2 44.7 34.3		III IV I	46008 19782 1487
23.5	47.9 44.5 34.3		III IV I	27569 22817 1505
24.2	47.9 44.6 34.3		III IV I	22461 23338 1228
26.6	47.7 44.4		III IV	6830 15695
27.4	44.3		IV	
28.3	44.1		IV	6424
31.5	43.7		IV→β'	7434
36.4	43.2		IV→β'	4625
38.8	43.0	41.7 (PPP)	β'	3378
46.1	-		-	-

Table 5.23. Small angle X-ray diffraction data collected during heating of the 6 mole percent solution of PPP in cocoa butter. The table also includes the d-spacing values observed for PPP and cocoa butter alone.

5.3.9 *5% and 4% of Tripalmitin in Cocoa Butter*

During cooling, the 5 mole percent solution crystallises at 25.4°C with a long spacing of 47.8Å, similar to that of Form III of cocoa butter alone (Table 5.24). Then, the system was kept at 25°C for approximately 20 minutes. In this case, the temperature was not low enough to allow the mixture to crystallise in Form I, while Form IV was detected as a shoulder on the peak for Form III. Heating up, Form III melts leaving Form IV, which becomes the dominant crystalline phase (Table 5.25). Form III disappears at 27.6°C. As observed for the previous mixtures at higher temperatures, the peak for Form IV shifts to 42.9Å, because cocoa butter melts and the crystalline phase becomes richer in solid tripalmitin (Figure 5.11). Like for the 6 mole

percent solution of tripalmitin in cocoa butter, this suggests the presence of a form similar to β'. The crystals completely melts at 41.0°C.

Studying the 4 mole percent solution of PPP in cocoa butter, it has been observed that both percentages (5% and 4%) crystallise in a similar way. The solid phase is very rich in cocoa butter, although the presence of tripalmitin can still influence the d-spacing shifting.

The first crystallisation of the 4 mole percent solution appears at 23.2°C (Table 5.26). Cooling the system to 15°C, led to Forms I and IV to crystallising. The Form I peak has very low intensity and cannot be observed in a three-dimensional plot. During heating, the Form IV peak increases in intensity and Forms I and III melt at approximately 24.6°C (Table 5.27). This can be explained in terms of cocoa butter crystallising in a more stable polymorphic form such as Form IV. It can be noted that the intensity of Form IV drops down between 24.6°C and 26.8°C. The latter temperature is very close to the melting point reported in literature for Form IV of cocoa butter [Wille and Lutton, 1966]. Now the solid phase is richer in tripalmitin but, because of the small percentage of tripalmitin present (only 4%), the amount of solid phase cannot be very high (Figure 5.12). The system finally melts completely at 38.4°C.

Temperature (°C)	d-spacing (Å)	d-spacing observed for CB (Å)	Polymorphic form	Intensity
25.4	47.9	49.0-48.5	III	423
25.0	47.9		III	904

Table 5.24. Small angle X-ray diffraction data collected during cooling of the 5 mole percent solution of PPP in cocoa butter. The table also includes the d-spacing value observed for cocoa butter alone.

Temperature (°C)	d-spacing (Å)	d-spacing observed for PPP and CB alone	Polymorphic form	Intensity
25.4	47.4 44.6	49.0 (CB) 44.7 (CB)	III IV	2447 679
26.0	47.4 44.6		III IV	1477 771
26.8	47.4 44.6		III IV	858 1000
27.6	44.6		IV	1401
28.9	44.3		IV	1754
29.7	43.8		IV→β'	1877
33.2	43.2		IV→β'	1745
35.4	42.9	41.7 (PPP)	β'	1474
41.0	-		-	-

Table 5.25. Small angle X-ray diffraction data collected during heating of the 5 mole percent solution of PPP in cocoa butter. The table also includes the d-spacing values observed for PPP and cocoa butter alone.

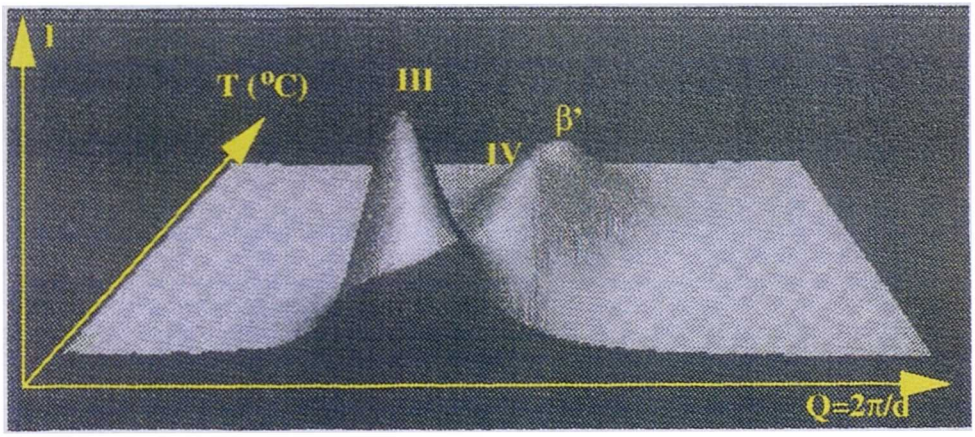

Figure 5.11 A three-dimensional plot of SAXS data collected during the heating stage of 5 mole percent solution of PPP in cocoa butter. The mixture was heated from 25 to 50°C. The Q range is from 0.10 to 0.18.

Temperature (°C)	d-spacing (Å)	d-spacing observed for CB (Å)	Polymorphic form	Intensity
23.2	48.7	49.0-48.5	III	602
22.4	48.6		III	3222
21.0	48.3		III	8999
20.3	48.3		III	11595
19.0	48.3		III	17173
17.8	48.3		III	24178

Table 5.26. Small angle X-ray diffraction data collected during cooling of the 4 mole percent solution of PPP in cocoa butter. The table also includes the d-spacing value observed for cocoa butter alone.

Temperature (°C)	d-spacing (Å)	d-spacing observed for PPP and CB alone	Polymorphic form	Intensity
14.9	48.5 44.6 34.3	49.0 (CB) 44.7 (CB) 54.1 (CB)	III IV I	28358 17762 409
16.3	48.5 44.6 34.3		III IV I	26676 18150 337
19.3	48.3 44.5 34.3		III IV I	21311 19459 372
20.8	48.3 44.5 34.3		III IV I	17712 20312 354
23.8	48.3 44.4		III IV	7637 22193
24.6	44.4		IV	20887
26.8	44.3		IV	12345
28.3	44.1		IV	2325
29.3	43.8	41.7 (PPP)	IV→β'	2582
32.8	43.6		IV→β'	1896
35.8	43.3		IV→β'	674
36.7	43.2		IV→β'	425
38.4	-		-	-

Table 5.27. Small angle X-ray diffraction data collected during heating of the 4 mole percent solution of PPP in cocoa butter. The table also includes the d-spacing values observed for PPP and cocoa butter alone.

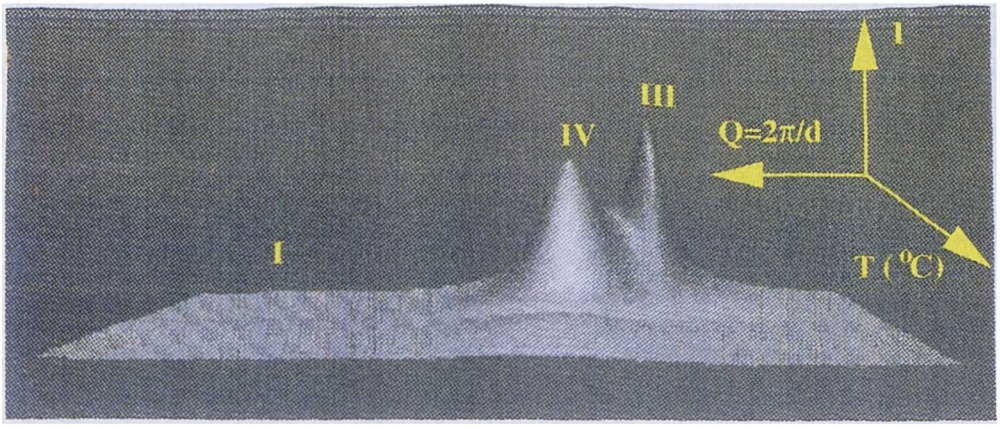

Figure 5.12. A three-dimensional plot of SAXS data collected during the heating stage of 4 mole percent solution of PPP in cocoa butter. The mixture was heated from 15 to 50°C. The Q range is from 0.08 to 0.21.

5.3.10 *3% Tripalmitin in Cocoa Butter*

The mixture was cooled from 60°C to 15°C. The cooling phase shows the same behaviour as that observed for the 6, 5 and 4 mole percent solutions. The system crystallises at 22.0°C. The long spacing observed was 48.9Å, which is consistent with Form III of cocoa butter. The small percentage of tripalmitin does not seem to influence the crystallisation of the system during cooling. In fact, the d-spacing value does not shift (Table 5.28) (Figure 5.13(a)).

After keeping the system at 15°C for approximately 30 minutes, it was heated up to 54°C. The first frame collected shows the presence of three new peaks (Figure 5.13(b)). They have long spacing values of 44.5Å, 34.3Å and 24.1Å, respectively (Table 5.29). The peak at 44.5Å corresponds to Form IV of cocoa butter, while the peak at 24.1Å is consistent with 2nd order of Form III. The latter peak was not present in the systems described in the previous sections. The d-spacing value of 34.3Å is consistent with Form I. Form III is still the dominant crystalline phase, while Form I has very low intensity peak. During the heating phase of the cycle, Form III (2nd order) disappears quickly, it melts at only 18.8°C. The intensity of the Form III (1st

order) peak decreases. Step by step, Form III melts and it transforms gradually to Form IV. At 21.0°C, Form IV is the dominant solid phase, being the only phase remaining when both Forms I and III melt at 24.6°C. Heating further, the d-spacing of Form IV does not change and this could be explained in terms of the concentration of tripalmitin being too low to interfere with the crystal packing of the system. Finally, Form IV melts at 34.8°C and this value is too high for Form IV of pure cocoa butter [Wille and Lutton, 1966]. In conclusion, the low presence of tripalmitin can affect the dissolution process.

Temperature (°C)	d-spacing (Å)	d-spacing observed for CB (Å)	Polymorphic form	Intensity
22.0	48.9	49.0-48.5	III	2072
18.1	48.7		III	30415
16.9	48.7		III	46216

Table 5.28. Small angle X-ray diffraction data collected during cooling of the 3 mole percent solution of PPP in cocoa butter. The table also includes the d-spacing value observed for cocoa butter alone.

Temperature (°C)	d-spacing (Å)	d-spacing observed for CB (Å)	Polymorphic Form	Intensity
15.2	48.7	49.0	III (1st order)	72630
	44.5	44.7	IV	15314
	34.3	54.1	I	616
	24.1		III (2nd order)	240
18.8	48.7		III (1st order)	39657
	44.5		IV	20376
	34.3		I	738
21.0	48.6		III (1st order)	22929
	44.5		IV	23104
	34.3		I	759
24.6	44.4		IV	19869
26.0	44.4		IV	6842
34.8	-		-	-

Table 5.29. Small angle X-ray diffraction data collected during heating of the 3 mole percent solution of PPP in cocoa butter. The table also includes the d-spacing value observed for cocoa butter alone.

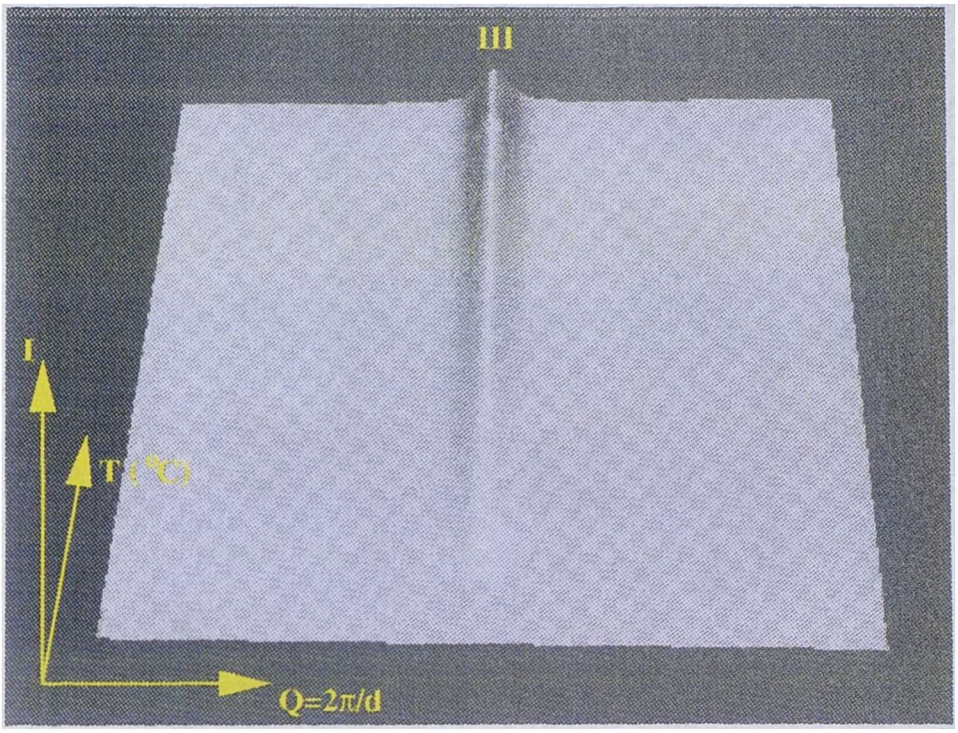

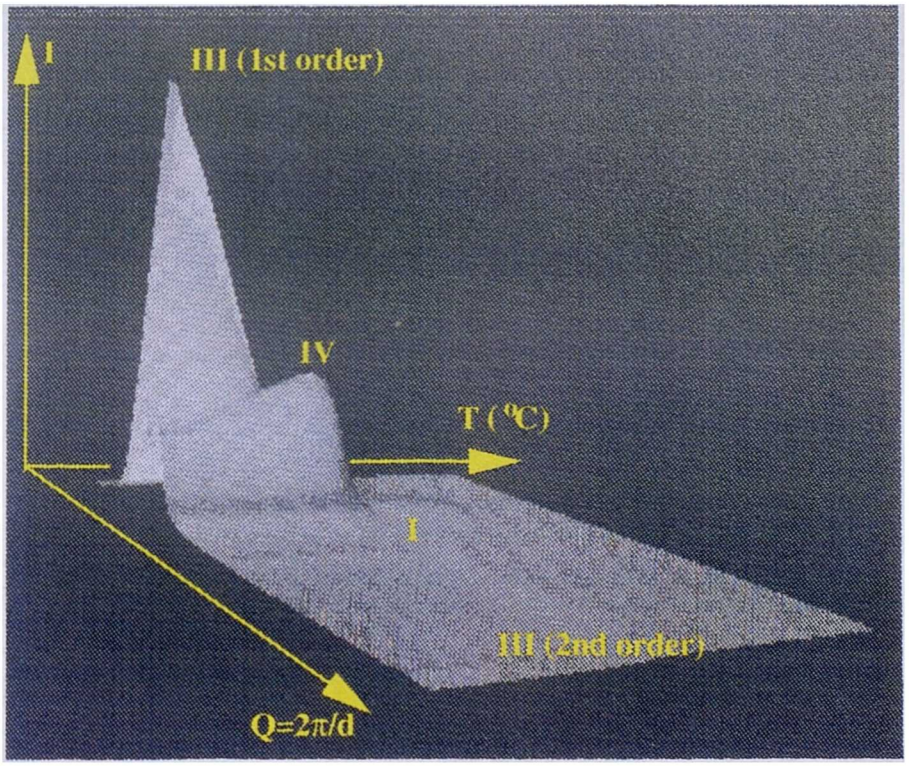

Figure 5.13. A three-dimensional plot of SAXS data of 3 mole percent solution of PPP in cocoa butter collected during: (a) cooling and (b) heating. The Q range is from 0.08 to 0.21.

5.3.11 *2% and 1% of Tripalmitin in Cocoa Butter*

These mixtures show similarity with the previous mixtures. Both systems were cooled to 15°C. In the case of the 2 mole percent solution of tripalmitin in cocoa butter, the cooling stage is characterised by the formation of a solid phase at 21.3°C (Table 5.30). The related long spacing is 48.4Å, which corresponds to Form III of cocoa butter. The heating stage does not show the presence of the peak corresponding to the 2nd order of Form III. This is due to the fact that the system was held at 15°C for 2 hours to allow the refilling of the synchrotron beam. It was not possible to collect frames and detect any changes during this period of time. Moreover, it is possible that the peak corresponding to the 2nd order of Form III is formed at 15°C, but it is of very low intensity.

From Table 5.31 and Figure 5.14 it should also be noted that in the first frame, collected during the heating stage, the intensity of Form IV is bigger than the intensity of Form III. It can be deduced that the morphological modifications do not depend only on the temperature of the system, but also on the time at a particular temperature.

During the heating stage, Form III melts at 22.4°C, while Form I disappears completely at 24.4°C. Also in this case, this agrees with the hypothesis that the two forms are related to the same solid phase. Heating further, Form IV melted at 33.2°C.

Temperature (°C)	d-spacing (Å)	d-spacing observed for CB (Å)	Polymorphic Form	Intensity
21.3	49.1	49.0-48.5	III	1306
20.6	49.1		III	6076
19.9	49.0		III	11849
19.3	49.0		III	17133
18.7	49.0		III	27958
17.4	48.9		III	34098
16.8	48.9		III	41405

Table 5.30. Small angle X-ray diffraction data collected during cooling of the 2 mole percent solution of PPP in cocoa butter. The table also includes the d-spacing value observed for cocoa butter alone.

Temperature (°C)	d-spacing (Å)	d-spacing observed for CB (Å)	Polymorphic form	Intensity
15.6	48.37 44.67 34.36	49.0 44.7 54.1	III IV I	12138 19156 454
22.4	44.42 34.31		IV I	20961 399
24.4	44.42		IV	15914
33.2	-		-	-

Table 5.31. Small angle X-ray diffraction data collected during heating of the 2 mole percent solution of PPP in cocoa butter. The table also includes the d-spacing value observed for cocoa butter alone.

The 1 mole percent solution of tripalmitin in cocoa butter crystallised at 22.1°C, as Form III (Table 5.32). Cooling further, another solid phase appears at 17.9°C and it has a d-spacing of 24.1 Å. Then, in the case of this system, the Form III (2nd order) is formed before the temperature reaches the value of 15°C.

The first frame, collected during the heating stage, shows the presence of Forms IV and I, but the Form III is still predominant (Figure 5.15). All data collected during the heating stage are summarised in Table 5.33. Heating further, the Form III 2nd order peak disappears at 20.7°C, while the peak intensities of Form III (1st order) and IV decrease and increase, respectively. At 22.1°C, it is observed that Form IV becomes the predominant solid phase. Form III disappears at 24.1°C, while Form I melts at 27.0°C.

The melting point of Form IV is 30.6°C.

Temperature (°C)	d-spacing (Å)	d-spacing observed for CB (Å)	Polymorphic Form	Intensity
23.5	48.9	49.0-48.5	III	77
22.8	48.9		III	835
21.4	48.7		III	2441
20.0	48.7		III	4959
17.9	48.5 24.1		III (1st order) III (2nd order)	7418 49
16.0	48.5 24.1		III (1st order) III (2nd order)	13008 74
15.9	48.5 24.1		III (1st order) III (2nd order)	17696 80

Table 5.32. Small angle X-ray diffraction data collected during cooling of the 1 mole percent solution of PPP in cocoa butter. The table also includes the d-spacing value observed for cocoa butter alone.

Temperature (°C)	d-spacing (Å)	d-spacing observed for CB (Å)	Polymorphic form	Intensity
16.0	48.3 44.5 34.2 24.0	49.0 44.7 54.1	III (1st order) IV I III (2nd order)	17374 2110 172 67
20.7	48.4 44.2 34.2		III (1st order) IV I	6279 4101 240
22.1	48.4 44.2 34.2		III (1st order) IV I	3465 4501 256
24.1	44.1 34.2		IV I	5002 262
27.0	44.1		IV	2809
28.5	44.0		IV	898
30.6	-		-	-

Table 5.33. Small angle X-ray diffraction data collected during heating of the 1 mole percent solution of PPP in cocoa butter. The table also includes the d-spacing value observed for cocoa butter alone.

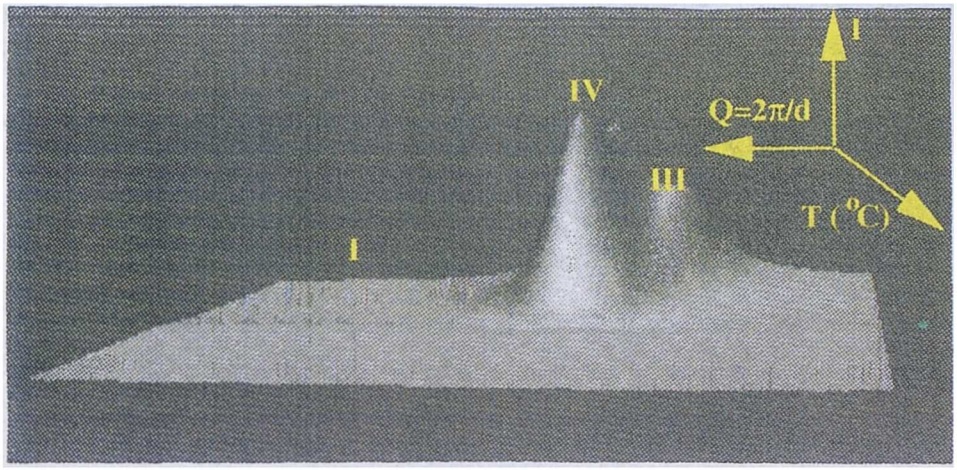

Figure 5.14. A three-dimensional plot of SAXS data collected during the heating stage of 2 mole percent solution of PPP in cocoa butter. The mixture was heated from 15 to 40°C. The Q range is from 0.08 to 0.25.

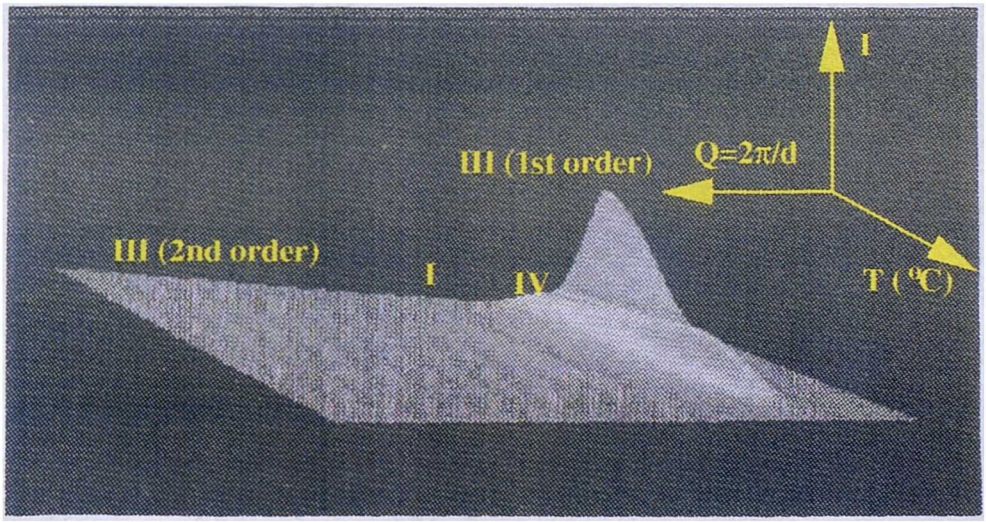

Figure 5.15. A three-dimensional plot of SAXS data collected during the heating stage of 1 mole percent solution of PPP in cocoa butter. The mixture was heated from 15 to 40°C. The Q range is from 0.08 to 0.28.

5.3.12 *Discussions*

5.3.12.1 *Study of stability of Form I at different concentration of PPP in CB*

Form I of cocoa butter has always been considered the least stable form. Wille and Lutton (1966) obtained Form I by rapidly cooling cocoa butter to low temperatures. Heating up at 0.5°C/min, this form melted at 17.3°C and transformed into Form IV via Forms II and III. Chapman (1971) reported a melting point of 15.7°C for Form I, while Witzel and Becker (1969), who studied the polymorphic forms of cocoa butter, do not report any data on Form I. According to Lutton and Chapman, an important condition to obtain the unstable forms I and III was to rapidly cool the sample so as to prevent the crystallisation of more stable forms (IV and V).

In this work the results on cocoa butter from the experiments carried out at NSLS at Brookhaven, confer a greater stability to Form I than previously suggested. It is important to underline that all samples were subjected to a cooling/heating cycle at a slow rate (0.75°C/min). Cooling cocoa butter, Form I was formed at 16.3°C and is characterised by two long spacing values at 54.2 Å and 26.7 Å. The sample was held at 10°C for approximately 40 minutes. During this period of time, the crystal lattice was reorganised and Form I transformed to Form III. The melting point of Form I was not recorded. But it is not possible to exclude completely the possibility that Form I would not have lasted at higher temperature if the sample had been heated up immediately.

Adding tripalmitin to cocoa butter, the formation of Form I was observed for all the different concentrations of PPP in the mixture PPP/CB, with the exception of 15, 10 and 5 mole percent solutions of PPP in cocoa butter. These mixtures were not cooled to a temperature low enough to allow the crystallisation of Form I. For all the other mixtures examined, Form I was formed and showed a long spacing value of 34.3Å [Wille and Lutton, 1966]. Comparing the data obtained from cocoa butter alone with those obtained from the mixtures of tripalmitin and cocoa butter, it is clearly evident that the two systems crystallise in two different types of molecular packing, but both related to Form I. Obviously, tripalmitin influences the molecular arrangement of cocoa butter and, at the same time, increases the stability of Form I at

higher temperatures.

In Figure 5.16 the intensity of Form I (d = 34.1Å) versus temperature is plotted for the system tripalmitin/cocoa butter at different concentrations of tripalmitin. The melting point of Form I varies within a range of temperatures between 23.8°C and 26.6°C. The maximum intensity of this polymorphic form occurs at 9 and 6 mole percent of tripalmitin.

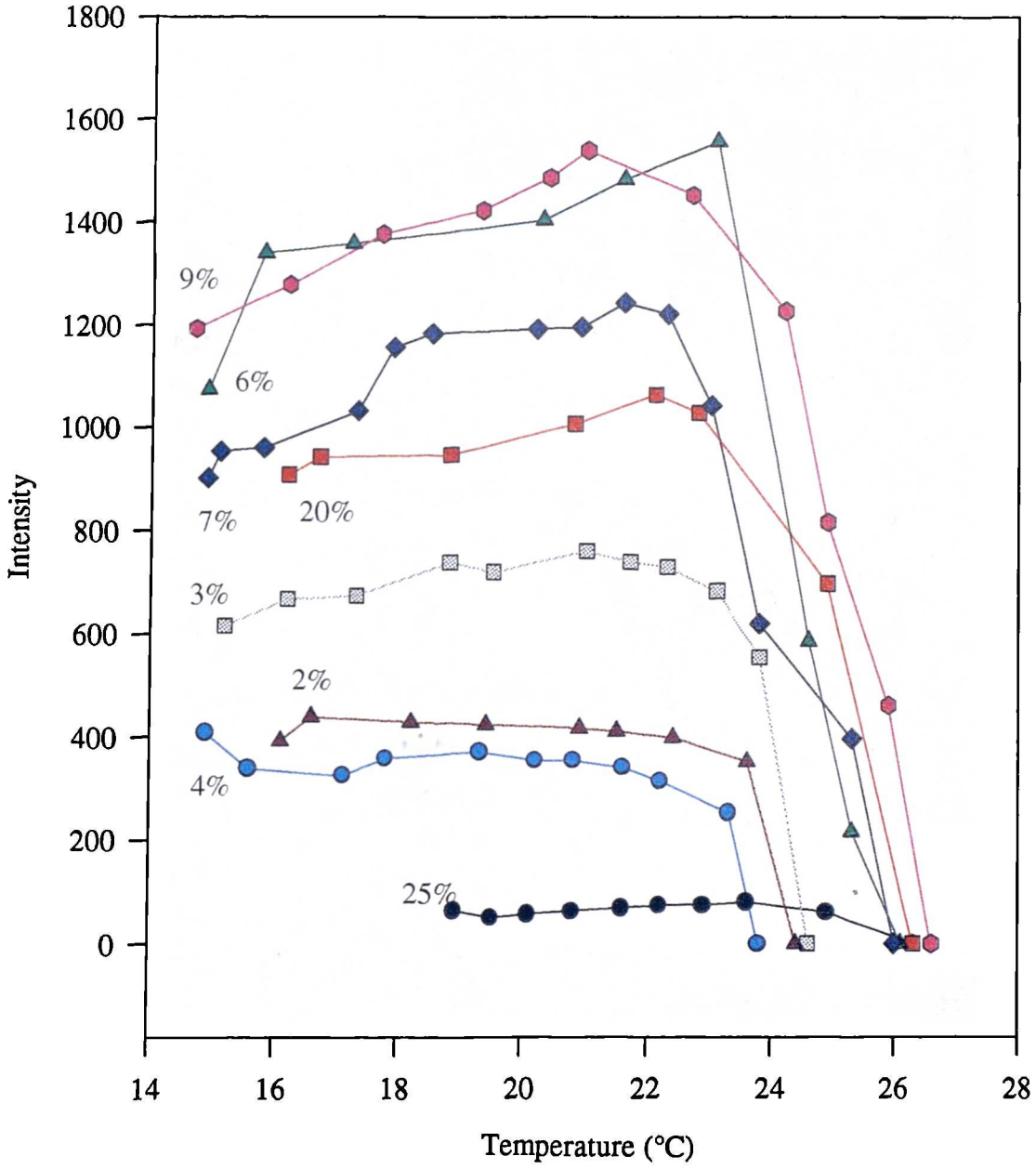

Figure 5.16. A plot of intensity of Form I versus temperature at different concentration of tripalmitin in cocoa butter.

5.3.12.2 *Influence of the concentration of the mixture on the crystallisation process*

Examining the data obtained for the binary system tripalmitin/cocoa butter at different concentrations, the predominance of one component over the other during the crystallisation process has been observed. Between 25 and 10 mole percent solutions, tripalmitin predominates in the solid phase and influences the molecular packing. In this range of concentrations, the cooling phase is characterised by the formation of Forms α and β' of tripalmitin. Form β' is the dominant polymorph and this condition persists also when the system is heated up. A peak consistent with Form I of cocoa butter also appears, and, besides, at higher temperatures the polymorphic transformation from β' to β takes place.

The three mixtures 9, 8 and 7 mole percent of PPP have a similar crystallisation behaviour, forming the three polymorphic forms I, III and IV at low temperatures. The cooling stage is dominated by cocoa butter crystallisation, while, during heating, the composition of the solid becomes richer in tripalmitin. Hence it causes a molecular rearrangement with the formation of form β', followed by the polymorphic transition from β' to β.

The crystallisation process in the mixtures with lower concentration of tripalmitin are clearly controlled by cocoa butter. The system crystallises like Forms I, III and IV of cocoa butter. Form III is the dominant solid phase. At higher temperature, form β' is formed only for the concentrations of tripalmitin 6, 5 and 4 mole percent. But it has to be noted that between 6 and 1 mole percent mixtures the polymorphic transition from β' to β does not take place. This transition is probably forbidden because of the high concentration of cocoa butter. It has been found [Gibon et al., 1986] that, in mixtures very rich in monounsaturated triglycerides, the β-form of saturated triglycerides is not observed.

Besides, a correlation with the melting of Form III and increasing of concentration of Form IV is observed during the heating stage. Figures 5.17(a) and (b) show the variation of intensity of Form III and IV, respectively, as a function of temperature for the system tripalmitin/cocoa butter at different concentrations of tripalmitin. For the 3, 6 and 7 mole percent solutions of tripalmitin in cocoa butter, the

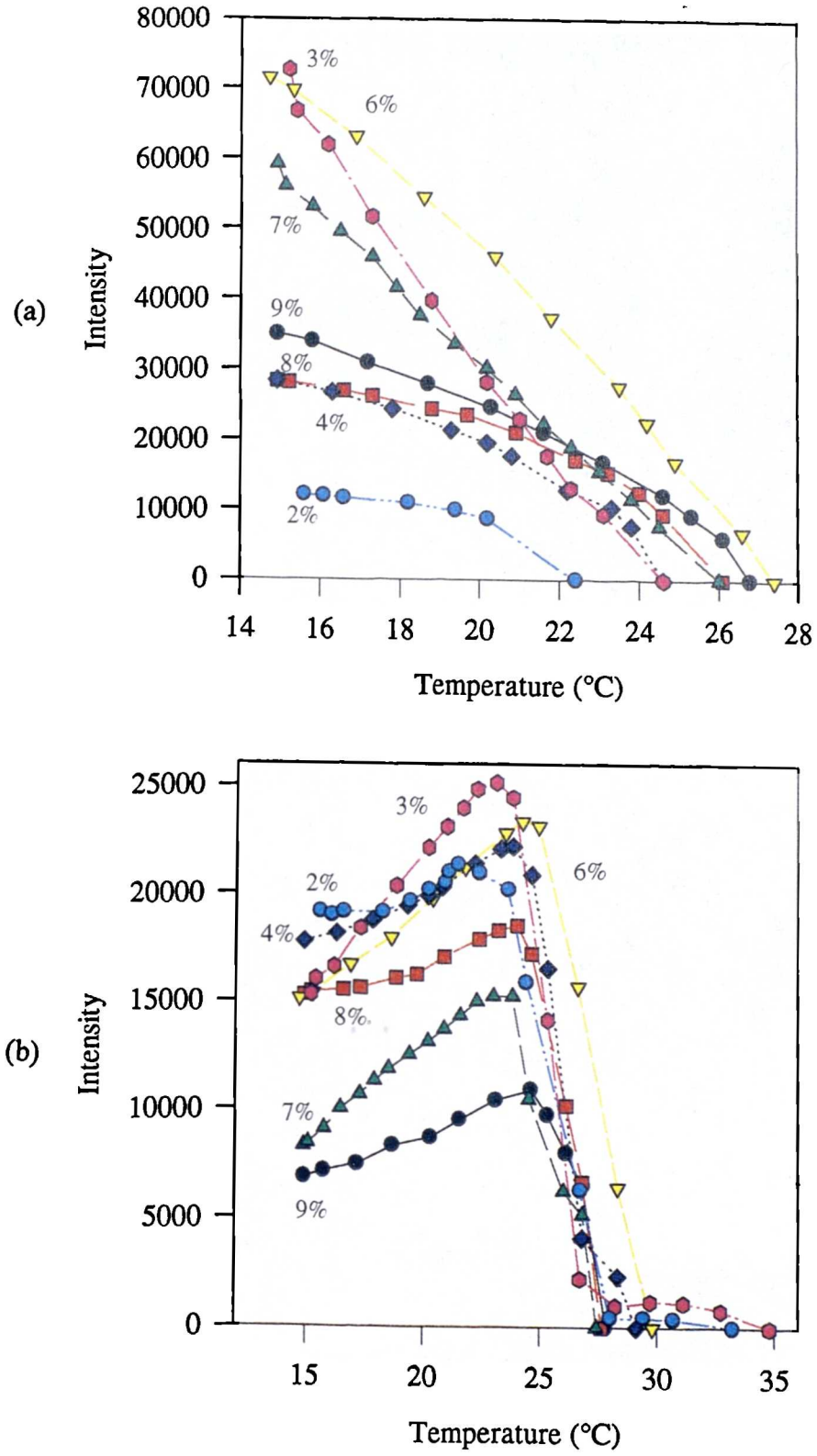

Figure 5.17. Plots of intensity of Form III (a) and Form IV (b) versus temperature at different concentrations of tripalmitin in cocoa butter.

intensity of Form III decreases constantly by increasing the temperature. Subsequently, the intensity of Form IV increases and the maximum of the curve is observed at a temperature corresponding to the melting point of Form III. In the case of 9, 8, 4 and 2 mole percent solutions of tripalmitin in cocoa butter, the intensity of Form III and IV remains almost constant for a wider range of temperature. This behaviour is more evident for 2 and 8 mole percent solutions.

The diffraction results are in excellent agreement with the conclusions reached in Chapter 4. The nucleation studies of PPP/CB systems showed different degrees of phase separations between 25 and 1 mole percent solutions of PPP in cocoa butter. In Figure 4.20 two different trends were observed and, subsequently, two enthalpy/entropy values were calculated. The diffraction data discussed in this chapter confirm the existence of different phases involved in the crystallisation and dissolution process.

Finally, it is important to underline further considerations:

- In the mixed system both components have an influence on the recorded long axis d-spacing. The d-spacings of the mixture are slightly shifted from those of the pure component making up the mixture. This shifting effect is enhanced during the formation of the polymorphic form III during the cooling stage.

- The crystallisation and the melting points of Forms III and IV do not show any trends as a function of the mixture composition.

- In static (unstirred) conditions with a cooling/heating rate of 0.75°C/min, the most stable Forms V and VI of cocoa butter are not formed.

- In all the systems studied, when the raw data is integrated a constant intensity is present throughout the 360° thus showing that no preferred orientation is observed.

5.4 *Effect of the presence of milk fat on the crystallisation of cocoa butter*

The study of crystallisation of milk fat and its mixtures with other components is more complicated, because milk fat is the most complex natural fat with respect to its triglyceride composition. More than 200 individual molecular species of even-numbered triglycerides have been quantified [Laakso, 1992; Bornaz, 1993; Gresti, 1993]. As it can be seen from Table 4.18, the GC analysis shows that 39 peaks have been found, most of which cannot be identified. For this reason, it is difficult to define, for certain, which polymorphic forms have formed during a cooling/heating cycle.

5.4.1 *Milk Fat*

Milk fat was cooled from 50°C to 8°C at a rate of 0.75°C/min. All small angle X-ray diffraction data, collected during cooling, are summarised in Table 5.34. Since it is very difficult to know for certain which polymorphic form corresponds to any peak formed, a number is given to each peak. Figure 5.18 shows a three-dimensional plot of SAXS diffraction data as a function of the temperature.

The first crystallisation was observed at 20.6°C. The d-spacing value recorded for this form is equal to 47.7Å. This is related to the formation of a bilayered structure [Keller, 1996]. According to previous studies of milk fat crystallisation [Small, 1986; Hagemann, 1988; Ollivon, 1992], this structure is generated mostly by long-chain, high melting, trisaturated triglycerides. At 18.3°C another solid phase is detected. Initially, the d-spacing of this form is equal to 42.0Å. Cooling further, the long-spacing slightly shifts assuming a value of 40.5Å.

Two more forms appear at 13.0°C. They have long spacings of 71.8Å and 35.8Å, respectively. The two peaks are related, because they are the first and the second order peaks of the same polymorph. This phase is probably due to the low-melting, long-chain, monounsaturated and mixed long- and short-chain triglycerides [Small, 1986; Ollivon, 1992; Hagemann, 1988].

At 10.1°C two further peaks are detected in the diffraction patterns. These two

peaks have long spacings of 64.7Å and 32.9Å. Also in this case, they can be considered as the first and the second order peaks, respectively, of the same phase. This phase occurred only at low temperatures. The value of d-spacing of 64.7Å is very similar to the value found in the literature for Form V (and VI) of cocoa butter sample [Wille and Lutton, 1966].

During the whole cooling stage, the 2nd order peak of Form 1 was the dominant solid phase. However, all peaks are of very low intensity.

The system was kept at 10°C for approximately 20 minutes. The first frame (Figure 5.19), collected during the heating stage of the cycle, shows that a change had taken place in the period of time the system was kept at 10°C (Table 5.35). During this time, the peaks related to Form 1 have disappeared. This confirms that the two peaks are related to the same phase. Moreover, the peaks corresponding to Forms 4 and 5 are merged together to form a peak 4x with d-spacing value equal to 40.1Å. This new peak 4x was the most intense.

Heating further, the two peaks consistent with Form 2 melt at approximately 14.0°C. Form 3 disappears at 17.1°C. At this temperature, Form 4x is the only one present. At higher temperatures, the d-spacing of Form 4x shifts gradually to 42.1Å (Figure 5.20) till Form 4x melts at 34.5°C.

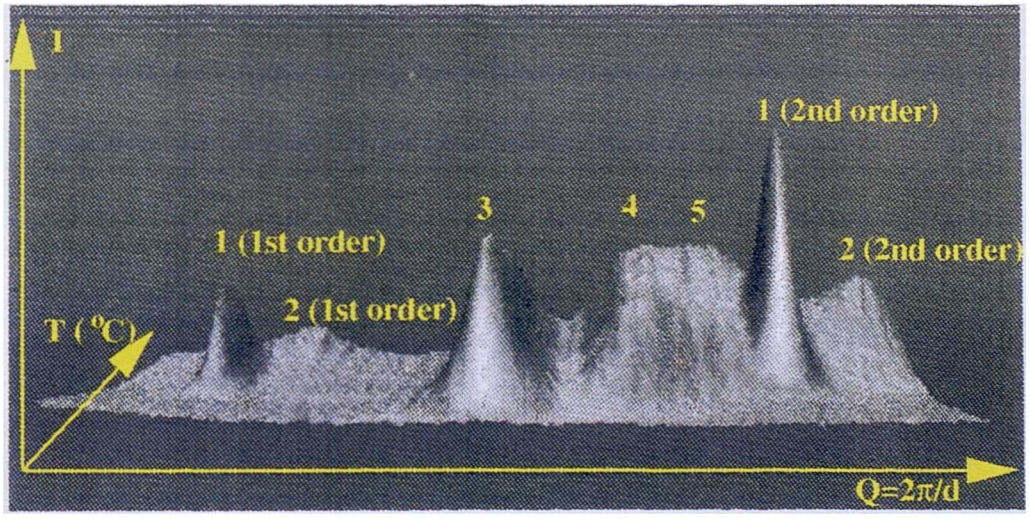

Figure 5.18. A three-dimensional plot of SAXS data collected during the crystallisation process of milk fat. The sample was cooled from 50 to 8°C. The Q range is from 0.05 to 0.21.

Temperature (°C)	d-spacing (Å)	Polymorphic form	Intensity
20.6	47.7	3	688
18.3	47.7	3	1012
	42.0	4	397
13.0	71.8	1 (1st order)	361
	47.4	3	1072
	40.7	4	759
	36.0	1 (2nd order)	531
10.0	71.8	1 (1st order)	585
	64.7	2 (1st order)	420
	47.5	3	984
	40.3	4	854
	37.8	5	858
	35.8	1 (2nd order)	1105
	32.9	2 (2nd order)	511

Table 5.34. Small angle X-ray diffraction data collected during cooling of milk fat.

Temperature (°C)	d-spacing (Å)	Polymorphic form	Intensity
9.9	64.7	2 (1st order)	520
	47.5	3	770
	40.1	4x	1414
	32.4	2 (2nd order)	764
13.9	47.5	3	720
	40.1	4x	1510
14.6	47.5	3	684
	40.3	4x	1622
17.1	40.4	4x	1828
21.7	40.9	4x	1670
25.8	41.3	4x	1320
29.8	41.7	4x	960
32.5	42.1	4x	471
34.5	-	-	-

Table 5.35. Small angle X-ray diffraction data collected during heating of milk fat.

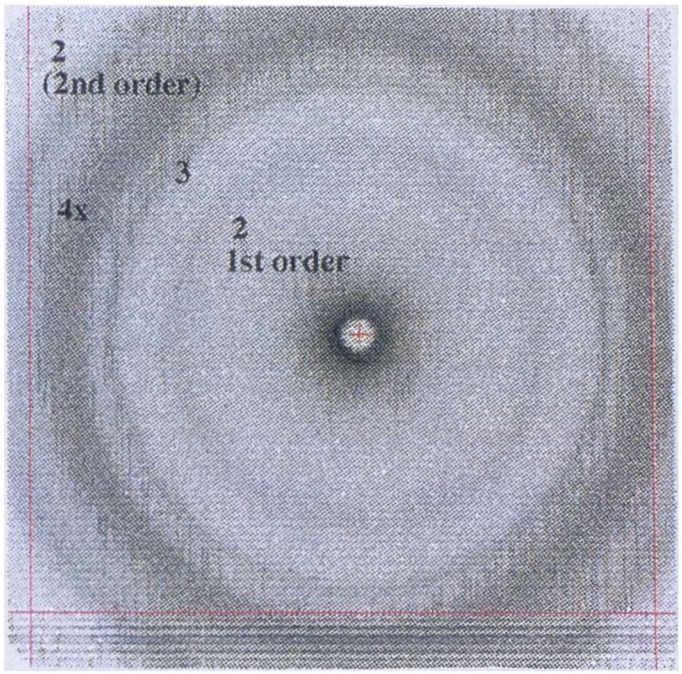

Figure 5.19. Small angle X-ray diffraction spectrum collected during heating of milk fat at 10°C.

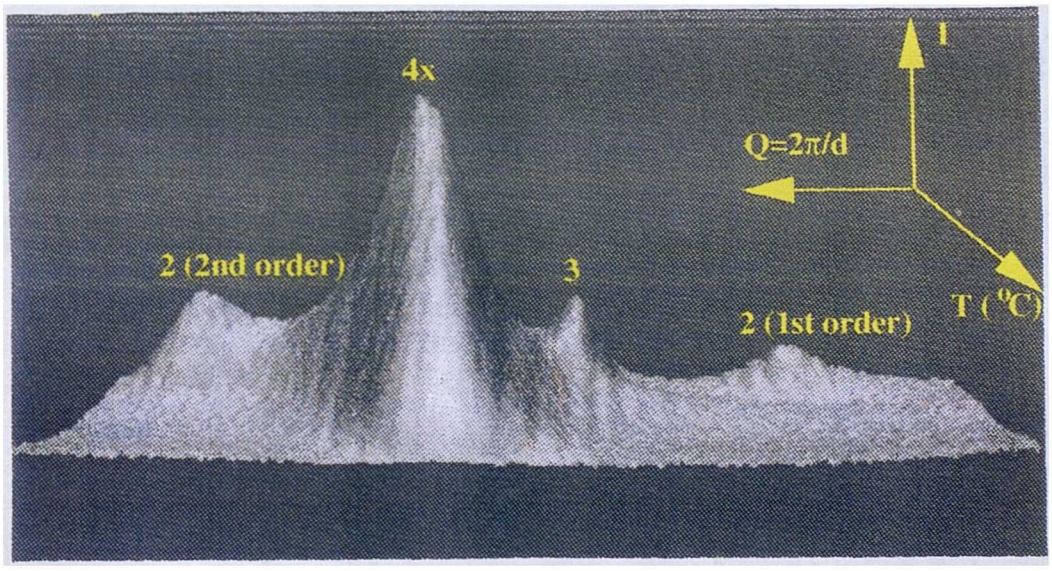

Figure 5.20. A three-dimensional plot of SAXS data collected during the dissolution process of milk fat. The sample was heated from 10 to 40°C. The Q range is from 0.05 to 0.21.

After the study of crystallisation process of milk fat and cocoa butter (see section 5.3.1), several mixtures of these two components have been examined in order to understand the structural mechanism occurring.

5.4.2 *75% Milk Fat in Cocoa Butter*

While cooling the mixture at a rate of 0.75°C/min, the first crystallisation has been observed at 18.6°C (Table 5.36). The peak formed 2 has a d-spacing value of 47.7Å. The polymorph corresponding to this peak is the same one that has been formed in the case of milk fat alone. The presence of cocoa butter does not shift the d-spacing, but it decreases the temperature of crystallisation of this polymorph by 2°C. At 14.6°C, a shoulder is formed on peak 2. The new polymorph 1x has a long spacing value of 41.4Å. Also this form was observed during the crystallisation of milk fat, with the same value of d-spacing, but there is approximately a 4°C difference in the temperature of crystallisation between the two systems.

Cooling further, peak 1x gradually shifts to 38.0Å transforming in the polymorphic form 1. At 12.7°C an other peak is formed with a long spacing of 75.3Å. The two peaks at 75.3Å and 38.0Å could be the 1st and 2nd order, respectively, of the same solid phase, being 38.0Å ca. half of 75.3Å. From Figure 5.21 it is evident that the 2nd order peak of Form 1 is the most intense.

It is important to emphasise that the two related peaks at 64.7Å (1st order) and 32.4Å (2nd order), present during the crystallisation process of milk fat, are not formed in the case of the mixture 75% of milk fat in cocoa butter.

The first frame (Figure 5.22), collected during the heating stage of the cycle, shows the presence of a shoulder on the peak at 38.0Å. Step by step, the intensities of the two peaks related to Form 1 decrease, while the intensity of peak 2 slightly increases. At 12.0°C, the shoulder of the peak at 38.0 Å becomes an independent peak (3), showing that the proportion of this polymorph is increasing (Table 5.37).

Temperature (°C)	d-spacing (Å)	d-spacing observed for Milk fat (Å)	Polymorphic form	Intensity
18.6	47.7	47.7	2	
14.6	47.7	47.7	2	
	41.4	42.0 - 40.3	1x	
12.7	75.3	71.8	1 (1st order)	373
	47.7	47.7	2	637
	38.0	38.0	1 (2nd order)	737
10.1	75.0		1 (1st order)	744
	47.3		2	539
	38.0		1 (2nd order)	2907

Table 5.36. Small angle X-ray diffraction data collected during cooling of the 75 mole percent of milk fat in cocoa butter. The table also includes the d-spacing value observed for milk fat alone.

Temperature (°C)	d-spacing (Å)	d-spacing observed for Milk fat (Å)	Polymorphic form	Intensity
9.7	75.3	71.8	1 (1st order)	705
	47.5	47.7	2	567
	38.0	38.0	1 (2nd order)	2860
11.3	75.3		1 (1st order)	521
	47.3		2	602
	38.0		1 (2nd order)	1848
12.0	75.3		1 (1st order)	441
	47.3		2	619
	39.3		3	1196
	38.0		1 (2nd order)	1393
12.6	75.3		1 (1st order)	379
	47.3		2	645
	39.3		3	1236
13.2	47.3		2	350
	39.7		3	1245
19.8	41.7		3x	1250
21.8	41.7		3x	1394
23.7	41.9		3x	1092
24.3	42.0		3x	991
32.5	-		-	-

Table 5.37. Small angle X-ray diffraction data collected during heating of the 75 mole percent of milk fat in cocoa butter. The table also includes the d-spacing value observed for milk fat alone.

The 2nd order of Form 1 gradually disappears until it merges at 12.6°C with Form 3, which becomes the dominant crystalline phase. Meanwhile, the 1st order peak of Form 1 disappears at 13.2°C. This confirms that these two peaks are related to the same solid phase.

Heating further, Form 2 melts at 19.8°C. At this point, Form 3 is the only crystalline phase. From Table 5.37 and Figure 5.23, it is evident that the peak relative to Form 3 is gradually shifted to 42.0Å during whole heating, following a structure reorganisation of this crystalline packing (Form 3x) and an increase of intensity is observed at 21.8°C. The polymorph relative to peak 3x melts at 32.5°C.

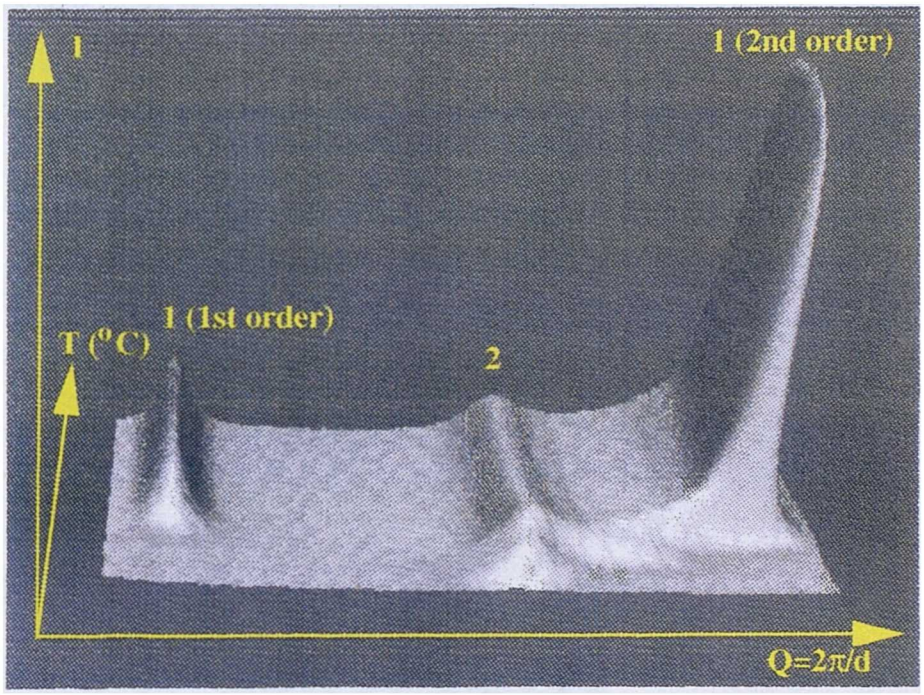

Figure 5.21. A three-dimensional plot of SAXS data during the crystallisation process of 75 mole percent mixture of milk fat in cocoa butter. The mixture was cooled from 50 to 10°C. The Q range is from 0.05 to 0.18.

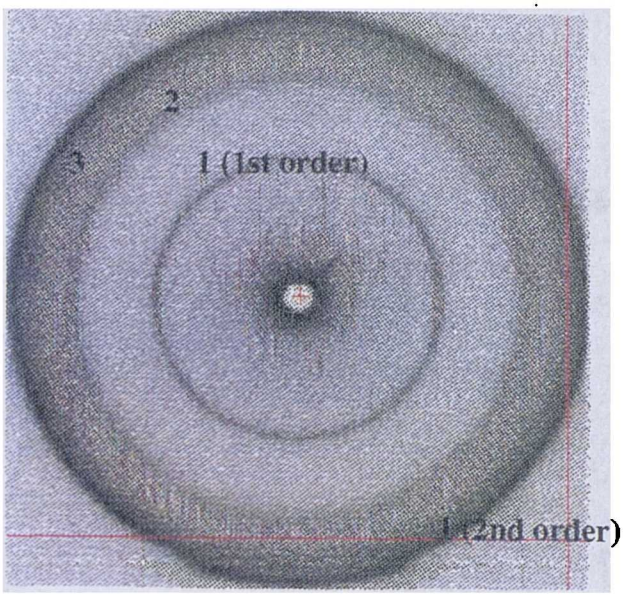

Figure 5.22. Small angle X-ray diffraction spectrum collected during heating of 75 mole percent of milk fat in cocoa butter at 9.7°C.

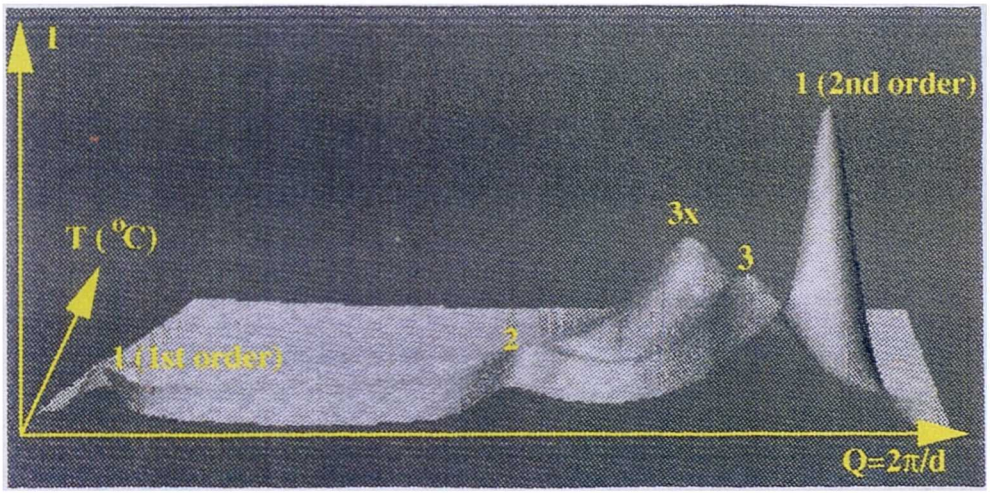

Figure 5.23. A three-dimensional plot of SAXS data collected during the dissolution process of 75 mole percent mixture of milk fat in cocoa butter. The mixture was heated from 10 to 40°C. The Q range is from 0.05 to 0.18.

5.4.3 *50% Milk fat in cocoa butter*

The study of the crystallisation process of the 50 mole percent mixture of milk fat in cocoa butter has shown different behaviour compared with those observed in the sections 5.4.1 and 5.4.2. The diffraction data, collected during cooling, are summarised in Table 5.38, while a three-dimensional plot of the whole cooling stage is shown in Figure 5.24.

The system starts to crystallise at 19.8°C. The value of d-spacing recorded for the peak 2 was 48.4Å. The polymorph corresponding to this peak could be consistent with double packing (β'), similar to Form III of cocoa butter [Wille and Lutton, 1966].

Cooling further, three more peaks are formed. The first two peaks appear at 14.1°C and they have d-spacing values of 51.3Å and 25.6Å. These two peaks are the 1st order and 2nd order, respectively, of the same polymorph, being 25.6Å ca. half of 51.3Å. The long spacing of 51.3Å is close to the long spacing observed for Form I of cocoa butter (55Å). The third peak is formed at 13.1°C and has a value of d-spacing of 45.5Å. The crystalline form corresponding to this peak 3 could have structural packing similar to Form IV of cocoa butter. From Figure 5.24 it is evident that, during cooling of this mixture, the 1^{st} order peak of Form 1 is the dominant solid phase. Comparing these results with those obtained in the case of milk fat alone and 75 mole percent mixture of milk fat in cocoa butter, it is clearly evident that the 50 mole percent mixture crystallises in a different way from the two previous systems. The peaks at approximately 71Å, 64.7Å, 35.9Å and 32.9Å are not present in the 50 mole percent mixture. An addition of cocoa butter to the mixture could cause an increase in the concentration of unsaturated triglycerides such as POP, POS and SOS. Therefore, the change of composition of the mixture might involve a different molecular packing.

The system was held at 13°C for ca. 2 hours to allow the synchrotron beam to be refilled. During this period of time, it was not possible to detect any changes. Then, the sample was heated up to 40°C. The first frame, collected during the heating stage of the cycle, shows that the two peaks corresponding to Form 1 have disappeared, only Forms 2 and 3 are present (Table 5.39). Form 3 is the dominant solid phase. Form 2 melts at 21.7°C, while Form 3 disappeared at 32.5°C.

Temperature (°C)	d-spacing (Å)	d-spacing observed for CB alone (Å)	Polymorphic form	Intensity
19.8	48.4	49 - 48.5	2	
14.1	51.3	54.1	1 (1st order)	906
	48.4	49 - 48.5	2	1238
	25.6	26.7	1 (2nd order)	463
12.8	51.3	54.1	1 (1st order)	1417
	48.4	49 - 48.5	2	1267
	45.5	44.7	3	850
	25.6	26.7	1 (2nd order)	602
11.6	51.3		1 (1st order)	2294
	48.4		2	1297
	45.5		3	897
	25.6		1 (2nd order)	814
9.8	51.3		1 (1st order)	2671
	48.4		2	1002
	45.5		3	826
	25.6		1 (2nd order)	837

Table 5.38. Small angle X-ray diffraction data collected during cooling of the 50 mole percent solution of milk fat in cocoa butter. The table also includes the d-spacing value observed for milk fat alone.

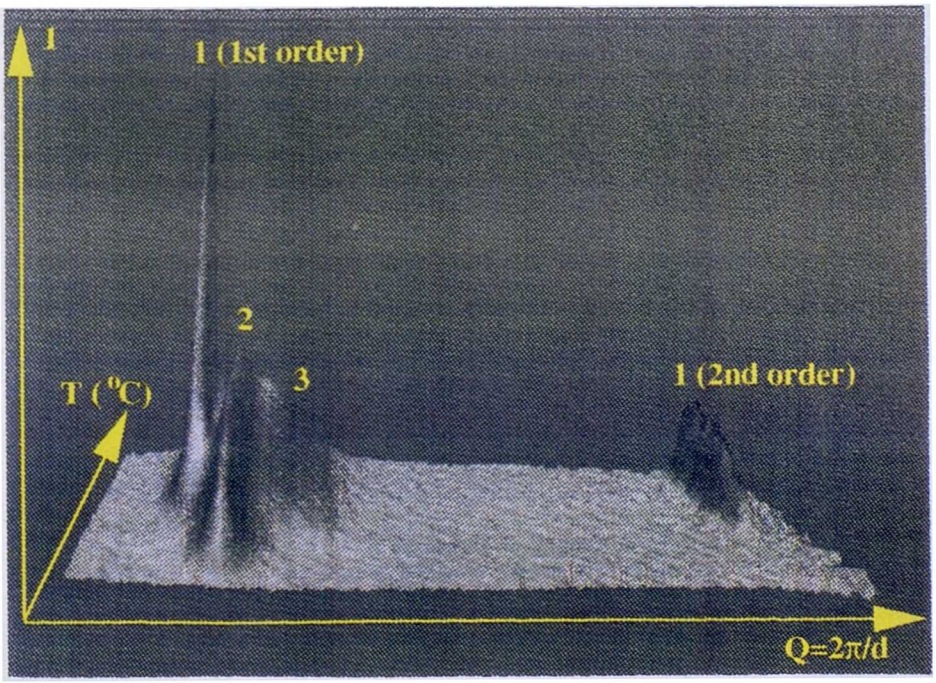

Figure 5.24. A three-dimensional plot of SAXS collected during the crystallisation process of 50 mole percent mixture of milk fat in cocoa butter. The sample was cooled from 50 to 10°C. The Q range is from 0.08 to 0.27.

Temperature (°C)	d-spacing (Å)	d-spacing observed for CB alone (Å)	Polymorphic form	Intensity
15.8	48.4 45.5	49 - 48.5 44.7	(2) (3)	875 1361
18.9	48.4 45.5	49 - 48.5 44.7	(2) (3)	348 970
21.7	45.5		(3)	814
32.5	-	-	-	-

Table 5.39. Small angle X-ray diffraction data collected during cooling of the 50 mole percent solution of milk fat in cocoa butter. The table also includes the d-spacing value observed for cocoa butter alone.

5.4.4 *25% milk fat in cocoa butter*

This mixture shows a crystallisation behaviour similar to that observed for 50 mole percent mixture. Figure 5.25 shows 3-D plot of the crystallisation process occurring during cooling, while the diffraction patterns are summarised in Table 5.40. It must be noted that all peaks formed are slightly shifted toward higher values of d-spacing, especially the two peaks corresponding to Form 1. Comparing the results obtained for this mixture with the previous results, it is notable that, whilst increasing the concentration of cocoa butter in the system, the two peaks consistent with Form 1 assume d-spacing value closer to that recorded for Form I of pure cocoa butter [Wille and Lutton, 1966]. The d-spacing shifting is observed for all polymorphs formed, confirming that a higher concentration of cocoa butter influences the crystallisation process. But, an increase of cocoa butter in the mixture does not make a significant change on the temperature of crystallisation of Form 2.

From Table 5.40 and Figure 5.25, it can be observed that the change in the peak intensity of the polymorph formed happens during the whole cooling stage. Initially, Form 2 is the dominant solid phase, but this does not last for long. At 14.0°C the intensity of the 1st order peak of Form 1 is higher than that of Form 2. Cooling further, the peaks for the two polymorphs 1 and 2 increase and become more intense; however the 1st order peak of Form 1 is still the dominant solid phase.

Then, the mixture was held at 10°C for approximately 30 minutes. During this period of time, a change in molecular arrangement is observed. Form 2 becomes more intense than Form 1. The low temperature promotes the reorganisation of the structural packing into a more stable form.

The first frame, collected during the heating stage of the cycle, shows the presence of another peak at 43.9Å. The polymorph corresponding to this peak was observed also in the case of the 50 mole percent mixture. The diffraction patterns collected during heating are summarised in Table 5.41. The slight difference in d-spacing for the polymorph corresponding to peak 3 is due to the different composition of the two systems. Heating up, the solid phase corresponding to the peaks 1 and 4 melts at 11.8°C. Form 3 becomes gradually more intense until it is the dominant crystalline phase. Form 2 melts at 23.1°C, while Form 3 disappears at 25.8°C.

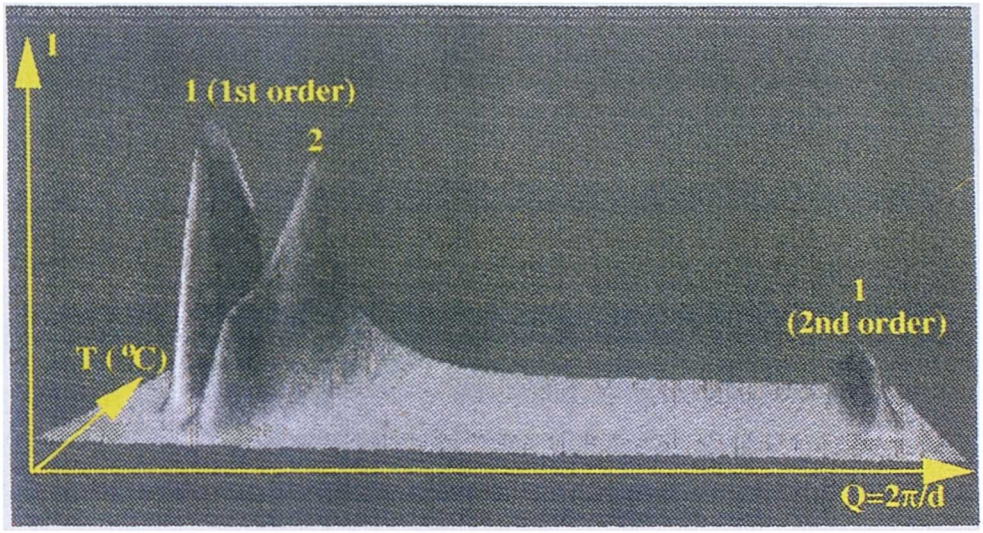

Figure 5.25. A three-dimensional plot of SAXS data collected during the crystallisation process of 25 mole percent mixture of milk fat in cocoa butter. The system was cooled from 50 to 10°C. The Q range is from 0.08 to 0.26.

Temperature (°C)	d-spacing (Å)	d-spacing observed for CB alone (Å)	Polymorphic Form	Intensity
20.1	48.8	49 - 48.5	2	
15.3	53.1	54.1	1 (1st order)	733
	48.8	49.0 - 48.5	2	2421
	26.3	26.7	1 (2nd order)	432
14.4	53.1		1 (1st order)	2000
	48.8		2	2578
	26.3		1 (2nd order)	732
14.0	53.1		1 (1st order)	2750
	48.8		2	2618
	26.3		1 (2nd order)	895
12.8	53.1		1 (1st order)	4473
	48.8		2	2720
	26.3		1 (2nd order)	1212
12.1	53.1		1 (1st order)	5289
	48.8		2	2842
	26.3		1 (2nd order)	1427
10.8	53.1		1 (1st order)	6280
	48.8		2	2947
	26.3		1 (2nd order)	1587
10.5	53.1		1 (1st order)	6526
	48.8		2	3087
	26.3		1 (2nd order)	1665
10.0 (after 20 minutes)	53.1		1 (1st order)	4605
	48.8		2	5631
	26.3		1 (2nd order)	1171

Table 5.40. Small angle X-ray diffraction data collected during cooling of the 25 mole percent mixture of milk fat in cocoa butter. The table also includes the d-spacing value observed for cocoa butter alone.

Temperature (°C)	d-spacing (Å)	d-spacing observed for CB alone (Å)	Polymorphic form	Intensity
10.0	53.1 47.8 43.9 26.3	54.1 49.0 - 48.5 44.7 26.7	1 (1st order) 2 3 1 (2nd order)	2071 7285 3470 386
11.8	48.8 45.1		2 3	6345 3235
18.2	48.8 45.1		2 3	3156 2564
21.9	48.8 45.1		2 3	1690 1688
22.4	48.8 45.1		2 3	1145 1380
23.1	45.1		3	969
25.8	-		-	-

Table 5.41. Small angle X-ray diffraction data collected during heating of the 25 mole percent mixture of milk fat in cocoa butter. The table also includes the d-spacing value observed for cocoa butter alone.

5.4.5 *12.5% milk fat in cocoa butter*

The sample was cooled from 50°C to 8°C at 0.75°C/min. It starts to crystallise at 19.6°C, in a structure consistent with the previously observed Form 2. Comparing the results obtained for this mixture (Table 5.42) with those discussed in the sections 5.4.3 and 5.4.4, it should be noted that the crystallisation temperature of Form 2 is almost the same. However, the d-spacing of Form 2 shifts slightly to a higher value, changing from a concentration of 50 to 12.5 mole percent of milkfat in cocoa butter. The different composition of the mixture does not seem to influence the crystallisation temperature of this polymorph, while it controls a different molecular packing. Being the mixture richer in cocoa butter, the crystal packing of Form 2 becomes closer to that consistent with Form III of pure cocoa butter.

The same behaviour is observed in the case of the solid phase appearing at 15.7°C. The two peaks at 53.8Å and 26.7Å correspond to the 1st and 2nd order, respectively, of the same polymorph. The long spacing of this form is closer to that

found for Form I of pure cocoa butter. Cooling further, a shoulder is formed on peak 2 at 10.2°C. A 3-D plot of the integrated data of the whole cooling stage is shown in Figure 5.26.

A change in the dominant crystalline packing, during cooling, is observed also for this system (see Table 5.42 and Figure 5.26). But in the case of the 12.5 mole percent of milk fat in cocoa butter, the difference in intensity between Form 1 (1st order) and Form 2 is much bigger.

The first frame, collected during the heating stage, shows that the two peaks corresponding to Form 1 have disappeared (Figure 5.27). The shoulder, appearing on peak 2, has increased in intensity, becoming an independent peak 3. Heating further, the intensity of the Form 2 peak decreases gradually, while the intensity of the Form 3 peak increases, until at 20.2°C Form 3 becomes the dominant crystalline phase (Table 5.43). The d-spacing of Forms 2 and 3 shifts toward higher value, due to the change in composition of the solid phase. Form 2 melts at 22.3°C, while Form 3 disappears at 27.8°C.

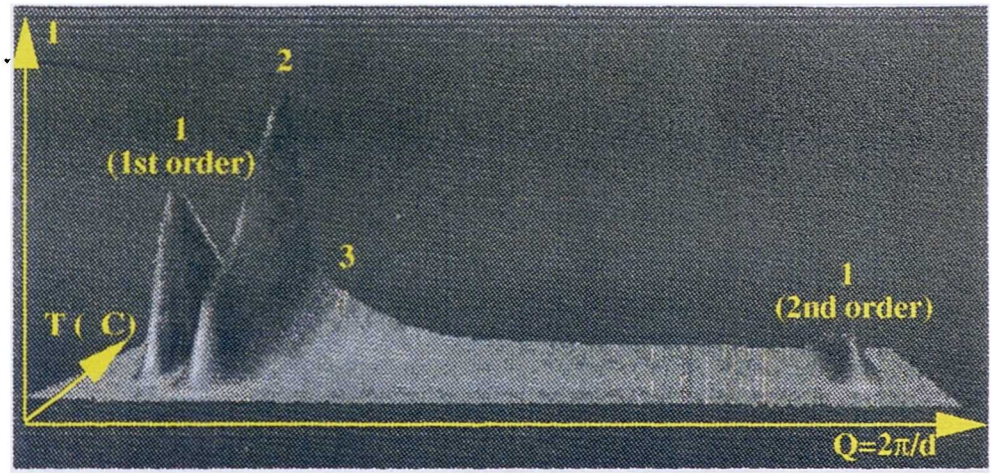

Figure 5.26. A three-dimensional plot of SAXS data collected during the crystallisation process of 12.5 mole percent of milk fat in cocoa butter. The sample was cooled from 50 to 8°C.

Temperature (°C)	d-spacing (Å)	d-spacing observed for CB alone (Å)	Polymorphic form	Intensity
19.6	49.2	49.0 - 48.5	2	
15.7	53.8	54.1	1 (1st order)	932
	49.2	49.0 - 48.5	2	3245
	26.7	26.7	1 (2nd order)	434
14.7	53.9		1 (1st order)	2578
	49.2		2	3578
	26.7		1 (2nd order)	822
13.7	53.9		1 (1st order)	4451
	49.2		2	3859
	26.7		1 (2nd order)	1232
11.1	53.9		1 (1st order)	6456
	49.2		2	5157
	26.7		1 (2nd order)	1551
10.5	53.9		1 (1st order)	6385
	49.2		2	5754
	26.7		1 (2nd order)	1534
10.5 (after 2 minutes)	53.9		1 (1st order)	6201
	49.2		2	6333
	26.7		1 (2nd order)	1494
10.5 (after 20 minutes)	53.9		1 (1st order)	3026
	49.2		2	10328
	26.7		1 (2nd order)	688

Table 5.42. Small angle X-ray diffraction data collected during cooling of the 12.5 mole percent of milk fat in cocoa butter. The table also includes the d-spacing value observed for cocoa butter alone.

Temperature (°C)	d-spacing (Å)	d-spacing observed for CB alone (Å)	Polymorphic form	Intensity
9.7	48.5 44.7	49.0 - 48.5 44.7	2 3	
16.2	48.8 45.6		2 3	6114 4439
18.8	49.1 45.6		2 3	4078 3583
20.2	48.9 45.1		2 3	2958 3159
22.3	44.7		3	2766
27.8	-		-	-

Table 5.43. Small angle X-ray diffraction data collected during heating of the 12.5 mole percent solution of milk fat in cocoa butter. The table also includes the d-spacing value observed for cocoa butter alone.

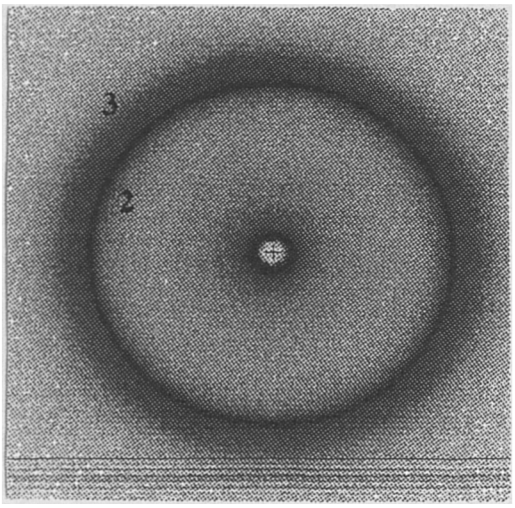

Figure 5.27. Small angle X-ray diffraction spectrum collected during heating of 12.5 mole percent of milk fat in cocoa butter at 9.7°C.

5.4.6 *Discussion*

Both milk fat and cocoa butter are a mixture of different triglycerides, especially milk fat which is the most complex natural fat with respect to its triglyceride composition. The complexity of the two components make it difficult to analyse the crystallisation process involved when milk fat and cocoa butter are mixed together. Also in this case, no preferred orientation is observed.

Moreover, examining the data obtained for the binary mixture of milk fat and cocoa butter at different concentrations, it can be observed that two different mechanisms of crystallisation occur as a function of the concentration of milk fat:

- the 75 mole percent mixture of milk fat in cocoa butter shows the closest crystallisation behaviour to that observed for "pure" milk fat. The two peaks consistent with Form 1 of milk fat are present in this mixture, but the d-spacing values are higher (ca. 75Å against 71Å in pure milk fat). This could be due to the influence of the unsaturated triglycerides present in cocoa butter. Form 3 is observed too, with similar long spacings. The two peaks related to Form 2 of milk fat have not been found in the mixture. Moreover, none of the peaks found for this mixture have similar long spacing to those observed for cocoa butter (see section 5.3.1);

- the 50 mole percent solution of milk fat in cocoa butter does not present any of the polymorphs observed in milk fat alone. The two peaks at 51.3Å and 25.6Å could be related to Form I of cocoa butter alone, even if these latter long spacing values are smaller than that expected for Form I (55Å). The polymorph observed at 48.4Å shows similarity to Form III of cocoa butter, while the d-spacing value of 45.5Å, observed for another polymorph of the mixture, is too high to be related to Form IV of cocoa butter.

- the 25 and 12.5 mole percent solutions of milk fat in cocoa butter have the closest crystallisation behaviour to that observed for cocoa butter alone. Both

systems show the formation of two polymorphs during the crystallisation process. The long spacing values for these forms are 53.1Å (1st order), 26.3 (2nd order) and 48.8Å. These polymorphs are more consistent with Forms I and III, observed for cocoa butter alone, than those found in the previous mixtures. During heating, a polymorphic transformation is observed. The peaks consistent with Form I melt and transform to a polymorph at 44 Å, which is consistent with Form IV of "pure" cocoa butter.

5.5 *The influence of 1% tripalmitin on crystallisation behaviour of the mixture 25% of milk fat in cocoa butter*

1 mole percent of tripalmitin was added to a mixture of 25 mole percent of milk fat in cocoa butter. The X-ray diffraction data obtained for this ternary system are compared with those already discussed in section 5.4.4 and they are summarised in the Tables 5.44 and 5.45.

The presence of tripalmitin does not make a significant change in the temperature of crystallisation of the two polymorphs formed during the cooling phase (see Table 5.44). On the binary system, Form 2 and Form 1 were formed at 20.1°C and 15.3°C, respectively. The addition of tripalmitin causes a change of only 0.5°C in the temperature of crystallisation of both polymorphs. As can be observed from Table 5.25, tripalmitin influences the stability of the polymorphs formed. In the three component system, Form 2 is the dominant crystalline structure until 10.4°C where the 1st order peak of Form 1 becomes the most intense. Compared with the binary mixture, this change in the dominant polymorph happens at 14.0°C. Thus, the addition of higher melting triglycerides, like tripalmitin, which might act as seed crystal [Hachiya et al., 1989], influences the kinetics of crystallisation of the system. PPP suppresses crystallisation but it does not change the phases present, except decreasing the phase 1/phase 2 ratio.

25mole % milk fat/ 75 mole % cocoa butter			25 mole% milk fat/74mole % cocoa butter/1 mole% PPP		
T (°C)	d-spacing (Å)	Intensity	T (°C)	d-spacing (Å)	Intensity
20.1	48.8 (2)		20.6	48.8 (2)	
15.3	53.1 (1) 48.8 (2) 26.3 (1)	733 2421 432	14.8	52.9 (1) 48.6 (2) 26.0 (1)	658 1467 358
14.4	53.1 (1) 48.8 (2) 26.3 (1)	2000 2578 732	13.9	52.9 (1) 48.5 (2) 26.0 (1)	1105 2105 396
14.0	53.1 (1) 48.8 (2) 26.3 (1)	2750 2618 895	12.8	52.9 (1) 48.5 (2) 26.0 (1)	1885 2092 585
12.8	53.1 (1) 48.8 (2) 26.3 (1)	4473 2720 1212	10.4	52.9 (1) 48.5 (2) 26.0 (1)	2144 2076 632
12.1	53.1 (1) 48.8 (2) 26.3 (1)	5289 2842 1427	10.0 (after 5 minutes)	52.9 (1) 48.5 (2) 26.0 (1)	2907 2144 856
10.8	53.1 (1) 48.8 (2) 26.3 (1)	6280 2947 1587	10.0 (after 2 minutes)	52.9 (1) 48.5 (2) 26.0 (1)	2868 2210 882
10.5	53.1 (1) 48.8 (2) 26.3 (1)	6526 3087 1665	10.0 (after 10 minutes)	52.9 (1) 48.1 (2) 26.0 (1)	2578 2592 852
10.0 (after 20 minutes)	53.1 (1) 48.8 (2) 26.3 (1)	4605 5631 1171	10.0 (after 10 minutes)	52.9 (1) 48.1 (2) 26.0 (1)	1842 3157 513

Table 5.44. Small angle X-ray diffraction data collected during cooling for the ternary and binary systems.

Keeping both binary and ternary mixtures at 10°C for a certain period of time, it is observed that a reorganisation of the crystalline structure has taken place. Form 2 becomes again the most intense polymorph and in both cases this happens after 20 minutes. The low temperature and the time play an important part in the morphology of the phases formed. But tripalmitin does not seem to influence this step.

The beginning, the heating stage does not show any remarkable differences between the two mixtures. In both systems, Form 1 is quickly melted and new polymorph (Form 3) appears. In the ternary mixture, the long spacing observed for Form 3 is slightly smaller than the corresponding value found in the binary system.

For both systems, Form 2 melted at 23.1°C, whilst it lasts longer in the case of the ternary mixture. This polymorph melted at 25.8°C in the two component system, while it disappeared at 33.4°C in the ternary mixture. The higher melting point could be explained by tripalmitin, possibly in a small percentage, present in the solid phase.

25 mole% milk fat/ 75 mole% cocoa butter			25 mole% milk fat/74 mole% cocoa butter/1 mole% PPP		
T (°C)	d-spacing (Å)	Intensity	T (°C)	d-spacing (Å)	Intensity
11.8	48.8 (2) 45.1 (3)	6345 3235	10.7	47.8 (2) 44.3 (3)	3473 1403
18.2	48.8 (2) 45.1 (3)	3156 2564	15.6	48.3 (2) 45.2 (3)	2342 1419
21.9	48.8 (2) 45.1 (3)	1690 1688	20.1	48.3 (2) 45.2 (3)	1250 795
22.4	48.8 (2) 45.1 (3)	1145 1380	21.5	48.3 (2) 45.2 (3)	738 693
23.1	45.1 (3)	969	23.1	45.5 (3)	546
25.4	-	-	33.4	-	-

Table 5.45. Small angle X-ray diffraction data collected during cooling for the ternary and binary systems.

5.6 *Effect of addition of the emulsifier YN on the crystallisation of fats mixture*

Small amounts of surface-active lipids can produce an immediate reduction in the viscosity of molten chocolate. In chocolate manufacturing, the reduction in viscosity is usually made at or near the end of the conching process, which has been described in Chapter 1. The most common emulsifier used by industries is soya lecithin, which is a natural phospholipid. An other surface-active agent widely used, especially in Britain, is sinthetic lecithin called YN (ammonium salts of phosphatidic acids). YN is obtained from partially hardened rapeseed oil after glycerolysis, phosphorylation and neutralisation.For the experiments described below, YN was provided by Cadbury Ltd.

An examination was made of the effects of YN on crystallisation of mixtures of milk fat and cocoa butter. Keeping mole percent of milk fat constant, YN was added to a mixture of milk fat and cocoa butter in a range of concentrations between 0.2 and 0.6 mole percent.

All the diffraction data are summarised in Tables 5.46 and 5.47 for the cooling stage and Tables 5.48 and 5.49 for the heating stage. In order to compare these results with those obtained, and already discussed in the previous sections, for the 25 mole percent mixture of milk fat in cocoa butter, Tables 5.46 and 5.49 include also the diffraction data of the binary mixture.

Form 2 crystallises at 20.1°C in the binary mixture. The addition of YN decreases the temperature of crystallisation of this crystalline phase by approximately 2°C. The major reduction is observed in the mixture with 0.4 mole percent concentration of YN. The two peaks consistent with Form 1 appear at the same temperature (15°C) for 0.2 and 0.4 mole percent concentrations of YN. This temperature is just 0.3°C below that observed in the binary mixture, while, in the case of the system with 0.6 mole percent concentration of YN, this latter polymorph crystallises at 14.4°C.

The long spacing values of Forms 1 and 2 do not change as a function of the concentration of YN present. Comparing these results with those observed in the binary mixture, it is noted that the peaks corresponding to Forms 1 and 2 are slightly

shifted to the right.

Another effect can be observed in the temperature at which Form 1 becomes the dominant solid phase. This step occurs at 14.0°C in the binary mixture. The presence of 0.2 mole percent of YN increases by only 0.2°C relative to the temperature at which this happens in the ternary system. The major difference (0.8°C) is observed for 0.6 mole percent solution of YN.

Cooling further, a reorganisation of the molecular packing is observed. The Form 2 peak becomes again the most intense. This transformation occurs at 10.0°C for all four systems considered, but at different times. In the case of 0.2 mole percent solution of YN in milk fat/cocoa butter system, this is observed just when the temperature reaches the value of 10.0°C. For 0.4 and 0.6 mole percent concentrations of YN and for the binary mixture, the systems have to be kept at 10.0°C for 10, 15 and 20 minutes, respectively, before the transformation has taken place.

As it can be noted from Tables 5.48 and 5.49, the first frame, collected during the heating phase, does not show the presence of the two peaks corresponding to Form 1. This polymorph disappeared during the time necessary to transfer the data collected for the cooling phase. Besides, a new crystalline phase appeared (Form 3). This could be explained as a polymorphic transformation taking place from Form 1 to Form 3.

Heating up, few differences can be noted between the binary and the ternary mixtures. Form 2 melts at 23.1°C in the 25 mole percent solution of milk fat in cocoa butter. The addition of YN to the system has the effect of decreasing the melting point of this polymorph. At 0.2 mole percent concentration of YN, the temperature at which Form 2 disappeared is 15.5°C, while, at 0.4 and 0.6 mole percent of YN, this happens at 19.8°C and 19.7°C, respectively.

In the case of Form 3, the presence of YN does not seem to make a remarkable change in his melting point. This polymorph melts around 25.4°C in the binary mixture. At 0.2 mole percent concentration of YN the value is increased by just 0.3°C, while for 0.4 and 0.6 mole percent of YN, a decrease of 0.2°C is observed.

25 mole% milk fat/ 75 mole% cocoa butter			25 mole% milk fat/74.8 mole% cocoa butter/0.2 mole% YN		
T (°C)	d-spacing (Å)	Intensity	T (°C)	-spacing (Å)	Intensity
20.1	48.8 (2)		18.3	48.5 (2)	
15.3	53.1 (1)	733	15.0	52.8 (1)	675
	48.8 (2)	2421		48.3 (2)	978
	26.3 (1)	432		26.1 (1)	368
14.0	53.1 (1)	2750	14.2	52.8 (1)	1237
	48.8 (2)	2618		48.3 (2)	1217
	26.3 (1)	895		26.1 (1)	557
12.8	53.1 (1)	4473	12.8	52.8 (1)	2408
	48.8 (2)	2720		48.1 (2)	1408
	26.3 (1)	1212		26.1 (1)	869
10.0 (after 20 minutes)	53.1 (1)	4605	10.0	52.8 (1)	3017
	48.8 (2)	5631		47.7 (2)	3035
	26.3 (1)	1171		26.1 (3)	1012

Table 5.46. Small angle X-ray diffraction data collected during cooling for the binary system and for 0.2 mole percent of YN in milk fat/cocoa butter system.

25 mole% milk fat/74.6 mole% cocoa butter/0.4 mole% YN			25 mole% milk fat/74.4 mole% cocoa butter/0.6 mole% YN		
T (°C)	d-spacing (Å)	Intensity	T (°C)	d-spacing (Å	Intensity
17.6	48.7 (2)		18.0	48.9 (2)	
15.0	52.8 (1)	702	14.4	52.8 (1)	688
	48.5 (2)	955		48.6 (2)	953
	26.0 (1)	304		26.1 (1)	345
13.7	52.9 (1)	1728	13.2	52.9 (1)	1144
	48.5 (2)	1552		48.7 (2)	1012
	26.1 (1)	770		26.1 (1)	453
11.5	52.9 (1)	3526	12.2	52.9 (1)	1903
	48.2 (2)	1771		48.5 (2)	1068
	26.0 (1)	1082		26.1 (1)	706
10.0 (after10 minutes)	52.9 (1)	3280	10.0 (after15 minutes)	52.9 (1)	1543
	47.8 (2)	3403		48.5 (2)	3017
	26.1 (1)	1043		26.1 (1)	503

Table 5.47. Small angle X-ray diffraction data collected during cooling for 0.4 and 0.6 mole percent of YN in milk fat/cocoa butter system.

25 mole% milk fat/ 75 mole% cocoa butter			25 mole% milk fat/74.8 mole% cocoa butter/0.2 mole% YN		
T (°C)	d-spacing (Å)	Intensity	T (°C)	-spacing (Å)	Intensity
11.8	48.8 (2) 45.1 (3)	6345 3235	9.7	47.5 (2) 45.2 (3)	4364 2267
18.2	48.8 (2) 45.1 (3)	3156 2564	14.2	47.5 (2) 45.2 (3)	2749 2337
23.1	45.1 (3)	969	15.5	45.2 (3)	2276
25.4	-	-	25.7	-	-

Table 5.48. Small angle X-ray diffraction data collected during heating for the binary system and for 0.2 mole percent of YN in milk fat/cocoa butter system.

25 mole% milk fat/74.6 mole% cocoa butter/0.4 mole% YN			25 mole% milk fat/74.4 mole% cocoa butter/0.6 mole% YN		
T (°C)	d spacing (Å)	Intensity	T (°C)	spacing (Å)	Intensity
9.8	47.6 (2) 45.2 (3)	5105	9.4	47.5 (2) 45.5 (3)	3473 1315
16.6	48.0 (2) 45.2 (3)	2171 1946	16.5	47.9 (2) 45.5 (3)	$I_2 \cong I_3$
19.8	45.2 (3)		19.7	45.5 (3)	
25.2	-	-	25.2	-	-

Table 5.49. Small angle X-ray diffraction data collected during heating for 0.4 and 0.6 mole percent of YN in milk fat/cocoa butter system.

5.6.1 *Discussion*

The addition of YN has more evident effects on polymorph 2, rather than on polymorph 1. 0.2 mole percent of YN speeds up the reorganisation of molecular packing and Form 2 becomes again the dominant polymorph in less time compared with that recorded for the binary system. 0.4 and 0.6 mole percent concentrations do not seem to influence the kinetics of crystallisation of Form 2. The presence of YN influences also the dissolution of Form 2. All the three concentrations of YN used decrease the melting point of Form 2: ca. 10°C for 0.2 mole percent of YN and ca. 6°C for 0.4 and 0.6 mole percent of YN.

Thus, different kinetics of crystallisation are observed for 0.2 and 0.4 mole

percent concentration of YN. This confirms the nucleation results discussed in the previous chapter (section 4.4.5.3).

5.7 *Conclusions*

- A higher stability of Form I of cocoa butter has been observed during the experiments carried out on tripalmitin/cocoa butter mixtures. Comparing the data obtained from single cocoa butter with those obtained with the mixtures tripalmitin/cocoa butter, it is clearly evident that the two systems crystallise in two different types of molecular packing, but both related to the same polymorphic phase. Obviously, tripalmitin influences the molecular arrangement of cocoa butter and, at the same time, increases the stability of Form I at higher temperatures.

- Examining the data obtained for the binary system tripalmitin/cocoa butter at different concentration, the predominance of one component over the other during the crystallisation process has been observed. Between 25 and 10 mole percent solutions, tripalmitin predominates in the solid phase and influences the molecular packing. In the range of 9 to 7 mole percent, the cooling phase is dominated by cocoa butter polymorph, whilst, during heating, the composition of the solid becomes richer in tripalmitin. The crystallisation process of the mixtures with lower concentrations of tripalmitin are clearly controlled by cocoa butter.

- A correlation with the melting of Form III and increasing of concentration of Form IV is observed during the heating stage. For the 3, 6 and 7 mole percent solutions of tripalmitin in cocoa butter, the intensity of Form III decreases constantly by increasing the temperature. Subsequently, the intensity of Form IV increases. In the case of 9, 8, 4 and 2 mole percent solutions of tripalmitin in cocoa butter, the intensity of Form III and IV remains almost constant for a

wider range of temperature.

- In the mixed system both component have an influence on the recorded long spacing. The d-spacings of the mixture are slightly shifted from those of the pure component making up the mixture. This shifting effect is enhanced during the formation of the polymorphic form III during the cooling stage.

- In the case of the binary mixture milk fat and cocoa butter it has been observed that two different mechanisms of crystallisation occur as a function of the concentration. The 75 mole percent solution of milk fat in cocoa butter shows the closest crystallisation behaviour to that observed for milk fat alone. The 50 mole percent solution of milk fat in cocoa butter does not present any of the polymorphs observed in milk fat alone. In contrast, the 25 and 12.5 mole percent solutions of milk fat in cocoa butter have the closest crystallisation behaviour to that observed for cocoa butter alone.

- The addition of 1 mole percent of tripalmitin to a mixture of 25 mole percent of milk fat in cocoa butter does not influence the temperature of crystallisation of the two polymorphs formed during the cooling phase, but less material is crystallised. Whereas, tripalmitin influences the stability of the polymorphs formed.

- The addition of synthetic lecithin YN to a 25 mole percent solution of milk fat in cocoa butter affects the stability of the polymorphs formed. Differences are observed between the two mixtures with 0.2 and 0.4 mole percent of YN. In contrast, the ternary system with 0.6 mole percent of YN shows similarity to the system with 0.4 mole percent concentration of YN.

- In all the systems studied, when the raw data is integrated a constant intensity is present throughout the 360°. No preferred orientation is observed.

5.8 *References*

Bornaz, S, Fanni, J and Parmentier, M, *J. Am. Oil Chem. Soc.*, 1993, 70, 11, 1075-1079.

Capel, M S, Smith, G C and Yu, B, *Review Scientific Instrumentation*, 1995, 66, 2, 2295-2299.

Capel, M S, at internet address: http://crim12b.nsls.bnl.gov/x12b_diff (2/9/1996).

Capel, M S, at internet address: http://crim12b.nsls.bnl.gov/x12b_optics(20/2/1997).

Capel, M S, at internet address: http://crim12b.nsls.bnl.gov/x12b_controls.gov (6/8/1997).

Chapman, G M, Akehust, A E and Wright, W B, *J. Am. Oil Chem. Soc.*, 1971, 48, 824-830.

Gibon, V, Durant, F and Deroanne, C I, *J. Am. Oil Chem. Soc.*, 1986, 63, 8, 1047-1055.

Gresti, J, Bugant, M, Maniongui, C and Bezard, J, *J. Dairy Sci.*, 1993, 76, 1850-1869.

Hachiya, I, Koyano, T and Sato, K, *J. Am. Oil Chem. Soc.*, 1989, 66, 12, 1757-1762.

Hachiya, I, Koyano, T and Sato, K, *J. Am. Oil Chem. Soc.*, 1989, 66, 12, 1763-1770.

Hagemann, J W, in *Crystallisation and polymorphism of fats and fatty acids*, eds by Garti, N and Sato, K, Marcel Decker Inc., New York, 1988, 9-95.

Kellens, M, Meeussen, R, Gehrke, R and Reynaers, H, *Chem. and Phys. of Lipids*, 1991, 58, 131-144.

Keller, G, Lavigne, F, Loisel, C, Ollivon, M and Bourgaux, C, *Journal of Thermal Analysis*, 1996, 47, 1545-1565.

Laakso, P H, Nurmela, K V V and Homer, D R, *J. Agric. Food Chem.*, 1992, 40, 2472-2482.

Lutton, E S and Fehl, A J, *Lipids*, 1969, 5, 91-99.

Ollivon, M and Perron, R, in *Manuel des corps gras AFECG*, A. Karleskund and J.P. Wolff eds., Lavoisier, Paris 1992, chap. 5.

Small, D M, in *The physical chemistry of lipids, Handbook of lipid research*, ed by Small, Plenum Press, New York, 1988, chapter 10.

Wille, R L and Lutton, E S, *J. Am. Oil Chem. Soc.*, 1966, 43, 491-496.

Witzel, H and Becker, K, *Fette Seifen Anstrichm.*, 1969, 71, 507-516.

Chapter 6

An exploratory examination of polymorphic phase transition in cocoa butter fat using wide angle X-ray scattering (WAXS)

6.1 *Introduction*

This chapter will examine the structural characterisation of cocoa butter using WAXS (wide angle X-ray scattering) diffraction at the SRS, Daresbury Laboratory.

6.2 *Wide angle X-ray scattering diffraction studies*

The crystallisation behaviour of the cocoa butter sample was studied using high resolution synchrotron radiation at station 2.3 at SRS, Daresbury. In contrast to SAXS studies, these experiments provided information on short spacing, which refer to the cross-sectional packing of the hydrocarbon chain and are independent of the chain length [Chapman, 1962; Jacobsberg, 1976].

6.2.1 *Description of station 2.3*

Station 2.3 is a monochromatic station situated on a dipole source with a two circle diffractometer. The schematic drawing (Figure 6.1) summarises the features of station 2.3. These include:

- a Si (111) monochromator which operates in the wavelength range 0.7-2.5Å;
- horizontal and vertical post monochromator slits which define the cross-section of the incident beam;
- a flat-plate stage which can rotate the powder sample or spinning goniometer, when capillary geometry is used or alternative a variable temperature stage can be mounted;
- two sets of scattered beam collimators under vacuum are attached to the 2θ arm, these reduce the scatter of the diffracted beam;
- a Ge proportional detector.

A polychromatic beam (2×15 mm^2) is incident on to a chanel cut Si (111) monochromator which is a monolithic single crystal. To achieve thermal stability, the temperature of the monochromator is constantly maintained at 30.0±0.1°C via water cooling cycle fed from a closed-circuit water bath. The entire device is housed in the monochromator chamber which is evacuated by a rotary vacuum pump. The emergent monochromatic beam is defined by centre opening slits before the sample position. The slits are housed inside a hutch beam pipe linked to the monochromator chamber. The vertical position of the slits can be controlled by a stepper motor. The defined beam passes through a 25 μm kapton foil mounted at 45°. The downward scattered radiation is monitored by the scintillation counter (monitor) positioned between the sample and the slits as shown in Figure 6.1. The beam emerges from the pipe and is incident on to the sample. The diffracted X-ray is recorded by the detector on the 2θ arm.

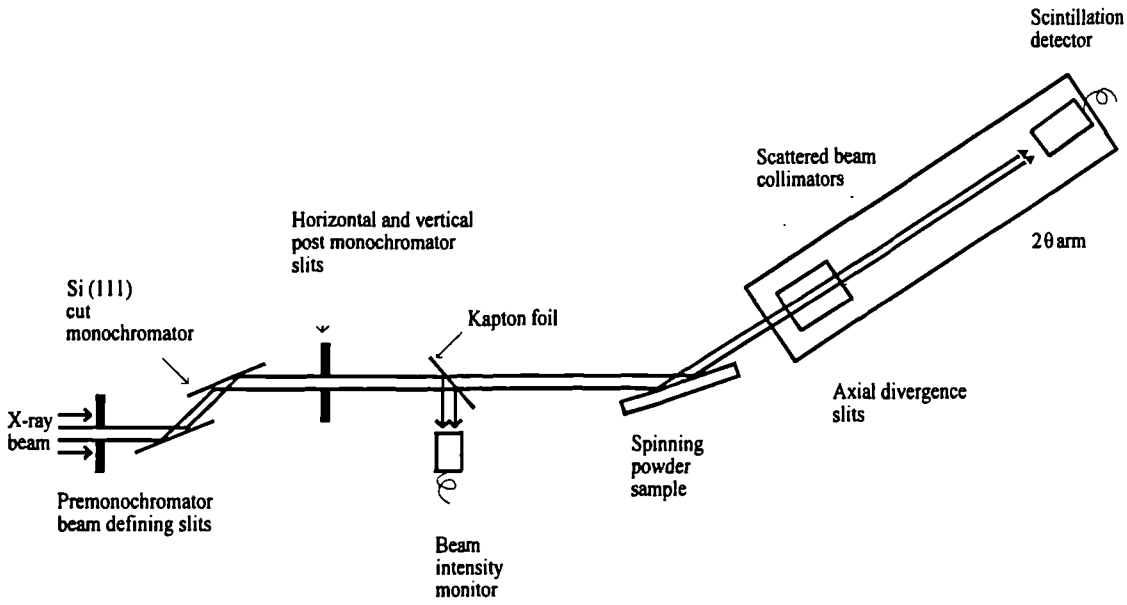

Figure 6.1. Schematic representation of station 2.3 at the Synchrotron Radiation Source, Daresbury Laboratory, after MacCalman [1996].

6.2.2 *In-situ cell for synchrotron studies*

The sample was held in a specially designed variable-temperature-cell (Figure 5.2), which has been described in detail by Cernik et al. (1995) and was mounted on the 2-circle diffractometer [Cernik, 1990] (Figure 6.2). The melted sample was pipetted into the sample holder and powder diffraction scans were recorded with a rotating sample in order to average out the effects of preferred orientation. The temperature of the sample was controlled by an integral water jacket fed from a Haake F3 recirculating bath (accurate to ± 0.01°C). The rate of heating and cooling was controlled by a Haake PG20 temperature programming unit.

The basic principles of the operating cell are very simple. The sample is mounted in a rotating stage which is kept in close sliding contact with a hollow copper block. The rotating shaft is lubricated with grease with a high thermal conductivity. The temperature of the block can be varied from -50°C to 80°C easily by changing the type of circulating fluid. The temperature can be measured by the K-type thermocouple that is buried in the copper block.

6.2.3 *Data collection and analysis*

Data were collected with 2θ values ranging from 1 to 30°, at intervals of 0.1° and at a collection time of 1 second. The data were normalised using the program PODSUM. The X-ray flux is not constant as the current of the electron beam in the storage ring decay. It is necessary to normalise the diffracted beam intensity against the incident beam intensity. The peak shapes and resulting peak positions analysis was carried out using the data manipulation and display program PLOTEK.

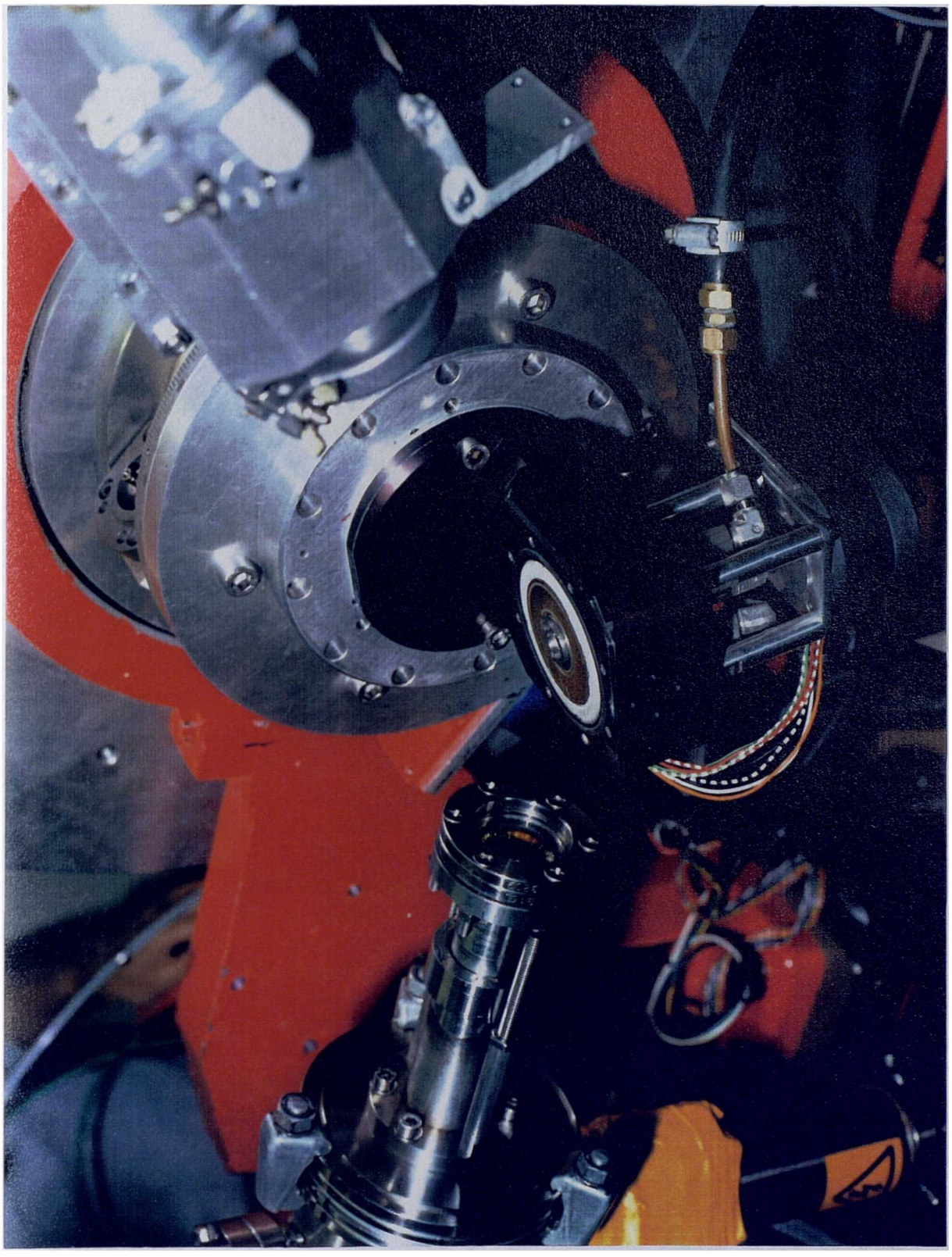

Figure 6.2. The in-situ cell attached to the diffractometer.

6.3 *Results and Discussion*

6.3.1 *Crystallisation of cocoa butter via slow cooling*

The cocoa butter sample was subjected to a cooling/heating cycle at a rate of 0.10°C. The X-ray wavelength used was 1.7002Å. The sample was cooled from 70°C to 15°C; it started to crystallise at 19°C. From the X-ray diffraction spectrum (Figure 6.3(a)) only one major peak is observed. The d-spacing value, corresponding to this latter peak, is 4.58 Å, which is consistent with Form V [Hicklin, 1985]. The intensity of the peak is very low and this is due to the wavelength chosen, the maximum photon flux is between 1.1Å and 1.5Å.

Cooling further, other peaks appear (Figure 6.3(b)). The d-spacing values corresponding to these peaks are: 5.4Å, 4.58Å, 3.96Å, 3.85Å, 3.75Å, and these values are all consistent with Form V. During the cooling phase of the cycle, no polymorphic transition was observed.

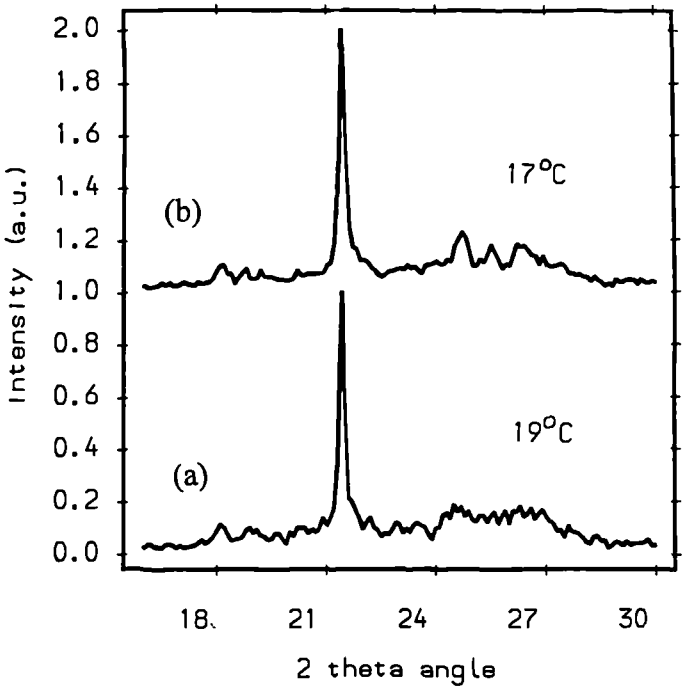

Figure 6.3. X-ray diffraction patterns taken at different temperatures: (a) 19°C, (b) 17°C.

The cocoa butter sample was then heated up to 40°C. No polymorphic transitions were observed. The sample melted at approximately 33.0°C and this agrees with the melting point of Form V [Wille and Lutton, 1966].

6.3.2 *Crystallisation of cocoa butter via quenched cooling*

In this experiment the X-ray wavelength used was 1.2002Å. The *in-situ* cell was set-up at 2°C. The cocoa butter sample was heated to 70°C in order to melt completely the high melting fraction of cocoa butter. The melt was pipetted into the sample holder a few drops at a time, allowing each addition to solidify before adding the next. This was done in order to avoid cocoa butter crystallising in stable polymorphic forms. Thus, the cell was heated up to 40°C at a rate of 0.75°C/min and the resultant polymorphic forms were studied. The X-ray diffraction data are summarised in Table 6.1; the values of short spacing observed are compared with the values found in literature [Hicklin, 1985; V. D'Souza, 1990]. As it can be observed from Table 6.1, the experimental data are consistent with the values found in the literature. Initially, cocoa butter crystallises in Form I. The X-ray diffraction pattern, collected at 4°C, shows a single peak at high intensity (Figure 6.4(a)). Form I is the only crystalline form present up to 15°C, where two other peaks appear (Figure 6.4(b)), that they are both concordant with Form III. Form I is still the predominant crystalline form.

Heating further, at 20°C another polymorphic form crystallises (Figure 6.4(c)); the d-spacing value, corresponding to this new peak, is 4.35 Å. This latter value is consistent with the Form IV. At 21°C, Form I is not the dominant crystalline form any longer, the peak at 4.35 Å becomes more intense than that at 4.19 Å (Figure 6.4(d)). Besides, two further peaks are present with d-spacing values of 4.6 Å and 3.99 Å, respectively. It is noteworthy that only a 1°C difference between the latter two spectra (Figure 6.4(c) and(d)) is necessary to influence the reorganisation of the crystal lattice into a more stable polymorphic form as Form V. Four polymorphic forms coexist

together, even if this situation does not last longer. The unstable polymorphic form (such as Forms I and III) transform into the more stable Form V.

Form I decreases in intensity up to melting at 24°C (Figure 5.4(f)). The melting point of Form I is not agreeing with the value of melting point of 17°C that Wille and Lutton (1966) observed during his studies on cocoa butter polymorphism. Form I seems to be more stable than expected from previous work [Wille and Lutton, 1966; Chapman, 1971]. This could confirm the conclusion reached in Chapter 5 concerning the higher stability of Form I.

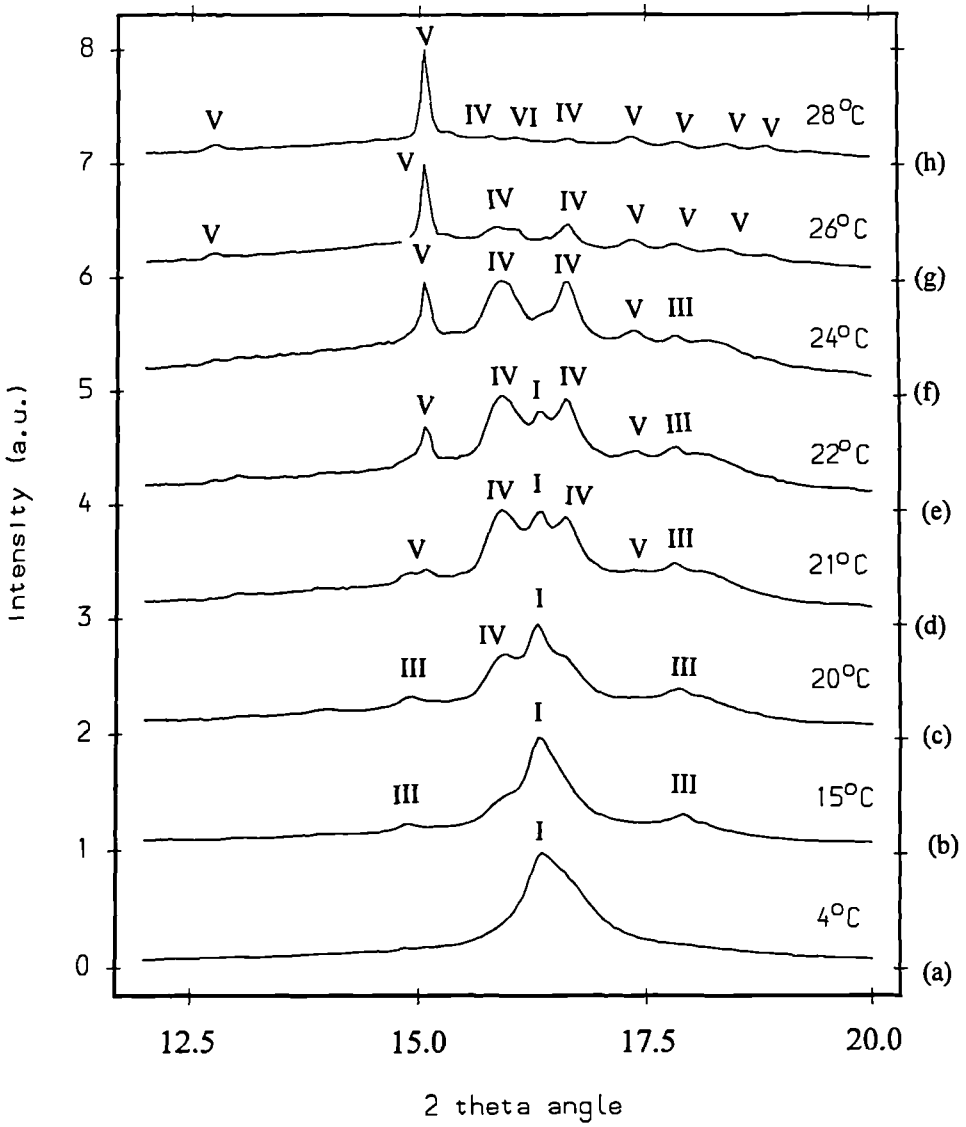

Figure 6.4. X-ray diffraction patterns taken at different temperatures: (a) 4°C; (b) 15°C; (c) 20°C; (d) 21°C; (e) 22°C; (f) 24°C; (g) 26°C; (h) 28°C.

T (°C)	d-spacing (Å) observed	d-spacing (Å) found in literature	Polymorphic forms
4	4.19	4.19	I (VS)
10	4.19	4.19	I (VS)
15	4.64	4.63	III (M)
	4.22	4.19	I (VS)
	3.86	3.87	III (M)
20	4.64	4.63	III (M)
	4.33	4.35	IV (VS)
	4.22	4.19	I (VS)
	3.86	3.87	III (M)
21	4.59	4.60	V (S)
	4.33	4.35	IV (VS)
	4.22	4.19	I (VS)
	4.16	4.17	IV (VS)
	3.98	3.99	V (M)
	3.86	3.87	III (M)
22	4.59	4.60	V (VS)
	4.33	4.35	IV (VS)
	4.22	4.19	I (M)
	4.16	4.17	IV (VS)
	3.98	3.99	V (M)
	3.86	3.87	III (M)
24	4.59	4.60	V (VS)
	4.33	4.35	IV (VS)
	4.16	4.17	IV (VS)
	3.98	3.99	V (S)
	3.86	3.87	III (M)
26	5.41	5.43	V (M)
	4.59	4.60	V (VS)
	4.33	4.35	IV (S)
	4.16	4.17	IV (S)
	3.98	3.99	V (M)
	3.86	3.87	V (W)
	3.77	3.76	V (W)
28	5.41	5.43	V (M)
	4.59	4.60	V (VS)
	4.33	4.35	IV (S)
	4.29	4.28	VI(W)
	4.16	4.17	IV (S)
	3.98	3.99	V (M)
	3.86	3.87	V (W)
	3.77	3.76	V (W)
	3.67	3.68	V (W)

Table 6.1 X-ray diffraction data collected at station 2.3 [S = strong; VS = very strong; M = medium; W = weak].

This behaviour is also consistent with the SAXS experiments carried out at NSLS at Brookhaven, as discussed in Chapter 5.

Form III melts around 26.0°C and this melting point is consistent with the value found by Wille and Lutton (1966). Figure 6.4(g) shows that Form V is the dominant polymorphic form, with peak intensity remarkable increased, although at 26°C part of the sample is already liquid. Besides, there are present two new peaks with d-spacing values of 5.41Å and 3.77Å, respectively. These latter two peaks are consistent with Form V.

At 28°C, there appears a peak of low intensity, consistent with Form VI (d = 4.29 Å). The two peaks relativing to Form IV have almost disappeared. The intensity of the peak at 4.59 Å increases even more to confirm that the system is gradually stabilising into a more stable polymorphic form. Heating further, cocoa butter melts finally at approximately 33°C.

There is no evidence for Form II in these studies.

6.4 *Conclusion*

- Cooling cocoa butter at a rate of 0.10°C, the system crystallises in a stable polymorphic form (Form V). Using the slowest cooling rate, the system has time to arrange the crystal lattice into a higher melting polymorphic form.

- Chilling the melt, cocoa butter crystallises first into the unstable forms, such as Forms I and III. The slow heating (0.75°C/min) allows reorganisation of the crystal lattice into the higher melting polymorphic form such as Form V and V, passing through Form IV and avoids the total disgregation, which corresponds to the melting phase.

- The melting point recorded for Form I was around 24.0°C, which is greater than the value of melting point found in the literature [Wille and Lutton, 1966; Witzel, 1969].

6.5 *References*

Cernik, R J, Murrey, P K, Pattison, P and Fitch, A N, *J. Appl. Crystallogr.*, 1990, 23, 292-296.

Cernik, R J, Craig, S R, Roberts, K J and Sherwood, J N, *J. Appl. Crystallogr.*, 1995, 28, 651-653.

Chapman, D, *Chem. Rev.*, 1962, 62, 433-456.

Chapman, G M, Akehust, A E and Wright, W B, *J. Am. Oil Chem. Soc.*, 1971, 48, 824-830.

D'Souza, V, deMan, J M and deMan, L, *J. Am. Oil Chem. Soc.*, 1990, 67, 11, 835-843.

Hicklin, J D, Jewell, G C and Heathcock, J F, *Food Microstructure*, 1985, 4, 2, 241-248.

Jacobsberg, B and OH, C H, *J. Am. Oil Chem. Soc.*, 1976, 53, 609-617.

MacCalman, L, in *Studies of the Crystallisation of Some Pharmaceutically Important Materials in Relation to Polymorphic Structural Stability*, PhD Thesis, University of Strathclyde, Glasgow, 1996.

Wille, R L and Lutton, E S, *J. Am. Oil Chem. Soc.*, 1966, 43, 491-496.

Witzel, H and Becker, K, *Fette Seifen Anstrichm.*, 1969, 71, 507-516.

Chapter 7

An examination of the effects of undercooling and mixing on induction times for single and mixed confectionery fats

7.1 *Introduction*

A new crash cool tempering cell was developed in order to measure induction times to a good degree of accuracy under well-controlled mixing conditions using a novel turbidity probe. This chapter will examine the results obtained on study of single and mixed fats using this new cell.

7.2 *Methodology*

If a solution is rapidly cooled to within the metastable zone region, a period of time will elapse before the onset of crystallisation, which is known as the induction time, τ. From the classical homogeneous nucleation theory, the induction time is due to the formation of a cluster of molecules having a critical size (r^*). Then, assuming that the induction time is primarily due to the formation of the first crystals, the period of time is considered inversely proportional to the rate of nucleation, J [Nancollas, 1964, Söhnel, 1992].

Using the technique of turbidimetry, the rate of change of light transmittance with respect to time is measured. This can be used to directly measure the induction time and by its inverse proportionality the nucleation rate.

The interfacial energy (γ) between the nuclei and surrounding solution can, in principle, be obtained from measurements of the time taken for nuclei formation as a function of supersaturation, S, [Walton, 1983; Elwell and Scheel, 1975]. Assuming spherical cluster formation, the interfacial energy can be found using the following equation:

$$\ln (1/\tau) = \ln (J) = \ln (A) - [-16 \pi \gamma^3 V_m^2 / 3k^3] [1/T^3 (\ln S)^2] \qquad (7.1)$$

where the V_m is the molar volume, K is Boltzmann constant and T is the crystallisation temperature (°K). A graph of ln (τ) versus T^{-3} $(\ln S)^2$ should yield a straight line of positive slope (γ^3 constant) from which the interfacial energy can be determined.

radius of the critical nucleus, r*, (the size of nucleus which has a maximum of Gibbs free energy) can be evaluated from the equation:

$$r^* = 2\gamma \, Vm / KT \ln (S) \qquad (7.2)$$

7.3 *A new crash cool tempering cell*

All samples were analysed using a tempering machine, provided by Cadbury (Figure 7.1). The fat mixture was put into a pot made from stainless steel and stirred by a U-shaped stainless steel mixer with scraper blades (Figure 7.2). Intensive mixing enables the formation of crystal nuclei and influences the growth and agglomeration of crystals. Moreover, the continuous removing of crystallised mass from the cooling surface is necessary for uniform heat transfer on the whole mass [Kleinert, 1976]. The mixer was driven by a low voltage servo motor.

The temperature of the system was monitored during the experiments, with a platinum resistance thermometer, fitted into the lid of the pot through a small hole. Heating and cooling was effected by the use of Peltier effect thermoelectric modules. The Peltier modules are capable of enabling fast (ca. 10°C/min) and they are controlled by a computer model MFI1010 manufactured by C.I.L. Ltd and an Electrocraft LA5600 servo amplifier to supply the current needed to drive the modules. An optical light probe was incorporated into the pot to detect nucleation. It was connected to a colorimeter, fabricated specifically for this purpose (Figure 7.3).

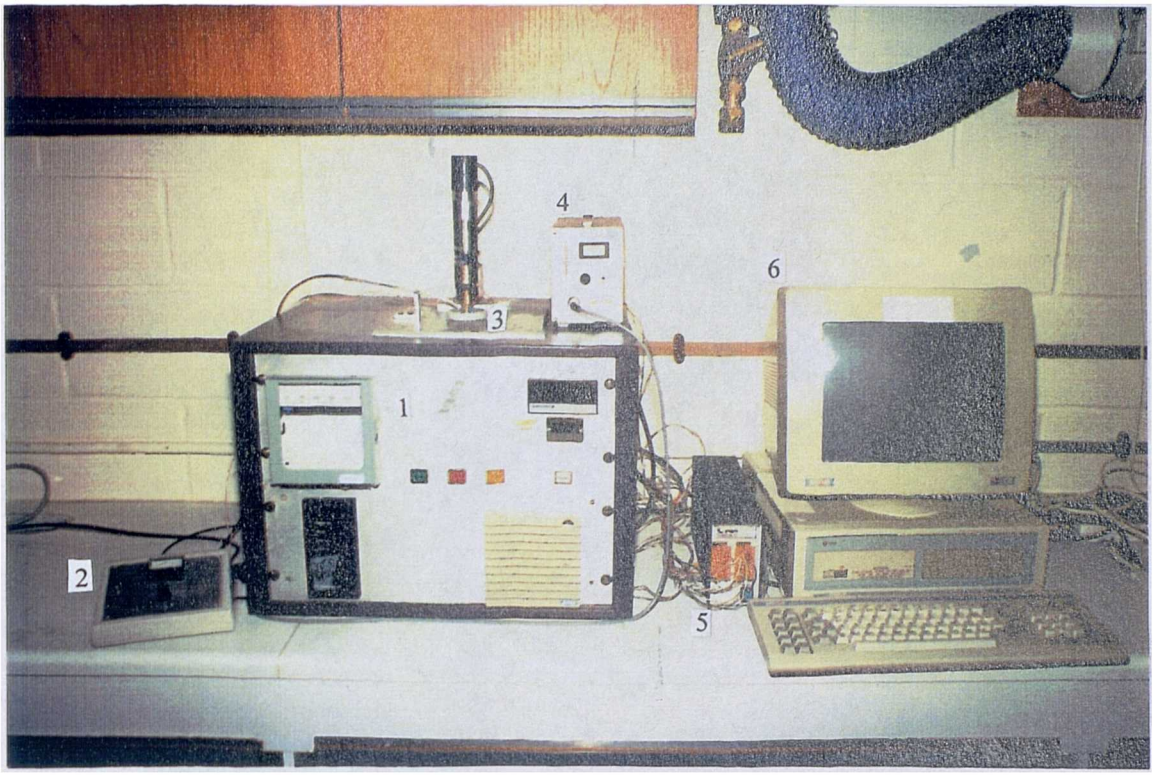

Figure 7.1. Photograph of the experimental arrangement and data acquisition used for crashcool measurements. 1. Tempering machine; 2. Colorimeter; 3. Sample pot containing Pt100 temperature probe, fibre optic light probe and mixer; 4. Temperature controller; 5. OASIS MADA interface; 6. Amstrad 1640 computer.

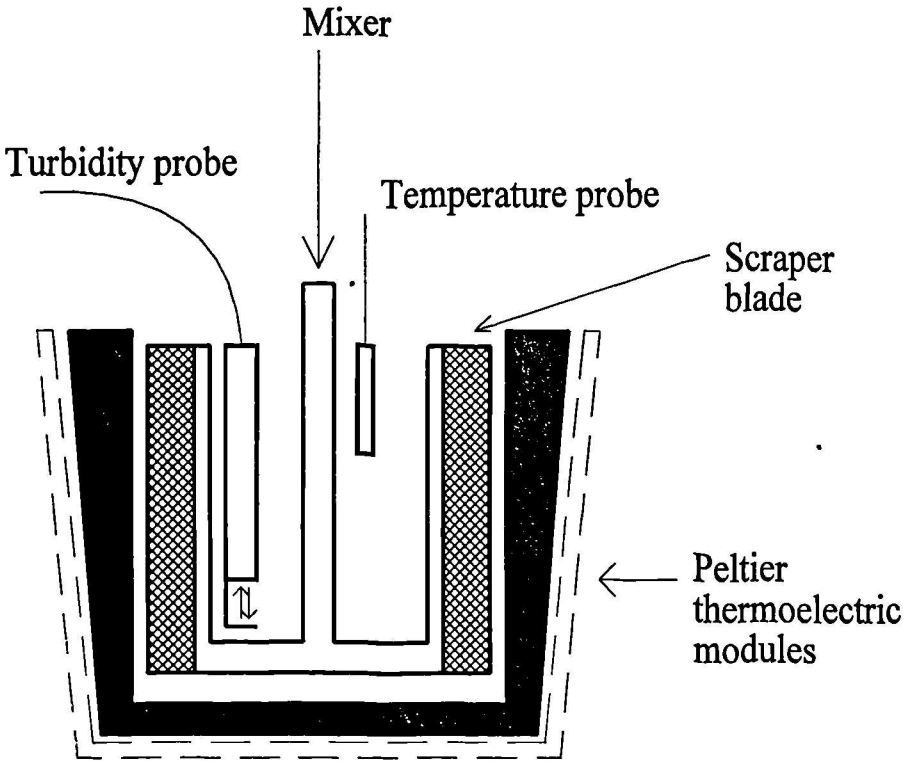

Figure 7.2. Expanded schematic view of sample pot containing Pt100 temperature probe, fibre optic light probe and mixer. Heating and cooling is effected by the use of Peltier effect thermoelectric modules.

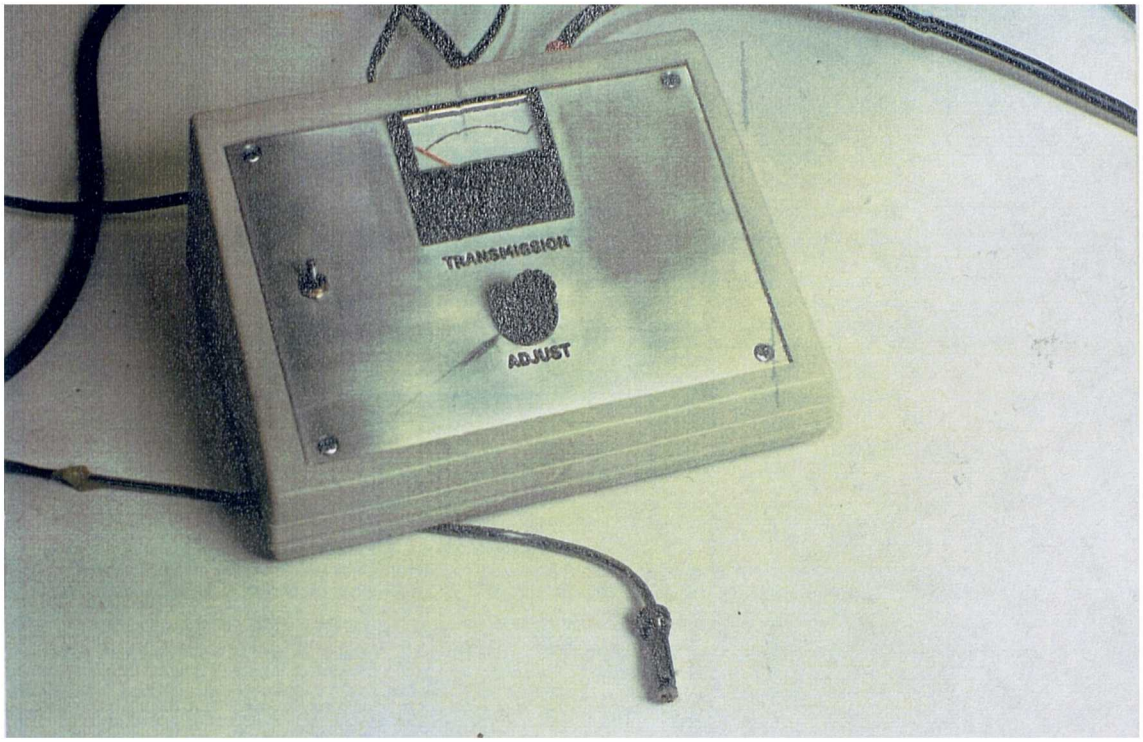

Figure 7.3. Fibre optic light probe connected to a colorimeter; note the curved stainless sheathing which enables the probe to fit into the sample pot without interfering with the stirrer motor.

7.4 *Experimentation*

The experimental methodology comprise of preheating the solution above the saturation temperature for a period of time to ensure all crystal nuclei have been dissolved. The solution is then crash cooled through the saturation temperature at a rate of 5°C/min to a base temperature within the metastable zone. A number of different base temperatures are used in order to vary the degree of supersaturation created within the solution. The temperature at which crystallisation occurs (T_{cryst}) is noted by a reduction in the solution's light transmittance, for these experiments a 10% reduction was found to be effective. The induction time (τ) is the period of time elapsed from passing the saturation temperature (determined previously in Chapter 4) to the detection of a crystallisation.

A typical experimental profile of crash cooling is shown in Figure 7.4.

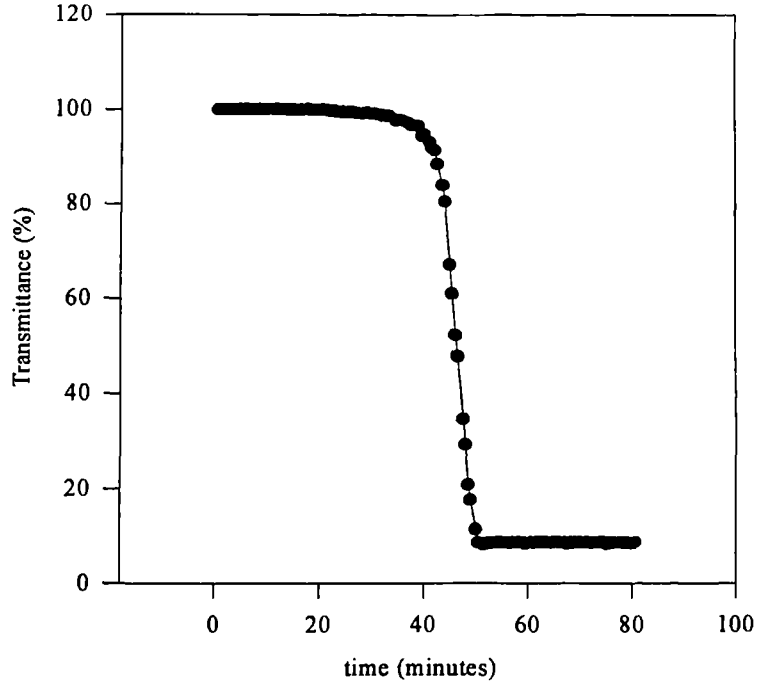

Figure 7.4 Experimental data for crash cool cycle for 10 mole percent solution of PPP in cocoa butter.

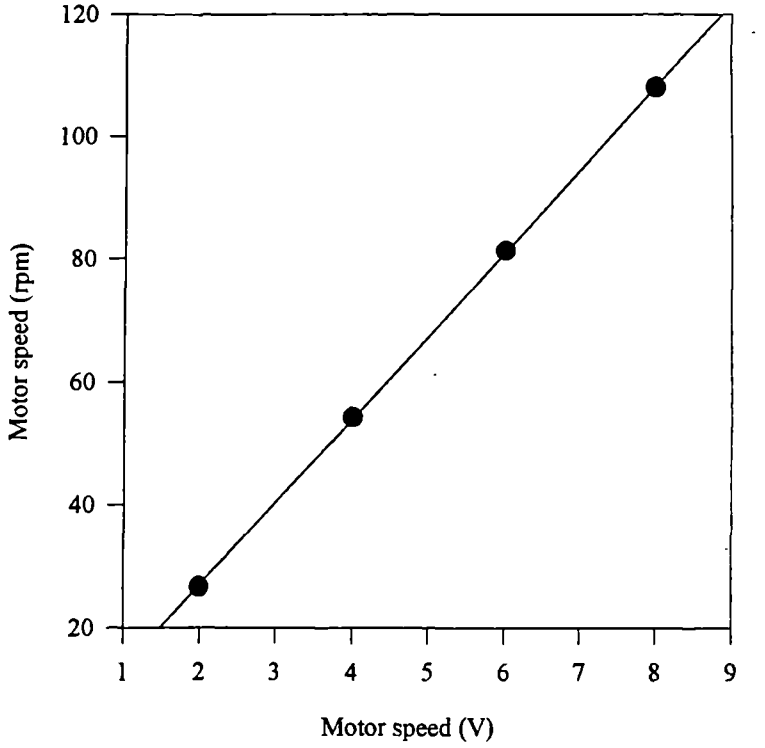

Figure 7.5 A plot of motor speed (volts) versus motor speed (rpm).

Different motor speeds were used to see the effects of mixing on the crystallisation temperature and the induction time. The motor control voltage was calibrated as motor speed. The calibration was accurate and very good correlation was found (see Figure 7.5 above).

A fresh sample was used for each analysis. It has been observed that the data were not reproducible when the same sample was used many times. This could be due to the fact that, during mixing, the pads of the stirrer scraped the wall and the bottom of the sample holder. Metallic particles could pass in the solution which sometimes turned green after many cycles. Metallic analysis of a green sample was carried out, which revealed traces of chromium (11 ppm) and nickel (2 ppm). It was felt that these impurities, presumably in the form of a salt of the fatty acids, could alter the crystallisation process which might explain the difference in induction time value found at the same conditions following repeated re-cycling. This inconvenient was minimised by putting a little piece of PTFE (polytetraflouroethylene) to avoid metal to metal contact in the bottom of the pot and substituting the metallic wipers with tufnol.

7.5 *Calculation of an estimated shear rate*

An estimation of the shear rate can be made as a function of the motor speed. Multiplying the motor speed (rpm) by the distance from the edge of wiper to the axis of rotation (1.405 cm) by 2π, it is worked out the distance per minute. Then, this latter parameter has to be divided by the gap between the wiper and the wall of the pot. This gives a value of shear rate.

$$\text{motor speed (rpm)} \times 2\pi r = \text{distance per minute} \qquad (7.3)$$

$$\text{distance per minute / gap} = \text{shear rate} \qquad (7.4)$$

The wipers are not fixed, but they move during the rotation. Then, it is impossible to measure accurately the gap width. The gap could vary from a maximum value of

0.0945 cm, which corresponds to the difference between the radius of the pot (1.4995 cm) minus the minimum distance of the wiper to the axis of rotation (1.405 cm), to 0 if the wipers touch the wall. In reality, this is not possible because the fats form like a film along the walls. The gap won't be equal to zero, but it can be assumed to be a very small value. Then, the shear rate will vary from a minimum to an infinite great value.

Using the equations (7.3) and (7.4), a minimum shear rate has been calculated for four different motor speed and summarised in Table 7.1

Motor speed (rpm)	Minimum shear rate (s^{-1})
26.7	41.5
54.3	84.5
81.3	126.5
108.0	168.1

Table 7.1. Calculation of minimum shear rate in function of motor speed.

7.6 *Results*

Cocoa butter, milk fat and several mixtures of two binary system (tripalmitin/cocoa butter and milk fat/cocoa butter) were investigated under well defined conditions of temperature and shear in order to study the variation of induction time.

7.6.1 *The effect of mixing on cocoa butter crystallisation*

From the slowcool measurements, the values found for temperature of saturation and meta stable zone width were 33.5°C and 8.1°C, respectively. The temperature of saturation and the difference between the T_{sat} and meta stable zone region provide the limit within which the base temperatures may be chosen.

The cocoa butter was preheated to 70°C to ensure all crystal nuclei were destroyed. Then, the sample was crash cooled to three different base temperatures. For each base temperature, the sample was analysed at four different shear rates. The experimental data are summarised in Table 7.2. A graph of induction time versus the base temperature is shown in Figure 7.6(a).

The shear rate plays an important role on crystallisation of cocoa butter. For each base temperature, at higher shear rate correspond small induction time values. The effect of mixing is more evident at the highest base temperature. At a base temperature of 25°C, cocoa butter crystallises quickly, due to the high degree of supersaturation. In the case of the two fastest shear rates, the values found for induction time are much smaller than ten minutes. Increasing the base temperature, the difference on induction time at different shear rate become bigger. At 28°C, cocoa butter crystallises in 3 hours at a shear rate of 41.5 s^{-1}, while it needs only 24 minutes to crystallise using a shear rate of 168.1 s^{-1}.

The shear rate has also an influence on the temperature at which crystallisation is occurred. The onset temperature for crystallisation is highest at the largest shear rate. Higher shear rate might help the formation of nuclei.

Base Temperature (°C)	Shear rate (s^{-1})	T_{cryst} (°C)	τ (minutes)
25.0	41.5	25.2	22
	84.5	25.4	10
	126.5	26.5	6
	168.1	26.4	3
26.0	41.5	26.0	60
	84.5	26.2	47
	126.5	27.7	25
	168.1	27.8	12
28.0	41.5	28.0	180
	84.5	28.1	88
	126.5	28.2	44
	168.1	28.7	24

Table 7.2. Base temperature chosen, minimum shear rates, temperatures of crystallisation and induction time (τ) for cocoa butter.

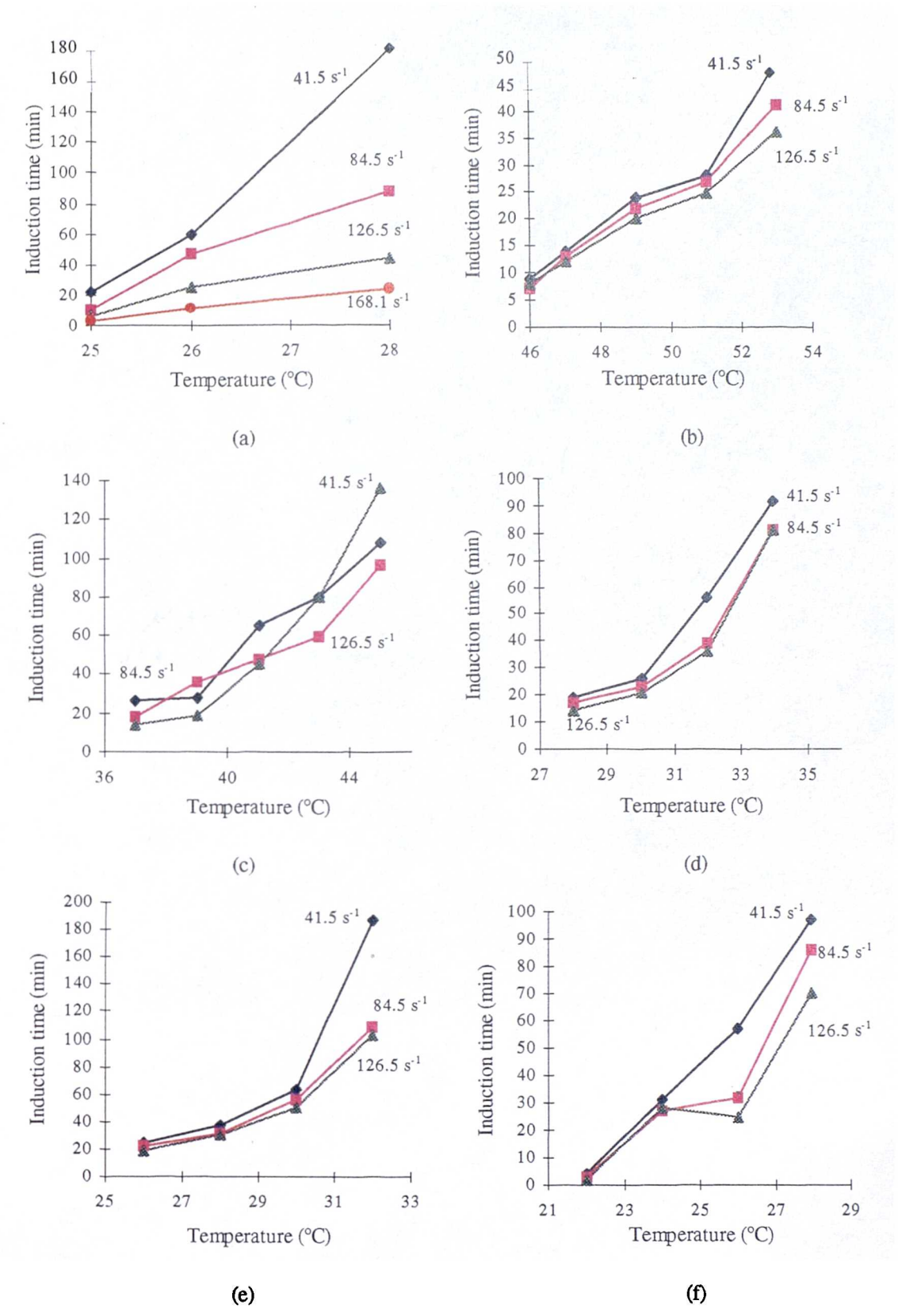

Figure 7.6. Plots of induction time versus base temperature at different shear rate: (a) cocoa butter, (b) 20 mole% of PPP in cocoa butter, (c) 10 mole% of PPP in cocoa butter, (d) 5 mole % of PPP in cocoa butter, (e) 3 mole% of PPP in cocoa butter and (f) 1 mole% of PPP in cocoa butter.

7.6.2 *Effect of mixing on mixture of tripalmitin and cocoa butter*

The changing of induction time as a function of three different shear rates was investigated for 20, 10, 5, 3 and 1 mole percent solutions of tripalmitin in cocoa butter. Five base temperature were choosen in the case of 20 and 10 mole percent solutions, while four base temperature for 5, 3 and 1 mole percent solutions.

7.6.2.1 *20% of tripalmitin in cocoa butter*

From the slowcool measurements, the values found for temperature of saturation and meta stable zone width were 56.0°C and 11.5°C, respectively. The experimental results are summarised in Table 7.3, and a plot of induction time versus base temperature temperature shown in Figure 7.6(b). No significant changes in induction times have been observed at the lowest predetermined temperatures.

Base Temperature (°C)	Shear rate (s^{-1})	T_{cryst} (°C)	τ (minutes)
46.0	41.5	45.8	9
	84.5	45.8	7
	126.5	45.3	8
47.0	41.5	46.5	14
	84.5	46.6	13
	126.5	46.9	12
49.0	41.5	48.3	24
	84.5	48.3	22
	126.5	48.5	20
51.0	41.5	50.0	28
	84.5	50.6	27
	126.5	50.8	25
53.0	41.5	51.8	49
	84.5	52.2	41
	126.5	52.4	36

Table 7.3. Base temperature chosen, minimum shear rates, temperatures of crystallisation and induction time (τ) for 20 mole percent solution of tripalmitin in cocoa butter.

At a base temperature of 46°C, the induction time values are very close, within a difference of only a minute between each value. The same behaviour was observed at 47°C. At the base temperatures of 49°C and 51°C it shown a slightly bigger difference in induction time at different shear rate. But the effect of mixing is more evident at 53°C. At this latter base temperature, the degree of supersaturation is small, then a higher shear rate might help the formation of nuclei.

Due to the high concentration of tripalmitin in the mixture, the nuclei formed are probably attributable to the polymorphs typical of tripalmitin. However, all base temperatures chosen are too high to allow the crystallisation of cocoa butter polymorphs.

7.6.2.2 *10% Tripalmitin in Cocoa Butter*

The experimental data are summarised in Table 7.4, while a plot of the induction time versus base temperature at different shear rate is shown in Figure 7.6(c). The values found for temperature of saturation and meta stable zone width were 52.1°C and 15.8°C, respectively.

As it can be observed from Figure 7.6(c), the variation of the induction time shows different trends as a function of the base temperature choosen. At the lowest base temperature, the induction time increases as the shear rate decreases. This behaviour is also observed at 41°C, even if the induction times at the two shear rates of 41.5 and 84.5 s^{-1} are very close. Besides, at 39°C, the induction time recorded at a shear rate of 41.5^{s-1} is smaller than that observed at a shear rate of $84.5s^{-1}$.

The main variation can be noted at base temperatures higher than 41°C. The degree of supersaturation decreases but the fastest shear rate does not seem to increase the nucleation rate. This could be due to the presence of different polymorphic forms crystallising out or to a change in the fat composition. Even if the base temperatures are too high to allow the crystallisation of cocoa butter, the high concentration of this latter component might influence the molecular packing of the mixture. At the base temperatures of 43 and 45°C, the highest values of induction time are recorded at the faster shear rate, while the system crystallises in a shorter time at a rate of $84.5s^{-1}$.

Base Temperature (°C)	Shear rate (s^{-1})	T_{cryst} (°C)	τ (minutes)
37.0	41.5	36.2	26
	84.5	36.3	18
	126.5	36.3	14
39.0	41.5	38.4	28
	84.5	38.0	36
	126.5	38.3	19
41.0	41.5	40.2	65
	84.5	40.4	48
	126.5	40.4	45
43.0	41.5	42.3	80
	84.5	42.5	59
	126.5	42.2	80
45.0	41.5	44.1	108
	84.5	44.4	96
	126.5	44.2	136

Table 7.4. Base temperature chosen, minimum shear rates, temperatures of crystallisation and induction time (τ) for 10 mole percent solution of tripalmitin in cocoa butter.

7.6.2.3 *5%, 3% and 1% of Tripalmitin in Cocoa Butter*

The values found from the slowcool measurement for temperature of saturation and meta stable zone width are summarised in Table 7.5, whilst the crashcool data are summarised in Tables 7.6, 7.7 and 7.8. The plots of the induction time versus base temperature are shown in Figure 7.6(d) - (f).

These three mixtures show similar crystallisation behaviour in function of the shear rate. In the case of 5 mole percent solution of tripalmitin in cocoa butter, the induction time decreases as the shear rate increases. This is observed at all base temperatures. At 28 and 30°C, the difference between the values of induction time is small, while at 32°C the difference is deeper between the shear rates of 84.5 and $126.5s^{-1}$.

The crystallisation behaviour of the 3 mole percent concentration shows similarity to the previous mixture. The induction time increases as the shear rate

decreases, but a small differences are observed between 26 and 30°C. At 32°C, the system takes long time before crystallise. There is a difference of more than an hour between the induction time recorded at the shear rates of 41.5 and 126.5s^{-1}.

Concentration of PPP in cocoa butter (mole%)	T_{sat} (°C)	MSZW (°C)
5	40.4	11.4
3	40.4	14.5
1	37.1	16.7

Table 7.5. Summary of saturation temperature and metastable zone width from the sloocool experiments discussed in Chapter 4 for 5, 3 and 1 mole percent solutions of tripalmitin in cocoa butter.

Base Temperature (°C)	Shear rate (s^{-1})	T_{cryst} (°C)	τ (minutes)
28	41.5	28.3	19
	84.5	28.3	17
	126.5	28.4	14
30	41.5	30.2	26
	84.5	30.3	23
	126.5	30.4	21
32	41.5	32.0	56
	84.5	32.8	39
	126.5	32.1	36
34	41.5	34.0	92
	84.5	34.0	81
	126.5	34.0	81

Table 7.6. Base temperature chosen, minimum shear rates, temperatures of crystallisation and induction time (τ) for 5 mole percent solution of tripalmitin in cocoa butter.

Base Temperature (°C)	Shear rate (s^{-1})	T_{cryst} (°C)	τ (minutes)
26	41.5	26.3	24
	84.5	26.4	22
	126.5	26.2	19
28	41.5	28.2	38
	84.5	28.3	31
	126.5	28.1	30
30	41.5	30.1	63
	84.5	30.1	56
	126.5	30.2	50
32	41.5	31.5	187
	84.5	31.9	109
	126.5	32.0	103

Table 7.7. Base temperature chosen, minimum shear rates, temperatures of crystallisation and induction time (τ) for 3 mole percent solution of tripalmitin in cocoa butter.

Base Temperature (°C)	Shear rate (s^{-1})	T_{cryst} (°C)	τ (minutes)
22	41.5	24.0	4
	84.5	24.2	3
	126.5	26.1	1.5
24	41.5	24.2	31
	84.5	24.3	27
	126.5	24.4	28
26	41.5	26.1	57
	84.5	26.1	32
	126.5	26.3	25
28	41.5	28.0	97
	84.5	28.1	86
	126.5	28.0	70

Table 7.8. Base temperature chosen, minimum shear rates, temperatures of crystallisation and induction time (τ) for 1 mole percent solution of tripalmitin in cocoa butter.

In the case of 1 mole percent solution of tripalmitin in cocoa butter, very small induction time (less than 5 minutes) are recorded when the system is crashcooled to 22°C. From table 7.8, it can be observed that this mixture crystallises even before to reach the value of the base temperature chosen. At a shear rate of 126.5s^{-1}, the temperature of crystallisation is approximately 26.1°C (4°C higher) and the induction time is only 90 seconds. Moving to a base temperature of 24°C, the induction times deeply increase with respect to the values observed at 22°C. However, the shear rates do not make sensible change on the induction time.

The effect of mixing can be noted at the two highest base temperatures, even if it is more evident at 26°C. There is a difference of approximately 25 minutes between the values of induction time recorded at the shear rates of 41.5 and 84.5s^{-1}. This is the highest difference observed in function of mixing speed.

7.6.2.4 *Crystallisation behaviour in static conditions*

The induction measurements were also done in static conditions for three samples: cocoa butter, 20 and 5 mole percent solutions of PPP in cocoa butter. The values obtained are compared with those recorded at a shear rate of 41.5 s^{-1} and summarised in Table 7.9.

Concentrations (mole%)	Base Temperature (°C)	Shear rate (s^{-1})	T_{cryst} (°C)	τ (minutes)
20% PPP	46	0	45.8	9
		41.5	44.9	76
5% PPP	28	0	28.3	19
		41.5	28.2	105
100% Cocoa Butter	25	0	25.2	22
		41.5	24.7	113

Table 7.9. Comparison of induction times in static and dynamic conditions for: cocoa butter, 20 and 5 mole percent solutions of PPP in cocoa Butter.

As it can be observed from Table 7.9, in static conditions, all systems take much more than an hour to crystallise. At the base temperatures chosen, the degree of supersaturation is high, but this condition is not enough to enable the systems to crystallise in short period of time.

7.6.2.5 *Discussion*

With the exception of the 10 mole percent solution of tripalmitin in cocoa butter, all systems show a decrease of induction time as the shear rate increases. In the case of the 20 mole percent solution of PPP in cocoa butter, the system crystallises in a relative short time and this could relate to the high concentration of tripalmitin. Analysing the results relative to the 10 mole percent solution of tripalmitin in cocoa butter, the induction time measurements do not show linear variation depending on the shear rate applied. This behaviour could be due to the presence of different polymorphic forms crystallising out or to a change in the fat composition.

The data obtained at similar undercooling for different concentrations of tripalmitin have been compared and summarised in Table 7.10.

		induction time (min)			Solution's ideality
Concentration of PPP in CB (mole%)	undercooling (°C)	41.5 s^{-1}	84.5 s^{-1}	126.5 s^{-1}	
0%	8.5	22	10	6	
1%	9.0	97	86	70	no-ideal
3%	9.1	187	109	103	no-ideal
5%	8.4	56	39	36	no-ideal
10%	8.4	80	59	80	ideal
20%	9.1	14	13	12	ideal

Table 7.10. A comparison of the induction times collected at similar undercooling for cocoa butter and 1, 3, 5, 10 and 20 mole percent solutions of PPP in cocoa butter.

The addition of tripalmitin to cocoa butter slightly reduces the induction time only at the highest concentration of tripalmitin. Whereas, the 5, 3 and 1 mole percent solutions of PPP in cocoa butter show induction times much higher than those recorded for cocoa butter alone. As it was discussed in Chapter 4, these three mixtures deviate from ideal behaviour.

7.6.3 *The effect of mixing on milk fat*

From the slowcool measurements, the values found for temperature of saturation and meta stable zone width were 34.2°C and 7.8°C, respectively. Three different base temperatures were chosen. For each base temperature, the effect of mixing was investigated by using four different shear rates. As it can be observed in Table 7.11 and Figure 7.7(a), faster shear rates correspond to shorter induction times. As the mixture is crash cooled to 28°C, it crystallises at approximately 28.2°C. No variations of temperature at which crystallisation is occurred is observed at different shear rates. The induction time varies between 16 to 28 minutes from the fastest to the slowest minimum shear rate.

Increasing the base temperature, the difference in terms of induction time at different shear rates increases. But the shearing effect is especially noted at a base temperature of 32°C where the induction time values are more distant. At the two lowest shear rates, the sample takes more than two hours before the formation of nuclei is detected. In contrast, at a shear rate of 168.1 s^{-1}, the crystallisation of milk fat occurs in 48 minutes.

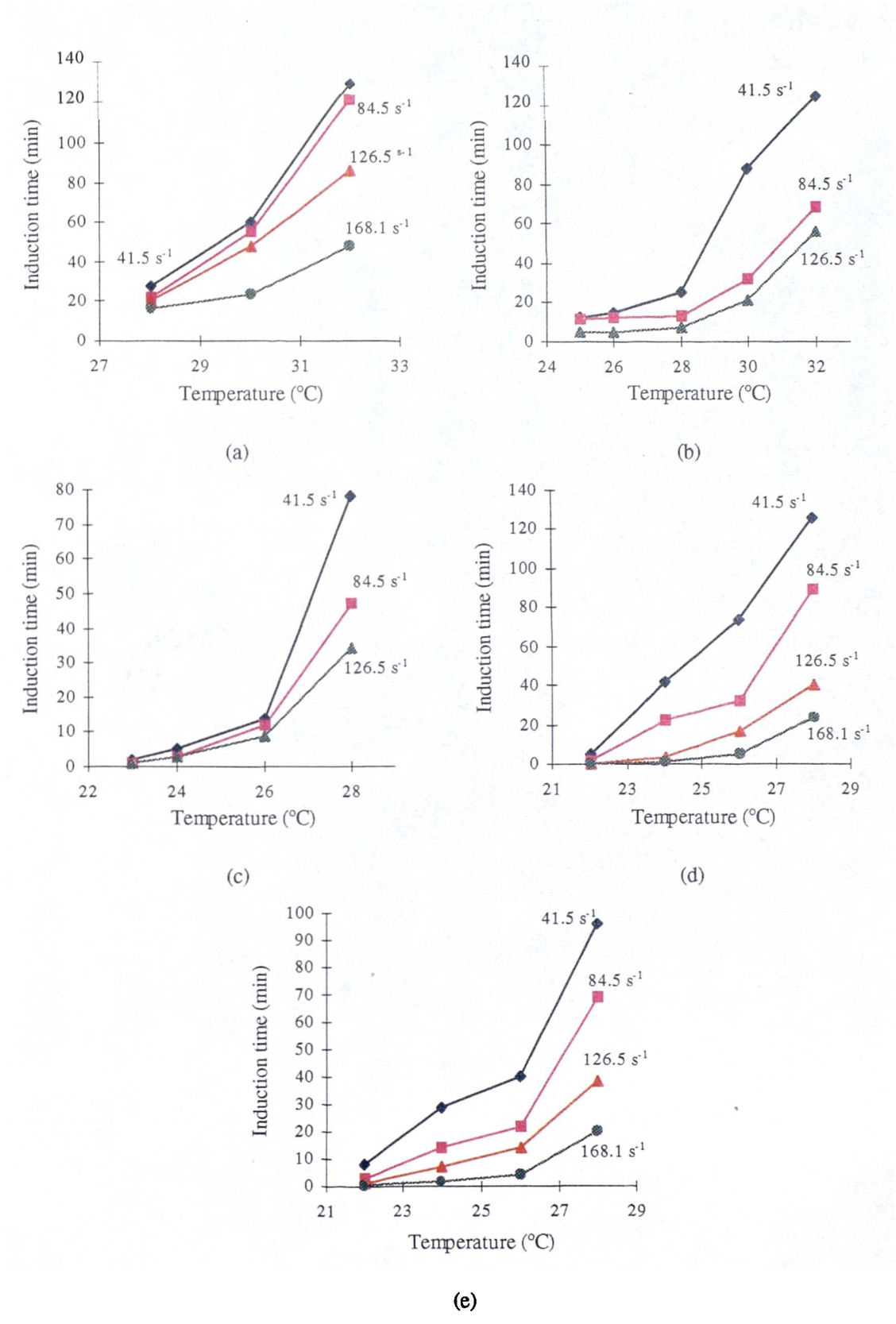

Figure 7.7. Plots of induction time versus base temperature at different shear rate: (a) milk fat, (b) 75 mole% of milk fat in cocoa butter, (c) 50 mole% of milk fat in cocoa butter, (d) 25 mole % of milk fat in cocoa butter and (e) 12.5 mole% of milk fat in cocoa butter.

Base Temperature (°C)	Shear rate (s^{-1})	T_{cryst} (°C)	τ (minutes)
28	41.5	28.2	28
	84.5	28.2	22
	126.5	28.2	20
	168.1	28.3	16
30	41.5	29.7	60
	84.5	29.8	55
	126.5	29.9	48
	168.1	30.0	24
32	41.5	31.6	132
	84.5	31.7	123
	126.5	31.9	86
	168.1	32.1	48

Table 7.11. Base temperature chosen, minimum shear rates, temperatures of crystallisation and induction time (τ) for milk fat.

7.6.4 *The effect of mixing on mixture of milk fat and cocoa butter*

The variation of induction time in function of three different shear rates was investigated for 75, 50, 25 and 12.5 mole percent solutions of milk fat in cocoa butter. Five base temperatures were chosen in the case of 75 mole percent solution, while four base temperatures for 50, 25 and 12.5 mole percent solutions.

7.6.4.1 *75% Milk Fat in Cocoa Butter*

The experimental data are summarised in Table 7.12 and a plot of induction time versus base temperature is shown in Figure 7.7(b). From slowcool measurements the values found for temperature of saturation and meta stable zone width were 34.2°C and 10.4°C, respectively.

Also in this mixture, the induction time increases as the shear rate decreases. The main effect of mixing is observed in the differences between the induction times

at the same base temperature, especially at the highest base temperatures. As the system is crash cooled to 25°C, it takes only 5 minutes to crystallise at a shear rate of 126.5 s^{-1}, whilst it needs 12 minutes before one detects the formation of nuclei at a shear rate of 41.5 s^{-1}. At a base temperature of 26°C, the mixture shows the same behaviour observed at a base temperature of 25°C, even if small differences are detected in the induction time recorded at a shear rate of 41.5 s^{-1}. Increasing the base temperature, the difference between the induction times at different shear rates increase. This is more evident at 30 and 32°C. There is approximately one hour difference between the values recorded at the two shear rates of 41.5 and 84.5 s^{-1}, whilst only 10 minutes of difference is observed between the 84.5 and 126.5 s^{-1}.

The onset temperature for crystallisation does not vary as a function of different mixing speed in any clearly-defined way.

Base Temperature (°C)	Shear rate (s^{-1})	T_{cryst} (°C)	τ (minutes)
25	41.5	25.6	12
	84.5	25.7	11
	126.5	25.9	5
26	41.5	26.3	15
	84.5	26.4	12
	126.5	27.7	5
28	41.5	28.5	25
	84.5	28.1	13
	126.5	28.8	7
30	41.5	29.4	88
	84.5	29.7	32
	126.5	29.7	21
32	41.5	31.8	125
	84.5	31.8	68
	126.5	31.8	56

Table 7.12. Base temperature chosen, minimum shear rates, temperatures of crystallisation and induction time (τ) for 75 mole% of milk fat in cocoa butter.

7.6.4.2 *50% Milk Fat in Cocoa Butter*

From slowcool measurements, the values found for temperature of saturation and meta stable zone width were 34.0°C and 10.5°C, respectively.

An increasing of concentration of cocoa butter in the mixture leads to a decreasing of the induction time. At the lowest base temperature, the system crystallises at higher temperatures in 2 minutes at a shear rate of 41.5 s^{-1} and only 1 minute at the next two shear rates (Table 7.13). Higher onset temperatures for crystallisation are also observed when the mixture is crash cooled to 24°C. The induction times are still very low, but little bit higher than those recorded at 22°C. At the next two base temperatures (26 and 28°C), small variations in the onset temperature for crystallisation from the base temperatures chosen are noted. Moreover, the system takes more time to crystallise, especially when the mixture is crash cooled to 28°C. At this latter base temperature, a big difference of induction time is detected between the shear rate of 41.5 and 126.5s^{-1} (Figure 7.7(c)).

Base Temperature (°C)	Shear rate (s^{-1})	T_{cryst} (°C)	τ (minutes)
23	41.5	26.8	2
	84.5	27.8	1
	126.5	28.8	1
24	41.5	26.4	5
	84.5	26.8	3
	126.5	26.6	3
26	41.5	26.7	14
	84.5	26.4	12
	126.5	26.6	9
28	41.5	28.0	78
	84.5	28.1	47
	126.5	28.2	34

Table 7.13. Base temperature chosen, minimum shear rates, temperatures of crystallisation and induction time (τ) for 50 mole% of milk fat in cocoa butter.

7.6.4.3 *25 and 12.5 % of Milk Fat in Cocoa Butter*

The values found from the slowcool measurement for temperature of saturation and meta stable zone width are summarised in Table 7.14, whilst the crashcool data are summarised in Tables 7.15 and 7.16. The plots of the induction time versus base temperature are shown in Figure 7.7(e) and (f).

Both mixtures show very high temperatures of crystallisation, compared to the base temperatures chosen and this phenomenon is more evident in the case of the 25 mole percent solution. This could be due to the crystallisation of metastable polymorphs.

At a shear rate of 126.5 s^{-1}, both systems crystallise very quickly: 3 and 30 seconds for 25 and 12.5 mole percent solutions, respectively. Besides, at the highest shear rate correspond small induction times for each base temperatures chosen.

Comparing the results obtained for these two mixtures, it can be observed that the mixing rates play different effect depending on the base temperature chosen. At the base temperatures of 22 and 24°C, the 25 mole percent of milk fat in cocoa butter crystallises very quickly at the two shear rate of 126.5 and 168.1s^{-1}, and, besides, very high temperatures of crystallisation are detected. At the same conditions of temperature and shearing, the 12.5 mole percent solution shows slightly higher induction times, whilst the temperature of crystallisation are smaller than those recorded for 25 mole percent solution.

In contrast, at the two base temperatures of 26 and 28°C, for all shear rates, the induction time values are smaller for the 12.5 mole percent solution (see also Figure 7.7(e)).

Concentration of milk fat in cocoa butter (mole%)	T_{sat} (°C)	MSZW (°C)
25 (A)	29.2	8.5
12.5 (A)	30.6	9.7

Table 7.14. Summary of saturation temperature and metastable zone width from the sloocool experiments discussed in Chapter4 for 25 and 12.5 mole percent of milk fat in cocoa butter.

Base Temperature (°C)	Shear rate (s^{-1})	T_{cryst} (°C)	τ (minutes)
22	41.5	23.5	5
	84.5	27.2	1.5
	126.5	33.3	0.1
	168.1	34.6	0.05
24	41.5	24.2	42
	84.5	25.4	22
	126.5	29.3	3.5
	168.1	33.9	0.5
26	41.5	26.1	74
	84.5	26.2	32
	126.5	26.9	16
	168.1	27.3	5
28	41.5	27.9	126
	84.5	28.1	89
	126.5	29.2	40
	168.1	30.1	24

Table 7.15. Base temperature chosen, minimum shear rates, temperatures of crystallisation and induction time (τ) for 25 mole% of milk fat in cocoa butter.

Base Temperature (°C)	Shear rate (s^{-1})	T_{cryst} (°C)	τ (minutes)
22	41.5	22.8	8
	84.5	23.8	3
	126.5	28.4	1
	168.1	30.5	0.5
24	41.5	24.4	29
	84.5	25.1	14
	126.5	26.5	7
	168.1	29.5	2
26	41.5	26.5	40
	84.5	26.9	22
	126.5	27.1	14
	168.1	31.6	4
28	41.5	27.7	96
	84.5	27.9	69
	126.5	28.6	38
	168.1	29.9	20

Table 7.16. Base temperature chosen, minimum shear rates, temperatures of crystallisation and induction time (τ) for 12.5 mole% of milk fat in cocoa butter.

7.6.4.4 *Crystallisation behaviour in static systems*

The induction measurements were done in static conditions for the following systems: milk fat, cocoa butter, 75, 50, 25 and 12.5 mole percent solutions of milk fat in cocoa butter. The values obtained are compared with those recorded at a shear rate of 41.5 s^{-1} and summarised in Table 7.17.

As it can be observed in Table 7.17, in static conditions, all systems take more time to crystallise. But, in milk fat, there is only six minutes of difference. In contrast, in the milk fat/cocoa butter mixtures, the shearing effect accelerate the crystallisation. However, the discrepancy between static and dynamic conditions it is more evident in the case of the binary system tripalmitin and cocoa butter.

Concentration (mole%)	Base Temperature (°C)	Shear rate (s^{-1})	T_{cryst} (°C)	τ (minutes)
Milk fat	28	0	28.2	28
		41.5	28.1	34
75% Milk fat	25	0	25.6	12
		41.5	25.9	42
50% Milk fat	23	0	26.8	2
		41.5	28.6	35
25% Milk fat	22	0	23.5	5
		41.5	22.6	26
12.5% Milk fat	22	0	22.8	8
		41.5	22.4	36
100% Cocoa butter	25	0	25.2	22
		41.5	24.7	113

Table 7.17. Comparison of induction times in static and dynamic conditions for: milk fat, 75, 50, 25 and 12.5 mole percent solutions of milk fat in cocoa Butter.

7.6.4.5 *Discussion*

Examining the induction time measurements for milk fat and the binary mixtures milk fat and cocoa butter at different concentrations, it has been observed an decreasing of induction time as the shear rate increases.

The mixtures at low concentration of milk fat show high temperatures of crystallisation, especially at the lowest base temperature and at the highest shear rate. High shearing force influences the crystallisation of the mixture and unstable polymorphs could be formed.

The data obtained at similar undercooling for different concentrations of milk fat in cocoa butter have been compared and summarised in Table 7.18. Only at the concentration of 75 mole percent of milk fat is observed a decrease of induction time from the values recorded for milk fat. According to the results discussed in Chapter 5, this concentration was the only one which showed a crystallisation behaviour similar to that observed for milk fat.

Due to much higher undercooling recorded for cocoa butter, it has not been possible make an useful comparison with the data summarised in Table 7.18.

		induction time (min)		
Concentration of milk fat in cocoa butter(mole%)	undercooling (°C)	41.5 s^{-1}	84.5 s^{-1}	126.5 s^{-1}
12.5%	6.6	29	14	7
25%	5.2	42	22	3.5
50%	6.0	78	47	34
75%	6.2	25	13	7
100%	6.2	28	22	20

Table 7.18. A comparison of the induction times collected at similar undercooling for milk fat and 12.5, 25, 50 and 75 mole percent solutions of milk fat in cocoa butter.

7.7 *Conclusions*

The use of the new crash cool tempering cell allowed the study of the variation of induction time as a function of the shearing effect.

- The induction time measurements for the binary mixture tripalmitin/cocoa butter shown a decrease of induction time as the shear rate increases. But in the case of the 10 mole percent solution of tripalmitin in cocoa butter, the induction time measurements do not show linear variation depending on the shear rate applied. This behaviour could be due to the presence of different phase coming out or to a different crystallisation mechanism.
  Comparing the results recorded at similar undercooling, it is observed that the induction times decreases only at the highest concentration of tripalmitin. In the case of 5, 3 and 1 mole percent solutions of PPP in cocoa butter the induction times are much higher than those recorded for cocoa butter alone.

- Also in the case of milk fat and the binary mixtures milk fat and cocoa butter, a decrease of induction time has been observed as the shear rate increases.

7.8 *References*

Nancollas, G H and Purdie, N, *Q. Rev. Chem. Soc.*, 1964, 18, 1-20..

Walton, A G and Zettlemoyer, A C, in *Nucleation*, Dekker, New York, 1983.

Elwell, D and Scheel, H J, in *Crystal Growth From High Temperature Solutions*, Academic Press, London, 1975.

Söhnel, O and Garside, J, in *Precipitation Basic Principles and Industrial Application*, Butterworth Heinemann, Oxford, 1992.

Kleinert, J, *Chocolate, Confectionery and Bakery*, 1976, 1, 2, 3-7.

Chapter 8

In-situ studies of confectionery fats under shearing conditions using small angle X-ray scattering

8.1 *Introduction*

In Chapters 4 and 5 the effect of ingredient composition and temperature profile on the phase composition of mixed confectionery fats was considered. However, it is well known that in commercial chocolate manufacturing processes mixing plays an important role.

A new variable temperature variable shear processing cell was developed in order to study in-situ the crystallisation process under conditions which are more representative of the industrial process.

The new cell was used in combination with SAXS beam lines 16.1 and 2.1 at the Synchrotron Radiation Source (SRS) at Daresbury Laboratory (UK).

This chapter will describe in detail the new cell and examine the effects of shearing, time and temperature on the formation of polymorphic forms of cocoa butter and a mixture of fats. The composition of the mixture is made up of cocoa butter, milk fat, vegetable fat and YN, in the proportion similar to that used in real chocolate.

8.2 *The development of a new X-ray Cell for In-situ Processing*

The *in-situ* processing cell, summarised in Figure 8.1, is designed so that SAXS data have been collected under well defined conditions of temperature and shear with the aim to optimise processing conditions on a structural basis.

8.2.1 *Instrument design*

The instrument is based on a cone and plate rheometer design with two aluminium surfaces: a stationery cone and a flat plate which rotates with respect to the cone [van Gelder, 1996]. The cone angle (4°) ensures uniform shear (shear rate: 0.2 to 22 s^{-1}) throughout the cell and it allows to use a small volume of sample. The cone has a 10 mm aperture at a radius of 65 mm. The two parts of the aluminium body have

overall dimensions of 200 mm by 240 mm by 40 mm and are separated by 2 mm PVC (polyvinyl chloride) spacers to reduce heat transfer to the base plate.

A circular kapton sealed window in the stationery plate and three kapton (0.025 mm in thickness) sealed arced apertures in the rotating plate are provided to allow transmission of X-rays through the cell for 95% of each revolution.

Two 'O'-ring made from rubber are mounted in grooves on the outer edge of the fixed cone to seal against the inside edge of the bearing. These seals serve to prevent the sample seeping out of the cell; this is particularly important as the shearing plane is vertical. A window is made in the cone plate to allow observation of the sample level. The liquid sample is injected into the cell through a valve using a glass syringe.

The 12V DC-motor is fitted with a tacho feed-back system for accurate speed control. It drives the rotating plate through a clutch and a 300 to 1 reduction gear box. The cell is mounted on a base plate with two bolts, fitted with springs to ensure the stability of the cell under changing thermal conditions.

The cell design can also incorporate an optical light probe to detect nucleation. The temperature of the cell is controlled with eight Peltier cooling/heating blocks, capable of enabling fast (ca. 10°C/min) and well controlled cooling and heating. The peltier elements are bonded to brass cooling blocks which are connected via quick release connections to a thermostatically controlled bath recirculating cooling water. A Pt-100 platinum resistance thermometer is mounted in the stationary plate of the cell for an accurate temperature reading. It is controlled by a P.I.D. temperature control apparatus.

Instrument control is effected through the use of a modified tempering machine built by Cadbury Ltd, which acts as an interface between the cell and the computer. The computer controls the experiments and collects the data. The control computer is a C.I.L. multifunction instrument model MFI1010 and the computer program is written and compiled using the Microsoft Quick Basic.

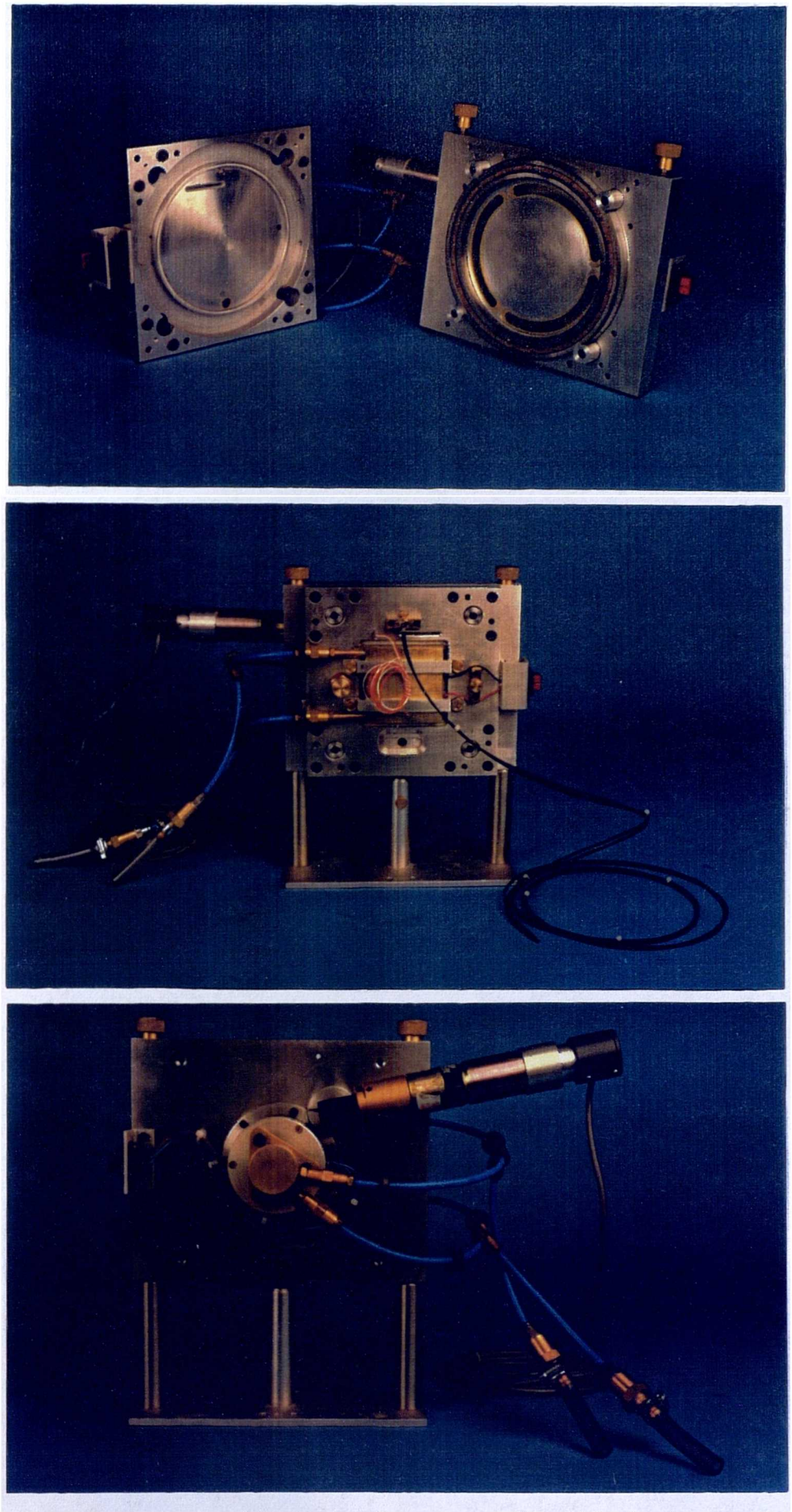

Figure 8.1. Photographs of the in-situ shear stress cell used for in-situ experiments.

Due to technical problems and software development it tooked over two years of the research to have the cell in reliable working conditions. In addition, the lack of beamtime allocation made impossible to continue to carry out experiments using this cell.

8.2.2 *Calculation of shear rate for cone and plate viscometer*

In this type of instrument the sample is contained in the space between a cone and a flat surface normal to its axis. A calculation of the shear rate can be made using the following equation [Van Wazer, 1963]:

$$\dot{\gamma} = \text{rps} \times 2\pi / \tan\theta \qquad (8.1)$$

where rps are revolution per seconds, θ is the angle of the cone plate.

Using the equation (8.1), a shear rate has been calculated for four different motor speed and summarised in Table 8.1.

Motor speed (rpm)	Shear rate (s^{-1})
5.3	8
6.7	10
10	15
16.7	25

Table 8.1 Shear rate calculation in function of the motor speed.

8.3 *Methodology*

8.3.1 *Materials*

Cocoa butter and fats mixtures were provided by Cadbury Ltd (UK). The samples were molten up to 70°C in order to melt also the high-melting fraction. Then, they were injected into the cell, already setup at 50°C, through a valve using a glass syringe. Each samples were then subjected to a cooling/heating process (tempering) which involved rapid cooling from 50°C to varies base temperatures ranging between 22 and 26°C for cocoa butter and 12 and 16°C for fats mixture. Subsequent, each samples were first heated up to 27°C to observe any polymorphic transition, then to 40°C.

8.3.2 *Data collection reduction*

The experiments we carried out at the fixed wavelength combined small and wide angle X-ray scattering stations 16.1 [Bliss et al., 1995] (Figure 8.2) and 2.1 at the synchrotron radiation source (SRS) in Daresbury (UK). These station were set-up for combined small and wide angle time-resolved x-ray scattering using two area detectors. The schematic layout is shown in Figure 8.3.

The SAXS detector was placed at a distance of 1.75m (station 16.1) or 1.40m (station 2.1) from the sample. The WAXS detector was placed at an angle of 45° above the sample distance so that only the top half of the diffraction rings of the wide angle data could be collected. A helium bag between the WAXS detector and the sample served to minimise air-scattering.

The spectra were analysed using the BSL program (Daresbury Laboratory). BSL is a program that is written specifically for analysing and manipulating 2D data. The SAXS data were calibrated upon comparisons with the d-spacing orders of wet rat tail collagen (Figure 8.4(a)), while, for the WAXS data, HDPE (high density polyethylene) was used (Figure 8.4(b)).

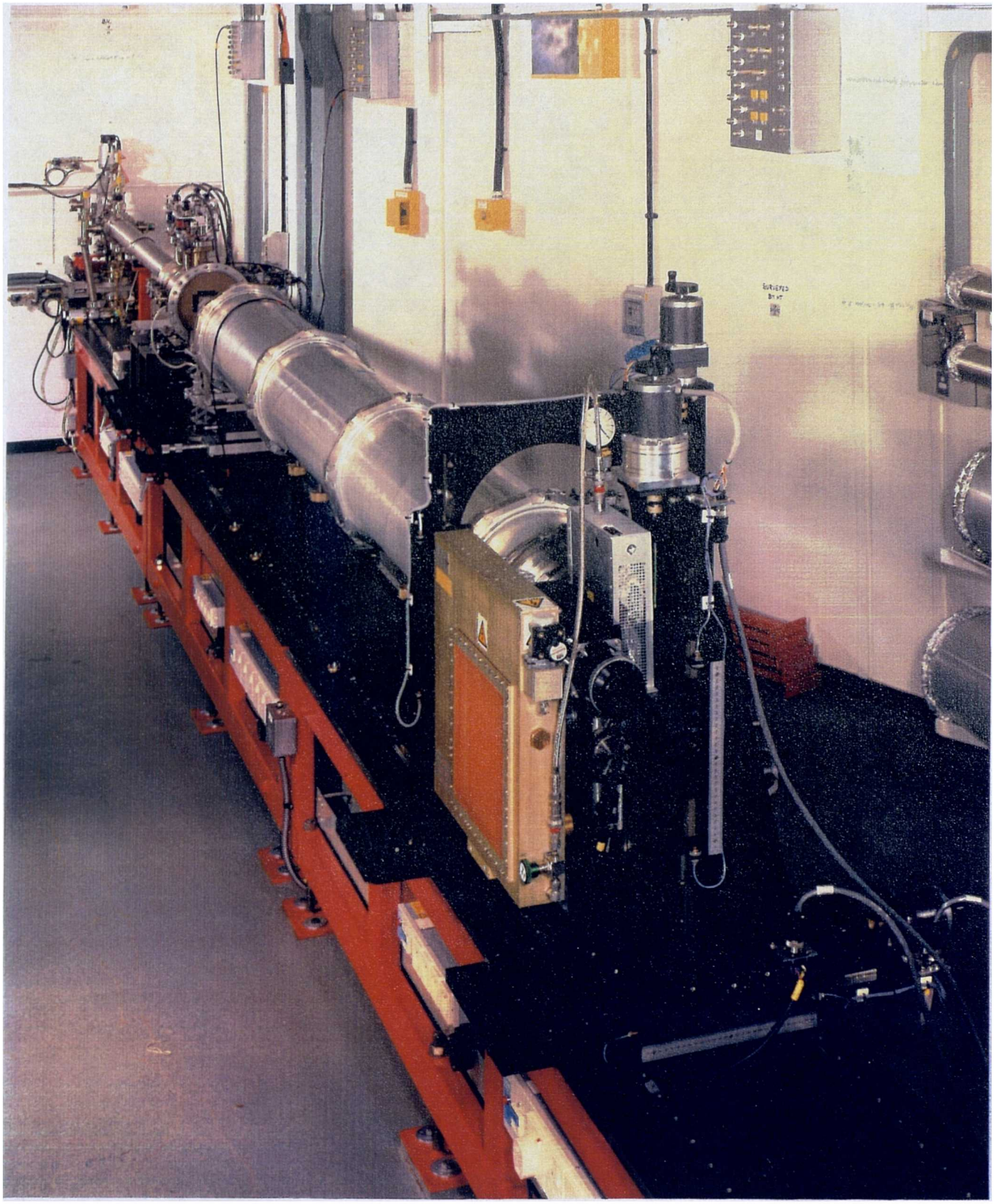

Figure 8.2. Photograph of beam line 16.1 (λ = 1.4Å).

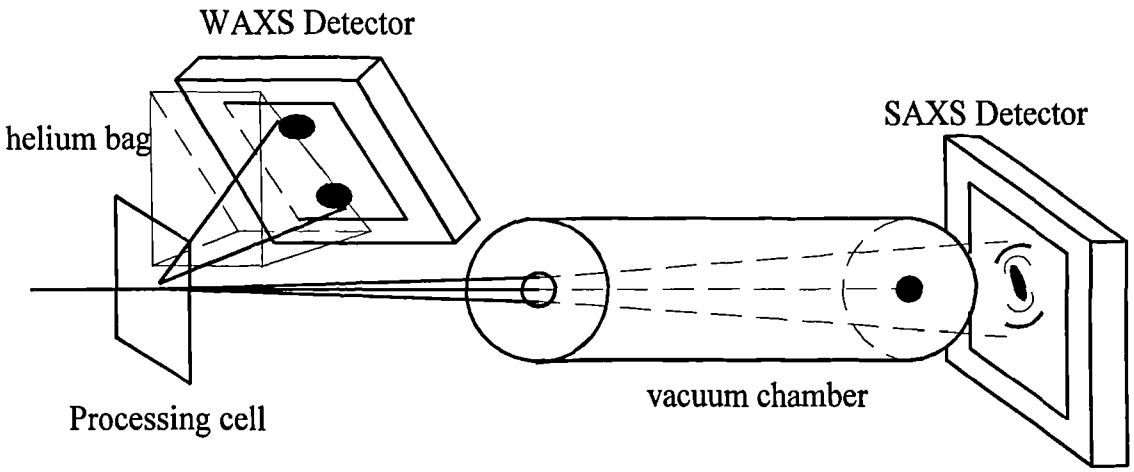

Figure 8.3. Schematic of Wiggler beamline 16.1 showing the experimental layout for combined small and wide angle X-ray scattering using two 2-D detectors.

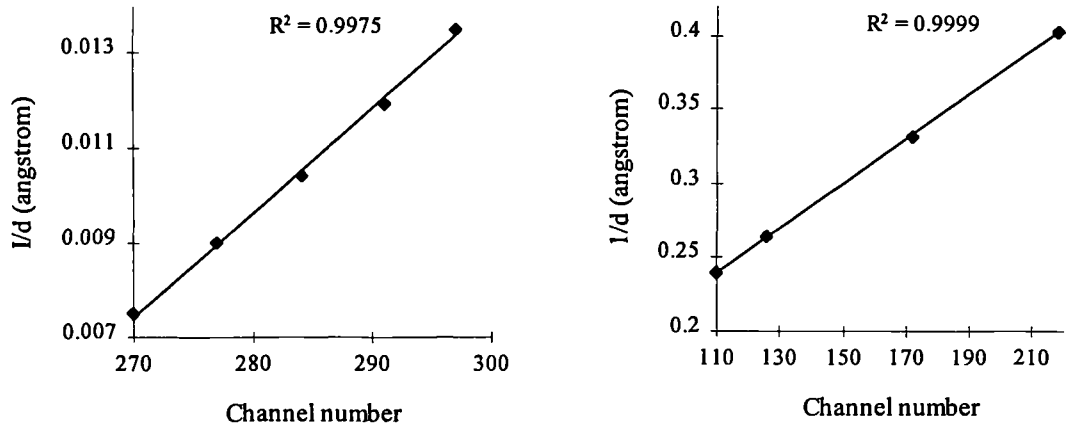

Figure 8.4. Calibration of SAXS/WAXS data using (a) wet rat tail collagen and (b) HDPE (high density polyethylene). The channel number indicates the position of the peak in the spectrum.

All data were normalised for beam-decay. Background subtraction was performed using empty cell for the background pattern and the small angle data were corrected for any inhomogenities in detector sensitivity. All frames were taken with a counting time of 90s.

8.4 *Results*

8.4.1 *Examination of cocoa butter*

8.4.1.1 *Preliminary experiments*

These experiments were carried out at the station 16.1 at the synchrotron radiation source (SRS) in Daresbury. Cocoa butter was subjected to a cooling/heating cycle at a rate of 0.75°C/min and at a shear rate of $8s^{-1}$. During the cooling phase of the cycle, liquid cocoa butter was cooled down from 50°C to 15°C and observed *in-situ* the crystallisation process which started to take place at 20.9°C. The resulting SAXS spectrum shows an intense ring, which corresponds to a long axis spacing of ca. 50 Å (Figure 8.5 (a)), while the WAXS spectrum shows an arc corresponding to a lattice spacing of ca. 4.2 Å (Figure 8.5 (a)). The data are consistent with Form III. The intense spots and the arc at 5 Å are due to diffraction from the mica windows of the cell. No polymorphic transitions were observed during this cooling process.

During the heating phase of the cycle a polymorphic transition was observed to take place at about 28.7°C. According to literature data [Wille and Lutton, 1966; Hicklin, 1985] this transition corresponds to the transition from Form III to Form V. The SAXS data (Figure 8.5 (b)) contains two rings: one at ca. 50Å and another at 66Å.

During the transition the peak at 50 Å reduces in intensity and disappears as the peak at 66 Å becomes more intense. At 30°C only the latter form is still present (Figure 8.5 (c)). In the WAXS spectra (Figure 8.5 (b) and (c)), during the polymorphic transition, two arcs were observed at ca. 3.91 Å and 3.76 Å, which are also consistent with transition to form V. At ca. 33.8°C the melting point of the latter form was observed and, according to literature data [Wille and Lutton, 1966], this is correspond to the melting point of Form V.

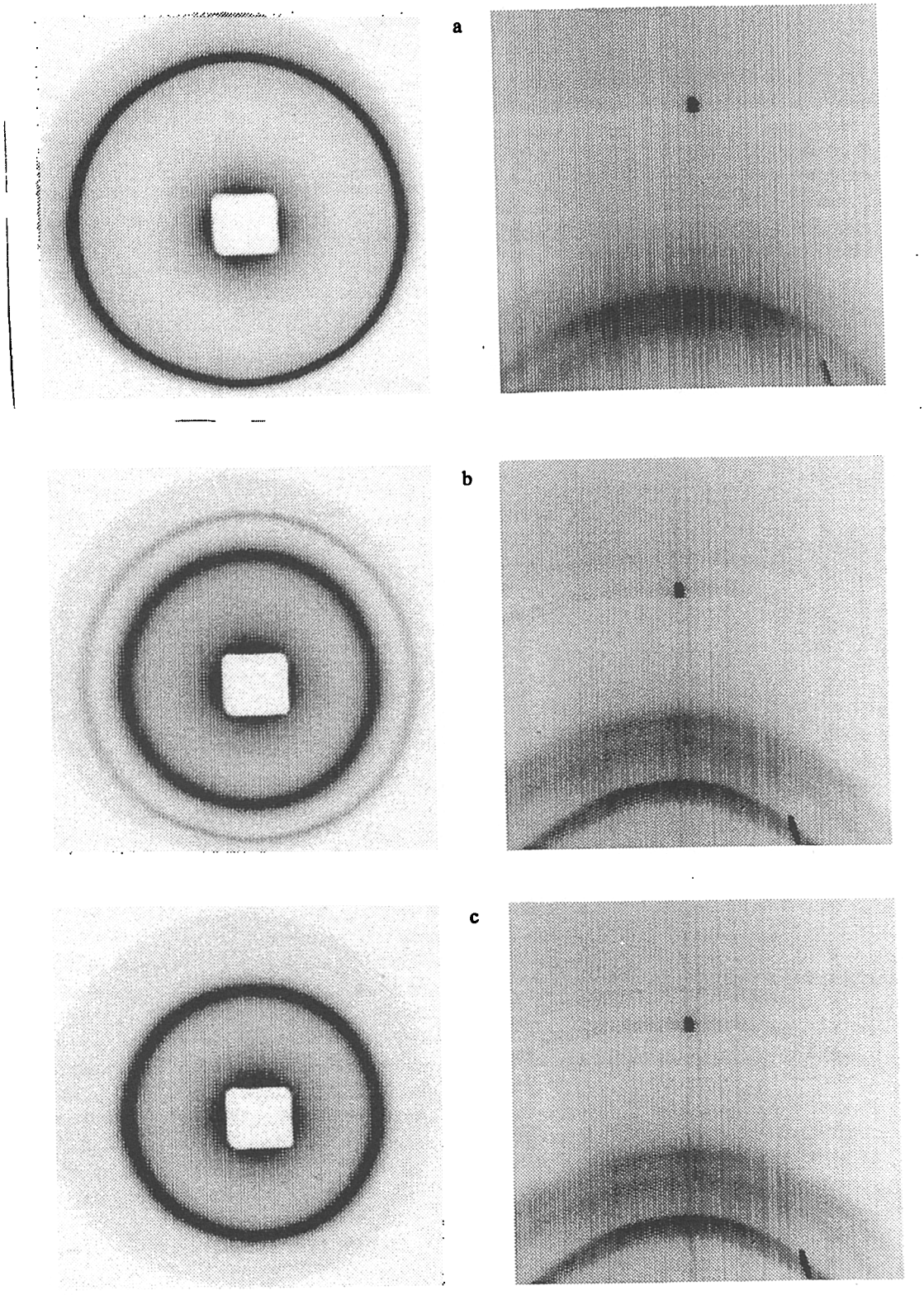

Figure 8.5. X-ray diffraction data of cocoa butter fat collected in-situ on beamline 16.1 at the Daresbury SRS. SAXS (left) and WAXS (right) data for: (a) 20.9°C; (b) 28.7°C; (c) 30°C.

8.4.1.2 *Effect of shear rate, temperature and time on crystallisation of cocoa butter*

Cocoa butter was subjected to cooling/heating cycle at a rate of 5°C/min. Each sample was cooled from 50°C to a base temperature ranging between 20 and 26°C. Then, the sample was held at the base temperature for a certain period of time, after which the sample was heated to 27°C to observe any polymorphic transformation. Finally, it was completely melted by heating up to 40°C. Due to the poor quality of WAXS spectra, for this set of data only the SAXS spectra have been used to follow the crystallisation process of cocoa butter. In these experiments the samples were cooled to 22 and 24°C base temperatures at two shear rates: 10 and $15s^{-1}$.

8.4.1.2.1 *22°C at a shear rate of $15s^{-1}$*

Cocoa butter was crash cooled to 22°C at a shear rate of $15s^{-1}$ and was held at this temperature for 10 minutes. A ring is initially formed during the cooling phase at 24.2°C with a long axis spacing of 50.8 Å (Figure 8.6(a)). This data is consistent with Form III [Wille and Lutton, 1966]. This polymorphic form grows up very slowly in the constant temperature region. After 6 minutes the sample was held at 22°C, other two rings appered (Figure 8.6(b)). They have long spacing of 67.3 Å and 34.4 Å, which correspond to the 1st and 2nd order, respectively, of Form V. Form III is still the dominant crystalline phase, but just after a minute the two rings relate to Form V become the most intense (Figure 8.6(c)).

After holding the temperature of cocoa butter at 22°C for 10 minutes, the sample was first heated to 27°C, where it is immediately observed that Form III melts and transform into Form V (Figure 8.6 (d)).

Then, cocoa butter was holded at 27°C for 5 minutes. Form V grows more until the system is heated up to 40°C and a melting of Form V is observed around 35°C.

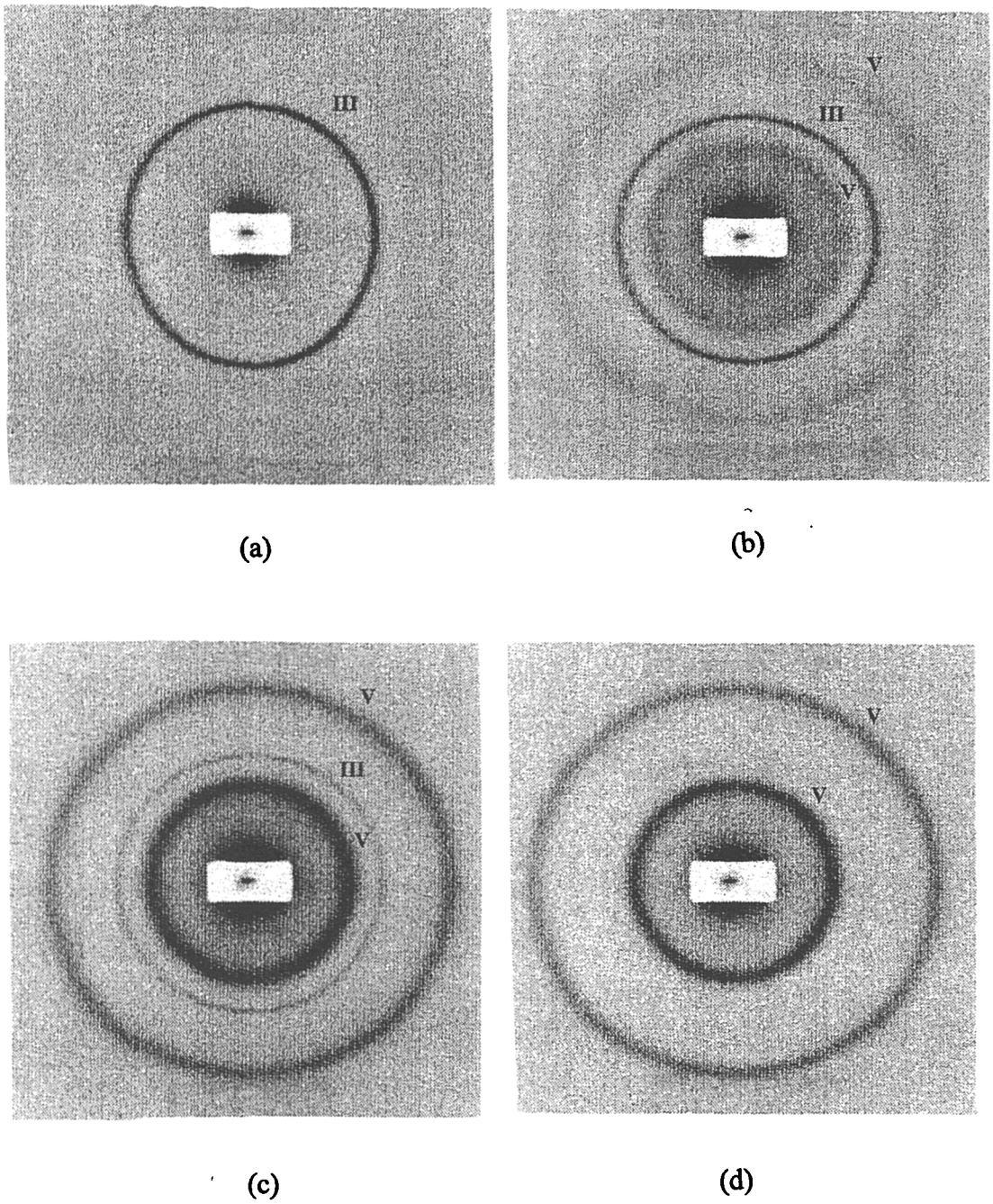

Figure 8.6. Small angle X-ray diffraction data of cocoa butter fat collected in-situ on beamline 2.1 at the Daresbury SRS: (a) 24.2°C; (b) 22.0°C, after 6 minutes; (c) 22.0 after 7 minutes; (d) 27.0°C.

8.4.1.2.2 *24°C at a shear rate of $15s^{-1}$*

Cooling cocoa butter to a base temperature of 24°C at a shear rate of $15s^{-1}$, Form III is immediately formed when this temperature is reached. But the induction of Form V is bigger than that was observed at a base temperature of 22°C. It takes 15 minutes before the two rings related to Form V appear. But, once Form V is crystallised, it becomes immediately the dominant solid phase.

Holding the temperature of the sample at 24°C for 30 minutes, the polymorphic transition from Form III to Form V is observed without heating up to 27°C. This occurs just after 8 minutes Form V was formed. Then, it is enough to keep the system at 24°C for at least 23 minutes to observe the melting of Form III into Form V.

8.4.1.2.3 *24°C at a shear rate of $10s^{-1}$*

As the experiment at a base temperature of 24°C is repeated at a shear rate of $10s^{-1}$, the same peak trends are observed. The only difference occurs in the induction time involved in the formation of Form V. As the shear rate is reduced from $15s^{-1}$ to $10s^{-1}$, the induction time is increased of 2 minutes.

8.4.1.2.4 *Using a base temperature above 24°C*

At a base temperature above 24°C, the formation of Form III is not observed. Cocoa butter was held at 26°C for 50 minutes and sheared at a rate of $15s^{-1}$. The sample crystallises as Form V after 35 minutes. The intensities of the two rings related to Form V are very low, at this temperature Form V has difficult to grow up.

8.4.1.2.5 *Discussion*

During all the experiments carried out on cocoa butter sample, Forms III and V were formed. However, different shear rates and base temperatures have the effect to vary the induction time involved in the crystallisation of cocoa butter as of Form V, whereas the formation of Form III is inhibited at temperature above 24°C. When the sample is cooled to a base temperature of 22 or 24°C, in both cases Form III is formed during cooling around 24°C. At 26°C, the formation of Form III is not observed.

The formation of Form V occurs for all the base temperature chosen, but the induction time varies (Table 8.2). It takes 6 minutes to observe the formation of Form V at a base temperature of 22°C, while 15 minutes at 24°C and 35 minutes at 26°C.

Also the polymorphic transformation from Form III to Form V occurs in different moments. At a base temperature of 22°C, the two polymorphs coexist during the majority of the constant temperature region. The melting of Form III is observed during heating to 27°C and corresponds to 23.5°C. This value agrees with the melting point of Form III found in literature [Wille and Lutton, 1966]. In the case of a base temperature of 24°C, the transformation occurs during the constant temperature region. The shearing force increases the temperature of crystallisation of the metastable Form III. Moreover, a base temperature of 24°C is too high to avoid the melting of Form III at expense of growing of Form V.

Shear rate (s^{-1})	Induction time (mins)
15 (crashcool to 22°C)	6
15 (crashcool to 24°C)	15
10 (crashcool to 24°C)	17
15 (crashcool to 26°C)	35

Table 8.2. Summary of induction times observed for Form V as a function of shear rate and base temperature.

8.4.2 *Crystallisation study of mixture of fats*

The fats mixture was subjected to cooling/heating cycle at a rate of 5°C/min. Each sample was cooled from 50°C to a base temperature ranging between 12 and 16°C. Then, the sample was held at the base temperature for a certain period of time, after which the sample was heated up to 25°C to observe any polymorphic transformation. Finally, it was completely melted by heating up to 40°C. Besides, keeping the base temperature constant to 14°C, three different shear rate were used: 10, 15 and 25s^{-1}. Also for the fats mixture, only the SAXS data have been used to follow the crystallisation process.

8.4.2.1 *16°C at a shear rate of 15s^{-1}*

The sample was crash cooled to 16°C at a shear rate of 15s^{-1} and was held at this temperature for 15 minutes. A ring was initially formed during the cooling phase at 21.7°C with a long axis spacing of 49.1 Å (Figure 8.7 (a)), which probably corresponds to Form III of cocoa butter [Wille and Lutton, 1966]. This polymorphic form grows up slowly for all remain cooling phase. After 9 minutes the sample is held at 16°C, the shadow of two other rings appears (Figure 8.7 (b)). The two weak rings have long spacing values of 66.2 Å and 35.9 Å, respectively. The former is consistent with Form V of cocoa butter [Wille and Lutton, 1966], whilst the latter is probably related to milk fat. The long spacing of 35.9 Å was also found during the static studies of milk fat, which have been described in chapter 5. This phase is probably due to the low-melting, long-chain, monounsaturated and mixed long- and short-chain triglycerides [Small, 1986; Hagemann, 1988; Ollivon, 1992]. Three minutes later, also a shoulder is formed on Form III with long spacing of 47.1 Å (Figure 8.7 (c)). This latter value is consistent with that found during static experiments of crystallisation of milk fat. As it was already explained in Chapter 5, it could be related to the formation of a bilayered structure. According to the literature [Small, 1986; Hagemann, 1988; Ollivon, 1992], this structure is generated mostly by long-chain, high melting,

trisaturated triglycerides.

After 15 minutes at 16°C, the mixtures was heated up to 25°C. During heating, the shoulder of Form III melts at 20.4°C. When the system reach the temperature of 25°C, it is noted that the ring at 35.9Å is shifted and has assumed long spacing of 33.6Å, which corresponds to 2nd order of Form V of cocoa butter. At this point, only the two rings related to Form V are present (Figure 8.7 (d)). The mixture is kept at this temperature for 10 minutes, but more changes were not observed. Then, it was heated up to 40°C, and the melting point of Form V was recorded around 35°C.

8.4.2.2 *14°C at a shear rate of $15s^{-1}$*

Cooling the fat mixture at a base temperature of 14°C, at a shear rate of $15s^{-1}$, the formation of the two rings at 47.1 Å and 35.9 Å are not observed. Form III of cocoa butter crystallised around 21°C during cooling (Figure 8.8 (a)). Once the system has reached the temperature of 14°C, it is observed the presence of two new rings (Figure 8.8 (b)), with long spacing of 53.1 Å and 27.8 Å. These values are consistent with the 1st and 2nd order, respectively, of Form I of cocoa butter [Wille and Lutton, 1966]. After 11 minutes within the constant temperature region, the formation of the 1st and 2nd order of Form V of cocoa butter are observed (Figure 8.8 (c)). The polymorphs I, III and V coexist together during the remain constant temperature region, but Form III is the dominant one.

After 35 minutes at 14°C, the mixture was heated up to 25°C and held at this latter temperature for 10 minutes. During heating, Form I melts around 22°C, while Form III disappears at approximately 25°C. At this stage, only Form V is present (Figure 8.8 (d)). Finally, the sample was further heat up and the melting point of this polymorph was observed around 36°C.

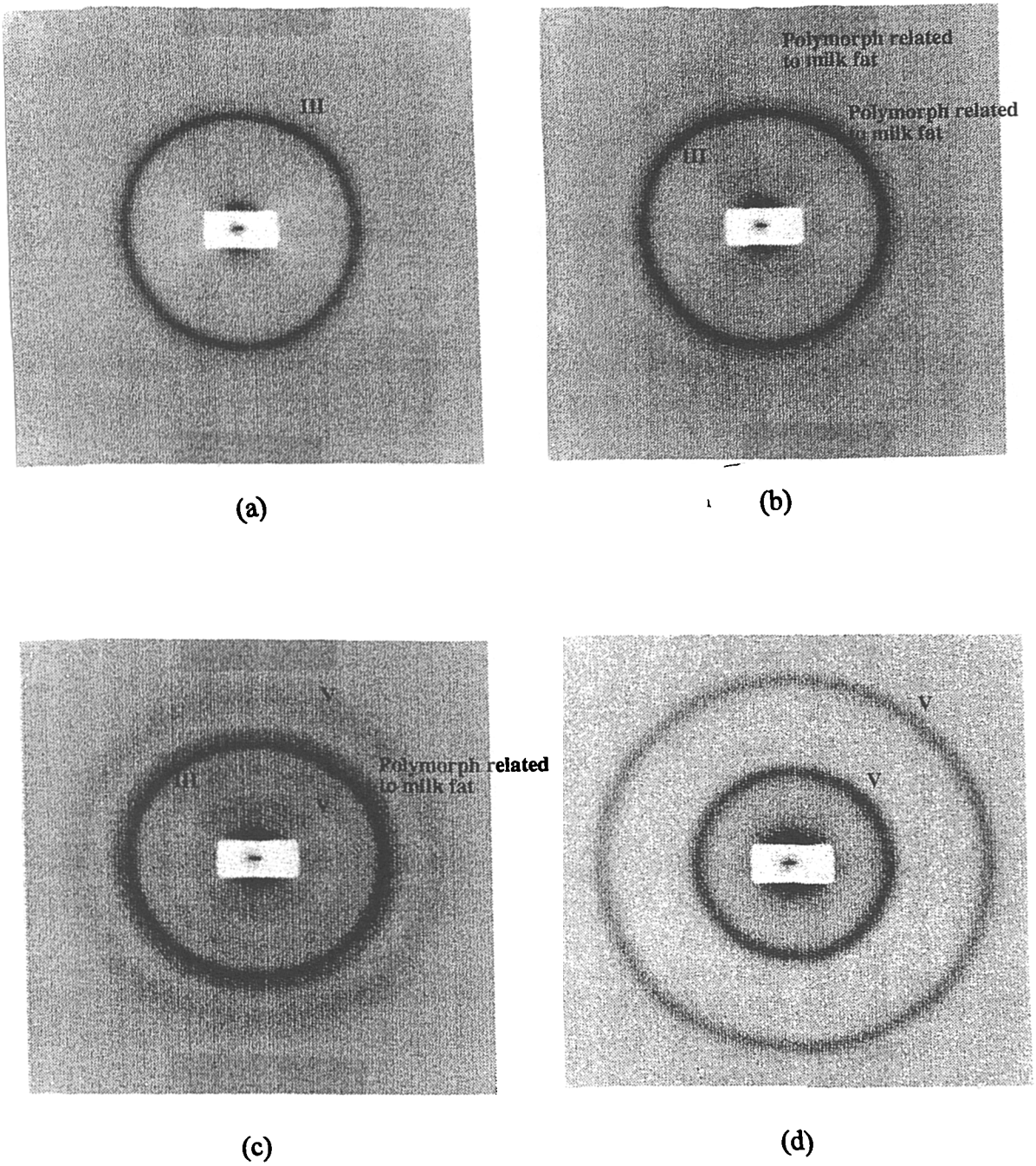

Figure 8.7 Small angle X-ray diffraction data of fats mixture collected in-situ on beamline 2.1 at the Daresbury SRS: (a) 21.7°C; (b) 16.0°C, after 9 minutes; (c) 21.7°C, after 12 minutes; (d) 25.0°C.

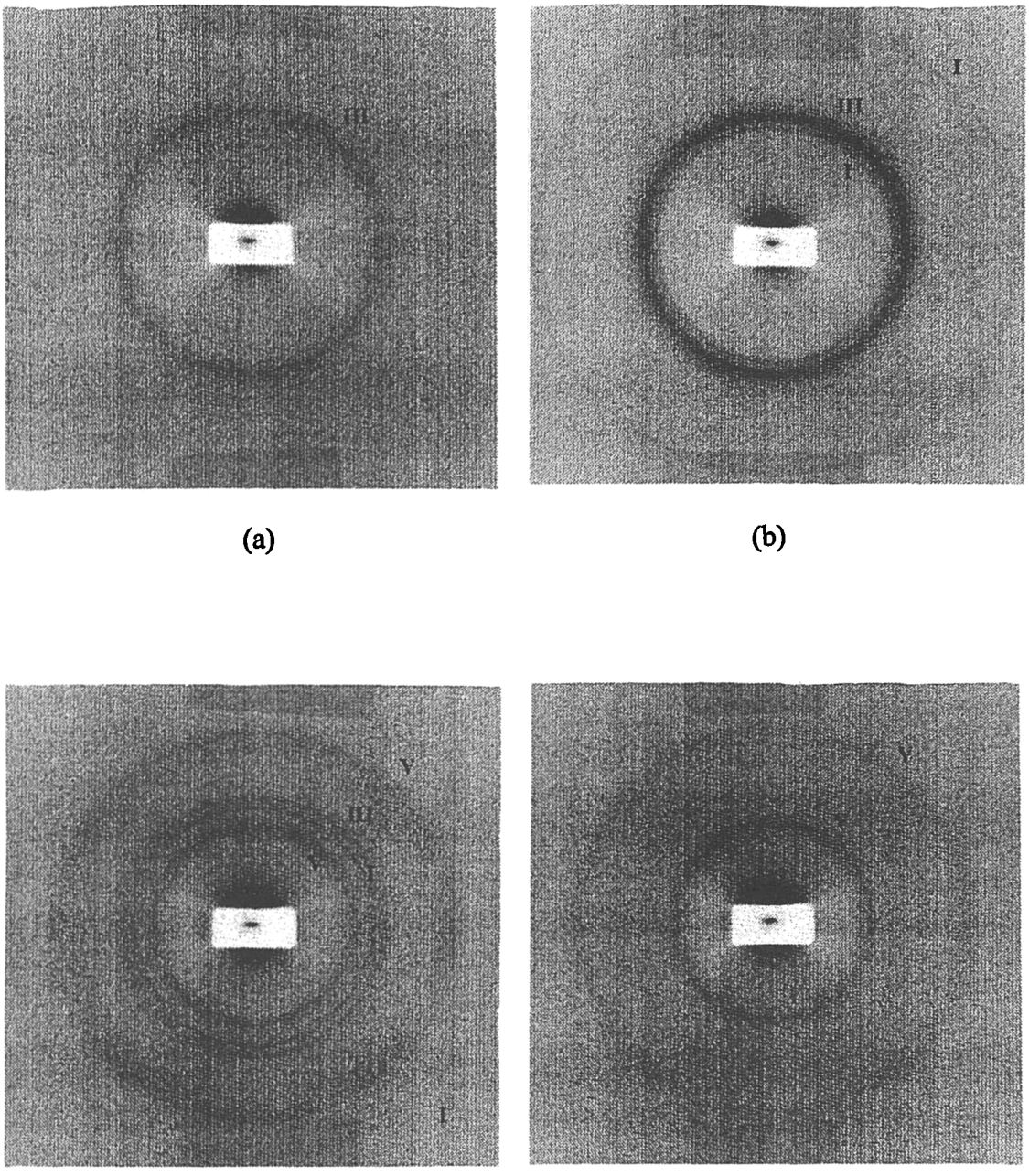

(a) (b)

(c) (d)

Figure 8.8. Small angle X-ray diffraction data of fats mixture collected in-situ on beamline 2.1 at the Daresbury SRS: (a) 21.0°C; (b) 14.0°C; (c) 14.0°C, after 11 minutes; (d) 25.0°C.

8.4.2.3 *14°C at a shear rate of $10s^{-1}$*

As the previous experiment is repeated at lower shear rate, the same peak trends are observed. The main difference is in the induction time involved in the formation of Form V. As the sample is cooled to the base temperature of 14°C, Form V crystallised after 14 minutes, against the 11 minutes required when the system is sheared at a rate of $15s^{-1}$.

8.4.2.4 *14°C at a shear rate of $25s^{-1}$*

When a sample is cooled to the same base temperature but a shear rate of $25s^{-1}$, two differences are observed. First, the induction time is reduced, it takes 7 minutes to Form V to crystallise. Second, Form I melts and transforms in Form V. The higher shearing force allows the reorganisation of the crystal packing at low temperature. Then, only Forms III and V are present during the remain time of the constant temperature region. However, the higher shear rate does not seem to influence the temperatures at which Form III and V melt during the heating phase.

8.4.2.5 *12°C at a shear rate of $15s^{-1}$*

As the base temperature is reduced to 12°C, at a shear rate of $15s^{-1}$ it is observed the same crystallisation behaviour occurring at 14°C. However, a base temperature of 12°C is too low. The sample completely solidified, causing the block of the motor. Then, it was not possible to follow the crystallisation process under shearing conditions.

8.4.2.6 *Discussion*

Both temperature and shear influence significantly the determination of the polymorphic structures. A base temperature of 16°C allows the formation of two polymorphs with long spacing of 35.9Å and 47.1Å, which are related to milk fat. These crystalline phases are not present at temperature below 16°C. Besides, this latter temperature is too high for the crystallisation of the unstable Form I of cocoa butter.

At lower base temperature (14°C), the mixture crystallises in the polymorphic forms I, III and V, which coexist together at the shear rates of 10 and $15s^{-1}$. A difference is observed with respect to the induction time of Form V: 14 minutes at $10s^{-1}$ against 11 minutes at $15s^{-1}$ (Table 8.3). In both cases, Form III results to be the dominant solid phase. An increasing on shearing force affects both induction time of Form V and stability of Form I. At a shear rate of $25s^{-1}$, Form V is formed after 7 minutes the sample is held at 14°C. But the formation of Form V takes place at the expense of Form I, which melts and transforms into Form V.

Finally, it has been observed that a base temperature of 12°C is too low to observe dynamically the crystallisation process involved. The sample solidified in less than 10 minutes causing the block of the motor.

Shear rate (s^{-1})	Induction time (mins)
15 (crashcool to 16°C)	9
15 (crashcool to 14°C)	11
10 (crashcool to 14°C)	14
25 (crashcool to 14°C)	7

Table 8.3. Summary of induction times observed for Form V in the fat mixture as a function of shear rate and base temperature.

8.6 *Conclusions*

The utility of this new variable temperature shear processing cell has been demonstrated in order to simulate the tempering process of cocoa butter fat and mixture of fats in combination with x-ray diffraction on a real-time basis.

- During all the experiments carried out on cocoa butter sample, Forms III and V were formed. However, different shear rate and base temperature have the effect to vary the induction time involved in the crystallisation of cocoa butter as of Form V, while the formation of Form III is inhibited at temperature above 24°C.

- Both temperature and shear influence significantly the determination of the polymorphic structures of fat mixtures. A base temperature of 16°C allows the formation of two polymorphs with long spacing of 35.9Å and 47.1Å, which are related to milk fat. These crystalline phases are not present at temperature below 16°C. At lower base temperature, the mixture crystallises in the polymorphic forms I, III and V, which coexist together at the shear rates of 10 and $15s^{-1}$. At a shear rate of $25s^{-1}$, Form V is formed after 7 minutes the sample is held at 14°C. But the formation of Form V takes place at the expense of Form I, which melts and transforms into Form V.

8.7 *References*

Bliss, N, Bordas, J, Fell, B D, Harris, N W, Helsby, W I, Mant, G R, Smith, W and Towns-Andrews, E, *Rev. Sci. Instrum.*, 1995, 66, 2, 1311-1313.

Rossi, A, van Gelder, R N M R, Hodgson, N and Roberts, K J, *ACS Conference Proceedings Series*, 1996, 209-215.

Hagemann, J W, in *Crystallisation and Polymorphism of Fats and Fatty Acids*, N Garti and K Sato eds., Marcel Dekker, New York, 1988.

Hicklin, J D, Jewell, G G and Heathcock, J F, *Food Microstructure*, 1985, 4, 2, 241-248.

Ollivon, M and Perron, R, in *Manuel des corps gras*, AFECG, A. Karleskind and J. P. Wolff Ed., Lavoisier, Paris 1992, chap. 5.

Small, D M, in *The Physical Chemistry of Lipids. From alkanes to phospholipids*, Plenum Press, New York, 1986, chap. 10.

van Wazer, J R et al., in *Viscosity and Flow Measurement - A Laboratory Handbook of Rheology*, Interscience Publishers, New York, 1963.

Wille, R L and Lutton, E S, *J. Am. Oil Chem. Soc.*, 1966, 43, 491-496.

Chapter 9

Conclusions

9.1 *Introduction*

The aims of this thesis were to investigate the inter-relationship between structure and kinetics associated with the crystallisation of the single and mixed chocolate confectionery fats. The conclusions drawn for this study are summarised in section 9.2 and suggestions for further work are outlined in section 9.3.

9.2 *Conclusions*

An examination of the nucleation behaviour of tripalmitin has revealed differences depending on the type of solvent used. Tripalmitin shows a very low solubility in triacetin, and this probably depends on the different length of the fatty acid chain in the two triglycerides. However, a very large positive deviation from the ideal behaviour is observed. This could be due to the fact that cohesive forces between like molecules are stronger than those between tripalmitin and triacetin. Then, the difficulty in dissolving tripalmitin in triacetin tends to suggest that the two components are not very compatible and the mixture is almost behaving as a two component mixture with the melting behaviour being close to that of pure tripalmitin.

In the case of the binary mixture tripalmitin/triolein, the experimental data follow the ideal behaviour. This might be due to the fact that the two components tripalmitin and triolein are more compatible than tripalmitin and triacetin. In fact, the values of temperature of saturation recorded for the mixture tripalmitin/triolein are very much lower than the value of melting point recorded for pure tripalmitin. An other explanation to this behaviour could be found considering the diffusion of the molecules from the surface depending on the different viscosity between triacetin and triolein.

The tripalmitin and cocoa butter system follows the Hildebrand solubility law only at high concentrations of tripalmitin. The experimental data follow the ideal behaviour at 25, 20, 15 and 10 mole percent solutions of tripalmitin in cocoa butter. Between 8 and 1 mole percent solutions, remarkable difference are detected on

temperature of saturation. The data was consistent with the phase separation of the fat component.

Examining the diffraction data collected for the binary system tripalmitin/cocoa butter at different concentration, it has been observed the predominance of one component over the other during the crystallisation process. Between 25 and 10 mole percent solutions, tripalmitin predominates in the solid phase and influences the molecular packing. In the range of 9 and 7 mole percent, the cooling phase is dominate by cocoa butter, while, during heating, the composition of the solid becomes richer on tripalmitin. The crystallisation process of the mixtures with lower concentration of tripalmitin are clearly controlled by cocoa butter.

In the case of the milk fat and cocoa butter system, two different crystallisation and dissolution process occur, depending on the concentration. The 75 and 50 mole percent solutions of milk fat in cocoa butter show a nucleation behaviour closest to that observed for pure milk fat. In contrast, the 25 and 12.5 mole percent solutions of milk fat in cocoa butter show that a polymorphic transformation has taken place. It was observed that this depends on the cooling/heating rate.

Examining the SAXS data on the binary mixture milk fat and cocoa butter it has been observed that two different mechanisms of crystallisation occur as a function of the concentration. The 75 mole percent solution of milk fat in cocoa butter shows the closest crystallisation behaviour to that observed for milk fat alone. The 50 mole percent solution of milk fat in cocoa butter does not present any of the polymorphs observed in milk fat alone. In contrast, the 25 and 12.5 mole percent solutions of milk fat in cocoa butter have the closest crystallisation behaviour to that observed for cocoa butter alone.

Examining the nucleation data, the effect of addition of the synthetic lecithin YN to a 25 mole percent solution of milk fat in cocoa butter is observed between 0.2 and 0.4 mole percent of YN. The 0.2 mole percent concentration of YN shows the closest crystallisation and dissolution processes to those of the binary mixture with no YN. But the addition of YN to 25 mole percent of milk fat in cocoa butter affects the presence of the two phases observed in the binary mixture. Phase separation is observed only in the case of the 0.2 mole percent solution of YN, at a rate of

0.50°C/min. The 0.4 and 0.6 mole percent solutions of YN do not show any significant differences.

The SAXS data revealed that the addition of synthetic lecithin YN to a 25 mole percent solution of milk fat in cocoa butter affects the stability of the polymorphs formed. Differences are observed between the two mixtures with 0.2 and 0.4 mole percent of YN. In contrast, the ternary system with 0.6 mole percent of YN shows similarity to the system with 0.4 mole percent concentration of YN.

A higher stability of Form I of cocoa butter has been observed during the SAXS experiments carried out on tripalmitin/cocoa butter mixtures. Comparing the data obtained from single cocoa butter with those obtained with the mixtures tripalmitin/cocoa butter, it is clearly evident that the two systems crystallise in two different types of molecular packing, but both related to the same polymorphic phase. Obviously, tripalmitin influences the molecular arrangement of cocoa butter and, at the same time, increases the stability of Form I at higher temperatures.

The addition of 1 mole percent of tripalmitin to a mixture of 25 mole percent of milk fat in cocoa butter does not influence the temperature of crystallisation of the two polymorphs formed during the cooling phase, but less material is crystallised. Whereas, tripalmitin influences the stability of the polymorphs formed.

Measurements of the induction time for the binary mixture tripalmitin/cocoa butter showed a decreasing of induction time as the shear rate increases. But in the case of the 10 mole percent solution of tripalmitin in cocoa butter, the induction time measurements do not show linear variation depending on the shear rate applied. This behaviour could be due to the presence of different phase crystallising out of solution. Also in the case of milk fat and the binary mixtures milk fat and cocoa butter, it has been observed a decreasing of induction time as the shear rate increases.

During the experiments carried out on cocoa butter fat using the shear processing cell, Forms III and V were formed. However, different shear rate and base temperature have the effect to vary the induction time involved in the crystallisation of cocoa butter as of Form V, while the formation of Form III is inhibited at temperature above 24°C.

Both temperature and shear influence significantly the determination of the

polymorphic structures of fat mixtures. A base temperature of 16°C allows the formation of two polymorphs with long spacing of 35.9Å and 47.1Å, which are related to milk fat. These crystalline phases are not present at temperature below 16°C. At lower base temperature, the mixture crystallises in the polymorphic forms I, III and V, which coexist together at the shear rates of 10 and $15s^{-1}$. At a shear rate of $25s^{-1}$, Form V is formed after 7 minutes the sample is held at 14°C. But the formation of Form V takes place at the expense of Form I, which melts and transforms into Form V.

9.3 *Suggestions for future work*

Many of the systems discussed in this thesis would merit further research. Further diffraction studies on the tripalmitin/cocoa butter and milk fat/cocoa butter systems as a function of the cooling rate could help to elucidate the phase separations observed in Chapter 4. A detailed diffraction studies of the binary mixture tripalmitin/triacetin could give useful informations on the crystallisation behaviour of this non-ideal mixture.

As it has been shown that the new variable temperature shear processing cell has been able to simulate the tempering process of cocoa butter fat, a continuation of this investigation using further parameters of shear, temperature and concentration should be undertaken.

It could be also interesting to determine the crystal structure of the three dominant triglyceride components in cocoa butter notably POP, POS and SOS and investigate the phase diagram for binary and tertiary mixtures of these components in order to evolve a realistic structural model for mixed fat system.